ISSN 1007-9327 (print)
ISSN 2219-2840 (online)

World Journal of *Gastroenterology*

World J Gastroenterol 2019 February 14; 25(6): 644-743

Published by Baishideng Publishing Group Inc

World Journal of Gastroenterology

Contents

Weekly Volume 25 Number 6 February 14, 2019

ABOUT COVER

Editorial board member of *World Journal of Gastroenterology*, Cristina Stasi, MD, PhD, Research Scientist, Department of Experimental and Clinical Medicine, University of Florence, Florence 50141, Italy

AIMS AND SCOPE

World Journal of Gastroenterology (*World J Gastroenterol*, *WJG*, print ISSN 1007-9327, online ISSN 2219-2840, DOI: 10.3748) is a peer-reviewed open access journal. The *WJG* Editorial Board consists of 642 experts in gastroenterology and hepatology from 59 countries.

The primary task of *WJG* is to rapidly publish high-quality original articles, reviews, and commentaries in the fields of gastroenterology, hepatology, gastrointestinal endoscopy, gastrointestinal surgery, hepatobiliary surgery, gastrointestinal oncology, gastrointestinal radiation oncology, *etc*. *WJG* is dedicated to become an influential and prestigious journal in gastroenterology and hepatology, to promote the development of above disciplines, and to improve the diagnostic and therapeutic skill and expertise of clinicians.

INDEXING/ABSTRACTING

World Journal of Gastroenterology (*WJG*) is now indexed in Current Contents®/Clinical Medicine, Science Citation Index Expanded (also known as SciSearch®), Journal Citation Reports®, Index Medicus, MEDLINE, PubMed, PubMed Central, Scopus and Directory of Open Access Journals. The 2018 edition of Journal Citation Report® cites the 2017 impact factor for *WJG* as 3.300 (5-year impact factor: 3.387), ranking *WJG* as 35th among 80 journals in gastroenterology and hepatology (quartile in category Q2).

RESPONSIBLE EDITORS FOR THIS ISSUE

Responsible Electronic Editor: *Shu-Yu Yin* **Proofing Editorial Office Director:** *Ze-Mao Gong*

NAME OF JOURNAL
World Journal of Gastroenterology

ISSN
ISSN 1007-9327 (print) ISSN 2219-2840 (online)

LAUNCH DATE
October 1, 1995

FREQUENCY
Weekly

EDITORS-IN-CHIEF
Subrata Ghosh, Andrzej S Tarnawski

EDITORIAL BOARD MEMBERS
http://www.wjgnet.com/1007-9327/editorialboard.htm

EDITORIAL OFFICE
Ze-Mao Gong, Director

PUBLICATION DATE
February 14, 2019

INSTRUCTIONS TO AUTHORS
https://www.wjgnet.com/bpg/gerinfo/204

GUIDELINES FOR ETHICS DOCUMENTS
https://www.wjgnet.com/bpg/GerInfo/287

GUIDELINES FOR NON-NATIVE SPEAKERS OF ENGLISH
https://www.wjgnet.com/bpg/gerinfo/240

PUBLICATION MISCONDUCT
https://www.wjgnet.com/bpg/gerinfo/208

ARTICLE PROCESSING CHARGE
https://www.wjgnet.com/bpg/gerinfo/242

STEPS FOR SUBMITTING MANUSCRIPTS
https://www.wjgnet.com/bpg/GerInfo/239

ONLINE SUBMISSION
https://www.f6publishing.com

World Journal of Gastroenterology

Submit a Manuscript: https://www.f6publishing.com

World J Gastroenterol 2019 February 14; 25(6): 644-658

DOI: 10.3748/wjg.v25.i6.644

ISSN 1007-9327 (print) ISSN 2219-2840 (online)

REVIEW

Evolving role of magnetic resonance techniques in primary sclerosing cholangitis

Emmanuel A Selvaraj, Emma L Culver, Helen Bungay, Adam Bailey, Roger W Chapman, Michael Pavlides

ORCID number: Emmanuel A Selvaraj (0000-0001-9479-2464); Emma L Culver (0000-0001-9644-8392); Helen Bungay (0000-0003-1016-3121); Adam Bailey (0000-0002-8371-2147); Roger W Chapman (0000-0001-9147-285); Michael Pavides (0000-0001-9882-8874).

Author contributions: All authors have contributed to write, revise and submit this review.

Supported by the National Institute of Health Research (NIHR) Biomedical Research Centre, based at Oxford University Hospitals NHS Foundation Trust; and Oxfordshire Health Service Research Committee (OHSRC) as part of Oxford Hospitals Charity, Oxford.

Conflict-of-interest statement: Pavlides M is a shareholder for the company Perspectum Diagnostics and has applied for a patent for medical imaging. All other authors declare no conflicts of interest.

Emmanuel A Selvaraj, Michael Pavlides, Oxford Centre for Clinical Magnetic Resonance Research, Division of Cardiovascular Medicine, Radcliffe Department of Medicine, University of Oxford, John Radcliffe Hospital, Oxford OX3 9DU, United Kingdom

Emmanuel A Selvaraj, Emma L Culver, Adam Bailey, Roger W Chapman, Michael Pavlides, Translational Gastroenterology Unit, Nuffield Department of Medicine, University of Oxford, John Radcliffe Hospital, Oxford OX3 9DU, United Kingdom

Emmanuel A Selvaraj, Emma L Culver, Adam Bailey, Michael Pavlides, Oxford NIHR Biomedical Research Centre, Oxford University Hospitals NHS Foundation Trust and the University of Oxford, Oxford OX3 9DU, United Kingdom

Helen Bungay, Department of Radiology, John Radcliffe Hospital, Oxford OX3 9DU, United Kingdom

Corresponding author: Michael Pavlides, BSc, DPhil, MBBS, MRCP, Doctor, Oxford Centre for Clinical Magnetic Resonance Research, Division of Cardiovascular Medicine, Radcliffe Department of Medicine, University of Oxford, Level 0, John Radcliffe Hospital, Headley Way, Headington, Oxford OX3 9DU, United Kingdom. michael.pavlides@cardiov.ox.ac.uk
Telephone: +44-1865-234577

Abstract

Development of non-invasive methods to risk-stratify patients and predict clinical endpoints have been identified as one of the key research priorities in primary sclerosing cholangitis (PSC). In addition to serum and histological biomarkers, there has been much recent interest in developing imaging biomarkers that can predict disease course and clinical outcomes in PSC. Magnetic resonance imaging/magnetic resonance cholangiopancreatography (MRI/MRCP) continue to play a central role in the diagnosis and follow-up of PSC patients. Magnetic resonance (MR) techniques have undergone significant advancement over the last three decades both in MR data acquisition and interpretation. The progression from a qualitative to quantitative approach in MR acquisition techniques and data interpretation, offers the opportunity for the development of objective and reproducible imaging biomarkers that can potentially be incorporated as an additional endpoint in clinical trials. This review article will discuss how the role of MR techniques have evolved over the last three decades from emerging as an alternative diagnostic tool to endoscopic retrograde cholangiopancreatography, to being instrumental in the ongoing search for imaging biomarker of disease stage, progression and prognosis in PSC.

Key words: Primary sclerosing cholangitis; Magnetic resonance imaging; Magnetic

Manuscript source: Invited manuscript

Received: November 28, 2018
Peer-review started: November 28, 2018
First decision: January 18, 2019
Revised: January 25, 2019
Accepted: January 28, 2019
Article in press: January 28, 2019
Published online: February 14, 2019

resonance cholangiopancreatography; Magnetic resonance elastography; Diffusion magnetic resonance imaging; Endoscopic retrograde cholangiopancreatography

Core tip: Magnetic resonance imaging/magnetic resonance cholangiopancreatography (MRI/MRCP) remains the cornerstone in the diagnosis and follow-up of primary sclerosing cholangitis (PSC) patients. However, heterogeneity in acquisition, image processing and interpretation varies significantly. There is ongoing interest in establishing non-invasive methods to predict clinical endpoints in PSC. A number of recent publications have focused on objectively quantifying output from various magnetic resonance (MR) techniques and have suggested MR parameters as potential prognostic risk-stratification tool in PSC. Our aim is to revisit the historical use of imaging in PSC and consolidate the evolving role of the different MR techniques to date in the quest for establishing a validated imaging biomarker for PSC.

Citation: Selvaraj EA, Culver EL, Bungay H, Bailey A, Chapman RW, Pavlides M. Evolving role of magnetic resonance techniques in primary sclerosing cholangitis. *World J Gastroenterol* 2019; 25(6): 644-658
URL: https://www.wjgnet.com/1007-9327/full/v25/i6/644.htm
DOI: https://dx.doi.org/10.3748/wjg.v25.i6.644

INTRODUCTION

Primary sclerosing cholangitis (PSC) is a rare, chronic, immune-mediated liver disease, characterised by intrahepatic and extrahepatic bile duct inflammation, leading to chronic cholestasis, biliary fibrosis and liver cirrhosis with portal hypertension[1]. It has a male preponderance, with a mean age of diagnosis of 40 years, and a strong association with concomitant inflammatory bowel disease (IBD)[2]. The population incidence ranges from 0 to 1.3 per 100000 persons annually, and the prevalence ranges from 0 to 16.2 per 100000 persons[3]. A clinical definition for PSC was based upon three landmark papers in the 1980s from the United States, United Kingdom and Norway[4-6]. Subsequently, four sub-types of PSC were described. 'Classical' large-duct PSC (LD-PSC), accounting for 90% of patients, involves either the intrahepatic bile ducts, extra hepatic bile ducts or both. It is usually diagnosed on the basis of cholestatic liver biochemistry and characteristic changes in the bile ducts on cholangiography. Magnetic resonance imaging/magnetic resonance cholangiopancreatography (MRI/MRCP) is the standard imaging modality to confirm a diagnosis of LD-PSC[7]. 'Small duct' PSC that has normal cholangiography but affects only the small intrahepatic bile ducts on liver histology, accounts for 5% of patients[8]. PSC with 'autoimmune hepatitis (AIH) overlap', confirmed histologically in those with elevated transaminases and/or immunoglobulin G levels and an abnormal cholangiogram, presents in 5% of patients[9]. Lastly, 'PSC with high immunoglobulin G subclass 4 (IgG4) levels' in the serum and/or tissue, is reported in 12%-18% of LD-PSC patients, with a distinct clinical phenotype and natural history of disease[10,11].

PSC is insidious, with nearly half of patients being asymptomatic at diagnosis, identified after investigation for abnormal liver biochemistry[12]. PSC is considered a premalignant condition, associated with the development of hepatobiliary and colorectal cancers, the most common being cholangiocarcinoma[13]. In the absence of effective medical therapies to date, liver transplantation is the only proven life-extending intervention. PSC accounts for 10%-15% of all liver transplant activity in Europe and the median transplant-free survival of patients with PSC is 14.5 years[13]. There is interest in developing non-invasive clinical risk-stratification methods and surrogate markers in the disease.

This article will review how the role of magnetic resonance (MR) techniques have evolved over the last three decades from emerging as an alternative diagnostic tool to endoscopic retrograde cholangiopancreatography (ERCP), to being instrumental in the ongoing search for an imaging biomarker of disease stage, progression and prognosis in PSC. A summary of the MR techniques that will be discussed in this review is presented in Table 1.

Table 1 Summary of magnetic resonance techniques used in primary sclerosing cholangitis

MR technique	Description of technique	Role in PSC
T2-weighted MRCP	Non-contrast sequences that depict fluid-filled structures such as bile ducts as high-intensity (white) compared to low-intensity (grey/black) of adjacent structures.	Visualisation of biliary anatomy.
Three-dimensional MRCP	Respiratory-triggered, single volume thin slab acquisitions producing isotropic images.	Preferred sequences for optimal multi angle visualisation of the biliary anatomy.
Two-dimensional MRCP	Specific sequences combining coronal thin-slab and rotating oblique-coronal thick-slab image acquisition.	Single shot T2w MRCP sequences are used when three-dimensional MRCP has artefacts or not feasible.
T2-weighted liver axial	Measure of T2 relaxation time in liver parenchyma. Both fat and water appear bright.	Sequence for optimal visualisation of the liver parenchyma.
T1-weighted liver axial	Measure of T1 relaxation time in liver parenchyma. Fat appears bright, water appears dark.	Sequence for optimal visualisation of the liver parenchyma.
MR elastrography	Generates an elastogram map. Specific regions can be selected to obtain mean liver stiffness (kilopascals; kPa).	Quantification and distribution of liver fibrosis.
Diffusion-weighted MRI	Captures changes in the diffusion properties of water protons in tissue represented as the apparent diffusion coefficient.	Can be used to assess liver parenchymal morphological changes (*e.g.*, tumours) and as surrogate for liver fibrosis.
Dynamic contrast-enhanced MRI	Measures T1 changes in liver parenchyma following bolus administration of gadolinium in different phases of uptake and elimination.	Delineates flow in vessels, permeability and enhancement of parenchyma. Can be used to quantify liver function using flow and permeability parameters as surrogate for liver fibrosis.

MR: Magnetic resonance; PSC: Primary sclerosing cholangitis; MRI: Magnetic resonance imaging; MRCP: Magnetic resonance cholangiopancreatography.

EVOLUTION OF PSC DIAGNOSIS

Pathology and cholangiography

The earliest description of PSC was found in a publication by Hofmann 1867[14]. The German pathologist reported two post-mortem descriptions of obstruction of the common hepatic duct by thickening of the duct walls with the absence of malignancy and stones. However, it was not until 1924-1925 that the first well-documented case was reported by the French surgeons Delbet[15] and Lafourcade[16]. The first in the English literature was reported by Miller in 1927[17]. In 1958, Schwarts and Dale reported 13 cases who they felt were consistent with a diagnosis of PSC on review of worldwide literature[18].

PSC was historically a condition recognised intra-operatively when the accessible portion of the extrahepatic biliary system was involved. Subsequently, with the development of operative cholangiography, surgeons were better able to visualise the intra- and extrahepatic bile ducts, extent of the disease and plan optimum site for biliary drainage using T-tube cholangiograms. Reported series of PSC cases were small prior to 1980[5]. The advent of percutaneous transhepatic cholangiography (PTC) and ERCP paved the way for non-operative methods of obtaining a cholangiogram. This led to more detailed description of PSC with a rise in reporting in the medical literature worldwide. The first classification of intrahepatic and extrahepatic features of PSC using cholangiograms obtained from T-tube, PTC, or ERCP was reported in 1984 by Chen and Goldberg using a case series of 19 patients[19].

Emergence of MRCP

ERCP had been the standard of reference for obtaining a cholangiogram in diagnosing PSC until the emergence of MRCP. Whilst MRI of the liver was being performed for liver disease, it was not until 1991 that the first "MR cholangiography" sequence was performed by Wallner *et al*[20]. They developed a T2-weighted rapid sequential gradient-echo two-dimensional (2D) acquisition and a three-dimensional (3D) post-processing technique to produce coronal and sagittal images, without the need for ionising radiation or intravenous biliary contrast. Static fluid-filled structures in the abdomen have long T2 relaxation time in comparison to adjacent tissue. MRCP exploits these differences by using heavily T2-weighted sequences that depicts higher signal intensity (white) of slow-moving or static fluid within the bile and pancreatic ducts in comparison to lower signal intensity (grey/black) of adjacent solid structures.

Specific image acquisition sequences ensure that flowing blood has minimal or no measurable signal in order not to mistake blood vessels for bile or pancreatic ducts. Acquisition is performed in a fasted state (often for at least 4 h) to reduce signal overlap from fluid in the surrounding stomach and duodenum, reduce peristalsis and promote gallbladder distension. Some centres use a negative oral contrast agent, such as 200-400 mL of pineapple juice, 20-30 min prior to MRCP. The high concentration of manganese in pineapple juice is thought to have a paramagnetic effect, suppressing signal from overlapping fluid in the stomach and duodenum[21]. 2D and 3D MRCP has undergone significant advances since its first description with shorter acquisition time, better image quality and improved reconstruction algorithms. Optimal imaging protocol depends on the specific scanner used and parameters including field strength (*e.g.*, 1.5 or 3T), the manufacturer, institutional preference and experience. Good quality 3D MRCP acquisition also depends on good navigator-based respiratory-triggering of the diaphragm.

MRI/MRCP technical review

The International PSC Study Group has recently published a position statement from multidisciplinary experts offering recommendations on the minimum standard for performing MRI/MRCP in PSC as well as a more complete workup[22].

Bile duct imaging: T2-weighted MRCP is preferred to T1-weighted for improved visualisation of biliary ducts. 3D MRCP is preferred over 2D MRCP as the thinner 1mm sections result in higher spatial resolution with excellent signal-to-noise ratio. Post-processing 3D reconstruction using isotropic data allows creation of multiple projections. However, the trade-off for this is longer acquisition time and motion artefact. If a hepatobiliary contrast agent is used, 3D MRCP sequences should be acquired first or else the bile signal will be suppressed.

Liver parenchyma imaging: Cross sectional T2 and T1-weighted acquisition is recommended. T2-weighted coronal plane acquisitions covering most of the liver from anterior to posterior is important for evaluation of peripheral intrahepatic ducts. Fat-suppressed T1-weighted image is acquired as it adds information on the liver parenchyma. Gadolinium-based intravenous contrast agents form part of a more complete workup of PSC patients to detect and differentiate mass lesions and inflammation. MR contrast agents can be classified as purely extracellular or extracellular with a hepatocyte-specific (hepatobiliary) component. Depending on the contrast agent used, post-contrast images are acquired in different phases including arterial, portal venous, equilibrium (parenchyma), delayed and hepatobiliary phases. Some centres perform diffusion-weighted imaging (DWI) routinely for parenchymal and lesion characterisation.

Diagnosis of PSC

Cholangiography is required to make a diagnosis of LD-PSC. ERCP is invasive with potential serious complications including pancreatitis, cholangitis, perforation and bleeding[23]. Over the last twenty years, MRCP has replaced ERCP as the first line imaging method for the diagnosis of PSC. A large meta-analysis, including 189 PSC patients, compared the diagnostic accuracy of MRCP against combined clinical, biochemical, and ERCP or PTC endpoint as the reference standard for diagnosis. The study concluded that the sensitivity and specificity of MRCP for the diagnosis of PSC were 0.86 (95%CI: 0.80-0.90) and 0.94 (95%CI: 0.86-0.98) respectively, with an area under the receiver operating curve of 0.91, supporting a high diagnostic accuracy[24]. Advancement in imaging techniques with higher quality images and spatial resolution is likely to have increased the diagnostic accuracy further. Both the European Association for the Study of the Liver (EASL) and American Association for the Study of Liver Diseases (AASLD) recommend MRCP as the first-choice imaging modality in PSC[7,25]. Performing MRCP first has been shown to be a more cost-effective strategy[26,27]. Moreover, incomplete biliary tract distension mimicking the ductal irregularities of PSC can give rise to false-positive diagnosis on ERCP cholangiogram and false-negative diagnosis if a high-grade stricture causes inadequate opacification of the intrahepatic ducts[28,29]. However, ERCP is still performed when diagnostic doubt exists after MRCP scanning.

MRI/MRCP features of PSC

Identification of multifocal fibrotic strictures and areas of dilatation and ductal wall thickening of the intrahepatic or extrahepatic biliary systems, or both, underpins the diagnosis of LD-PSC. The majority of patients have involvement of both the intra- and extrahepatic bile ducts, with less than 25% with intrahepatic duct disease only[25]. Exclusive involvement of the extrahepatic duct is uncommon (less than 5%) and

should prompt a search for an alternative cause[1]. Figure 1 illustrates typical MRCP features of LD-PSC. The MRI/MRCP features of PSC that have been reported in the literature are summarised in Table 2[22,30-32].

As for any other imaging modality, MRI/MRCP is subject to inter-observer variability. The cholangiographic features of PSC on its own do not necessarily distinguish PSC from secondary sclerosing cholangitis, particularly in the absence of IBD diagnosis. Immunoglobulin G4-related sclerosing cholangitis (IgG4-SC) can often mimic PSC on MRCP. Features that support a diagnosis of IgG4-SC over PSC include dilatation proximal to confluent stricture, symmetrical bile duct wall thickening with smoother outer and inner margins, presence of continuous as opposed to skip disease in the bile ducts, common bile duct thickness greater than 2.5 mm, gallbladder and pancreatic involvement[33,34]. Other mimickers include ischaemic cholangiopathy, acquired immune deficiency syndrome-related cholangiopathy, secondary sclerosing cholangitis after repeated ascending cholangitis and portal biliopathy.

STAGING OF LIVER FIBROSIS

Liver biopsy

Liver biopsy, assessed using Ludwig staging system, has been shown to be an independent predictor of survival in PSC[35,36]. More recently, in a multicentre PSC cohort, three separate histological scoring systems (Nakanuma, Ishak and Ludwig), have been shown to have independent prognostic value in monitoring disease progression[37]. However, liver biopsy is not recommended in the current EASL and AASLD guidelines for the diagnosis and follow-up of PSC due to its invasive nature and risk of complications[7,25]. Moreover, distribution of disease in PSC is patchy and liver biopsy is prone to sampling variability[38]. A liver biopsy is usually performed when MRCP/ERCP is normal to diagnose small-duct PSC and/or there is suspicion of an autoimmune overlap syndrome or IgG4-SC.

Serum markers of fibrosis

Several promising serum biomarkers have been studied as surrogate markers for liver fibrosis. The ELF test is based on three direct markers of fibrogenesis: hyaluronic acid (HA), tissue inhibitor of metalloproteinases-1 (TIMP-1) and procollagen III amino terminal peptide (PIIINP). It has been reported in two large, retrospective, cohort studies to be a strong predictor of clinical outcomes defined as liver-transplant or death, and independent of other risk factors or prognostic scores that predict outcomes[39,40]. Fibrosis-4 index (FIB-4) and aspartate aminotransferase to platelet ratio index (APRI) have been studied in other chronic liver diseases as a marker of liver fibrosis, but their roles in PSC have not been reported to date.

Liver stiffness measurement

Liver stiffness has also been shown to be a surrogate marker for liver fibrosis. Studies have shown correlation with stages of liver fibrosis, liver decompensation and survival[41,42]. Liver stiffness can be measured using shear-wave-based technology such as vibration controlled transient elastography (VCTE) or magnetic resonance elastography (MRE). Two retrospective studies have shown good correlation between baseline VCTE measurements and changes in VCTE measurements with stages of fibrosis and clinical outcomes[43,44]. Although widely available with relatively low-cost, false positive elevation of VCTE measurements can be caused by biliary obstruction and active inflammation such as occurs in PSC patients[45,46]. Technical failures and unreliable results have been reported to be as high as 10% in PSC patients[43]. There is limited data reported on the use of other ultrasound-based techniques such as point shear wave elastography and 2D shear wave elastography in PSC.

MRE has been shown to predict liver decompensation in a large single-centre retrospective study involving 266 PSC patients with median follow-up of 2 years[47]. In a small sub analysis of this study, MRE was also shown to correlate with different stages of liver fibrosis. In comparison to VCTE, it has the added advantage of being able to visualise the whole liver and identify patchy areas of fibrosis in PSC. MRE is able to assess more than 1000 times the volume of liver than VCTE[48]. Unlike VCTE, MRE can be performed regardless of patient's body habitus or presence of ascites. However, MRE is not widely available, is more costly and time-consuming[49]. Whilst MRE was found to have better diagnostic accuracy than VCTE for staging of liver fibrosis in non-alcoholic fatty liver disease[50], there has been no head-to-head comparison performed in a chronic cholestatic disease such as PSC. MRE has also been shown to correlate better with Mayo PSC risk score than VCTE and liver stiffness quantified by MRE is an independent predictor of worse score[51].

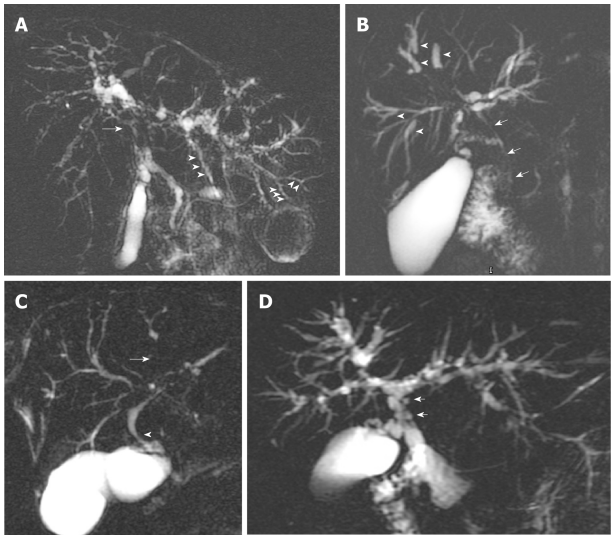

Figure 1 Magnetic resonance cholangiopancreatography annotating typical features of large-duct-primary sclerosing cholangitis. A: Common hepatic duct stricture (arrow) and intrahepatic duct beading (arrowheads); B: Dominant stricture (arrow) and dilated proximal intrahepatic ducts secondary to distal strictures (arrowheads); C: Area of non-filling of intrahepatic ducts indicating tight stricture (arrow) and common hepatic duct stricture (arrowhead); D: Pseudodiverticula.

MONITORING DISEASE PROGRESSION AND CLINICAL OUTCOMES

Disease progression in PSC can affect the biliary tree and/or the liver. A third domain of disease complications or progression includes extra-hepatic manifestations and symptoms, which can be independent of the stage of the biliary or liver disease. The complications of disease progression in PSC are summarised in Figure 2. Predicting which patients are at risk of developing these complications is challenging in clinical practice. Development of non-invasive methods to risk-stratify patients with PSC and predict clinical events was identified as a research priority in a 2016 survey by PSC Support, a registered United Kingdom charity[52]. It highlighted that patients experience significant anxiety due to the uncertainty about the future of their disease; in particular, the risk of disease progression, malignancy, and liver transplantation. In addition to the stage of liver fibrosis, a combination of serum biomarkers, clinical risk prediction model and cholangiographic features can be used to risk-stratify patients.

Serum prognostic markers

Serum alkaline phosphatase (ALP) has been the most widely studied serum biomarker in PSC. ALP levels can fluctuate throughout the disease course but persistently low ALP has been shown to correlate with better clinical outcomes. A cut-off value of 1.5 × the upper limit of normal (ULN) has been demonstrated in several patient cohorts to have prognostic implications[53-57]. However, patients can have normal serum ALP with advanced liver disease[58]. In one study with 10-year follow-up, 62% of patients did not experience any liver-related endpoints despite having a serum ALP that did not improve to levels less than 1.5 × ULN[57].

Clinical risk score and prognostic model

Several clinical risk scores have been developed to predict disease progression and clinical outcomes in PSC. The revised Mayo PSC risk score, based on age, bilirubin, albumin, AST and variceal bleeding, is the most commonly used clinical risk model[59]. The model was developed using multi-centre large cohort data (n = 405) and was subsequently validated in a separate cohort (n = 105). The risk score provides survival estimates up to 4-year follow-up but does not include time to liver transplant. Given that it is made up of markers predictive of advanced disease, it is not surprising that it has insufficient power and is not clinically useful in discriminating and predicting the clinical course of early disease.

The Amsterdam-Oxford risk score based on seven variables (PSC subtype, age at diagnosis, albumin, platelet, AST, ALP and bilirubin) predicted long-term transplant-free survival in a large derivation cohort (n = 692) and external validation cohort (n = 264)[60]. The PSC risk estimate tool (PREsTo) was recently developed using machine learning techniques. It consists of 9 variables (bilirubin, albumin, ALP times the ULN,

Table 2 Descriptive features of primary sclerosing cholangitis on magnetic resonance imaging/ magnetic resonance cholangiopancreatography[22,30-32]

Bile duct changes
Multiple annular or short segmental strictures (1-2 mm) with slightly dilated ducts among them: "beaded" appearance
Obliteration of small peripheral ducts "pruned tree"
Periductal inflammation
Thickening of walls of large ducts
Strictures seen at bile duct bifurcation
Angles between peripheral and central bile ducts become obtuse
Exclusive involvement of extrahepatic bile duct is infrequent
Bile duct dilatations are usually subtle
Retraction of papilla
Webs, diverticula and pigmented stones
Liver parenchymal changes
Segmental or lobular atrophy with compensatory hypertrophy attributed to chronic biliary obstruction
Patchy areas of peripheral parenchymal enhancement
Caudate lobe hypertrophy[1]
Spherical liver shape[2]
Peripheral wedge-shaped areas with focal increased signal intensity on T2-weighted images[3]
T2-weighted hyperintensity around portal vein branches
Regional changes
Gallbladder enlargement
Enlarged regional lymph nodes
Signs of portal hypertension including splenomegaly and collateral vessels

[1]Autoimmune process spares bile ducts in caudate lobe that results in compensatory hypertrophy. This feature is also seen in other cirrhotic livers because the caudate lobe has its own venous, lymphatic and biliary drainage.
[2]This is due to atrophy of left lateral segments and posterior segments of the right lobe.
[3]It remains unclear if this is caused by inflammatory or fibrotic conditions.

platelet, AST, haemoglobin, sodium, age and number of years since diagnosis)[61]. The model was derived using 509 patients and validated in an international multicentre cohort (278 patients) who did not have markers of advanced disease. It accurately predicted the 5-year risk of liver decompensation. None of the prognostic scores that have been developed to date has entered radiological features as a variable into their modelling methods, probably because of the significant inter-observer variability in radiological interpretation even among experienced experts[62].

Cholangiography

Given that cholangiography is required for the diagnosis of the majority cases of PSC, it would seem intuitive to use cholangiographic features as predictors of disease stage and prognosis. Whilst there are limited studies evaluating the use of ERCP cholangiogram findings, there is an increasing trend of utilising MR techniques to study both the liver parenchyma and cholangiography of PSC patients simultaneously to propose imaging biomarkers in PSC. The non-invasive nature of MR techniques makes this an attractive option as a surrogate marker.

ERCP: Craig *et al*[63] retrospectively reviewed ERCP cholangiograms of a cohort of 174 PSC patients with relatively advanced disease and found that both high-grade intrahepatic duct strictures and diffuse intrahepatic duct strictures were associated with a lower 3-year survival[63]. Similarly, Olsson *et al*[64] concluded that high-grade intrahepatic strictures predicted shorter survival in a study involving 94 PSC patients. The Amsterdam cholangiographic classification system was developed by Ponsioen *et al*[65], incorporating the previously reported classifications by Majoie *et al*[66] and Chen-Goldberg[19]. It is based on scoring intrahepatic and extrahepatic stricture and dilatation severity on ERCP cholangiograms as outlined in Table 3. In a large single-centre study with a long follow-up period, 133 patients' cholangiograms were scored. Cholangiographic scores were inversely correlated to survival, and together with age at ERCP, a prognostic model was derived[65]. It remains to be externally validated, perhaps reflecting the shift away from invasive biomarkers of disease.

MRI/MRCP: MRI/MRCP presents a more favourable option than ERCP as a marker

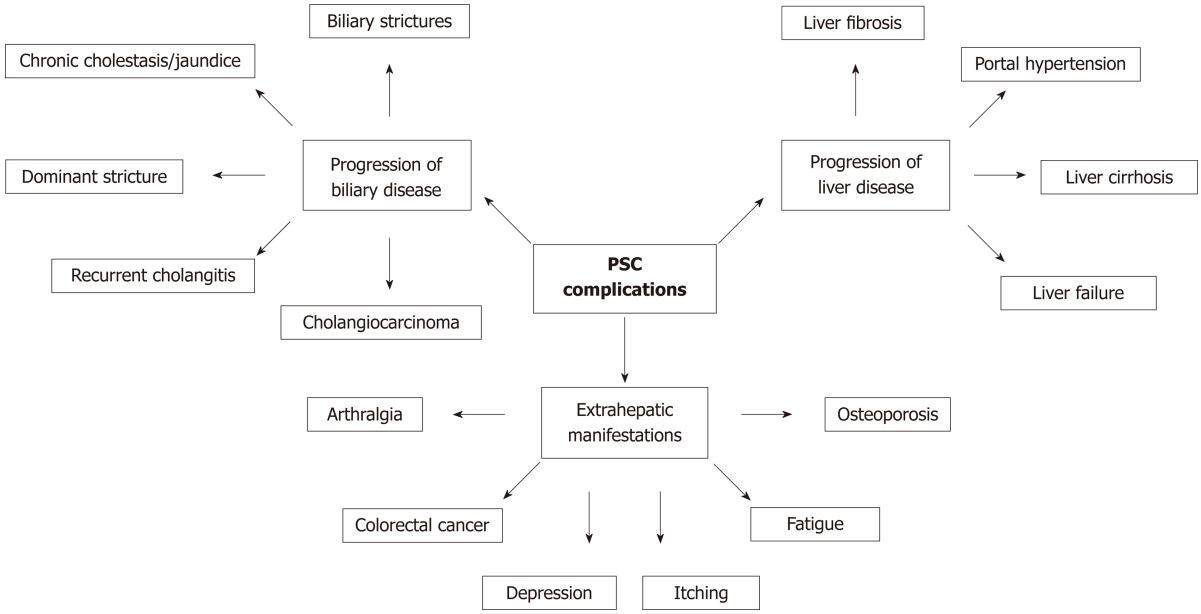

Figure 2 Summary of complications resulting from disease progression in primary sclerosing cholangitis. PSC: Primary sclerosing cholangitis.

of disease activity and prognosis in PSC as it allows co-assessment of liver parenchyma and biliary abnormalities. Petrovic *et al*[67] retrospectively examined the relationship between MRI/MRCP features and survival as predicted by the Mayo risk score. The severity of biliary stricture was graded using the Amsterdam cholangiographic classification. In this study involving 47 patients with PSC, delayed (3-min post contrast) peribiliary hyperenhancement in the liver parenchyma using extracellular gadolinium contrast, showed weak correlation with Mayo risk score. There was no correlation with peribiliary hyperenhancement at 2-min post contrast, intrahepatic or extrahepatic duct grading of strictures. Extrapolating ERCP-based cholangiographic findings to MR-based cholangiography cast doubts on the reproducibility of stricture grading, particularly with variability in contrast injection technique and volume used during ERCP. Tenca *et al*[68] reported only moderate agreement between ERCP and MRCP cholangiograms using a modified Amsterdam scoring system. Weak correlations were demonstrated between severity of biliary changes and serum ALP as well as clinical endpoints defined by liver transplantation or death.

Change in the morphological appearance of the biliary tree and liver on interval MRI/MRCP is often used to comment on whether the disease is stable or has progressed. Ruiz *et al*[69] designed the first MRI-based score to determine radiological disease progression on follow-up MRI/MRCP of 142 well-characterised PSC patients. They designed an interpretation standard model that converted radiological descriptors into categorical variables in this study, which allowed them to systematically analyse the bile ducts and liver parenchyma. An MRI progression risk score model was built using factors that predicted radiological progression between two successive MRIs, as shown in Figure 3.

This study demonstrated radiological progression in 58% of patients (n = 37) over a 4-year follow-up period. Both scores had area under receiver operating characteristic curve of 80% and 83% respectively for predicting radiological progression. However, the study did not take into account inter-observer variability, had no correlation with clinical outcomes and did not have ERCP as the reference standard. The MRI score is awaiting external validation. Kitzing *et al*[70] subsequently examined serial MRI/MRCP images and reported that liver morphological changes on surveillance imaging, specifically liver atrophy, was associated with adverse clinical outcome and shorter transplant-free survival over a mean intervening period of 5 years.

Several studies have evaluated the changes seen on contrast-enhanced MRI sequences in PSC with mixed evidence. Bader *et al*[71] studied 52 patients with PSC and reported that there were no correlations between liver parenchymal signal abnormalities or biliary ductal features and Childs-Pugh or Model for End-stage Liver Disease (MELD) score in a retrospective single time point analysis of MR images. Whilst delayed phase peribiliary hyperenhancement showed weak correlation with Mayo risk score as described earlier, Ni Mhuircheatiagh *et al*[72] reported that the presence and extent of arterial phase peribiliary hyperenhancement on MRI was

Table 3 The Amsterdam classification of endoscopic retrograde cholangiopancreatography cholangiographic changes in primary sclerosing cholangitis[65]

Type	Intrahepatic	Extrahepatic
0	No visible abnormalities	No visible abnormalities
I	Multiple calibre changes; minimal dilatation	Slight irregularities of duct contour; no stricture
II	Multiple strictures; saccular dilatations, decreased arborisation	Segmental strictures
III	Only central branches filled despite adequate filling pressure; severe pruning	Strictures of almost entire length of duct
IV	-	Extremely irregular margins; diverticulum-like outpouchings

associated with a higher Mayo risk score in a cohort of 60 PSC patients. They postulated that this is potentially a marker of active biliary inflammation and poorer prognosis. Bookwalter *et al*[73] retrospectively reviewed MRI that included dynamic contrast enhanced sequences, MRCP and MRE of 55 PSC patients to examine the relationship between liver parenchymal changes, biliary features and liver stiffness at a segmental, lobar and global level. They found weak correlation at segmental level between liver stiffness and liver parenchymal signal changes and ductal strictures. However, they found no significant correlation between the presence and absence of periductal enhancement in any of the three contrast enhanced phases with Mayo risk score or MELD score.

Dominant stricture and cholangiocarcinoma

A dominant bile duct stricture in PSC is defined as a stricture less than 1.5 mm diameter in the common bile duct, or less than 1 mm in the left or right main hepatic ducts on cholangiography[7]. However, there are currently no validated criteria for MR definition of a dominant stricture. Deterioration in clinical and biochemical parameters prompts evaluation for a dominant stricture and/or cholangiocarcinoma on MRI/MRCP. The presence of a dominant stricture either at diagnosis or follow-up is associated with an increased risk of developing cholangiocarcinoma and mortality[74,75].

Over one third of cholangiocarcinoma cases were detected within the first year following PSC diagnosis in a retrospective, international, observational cohort study involving 594 PSC patients[13]. This is likely due to length-time bias and detection of cholangiocarcinoma only when it becomes clinically overt. Serum tumour marker carbohydrate antigen (CA)19-9 is widely used in surveillance strategy but it lacks both sensitivity and specificity for the detection of cholangiocarcinoma[76,77]. The cholangiocarcinoma is usually too advanced for curable treatment by the time CA19-9 becomes persistently elevated[78]. Annual MRI/MRCP as a surveillance strategy is often performed, but with limited proven benefit. Nevertheless, the current recommendation for cholangiocarcinoma surveillance is annual CA19-9 and MRI/MRCP[79]. There is an unmet need for earlier detection of cholangiocarcinoma and closer monitoring of newly diagnosed patients.

Subclinical PSC

A population-based study of long-term IBD patients in Norway reported that 8.1% of 322 patients had MRCP lesions indicating PSC, a 3-fold higher prevalence than detected clinically before MRCP screening. Nearly two-thirds of these detected cases had 'subclinical' PSC with mild changes on cholangiography and no biochemical abnormalities[80]. A prospective controlled UK study demonstrated 14% of 51 patients with extensive ulcerative colitis and normal liver biochemistry had biliary abnormalities suggestive of PSC on MRCP, and over long-term (10-year) follow-up, one-third developed abnormal liver biochemistry, one-fifth developed progressive bile duct disease and over half developed malignancy, including two biliary and one colorectal carcinoma[81].

QUANTITATIVE LIVER IMAGING

DW-MRI

DW-MRI manipulates the altered diffusion properties of water protons in fibrotic tissue and allows assessment of liver fibrosis[82]. Addition of the short sequence to routine MRI/MRCP enables whole liver assessment of fibrosis distribution, particularly useful in a patchy disease such as PSC[32,83]. Since TE and MRE have shown better diagnostic accuracy for the staging of liver fibrosis[83,84], DWI has fallen

MRI progression risk score (without gadolinium) = 1 × intrahepatic bile duct dilatation + 2 × hepatic dysmorphy + 1 × portal hypertension
MRI progression risk score (with gadolinium) = 1 × hepatic dysmorphy + 1 × hepatic parenchymal enhancement heterogeneity
Intrahepatic bile duct dilatation score: 0 (≤ 3 mm), 1 (4 mm), or 2 (≥ 5 mm)

Figure 3 Magnetic resonance imaging progression risk score[69]. MRI: Magnetic resonance imaging.

out of favour but is still performed for better characterisation of lesions involving the liver parenchyma. In a recent prospective study involving 47 PSC patients, DWI-MRI performed better than dynamic contrast-enhanced MRI (DCE-MRI) in detecting and staging liver fibrosis using VCTE as the reference standard[85].

DCE-MRI

Administration of hepatocyte-specific contrast agents such as Gd-BOPTA (gadobenate dimeglumine) and Gd-EOB-DTPA (gadoxetate disodium) allows assessment of liver function by analysing the liver uptake and elimination of contrast. Several studies have attempted to quantify liver parenchymal changes with the administration of a contrast agent.

Ringe *et al*[86] demonstrated that hepatobiliary excretion of hepatocyte-specific contrast is significantly reduced in patients with PSC when compared to normal controls and correlated with bilirubin levels in PSC. Noren *et al*[87] quantitatively compared hepatocyte-specific contrast uptake with histopathological stage of fibrosis in a prospective study involving 38 patients with compensated chronic liver diseases of varying aetiology. They demonstrated that quantitative measurement of signal intensities using DCE-MRI was able to distinguish advanced fibrosis (F3-4) from no and moderate fibrosis (F0-2). Nilsson *et al*[88] developed a non-invasive imaging-based method using DCE-MRI to assess liver function at the segmental and global level, and showed significantly heterogeneity in the liver parenchyma of PSC patients compared to controls. This small study (involving PSC patients with mild disease) reported correlation between MRI-derived liver function indices and disease severity using Mayo risk score. Segmental liver function correlated with level of downstream biliary obstruction.

Hinrichs *et al*[89] reported that reduction in T1 relaxation time after hepatocyte-specific contrast administration correlated with liver biochemistry tests, MELD and Mayo risk score. They proposed that global liver function could be non-invasively assessed using this specific T1 mapping sequence technique in PSC. Nolz *et al*[90] performed retrospective quantitative analysis of liver parenchymal enhancement in T1-weighted MRCP images in a small cohort of PSC patients, and calculated the difference in signal intensity (SI) ratio between the hepatobiliary phase and unenhanced parenchyma [termed relative enhancement (RE)]. They demonstrated significant reduction in RE in localised areas of impaired liver parenchyma in comparison to normal areas, thus allowing regional functional assessment.

RE = [(hepatobiliary SI - unenhanced SI)/unenhanced SI × 100]

Keller *et al*[91] adapted the above technique to MRI scans performed with extracellular gadolinium-based instead of hepatocyte-specific contrast. They retrospectively reviewed scans and liver biopsies of 40 PSC patients to evaluate the utility of several quantitative MRI-derived parameters as markers of liver inflammation and fibrosis (LIF). Relative liver enhancement (RLE) in the delayed phase of T1-weighted MRI was shown to strongly correlate with stage of liver fibrosis. The same group also demonstrated an increased RLE within T2 hyperintense areas in the liver parenchyma on T2-weighted MRI and postulated that this could be early changes of patchy inflammation[92]. Schulze *et al*[93] calculated RLE in the hepatobiliary MRI phase in a prospective study using hepatocyte-specific contrast agent and evaluated its role as a prognostic marker. Moderate correlation was demonstrated with serum markers (ALP, albumin, bilirubin, INR) and prognostic scorings systems (MELD, Mayo risk score, Amsterdam-Oxford). They proposed a cut-off RLE value that predicted clinical endpoints with low sensitivity (74%) and reasonable specificity (94%), which remains to be externally validated.

Non-contrast T1 mapping

Liver*Multiscan*™ (Perspectum Diagnostics, Oxford, United Kingdom) is a software product that enables post-processing of liver MRI using T1 and T2* maps[94,95]. In a small proof of principle study, the LIF score derived from the iron corrected T1 (cT1) measurements, has been shown to strongly correlate with clinical outcomes in patients with chronic liver disease of mixed aetiologies[96]. This technique looks promising for the evaluation of patients with non-alcoholic fatty liver disease[97].

More recently, Arndtz *et al*[98,99] reported the distribution of imaging metrics derived

from quantitative maps of T1, T2* and cT1 of Liver*Multiscan*™ in autoimmune hepatitis (AIH), primary biliary cholangitis (PBC) and PSC. Using a machine-learning technique to analyse the skewness and kurtosis of the distribution as well as local regional variance, they demonstrated that addition of imaging metrics to serum ALT or ALP performed slightly better than serum ALT or ALP alone in disease differentiation between parenchymal liver disease (62 AIH patients) and biliary liver disease (124 PSC and PBC patients).

LIMITATIONS OF MRI/MRCP

Acquisition and 3D image reconstruction protocols still vary significantly across centres and there is no standard model for interpreting MRCP data. Current clinical utility of MRI/MRCP allows only qualitative assessment of the bile ducts and liver parenchyma, and is therefore susceptible to subjectivity in interpretation. Assessment of the distal common bile duct and subtle changes in the smaller peripheral intrahepatic bile ducts still remains a challenge despite the use of modern 3 Tesla (T) MRI scanners[22]. The position statement from the International PSC Study Group outlines areas of unmet need for imaging techniques in PSC, including (1) early detection of disease; (2) the determination of disease stage, activity and prognosis; (3) the assessment of treatment response; (4) a clinically meaningful definition of dominant bile duct stenosis; and (5) the early detection of cholangiocarcinoma.

CONCLUSION

The role of MRI/MRCP in establishing the diagnosis of PSC is well documented and has long superseded ERCP as the gold standard for obtaining cholangiography. Disease staging is based on the severity of the liver fibrosis component of PSC, which has prognostic implications. MRE appears to be a promising technique that generates a liver stiffness map of the whole liver for assessment of patchy liver fibrosis. However, there have been no comparative studies between MRE and other surrogate markers of fibrosis in PSC. Whilst there is some exciting work published on MR quantitative methods involving the liver parenchyma in PSC, there has been surprisingly little advancement in the last three decades on quantitative methods involving the bile ducts. Published studies to date have only proposed cholangiography-based scoring systems derived from interpretation of qualitative descriptors by two specialist radiologists assessing the morphological appearance of bile ducts and liver parenchyma. This method is highly variable even among experts and therefore limits its inclusion into reliable prognostic models. MRI/MRCP shows promising potential for prediction of disease course and clinical endpoints in PSC as MR techniques evolve towards 'quantifying' the disease. However, further development and validation of objective and reproducible MR-based parameters are needed before it can establish its role as an imaging biomarker in PSC.

REFERENCES

1 **Hirschfield GM**, Karlsen TH, Lindor KD, Adams DH. Primary sclerosing cholangitis. *Lancet* 2013; **382**: 1587-1599 [PMID: 23810223 DOI: 10.1016/S0140-6736(13)60096-3]

2 **Boonstra K**, Weersma RK, van Erpecum KJ, Rauws EA, Spanier BW, Poen AC, van Nieuwkerk KM, Drenth JP, Witteman BJ, Tuynman HA, Naber AH, Kingma PJ, van Buuren HR, van Hoek B, Vleggaar FP, van Geloven N, Beuers U, Ponsioen CY; EpiPSCPBC Study Group. Population-based epidemiology, malignancy risk, and outcome of primary sclerosing cholangitis. *Hepatology* 2013; **58**: 2045-2055 [PMID: 23775876 DOI: 10.1002/hep.26565]

3 **Boonstra K**, Beuers U, Ponsioen CY. Epidemiology of primary sclerosing cholangitis and primary biliary cirrhosis: a systematic review. *J Hepatol* 2012; **56**: 1181-1188 [PMID: 22245904 DOI: 10.1016/j.jhep.2011.10.025]

4 **Schrumpf E**, Elgjo K, Fausa O, Gjone E, Kolmannskog F, Ritland S. Sclerosing cholangitis in ulcerative colitis. *Scand J Gastroenterol* 1980; **15**: 689-697 [PMID: 7209379 DOI: 10.3109/00365528009181516]

5 **Chapman RW**, Arborgh BA, Rhodes JM, Summerfield JA, Dick R, Scheuer PJ, Sherlock S. Primary sclerosing cholangitis: a review of its clinical features, cholangiography, and hepatic histology. *Gut* 1980; **21**: 870-877 [PMID: 7439807 DOI: 10.1136/gut.21.10.870]

6 **Wiesner RH**, LaRusso NF. Clinicopathologic features of the syndrome of primary sclerosing cholangitis. *Gastroenterology* 1980; **79**: 200-206 [PMID: 7399227]

7 **European Association for the Study of the Liver**. EASL Clinical Practice Guidelines: management of cholestatic liver diseases. *J Hepatol* 2009; **51**: 237-267 [PMID: 19501929 DOI: 10.1016/j.jhep.2009.04.009]

8 **Angulo P**, Maor-Kendler Y, Lindor KD. Small-duct primary sclerosing cholangitis: a long-term follow-up study. *Hepatology* 2002; **35**: 1494-1500 [PMID: 12029635 DOI: 10.1053/jhep.2002.33202]

9 **Kaya M**, Angulo P, Lindor KD. Overlap of autoimmune hepatitis and primary sclerosing cholangitis: an evaluation of a modified scoring system. *J Hepatol* 2000; **33**: 537-542 [PMID: 11059857 DOI: 10.1016/S0168-8278(00)80004-5]

10 **Mendes FD**, Jorgensen R, Keach J, Katzmann JA, Smyrk T, Donlinger J, Chari S, Lindor KD. Elevated serum IgG4 concentration in patients with primary sclerosing cholangitis. *Am J Gastroenterol* 2006; **101**: 2070-2075 [PMID: 16879434 DOI: 10.1111/j.1572-0241.2006.00772.x]

11 **Björnsson E**, Chari S, Silveira M, Gossard A, Takahashi N, Smyrk T, Lindor K. Primary sclerosing cholangitis associated with elevated immunoglobulin G4: clinical characteristics and response to therapy. *Am J Ther* 2011; **18**: 198-205 [PMID: 20228674 DOI: 10.1097/MJT.0b013e3181c9dac6]

12 **Lazaridis KN**, LaRusso NF. Primary Sclerosing Cholangitis. *N Engl J Med* 2016; **375**: 1161-1170 [PMID: 27653566 DOI: 10.1056/NEJMra1506330]

13 **Weismüller TJ**, Trivedi PJ, Bergquist A, Imam M, Lenzen H, Ponsioen CY, Holm K, Gotthardt D, Färkkilä MA, Marschall HU, Thorburn D, Weersma RK, Fevery J, Mueller T, Chazouillères O, Schulze K, Lazaridis KN, Almer S, Pereira SP, Levy C, Mason A, Naess S, Bowlus CL, Floreani A, Halilbasic E, Yimam KK, Milkiewicz P, Beuers U, Huynh DK, Pares A, Manser CN, Dalekos GN, Eksteen B, Invernizzi P, Berg CP, Kirchner GI, Sarrazin C, Zimmer V, Fabris L, Braun F, Marzioni M, Juran BD, Said K, Rupp C, Jokelainen K, Benito de Valle M, Saffioti F, Cheung A, Trauner M, Schramm C, Chapman RW, Karlsen TH, Schrumpf E, Strassburg CP, Manns MP, Lindor KD, Hirschfield GM, Hansen BE, Boberg KM; International PSC Study Group. Patient Age, Sex, and Inflammatory Bowel Disease Phenotype Associate With Course of Primary Sclerosing Cholangitis. *Gastroenterology* 2017; **152**: 1975-1984.e8 [PMID: 28274849 DOI: 10.1053/j.gastro.2017.02.038]

14 **Hoffmann C**. Verschluß der Gallenwege durch Verdickung der Wandungen. *Arch Pathol Anat Physiol Klin Med* 1867; 49: 206-215.

15 **Delbet M**. Retrecissement due choledoque: Cholecystoduo-denostomie. *Bull Mem Soc Nat Chir* 1924; **50**: 1144

16 **Lafourcade M**. Deux observations d'obliteration cicatricelle de choledoque. *Bull Mem Soc Nat Chir* 1925; 50

17 **Miller RT**. Benign Stricture of the Bile Ducts. *Ann Surg* 1927; **86**: 296-303 [PMID: 17865730 DOI: 10.1097/00000658-192708000-00018]

18 **Schwartz SI**, Dale WA. Primary sclerosing cholangitis; review and report of six cases. *AMA Arch Surg* 1958; **77**: 439-451 [PMID: 13572239 DOI: 10.1001/archsurg.1958.01290030139016]

19 **Chen LY**, Goldberg HI. Sclerosing cholangitis: broad spectrum of radiographic features. *Gastrointest Radiol* 1984; **9**: 39-47 [PMID: 6724238 DOI: 10.1007/BF01887799]

20 **Wallner BK**, Schumacher KA, Weidenmaier W, Friedrich JM. Dilated biliary tract: evaluation with MR cholangiography with a T2-weighted contrast-enhanced fast sequence. *Radiology* 1991; **181**: 805-808 [PMID: 1947101 DOI: 10.1148/radiology.181.3.1947101]

21 **Arrivé L**, Coudray C, Azizi L, Lewin M, Hoeffel C, Monnier-Cholley L, Lacombe C, Vautier S, Poupon J, Tubiana JM. [Pineapple juice as a negative oral contrast agent in magnetic resonance cholangiopancreatography]. *J Radiol* 2007; **88**: 1689-1694 [PMID: 18065928]

22 **Schramm C**, Eaton J, Ringe KI, Venkatesh S, Yamamura J, MRI working group of the IPSCSG. Recommendations on the use of magnetic resonance imaging in PSC-A position statement from the International PSC Study Group. *Hepatology* 2017; **66**: 1675-1688 [PMID: 28555945 DOI: 10.1002/hep.29293]

23 **Chandrasekhara V**, Khashab MA, Muthusamy VR, Acosta RD, Agrawal D, Bruining DH, Eloubeidi MA, Fanelli RD, Faulx AL, Gurudu SR, Kothari S, Lightdale JR, Qumseya BJ, Shaukat A, Wang A, Wani SB, Yang J, DeWitt JM. Adverse events associated with ERCP. *Gastrointest Endosc* 2017; **85**: 32-47 [PMID: 27546389 DOI: 10.1016/j.gie.2016.06.051]

24 **Dave M**, Elmunzer BJ, Dwamena BA, Higgins PD. Primary sclerosing cholangitis: meta-analysis of diagnostic performance of MR cholangiopancreatography. *Radiology* 2010; **256**: 387-396 [PMID: 20656832 DOI: 10.1148/radiol.10091953]

25 **Chapman R**, Fevery J, Kalloo A, Nagorney DM, Boberg KM, Shneider B, Gores GJ; American Association for the Study of Liver Diseases. Diagnosis and management of primary sclerosing cholangitis. *Hepatology* 2010; **51**: 660-678 [PMID: 20101749 DOI: 10.1002/hep.23294]

26 **Talwalkar JA**, Angulo P, Johnson CD, Petersen BT, Lindor KD. Cost-minimization analysis of MRC versus ERCP for the diagnosis of primary sclerosing cholangitis. *Hepatology* 2004; **40**: 39-45 [PMID: 15239084 DOI: 10.1002/hep.20287]

27 **Meagher S**, Yusoff I, Kennedy W, Martel M, Adam V, Barkun A. The roles of magnetic resonance and endoscopic retrograde cholangiopancreatography (MRCP and ERCP) in the diagnosis of patients with suspected sclerosing cholangitis: a cost-effectiveness analysis. *Endoscopy* 2007; **39**: 222-228 [PMID: 17385107 DOI: 10.1055/s-2007-966253]

28 **Fulcher AS**, Turner MA, Franklin KJ, Shiffman ML, Sterling RK, Luketic VA, Sanyal AJ. Primary sclerosing cholangitis: evaluation with MR cholangiography-a case-control study. *Radiology* 2000; **215**: 71-80 [PMID: 10751470 DOI: 10.1148/radiology.215.1.r00ap2671]

29 **Angulo P**, Pearce DH, Johnson CD, Henry JJ, LaRusso NF, Petersen BT, Lindor KD. Magnetic resonance cholangiography in patients with biliary disease: its role in primary sclerosing cholangitis. *J Hepatol* 2000; **33**: 520-527 [PMID: 11059855 DOI: 10.1016/S0168-8278(00)80002-1]

30 **Parlak E**, Dişibeyaz S, Odemiş B, Köksal AŞ, Oğuz D, Çiçek B, Saşmaz N, Sahin B. Demonstration of retraction of the main papilla toward the biliary system in patients with primary sclerosing cholangitis with magnetic resonance cholangiopancreatography. *Dig Endosc* 2012; **24**: 384 [PMID: 22925300 DOI: 10.1111/j.1443-1661.2012.01288.x]

31 **Kovač JD**, Weber MA. Primary Biliary Cirrhosis and Primary Sclerosing Cholangitis: an Update on MR Imaging Findings with Recent Developments. *J Gastrointestin Liver Dis* 2016; **25**: 517-524 [PMID: 27981308 DOI: 10.15403/jgld.2014.1121.254.vac]

32 **Kovač JD**, Ješić R, Stanisavljević D, Kovač B, Maksimovic R. MR imaging of primary sclerosing cholangitis: additional value of diffusion-weighted imaging and ADC measurement. *Acta Radiol* 2013; **54**: 242-248 [PMID: 23386736 DOI: 10.1177/0284185112471792]

33 **Tokala A**, Khalili K, Menezes R, Hirschfield G, Jhaveri KS. Comparative MRI analysis of morphologic patterns of bile duct disease in IgG4-related systemic disease versus primary sclerosing cholangitis. *AJR Am J Roentgenol* 2014; **202**: 536-543 [PMID: 24555589 DOI: 10.2214/AJR.12.10360]

34 **Ohara H**, Okazaki K, Tsubouchi H, Inui K, Kawa S, Kamisawa T, Tazuma S, Uchida K, Hirano K, Yoshida H, Nishino T, Ko SB, Mizuno N, Hamano H, Kanno A, Notohara K, Hasebe O, Nakazawa T,

Nakanuma Y, Takikawa H; Research Committee of IgG4-related Diseases; Research Committee of Intractable Diseases of Liver and Biliary Tract; Ministry of Health, Labor and Welfare, Japan; Japan Biliary Association. Clinical diagnostic criteria of IgG4-related sclerosing cholangitis 2012. *J Hepatobiliary Pancreat Sci* 2012; **19**: 536-542 [PMID: 22717980 DOI: 10.1007/s00534-012-0521-y]

35 **Wiesner RH**, Grambsch PM, Dickson ER, Ludwig J, MacCarty RL, Hunter EB, Fleming TR, Fisher LD, Beaver SJ, LaRusso NF. Primary sclerosing cholangitis: natural history, prognostic factors and survival analysis. *Hepatology* 1989; **10**: 430-436 [PMID: 2777204]

36 **de Vries EM**, Verheij J, Hubscher SG, Leeflang MM, Boonstra K, Beuers U, Ponsioen CY. Applicability and prognostic value of histologic scoring systems in primary sclerosing cholangitis. *J Hepatol* 2015; **63**: 1212-1219 [PMID: 26095184 DOI: 10.1016/j.jhep.2015.06.008]

37 **de Vries EM**, de Krijger M, Färkkilä M, Arola J, Schirmacher P, Gotthardt D, Goeppert B, Trivedi PJ, Hirschfield GM, Ytting H, Vainer B, Buuren HR, Biermann K, Harms MH, Chazouilleres O, Wendum D, Kemgang AD, Chapman RW, Wang LM, Williamson KD, Gouw AS, Paradis V, Sempoux C, Beuers U, Hübscher SG, Verheij J, Ponsioen CY. Validation of the prognostic value of histologic scoring systems in primary sclerosing cholangitis: An international cohort study. *Hepatology* 2017; **65**: 907-919 [PMID: 27880989 DOI: 10.1002/hep.28963]

38 **Olsson R**, Hägerstrand I, Broomé U, Danielsson A, Järnerot G, Lööf L, Prytz H, Rydén BO, Wallerstedt S. Sampling variability of percutaneous liver biopsy in primary sclerosing cholangitis. *J Clin Pathol* 1995; **48**: 933-935 [PMID: 8537493 DOI: 10.1136/jcp.48.10.933]

39 **Vesterhus M**, Hov JR, Holm A, Schrumpf E, Nygård S, Godang K, Andersen IM, Naess S, Thorburn D, Saffioti F, Vatn M, Gilja OH, Lund-Johansen F, Syversveen T, Brabrand K, Parés A, Ponsioen CY, Pinzani M, Färkkilä M, Moum B, Ueland T, Røsjø H, Rosenberg W, Boberg KM, Karlsen TH. Enhanced liver fibrosis score predicts transplant-free survival in primary sclerosing cholangitis. *Hepatology* 2015; **62**: 188-197 [PMID: 25833813 DOI: 10.1002/hep.27825]

40 **de Vries EMG**, Färkkilä M, Milkiewicz P, Hov JR, Eksteen B, Thorburn D, Chazouillères O, Pares A, Nygård S, Gilja OH, Wunsch E, Invernizzi P, Carbone M, Bernuzzi F, Boberg KM, Røsjø H, Rosenberg W, Beuers UH, Ponsioen CY, Karlsen TH, Vesterhus M. Enhanced liver fibrosis test predicts transplant-free survival in primary sclerosing cholangitis, a multi-centre study. *Liver Int* 2017; **37**: 1554-1561 [PMID: 28267887 DOI: 10.1111/liv.13402]

41 **Singh S**, Fujii LL, Murad MH, Wang Z, Asrani SK, Ehman RL, Kamath PS, Talwalkar JA. Liver stiffness is associated with risk of decompensation, liver cancer, and death in patients with chronic liver diseases: a systematic review and meta-analysis. *Clin Gastroenterol Hepatol* 2013; **11**: 1573-1584.e1-2; quiz e88-89 [PMID: 23954643 DOI: 10.1016/j.cgh.2013.07.034]

42 **Singh S**, Venkatesh SK, Wang Z, Miller FH, Motosugi U, Low RN, Hassanein T, Asbach P, Godfrey EM, Yin M, Chen J, Keaveny AP, Bridges M, Bohte A, Murad MH, Lomas DJ, Talwalkar JA, Ehman RL. Diagnostic performance of magnetic resonance elastography in staging liver fibrosis: a systematic review and meta-analysis of individual participant data. *Clin Gastroenterol Hepatol* 2015; **13**: 440-451.e6 [PMID: 25305349 DOI: 10.1016/j.cgh.2014.09.046]

43 **Corpechot C**, Gaouar F, El Naggar A, Kemgang A, Wendum D, Poupon R, Carrat F, Chazouillères O. Baseline values and changes in liver stiffness measured by transient elastography are associated with severity of fibrosis and outcomes of patients with primary sclerosing cholangitis. *Gastroenterology* 2014; **146**: 970-9; quiz e15-6 [PMID: 24389304 DOI: 10.1053/j.gastro.2013.12.030]

44 **Ehlken H**, Wroblewski R, Corpechot C, Arrivé L, Rieger T, Hartl J, Lezius S, Hübener P, Schulze K, Zenouzi R, Sebode M, Peiseler M, Denzer UW, Quaas A, Weiler-Normann C, Lohse AW, Chazouilleres O, Schramm C. Validation of Transient Elastography and Comparison with Spleen Length Measurement for Staging of Fibrosis and Clinical Prognosis in Primary Sclerosing Cholangitis. *PLoS One* 2016; **11**: e0164224 [PMID: 27723798 DOI: 10.1371/journal.pone.0164224]

45 **Ehlken H**, Lohse AW, Schramm C. Transient elastography in primary sclerosing cholangitis-the value as a prognostic factor and limitations. *Gastroenterology* 2014; **147**: 542-543 [PMID: 24973676 DOI: 10.1053/j.gastro.2014.04.058]

46 **Millonig G**, Reimann FM, Friedrich S, Fonouni H, Mehrabi A, Büchler MW, Seitz HK, Mueller S. Extrahepatic cholestasis increases liver stiffness (FibroScan) irrespective of fibrosis. *Hepatology* 2008; **48**: 1718-1723 [PMID: 18836992 DOI: 10.1002/hep.22577]

47 **Eaton JE**, Dzyubak B, Venkatesh SK, Smyrk TC, Gores GJ, Ehman RL, LaRusso NF, Gossard AA, Lazaridis KN. Performance of magnetic resonance elastography in primary sclerosing cholangitis. *J Gastroenterol Hepatol* 2016; **31**: 1184-1190 [PMID: 26691631 DOI: 10.1111/jgh.13263]

48 **Shire NJ**, Yin M, Chen J, Railkar RA, Fox-Bosetti S, Johnson SM, Beals CR, Dardzinski BJ, Sanderson SO, Talwalkar JA, Ehman RL. Test-retest repeatability of MR elastography for noninvasive liver fibrosis assessment in hepatitis C. *J Magn Reson Imaging* 2011; **34**: 947-955 [PMID: 21751289 DOI: 10.1002/jmri.22716]

49 **Dulai PS**, Sirlin CB, Loomba R. MRI and MRE for non-invasive quantitative assessment of hepatic steatosis and fibrosis in NAFLD and NASH: Clinical trials to clinical practice. *J Hepatol* 2016; **65**: 1006-1016 [PMID: 27312947 DOI: 10.1016/j.jhep.2016.06.005]

50 **Hsu C**, Caussy C, Imajo K, Chen J, Singh S, Kaulback K, Le MD, Hooker J, Tu X, Bettencourt R, Yin M, Sirlin CB, Ehman RL, Nakajima A, Loomba R. Magnetic Resonance vs Transient Elastography Analysis of Patients With Nonalcoholic Fatty Liver Disease: A Systematic Review and Pooled Analysis of Individual Participants. *Clin Gastroenterol Hepatol* 2018 [PMID: 29908362 DOI: 10.1016/j.cgh.2018.05.059]

51 **Jhaveri KS**, Hosseini-Nik H, Sadoughi N, Janssen H, Feld JJ, Fischer S, Menezes R, Cheung AC. The development and validation of magnetic resonance elastography for fibrosis staging in primary sclerosing cholangitis. *Eur Radiol* 2019; **29**: 1039-1047 [PMID: 30051141 DOI: 10.1007/s00330-018-5619-4]

52 PSC Support. PSC Support Patient Unmet Needs and Research Implications: pscsupport.org.uk; 2016 Available from: http://www.pscsupport.org.uk/sites/default/files/files/PSC%20Support%20Patient%20Survey%20Results(2).pdf.

53 **de Vries EM**, Wang J, Leeflang MM, Boonstra K, Weersma RK, Beuers UH, Geskus RB, Ponsioen CY. Alkaline phosphatase at diagnosis of primary sclerosing cholangitis and 1 year later: evaluation of prognostic value. *Liver Int* 2016; **36**: 1867-1875 [PMID: 26945698 DOI: 10.1111/liv.13110]

54 **Rupp C**, Rössler A, Halibasic E, Sauer P, Weiss KH, Friedrich K, Wannhoff A, Stiehl A, Stremmel W, Trauner M, Gotthardt DN. Reduction in alkaline phosphatase is associated with longer survival in primary sclerosing cholangitis, independent of dominant stenosis. *Aliment Pharmacol Ther* 2014; **40**: 1292-1301 [PMID: 25316001 DOI: 10.1111/apt.12979]

55 **Lindström L**, Hultcrantz R, Boberg KM, Friis-Liby I, Bergquist A. Association between reduced levels of alkaline phosphatase and survival times of patients with primary sclerosing cholangitis. *Clin Gastroenterol Hepatol* 2013; **11**: 841-846 [PMID: 23353641 DOI: 10.1016/j.cgh.2012.12.032]

56 **Hilscher M**, Enders FB, Carey EJ, Lindor KD, Tabibian JH. Alkaline phosphatase normalization is a biomarker of improved survival in primary sclerosing cholangitis. *Ann Hepatol* 2016; **15**: 246-253 [PMID: 26845602 DOI: 10.5604/16652681.1193721]

57 **Al Mamari S**, Djordjevic J, Halliday JS, Chapman RW. Improvement of serum alkaline phosphatase to <1.5 upper limit of normal predicts better outcome and reduced risk of cholangiocarcinoma in primary sclerosing cholangitis. *J Hepatol* 2013; **58**: 329-334 [PMID: 23085647 DOI: 10.1016/j.jhep.2012.10.013]

58 **Balasubramaniam K**, Wiesner RH, LaRusso NF. Primary sclerosing cholangitis with normal serum alkaline phosphatase activity. *Gastroenterology* 1988; **95**: 1395-1398 [PMID: 3169503]

59 **Kim WR**, Therneau TM, Wiesner RH, Poterucha JJ, Benson JT, Malinchoc M, LaRusso NF, Lindor KD, Dickson ER. A revised natural history model for primary sclerosing cholangitis. *Mayo Clin Proc* 2000; **75**: 688-694 [PMID: 10907383 DOI: 10.4065/75.7.688]

60 **de Vries EM**, Wang J, Williamson KD, Leeflang MM, Boonstra K, Weersma RK, Beuers U, Chapman RW, Geskus RB, Ponsioen CY. A novel prognostic model for transplant-free survival in primary sclerosing cholangitis. *Gut* 2018; **67**: 1864-1869 [PMID: 28739581 DOI: 10.1136/gutjnl-2016-313681]

61 **Eaton JE**, Vesterhus M, McCauley BM, Atkinson EJ, Schlicht EM, Juran BD, Gossard AA, LaRusso NF, Gores GJ, Karlsen TH, Lazaridis KN. Primary Sclerosing Cholangitis Risk Estimate Tool (PREsTo) Predicts Outcomes of the Disease: A Derivation and Validation Study Using Machine Learning. *Hepatology* 2018 [PMID: 29742811 DOI: 10.1002/hep.30085]

62 **Zenouzi R**, Liwinski T, Yamamura J, Weiler-Normann C, Sebode M, Keller S, Lohse AW, Schramm C; International PSC Study Group (IPSCSG). Follow-up magnetic resonance imaging/3D-magnetic resonance cholangiopancreatography in patients with primary sclerosing cholangitis: challenging for experts to interpret. *Aliment Pharmacol Ther* 2018; **48**: 169-178 [PMID: 29741240 DOI: 10.1111/apt.14797]

63 **Craig DA**, MacCarty RL, Wiesner RH, Grambsch PM, LaRusso NF. Primary sclerosing cholangitis: value of cholangiography in determining the prognosis. *AJR Am J Roentgenol* 1991; **157**: 959-964 [PMID: 1927817 DOI: 10.2214/ajr.157.5.1927817]

64 **Olsson RG**, Asztély MS. Prognostic value of cholangiography in primary sclerosing cholangitis. *Eur J Gastroenterol Hepatol* 1995; **7**: 251-254 [PMID: 7743307]

65 **Ponsioen CY**, Vrouenraets SM, Prawirodirdjo W, Rajaram R, Rauws EA, Mulder CJ, Reitsma JB, Heisterkamp SH, Tytgat GN. Natural history of primary sclerosing cholangitis and prognostic value of cholangiography in a Dutch population. *Gut* 2002; **51**: 562-566 [PMID: 12235081 DOI: 10.1136/gut.51.4.562]

66 **Majoie CB**, Reeders JW, Sanders JB, Huibregtse K, Jansen PL. Primary sclerosing cholangitis: a modified classification of cholangiographic findings. *AJR Am J Roentgenol* 1991; **157**: 495-497 [PMID: 1651643 DOI: 10.2214/ajr.157.3.1651643]

67 **Petrovic BD**, Nikolaidis P, Hammond NA, Martin JA, Petrovic PV, Desai PM, Miller FH. Correlation between findings on MRCP and gadolinium-enhanced MR of the liver and a survival model for primary sclerosing cholangitis. *Dig Dis Sci* 2007; **52**: 3499-3506 [PMID: 17410447 DOI: 10.1007/s10620-006-9720-1]

68 **Tenca A**, Mustonen H, Lind K, Lantto E, Kolho KL, Boyd S, Arola J, Jokelainen K, Färkkilä M. The role of magnetic resonance imaging and endoscopic retrograde cholangiography in the evaluation of disease activity and severity in primary sclerosing cholangitis. *Liver Int* 2018; **38**: 2329-2339 [PMID: 29901259 DOI: 10.1111/liv.13899]

69 **Ruiz A**, Lemoinne S, Carrat F, Corpechot C, Chazouillères O, Arrivé L. Radiologic course of primary sclerosing cholangitis: assessment by three-dimensional magnetic resonance cholangiography and predictive features of progression. *Hepatology* 2014; **59**: 242-250 [PMID: 23857427 DOI: 10.1002/hep.26620]

70 **Kitzing YX**, Whitley SA, Upponi SS, Srivastava B, Alexander GJ, Lomas DJ. Association between progressive hepatic morphology changes on serial MR imaging and clinical outcome in primary sclerosing cholangitis. *J Med Imaging Radiat Oncol* 2017; **61**: 636-642 [PMID: 28432731 DOI: 10.1111/1754-9485.12610]

71 **Bader TR**, Beavers KL, Semelka RC. MR imaging features of primary sclerosing cholangitis: patterns of cirrhosis in relationship to clinical severity of disease. *Radiology* 2003; **226**: 675-685 [PMID: 12616016 DOI: 10.1148/radiol.2263011623]

72 **Ni Mhuircheartaigh JM**, Lee KS, Curry MP, Pedrosa I, Mortele KJ. Early Peribiliary Hyperenhancement on MRI in Patients with Primary Sclerosing Cholangitis: Significance and Association with the Mayo Risk Score. *Abdom Radiol (NY)* 2017; **42**: 152-158 [PMID: 27472938 DOI: 10.1007/s00261-016-0847-z]

73 **Bookwalter CA**, Venkatesh SK, Eaton JE, Smyrk TD, Ehman RL. MR elastography in primary sclerosing cholangitis: correlating liver stiffness with bile duct strictures and parenchymal changes. *Abdom Radiol (NY)* 2018; **43**: 3260-3270 [PMID: 29626258 DOI: 10.1007/s00261-018-1590-4]

74 **Chapman MH**, Webster GJ, Bannoo S, Johnson GJ, Wittmann J, Pereira SP. Cholangiocarcinoma and dominant strictures in patients with primary sclerosing cholangitis: a 25-year single-centre experience. *Eur J Gastroenterol Hepatol* 2012; **24**: 1051-1058 [PMID: 22653260 DOI: 10.1097/MEG.0b013e3283554bbf]

75 **Rudolph G**, Gotthardt D, Klöters-Plachky P, Kulaksiz H, Rost D, Stiehl A. Influence of dominant bile duct stenoses and biliary infections on outcome in primary sclerosing cholangitis. *J Hepatol* 2009; **51**: 149-155 [PMID: 19410324 DOI: 10.1016/j.jhep.2009.01.023]

76 **Petersen-Benz C**, Stiehl A. Impact of dominant stenoses on the serum level of the tumor marker CA19-9 in patients with primary sclerosing cholangitis. *Z Gastroenterol* 2005; **43**: 587-590 [PMID: 15986288 DOI: 10.1055/s-2005-858105]

77 **Levy MJ**, Baron TH, Clayton AC, Enders FB, Gostout CJ, Halling KC, Kipp BR, Petersen BT, Roberts LR, Rumalla A, Sebo TJ, Topazian MD, Wiersema MJ, Gores GJ. Prospective evaluation of advanced molecular markers and imaging techniques in patients with indeterminate bile duct strictures. *Am J Gastroenterol* 2008; **103**: 1263-1273 [PMID: 18477350 DOI: 10.1111/j.1572-0241.2007.01776.x]

78 **Chapman RW**, Williamson KD. Are Dominant Strictures in Primary Sclerosing Cholangitis a Risk Factor for Cholangiocarcinoma? *Curr Hepatol Rep* 2017; **16**: 124-129 [PMID: 28706774 DOI: 10.1007/s11901-017-0341-2]

79 **Razumilava N**, Gores GJ, Lindor KD. Cancer surveillance in patients with primary sclerosing cholangitis. *Hepatology* 2011; **54**: 1842-1852 [PMID: 21793028 DOI: 10.1002/hep.24570]

80 **Lunder AK**, Hov JR, Borthne A, Gleditsch J, Johannesen G, Tveit K, Viktil E, Henriksen M, Hovde Ø,

Huppertz-Hauss G, Høie O, Høivik ML, Monstad I, Solberg IC, Jahnsen J, Karlsen TH, Moum B, Vatn M, Negård A. Prevalence of Sclerosing Cholangitis Detected by Magnetic Resonance Cholangiography in Patients With Long-term Inflammatory Bowel Disease. *Gastroenterology* 2016; **151**: 660-669.e4 [PMID: 27342213 DOI: 10.1053/j.gastro.2016.06.021]

81 **Culver EL**, Bungay H, Betts M, Manganis C, Buchel O, Shrumpf E, Cummings JF, Keshav S, Travis SP, Chapman RW. Complications of primary sclerosing cholangitis in patients with ulcerative colitis and normal liver function tests: a prospective magnetic resonance cholangiographic study with long-term follow-up. *Journal of Crohn's and Colitis* 2017; **11** Suppl 1: S215 [DOI: 10.1093/ecco-jcc/jjx002.396]

82 **Taouli B**, Koh DM. Diffusion-weighted MR imaging of the liver. *Radiology* 2010; **254**: 47-66 [PMID: 20032142 DOI: 10.1148/radiol.09090021]

83 **Kovač JD**, Daković M, Stanisavljević D, Alempijević T, Ješić R, Seferović P, Maksimović R. Diffusion-weighted MRI versus transient elastography in quantification of liver fibrosis in patients with chronic cholestatic liver diseases. *Eur J Radiol* 2012; **81**: 2500-2506 [PMID: 22100369 DOI: 10.1016/j.ejrad.2011.10.024]

84 **Wang QB**, Zhu H, Liu HL, Zhang B. Performance of magnetic resonance elastography and diffusion-weighted imaging for the staging of hepatic fibrosis: A meta-analysis. *Hepatology* 2012; **56**: 239-247 [PMID: 22278368 DOI: 10.1002/hep.25610]

85 **Keller S**, Sedlacik J, Schuler T, Buchert R, Avanesov M, Zenouzi R, Lohse AW, Kooijman H, Fiehler J, Schramm C, Yamamura J. Prospective comparison of diffusion-weighted MRI and dynamic Gd-EOB-DTPA-enhanced MRI for detection and staging of hepatic fibrosis in primary sclerosing cholangitis. *Eur Radiol* 2019; **29**: 818-828 [PMID: 30014204 DOI: 10.1007/s00330-018-5614-9]

86 **Ringe KI**, Hinrichs J, Merkle EM, Weismüller TJ, Wacker F, Meyer BC. Gadoxetate disodium in patients with primary sclerosing cholangitis: an analysis of hepatobiliary contrast excretion. *J Magn Reson Imaging* 2014; **40**: 106-112 [PMID: 24923477 DOI: 10.1002/jmri.24381]

87 **Norén B**, Forsgren MF, Dahlqvist Leinhard O, Dahlström N, Kihlberg J, Romu T, Kechagias S, Almer S, Smedby Ö, Lundberg P. Separation of advanced from mild hepatic fibrosis by quantification of the hepatobiliary uptake of Gd-EOB-DTPA. *Eur Radiol* 2013; **23**: 174-181 [PMID: 22836161 DOI: 10.1007/s00330-012-2583-2]

88 **Nilsson H**, Blomqvist L, Douglas L, Nordell A, Jacobsson H, Hagen K, Bergquist A, Jonas E. Dynamic gadoxetate-enhanced MRI for the assessment of total and segmental liver function and volume in primary sclerosing cholangitis. *J Magn Reson Imaging* 2014; **39**: 879-886 [PMID: 24123427 DOI: 10.1002/jmri.24250]

89 **Hinrichs H**, Hinrichs JB, Gutberlet M, Lenzen H, Raatschen HJ, Wacker F, Ringe KI. Functional gadoxetate disodium-enhanced MRI in patients with primary sclerosing cholangitis (PSC). *Eur Radiol* 2016; **26**: 1116-1124 [PMID: 26205638 DOI: 10.1007/s00330-015-3913-y]

90 **Nolz R**, Asenbaum U, Schoder M, Wibmer A, Einspieler H, Prusa AM, Peck-Radosavljevic M, Ba-Ssalamah A. Diagnostic workup of primary sclerosing cholangitis: the benefit of adding gadoxetic acid-enhanced T1-weighted magnetic resonance cholangiography to conventional T2-weighted magnetic resonance cholangiography. *Clin Radiol* 2014; **69**: 499-508 [PMID: 24630133 DOI: 10.1016/j.crad.2013.12.008]

91 **Keller S**, Aigner A, Zenouzi R, Kim AC, Meijer A, Weidemann SA, Krech T, Lohse AW, Adam G, Schramm C, Yamamura J. Association of gadolinium-enhanced magnetic resonance imaging with hepatic fibrosis and inflammation in primary sclerosing cholangitis. *PLoS One* 2018; **13**: e0193929 [PMID: 29513767 DOI: 10.1371/journal.pone.0193929]

92 **Keller S**, Venkatesh SK, Avanesov M, Weinrich JM, Zenouzi R, Schramm C, Adam G, Yamamura J. Gadolinium-based relative contrast enhancement in primary sclerosing cholangitis: additional benefit for clinicians? *Clin Radiol* 2018; **73**: 677.e1-677.e6 [PMID: 29576223 DOI: 10.1016/j.crad.2018.02.010]

93 **Schulze J**, Lenzen H, Hinrichs JB, Ringe B, Manns MP, Wacker F, Ringe KI. An Imaging Biomarker for Assessing Hepatic Function in Patients With Primary Sclerosing Cholangitis. *Clin Gastroenterol Hepatol* 2019; **17**: 192-199.e3 [PMID: 29775791 DOI: 10.1016/j.cgh.2018.05.011]

94 **Banerjee R**, Pavlides M, Tunnicliffe EM, Piechnik SK, Sarania N, Philips R, Collier JD, Booth JC, Schneider JE, Wang LM, Delaney DW, Fleming KA, Robson MD, Barnes E, Neubauer S. Multiparametric magnetic resonance for the non-invasive diagnosis of liver disease. *J Hepatol* 2014; **60**: 69-77 [PMID: 24036007 DOI: 10.1016/j.jhep.2013.09.002]

95 **Tunnicliffe EM**, Banerjee R, Pavlides M, Neubauer S, Robson MD. A model for hepatic fibrosis: the competing effects of cell loss and iron on shortened modified Look-Locker inversion recovery T_1 (shMOLLI-T_1) in the liver. *J Magn Reson Imaging* 2017; **45**: 450-462 [PMID: 27448630 DOI: 10.1002/jmri.25392]

96 **Pavlides M**, Banerjee R, Sellwood J, Kelly CJ, Robson MD, Booth JC, Collier J, Neubauer S, Barnes E. Multiparametric magnetic resonance imaging predicts clinical outcomes in patients with chronic liver disease. *J Hepatol* 2016; **64**: 308-315 [PMID: 26471505 DOI: 10.1016/j.jhep.2015.10.009]

97 **Pavlides M**, Banerjee R, Tunnicliffe EM, Kelly C, Collier J, Wang LM, Fleming KA, Cobbold JF, Robson MD, Neubauer S, Barnes E. Multiparametric magnetic resonance imaging for the assessment of non-alcoholic fatty liver disease severity. *Liver Int* 2017; **37**: 1065-1073 [PMID: 27778429 DOI: 10.1111/liv.13284]

98 **Arndtz K**, Hodson J, Eddowes PJ, Kelly MD, Green D, Banerjee R, Neubauer S, Hirschfield GM. Multi-parametric MRI imaging correlates with clinically meaningful surrogates of disease activity in autoimmune hepatitis. *Hepatology* 2017; **66**: 188a-a

99 **Arndtz K**, Irving B, Eddowes PJ, Green D, Kelly MD, Jayaratne N, Banerjee R, Brady M, Hirschfield GM. Novel quantitative magnetic resonance imaging features with liver function tests to distinguish parenchymal and biliary disease. 22nd Conference of Medical Image Understanding and Analysis (MIUA); United Kingdom. Southampton: Springer, 2018: 37-43.

P- Reviewer: Ahmed M, Arrive L, Chow WK, Kitamura K
S- Editor: Ma RY **L- Editor:** A **E- Editor:** Yin SY

World Journal of Gastroenterology

Submit a Manuscript: https://www.f6publishing.com

World J Gastroenterol 2019 February 14; 25(6): 659-671

DOI: 10.3748/wjg.v25.i6.659

ISSN 1007-9327 (print) ISSN 2219-2840 (online)

MINIREVIEWS

Cancer risk in primary sclerosing cholangitis: Epidemiology, prevention, and surveillance strategies

Brian M Fung, Keith D Lindor, James H Tabibian

ORCID number: Brian M Fung (0000-0002-2558-5733); Keith D Lindor (0000-0003-1046-5621); James H Tabibian (0000-0001-9104-1702).

Author contributions: Tabibian JH and Fung BM reviewed the literature for relevant original studies and other content; Fung BM designed and/or formatted the figures; Tabibian JH and Lindor KD reviewed the figures; Fung BM drafted the manuscript; Tabibian JH and Lindor KD provided supervision; all authors provided critical input and approved of the manuscript.

Conflict-of-interest statement: The authors have no financial disclosures or conflicts of interest.

Manuscript source: Invited manuscript

Received: October 30, 2018
Peer-review started: November 1, 2018
First decision: November 29, 2018
Revised: January 10, 2019

Brian M Fung, UCLA-Olive View Internal Medicine Residency Program, Olive View-UCLA Medical Center, Sylmar, CA 91342, United States

Keith D Lindor, Office of the University Provost, Arizona State University, Phoenix, AZ 85004, United States

James H Tabibian, Division of Gastroenterology, Department of Medicine, Olive View-UCLA Medical Center, Sylmar, CA 91342, United States

Corresponding author: James H Tabibian, MD, PhD, Health Sciences Clinical Associate Professor, David Geffen School of Medicine at UCLA, Director of Endoscopy, Department of Medicine, Olive View-UCLA Medical Center, 14445 Olive View Drive, 2B-182, Sylmar, CA 91342, United States. jtabibian@dhs.lacounty.gov
Telephone: +1-747-2103205
Fax: +1-747-2104573

Abstract

Primary sclerosing cholangitis (PSC) is a rare cholestatic liver disease characterized by progressive fibroinflammatory destruction of the intra- and/or extrahepatic biliary ducts. While its features and disease course can be variable, most patients with PSC have concurrent inflammatory bowel disease and will eventually develop liver cirrhosis and end-stage liver disease, with liver transplantation representing the only potentially curative option. Importantly, PSC is associated with a significantly increased risk of malignancy compared to the general population, mainly cholangiocarcinoma, gallbladder carcinoma, hepatocellular carcinoma, and colorectal cancer, with nearly 50% of deaths in patients with PSC being due to cancer. Therefore, robust surveillance strategies are needed, though uncertainty remains regarding how to best do so. In this review, we discuss the epidemiology, prevention, and surveillance of cancers in patients with PSC. Where evidence is limited, we present pragmatic approaches based on currently available data and expert opinion.

Key words: Bile duct diseases; Cholangiocarcinoma; Gallbladder carcinoma; Hepatocellular carcinoma; Colorectal cancer; Chemoprotection; Inflammatory bowel disease

Core tip: Primary sclerosing cholangitis is a rare cholestatic liver disease characterized by progressive fibroinflammatory destruction of the bile ducts. It is associated with a

Accepted: January 14, 2019
Article in press: January 15, 2019
Published online: February 14, 2019

significantly increased risk of malignancy over the general population, with nearly 50% of deaths in patients with primary sclerosing cholangitis caused by cancer, thus necessitating robust surveillance strategies. In this article, we provide a synopsis of the epidemiology, prevention, and surveillance of cancers in patients with primary sclerosing cholangitis.

Citation: Fung BM, Lindor KD, Tabibian JH. Cancer risk in primary sclerosing cholangitis: Epidemiology, prevention, and surveillance strategies. *World J Gastroenterol* 2019; 25(6): 659-671
URL: https://www.wjgnet.com/1007-9327/full/v25/i6/659.htm
DOI: https://dx.doi.org/10.3748/wjg.v25.i6.659

INTRODUCTION

Primary sclerosing cholangitis (PSC) is a rare, progressive cholestatic liver disease characterized by chronic inflammation and fibrosis of the intra- and extrahepatic bile ducts[1-3]. It is a heterogenous disease often presenting with an insidious onset and variable disease course, though ultimately leading to cirrhosis and end-stage liver disease in most cases[4-6]. Its incidence and prevalence appear to vary depending on geography, with estimated incidence ranging from 0-1.3 per 100000 and prevalence from 0-16.2 per 100000, both of which appear to be rising for unclear reasons[7]. The disease has a male predominance, though it can affect men and women of nearly all ages[8]. It also has a strong association with inflammatory bowel disease (IBD), with a majority of patients with PSC also having IBD[9]. Associations with other immune-mediated diseases such thyroid disease, psoriasis, and sarcoidosis have also been reported[10-12]. Furthermore, patients with PSC have a significantly increased risk of developing various abdominal malignancies, which in fact account for 40%-50% of the mortality in patients with PSC[13-16]. Nevertheless, predictors of cancer in PSC are still largely unclear, preventive measures are for the most part unproven if not non-existent, and much is still unknown regarding prevention and surveillance of cancer in PSC[8]. Furthermore, there is significant ambiguity regarding surveillance strategies, with limited recommendations provided by society guidelines. In this article, we discuss the epidemiology, prevention, and surveillance of cancer in patients with PSC. We review current recommendations and avenues for cancer surveillance based on currently available evidence and expert opinion.

CANCER EPIDEMIOLOGY IN PRIMARY SCLEROSING CHOLANGITIS

PSC is associated with a major lifetime risk of gastrointestinal cancers. Compared with the general population, patients with PSC have double the risk of cancer in general and 40 times the risk of a primary hepatobiliary cancer[17]. Various studies have shown that patients with PSC have a significantly increased risk of developing cholangiocarcinoma (CCA), gallbladder carcinoma (GBC), hepatocellular carcinoma (HCC), and colorectal carcinoma (CRC) (Figure 1)[15,16,18,19]. We discuss each of these in forthcoming sections.

Cholangiocarcinoma risk

Patients with PSC are at particularly increased risk for CCA. The annual incidence of CCA in patients with PSC is estimated to be 0.5%-1.5%, with a reported lifetime incidence of 20%[5,6,20]. Recently, a large international multi-centered cohort study (n = 7121 patients from 37 countries) estimated the prevalence of hepatobiliary cancer in PSC to be 10%, with CCA being the most common malignancy[21]. Compared to the general population, patients with PSC have a 400- to 1500- fold increased lifetime risk of CCA[5,22]. Though the predictors of CCA in PSC remain somewhat unclear, several factors seem to be associated with CCA risk. For example, prolonged duration of IBD in PSC-IBD patients seems to (further) increase the risk of developing CCA, as does a history of colonic dysplasia[14]. Notably, cirrhosis does not appear to significantly increase the risk of (or at least is not required for development of) CCA in patients with PSC, and many patients do not carry a diagnosis of cirrhosis at the time of CCA

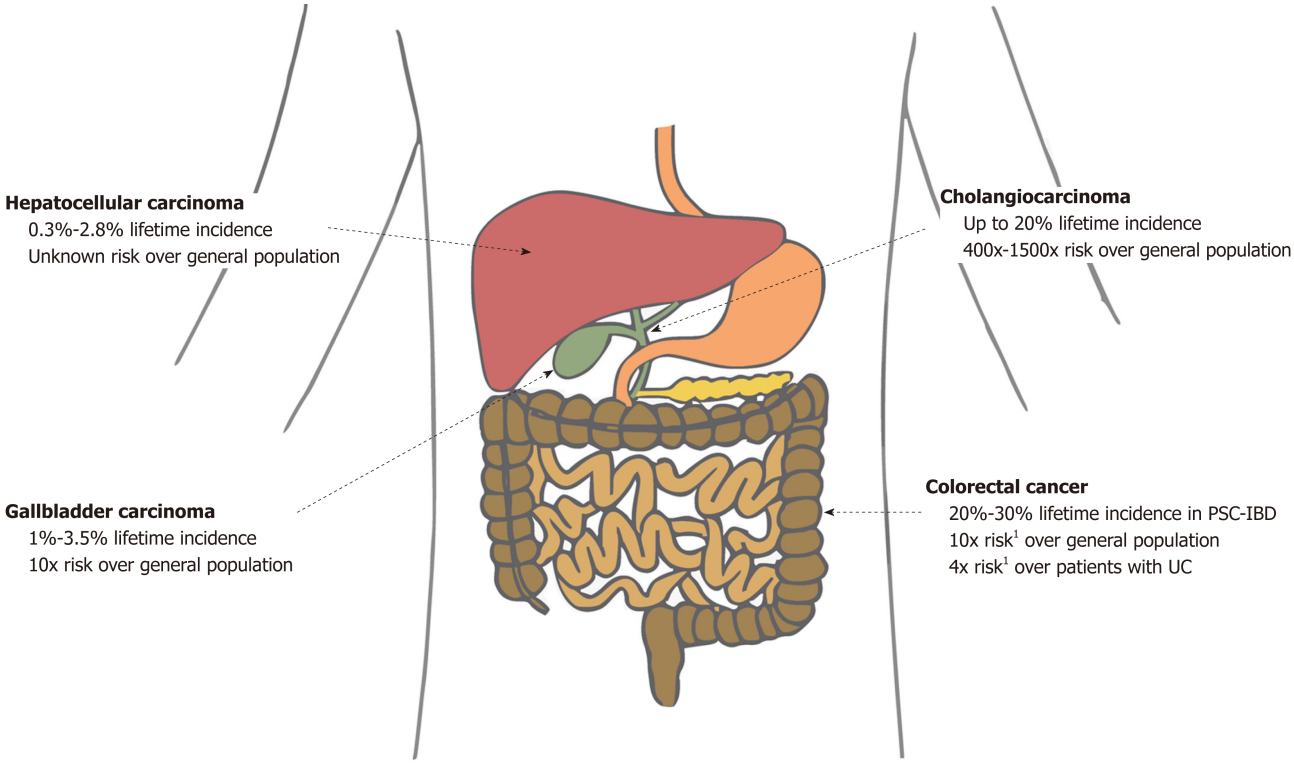

Figure 1 Lifetime incidence of various cancers associated with primary sclerosing cholangitis and their respective risks compared with the general population. Estimations of lifetime incidence are made from limited available data (predominantly based on 10- to 30-year longitudinal studies), and thus may often underestimate true lifetime risk. [1]The risk in patients with PSC-IBD (not PSC alone) is 4× the risk in patients with UC alone and 10× the risk in the general population. PSC: Primary sclerosing cholangitis; PSC-IBD: Inflammatory bowel disease co-existing with primary sclerosing cholangitis; UC: Ulcerative colitis.

diagnosis[6,23].

To better characterize and manage CCA, tumors are often classified into one of three subtypes based on their location: Intrahepatic (located proximal to the secondary branches of the left and right hepatic ducts), perihilar (between the cystic duct confluence and the secondary branches of the left and right hepatic ducts), and distal (between the cystic duct and the hepatopancreatic ampulla)[24]. Based on the limited number of studies that have evaluated CCA by subtype, it appears that patients with PSC may have a higher proportion of intrahepatic tumors compared with patients without PSC[23,25,26]. However, studies are very heterogenous; one study even reported no cases of intrahepatic tumors[27]. Overall, studies evaluating the features and outcomes of CCA by location specifically in patients with PSC are very limited, with various studies using different classification schemes/definitions[27-29] or including other cancers (*e.g.*, GBC) as CCA[30], thus limiting the ability to compare studies and draw meaningful conclusions in this regard.

Of note, though the median time between PSC diagnosis and CCA ranges from 4-6 years, as many as 50% of patients are diagnosed with CCA either at presentation or within 1 year of being diagnosed with PSC[6,20,22]. The presenting features of CCA are lamentably nonspecific, with extrahepatic CCA presenting with biliary obstruction symptoms [*e.g.*, abdominal pain, jaundice, dark urine (choluria), pruritis, malaise, weight loss, pale stools (from acholia), and increases in serum alkaline phosphatase and bilirubin above PSC baseline] and intrahepatic CCA more frequently presenting with "cancer" symptoms (*e.g.*, abdominal pain, fatigue, weight loss, diminished appetite, and night sweats; alkaline phosphatase is typically elevated above baseline, but bilirubin may remain unchanged)[31-33]. Unfortunately, CCA accounts for approximately a third of all-cause mortality in PSC[5], and up to 80% of patients who develop CCA die within 1 year[6]. Liver transplantation (LT) for PSC, though curative for many, does not preclude recurrence of PSC or PSC-associated CCA (though both occur in only a minority of patients). Moreover, CCA may develop post-LT, with at least several cases reporting de novo tumor growth in the remnant bile duct when the native bile duct was preserved[34-38]. For this reason, some have recommended avoiding choledochocholedochal anastomosis in patients with PSC[37]. Treatment of CCA and other PSC-associated malignancies has been recently reviewed and is discussed elsewhere[39,40].

Gallbladder carcinoma risk

Patients with PSC have an increased incidence of various gallbladder abnormalities, including gallstones, cholecystitis, gallbladder polyps, and GBC. It is important to note that although most gallbladder polyps are benign in the general population, patients with PSC have a high incidence of dysplastic or malignant polyps[41]. In a Swedish study of 286 patients with PSC, 6% had gallbladder masses, of which 56% harbored malignancy[19]. Similarly, in an American study of 102 patients with PSC undergoing cholecystectomy, 13.7% had a gallbladder mass, of which 57% had adenocarcinomas[42]. GBC can manifest on imaging as a mass replacing part or all of the gallbladder (seen in 45%-60%), wall thickening (20%-30%), or intraluminal polypoid lesion (15%-25%)[43]. Current societal guidelines recommend consideration of cholecystectomy in all patients with PSC with gallbladder polyps greater than 8 mm in size as well as gallbladder masses of any size due to the high risk of current or developing malignancy[19,44-46]. Smaller polyps, on the other hand, should be closely monitored, as cholecystectomy in patients with PSC may be associated with relatively high morbidity and should not be performed unless the benefit is believed to outweigh the potential risks[47]. The lifetime incidence of GBC in patients with PSC is estimated to be 3%-14%[48].

Hepatocellular carcinoma risk

There is an increased risk of HCC in patients with PSC[49]. Though the incidence of HCC in PSC has not been well studied, limited data suggest a lifetime incidence of 0.3% to 2.8%[49,50]. In a recent study of 830 patients with PSC, 23 patients had HCC, all of which had cirrhotic-stage PSC, suggesting the increased risk for HCC in patients with PSC may be solely in the setting of cirrhosis, as with most other chronic liver diseases[51].

Colorectal cancer risk

It is well known that patients with IBD are at increased risk for CRC. Although the exact mechanism is unclear, it is thought that chronic intestinal inflammation promotes pro-neoplastic changes, thus leading to dysplasia and IBD-associated cancer[52]. Most patients with PSC also have IBD, with an estimated prevalence of IBD in patients with PSC ranging from 50% to 80%, the majority of cases being of the ulcerative colitis (UC) subtype[53,54]. Remarkably, patients with PSC and IBD are at even higher risk for CRC than those with PSC alone or IBD alone. In one study, the reported 10-year and 20-year risks for CRC were 14% and 31%, respectively, compared to 2% and 2%, respectively, in patients with PSC alone[16,55]. Similarly, a large meta-analysis of 16844 patients revealed a 4-fold increased risk of CRC in patients with concurrent PSC and UC compared with patients with UC alone[56]. A more recent meta-analysis of 13379 IBD patients also came to the same conclusions[18]. Of note, although PSC has been found to be an independent risk factor for CRC in patients with UC, it is unclear whether PSC has the same influence in Crohn's disease. The few studies on this topic in the literature have had differing results[57,58]. In general, however, it is believed that the risk of CRC in extensive Crohn's colitis is similar to that of UC.

It should be mentioned that IBD co-existing with PSC (PSC-IBD) may represent a genetically and clinically distinct entity from IBD alone[59]. Intestinal disease in PSC-IBD is typically more quiescent and is often asymptomatic, thus only found on active screening with colonoscopy with biopsies[54,60]. Furthermore, the progression of colonic neoplasms from low grade dysplasia to advanced colorectal neoplasia occurs at a higher rate in patients with PSC-IBD (regardless of the apparent severity of PSC) compared with patients with IBD alone[61]. Patients with PSC-IBD also appear to have a younger age at onset of IBD symptoms (19 *vs* 29 years)[62], younger age at diagnosis of CRC (38 *vs* 48 years)[62], more extensive colitis[59], increased frequency of right sided cancers (67% *vs* 36%), and overall worse prognosis (5 year survival: 40% *vs* 75%)[63], compared to patients with IBD alone. Of note, unlike classical IBD where patients are considered to be at an increased risk of CRC after having IBD for a decade, patients with PSC-UC have an increased risk of CRC as soon as the initial diagnosis of both diseases is made[64,65]. In addition, for unclear reasons, the risk of CRC can increase after LT, thus routine surveillance for CRC is essential[66].

Pancreatic cancer risk

There is currently little data supporting an increased risk of pancreatic cancer in patients with PSC. A review of the literature reveals one study of 604 patients with PSC finding the risk of pancreatic cancer to be 14 times higher than the general population[15]. Subsequent studies, however, have not found such high rates of pancreatic cancer in patients with PSC. A study of 211 patients with PSC in the Netherlands found only 1 case of pancreatic cancer[16], and a study of 200 patients with

PSC in Belgium found 5 cases of pancreatic cancer, though one of the cases could not be distinguished from distal CCA[67]. Given the paucity of data to date, specific surveillance for pancreatic cancer is not recommended at this time but is an area which merits further investigation.

CANCER PREVENTION IN PRIMARY SCLEROSING CHOLANGITIS

Data regarding the prevention of cancer in PSC are scarce, largely due to the rarity of PSC and difficulty in amassing sufficient patient-years to power chemopreventive studies. There are currently no pharmacological agents that are routinely recommended for cancer prevention in patients with PSC. Multiple potential disease modifying agents and pharmacotherapeutics have been studied, including atorvastatin, azathioprine, colchicine, budesonide, docosahexaenoic acid, D-penicillamine, malotilate, methotrexate, metronidazole, minocycline, mycophenolate mofetil, nicotine, pentoxifylline, pirfenodone, prednisolone, tacrolimus, thalidomide, and silymarin, all without clear clinical benefit[46]. However, there are several pharmacological agents that may have potential benefit, thus necessitating further investigation.

Ursodeoxycholic acid (UDCA), a hydrophilic bile acid, has been one of the most studied pharmacological agents for PSC to date, with trials showing varying results. Although its mechanism for chemoprevention is still unclear, it is thought to act through alterations in colonic bile acid milieu (among other mechanisms), possibly lowering levels of carcinogenic compounds[68]. Several trials have shown that the use of UDCA reduces the risk of developing dysplasia or cancer in patients with PSC-IBD[68,69], while others show no benefit[70] or even deleterious effects when taken in high doses (28-30 mg/kg/day)[71]. In general, low- to intermediate-dose UDCA appears to have some chemopreventive benefit[69] while high-dose UDCA has been associated with an increased risk of adverse effects[72], including an increased risk of CRC[71], and thus should be avoided. The role of intermediate-dose UDCA in patients with PSC for chemopreventive purposes remains unclear at this time. The American Association for the Study of Liver Diseases (AASLD) and American College of Gastroenterology (ACG) both strongly recommend against the routine use of UDCA as chemoprevention for CRC in patients with PSC-IBD[44,46], while the European Association for Study of the Liver (EASL) does not provide specific recommendations for the general use of UDCA, but acknowledges consideration of UDCA in high-risk groups (*e.g.*, those with strong family history of CRC, previous history of colorectal dysplasia and cancer, or longstanding extensive colitis)[45].

Oral vancomycin, an immunomodulating bacterial glycopeptide antibiotic, has been used to treat PSC and found to result in significant improvement in clinical symptoms and liver biochemistries in some PSC-IBD patients[73-75]. However, data regarding the impact of vancomycin on cancer prevention (or prevention of recurrent PSC post-LT) are not yet available. The use of oral vancomycin in PSC remains an area of active and exciting research[76].

Curcumin, a naturally-occurring phytoextract from the turmeric (*Curcuma longa*) rhizome is another compound of interest. Preclinical studies have suggested that curcumin has anti-inflammatory, anti-fibrotic, and anti-neoplastic effects, primarily with regard to HCC and CCA[77]. Although there are no published clinical trials to date on the effects of curcumin on hepatobiliary malignancies, a phase 1/2 study for the use of curcumin in the treatment of PSC is currently underway[78], and if therapeutic effects are found, would support further studies to investigate its chemopreventive potential.

In addition to pharmacological agents, prevention can involve minimizing modifiable risk factors for hepatobiliary malignancies. Several studies have found smoking and alcohol consumption to be associated with an increased risk of CCA[22,25,79]. However, there have not been any published studies evaluating whether cessation of smoking or alcohol consumption can reduce the risk of hepatobiliary malignancies or survival in patients with PSC.

CANCER SURVEILLANCE IN PRIMARY SCLEROSING CHOLANGITIS

In the health sciences, surveillance refers to the observation and monitoring of asymptomatic, but at-risk populations for the occurrence of an outcome of interest.

When the outcome of interest is cancer, surveillance is performed to detect lesions before they become cancer and/or to detect cancers at an earlier stage, thereby increasing the chance of cure. For surveillance to be effective, the at-risk population must be identifiable, and tests used in the identification of patients with disease must be accurate, accessible, cost-effective, and with acceptable risks. Furthermore, the disease should be treatable with evidence-based modalities and should increase survival of the population under surveillance[48]. Strategies and recommendations for cancer surveillance in patients with PSC are discussed in the following sections.

Surveillance for cholangiocarcinoma

The development of surveillance guidelines for CCA has been challenging albeit an area of great interest. Patients with PSC are at risk for developing CCA, thus, a clear at-risk population can be identified for the purposes of developing an effective surveillance program. In addition, surveillance modalities are, for the most part, available and with acceptable risks to patients. However, early detection and tissue diagnosis of CCA have historically been challenging, limited treatment options are available if CCA is detected, and consequently, survival benefit of surveillance (until recently) has largely been unknown. Due to these limitations and others, unlike for GBC and CRC (Figure 2), there is currently no consensus, evidence-based societal guideline for CCA surveillance in PSC[32].

Despite the aforementioned shortcomings, many experts suggest the usage of regular imaging and measurement of the serum tumor marker carbohydrate antigen 19-9 (CA 19-9) for surveillance of CCA[13,46]. Indeed, the majority of large-volume centers perform yearly or biennial magnetic resonance imaging/magnetic resonance cholangiopancreatography (MRI/MRCP) for patients with PSC[80], which has a reported sensitivity and specificity of 89% and 75%, respectively[81]. Transabdominal ultrasound is another modality often considered given its lower cost, increased availability, and greater patient acceptability compared with MRI/MRCP; however, sensitivity is seemingly lower at 57% (while specificity is higher, 94%)[81]. Computed tomography has similar sensitivity and specificity to MRI/MRCP at 75% and 80%, respectively, but is not recommended due to the long-term risk of radiation and iodinated contrast and somewhat inferior diagnostic performance in some studies[13,51].

CA 19-9 is a serum biomarker that has been extensively studied for its role in the diagnosis of pancreatobiliary malignancy, including CCA. However, there is no agreement on cutoff for diagnosis, and its sensitivity and specificity is relatively low when used by itself without other diagnostic modalities (78% and 67%, respectively, when using a cutoff of 20 IU/mL)[81]. False positive results for CA 19-9 are frequently encountered, with one study finding approximately one third of patients with an increased CA 19-9 over 129 IU/mL not having CCA[82]. Nevertheless, CA 19-9 is still often used in clinical practice, and the combination of CA 19-9 levels greater than 20 IU/mL and suspicious findings on MRI/MRCP has been found to increase sensitivity of detecting CCA to near 100% (at the expense of decreased specificity of 38%)[81]. The use of CA 19-9 also increases the sensitivity of ultrasound to 91% (with specificity of 67%)[81]. Thus, we propose the use of annual abdominal imaging [ultrasound (US) or MRI/MRCP] combined with CA 19-9 for CCA surveillance (Figure 3). Of note, recent studies have explored other serum biomarkers (and even bile biomarkers) that may aid in the diagnosis of CCA, though more research is needed prior to their use in the clinical setting[82-84].

Endoscopic retrograde cholangiopancreatography (ERCP) with biliary sampling may be another surveillance strategy. When all definite, probable, and possible findings of CCA are included, the sensitivity of an abnormal ERCP is high (91%)[81]. However, the sensitivity of cytology for malignant lesions is low, with a systematic review and meta-analysis reporting a sensitivity of 43%[85]. Fluorescence *in situ* hybridization analysis has been found to improve this sensitivity[86,87], but the risks of post-ERCP complications, especially pancreatitis, cholangitis, and hospitalization rate of over 10% of patients with PSC make this an undesirable surveillance modality[88]. Thus, ERCP should be resorted to only when imaging and/or serum CA 19-9 are positive or indeterminate/insufficient.

New research has shown that surveillance for hepatobiliary cancers is associated with improved outcomes, including survival, in patients with PSC. A retrospective study of 830 patients with PSC found an association between hepatobiliary cancer surveillance and (1) earlier stage of cancer at diagnosis, (2) significantly lower 5-year risk of a cancer-related adverse event (32% *vs* 75%), and (3) significantly higher overall survival at 5 years (68% *vs* 20%) compared to patients that were not in a surveillance program[86]. Despite these promising results, care should still be exercised when implementing surveillance strategies, as diagnostic tools are still limited, and false positives are not uncommon. Furthermore, treatment options are limited, with curative surgical resection being appropriate in only a subset of patients and LT being

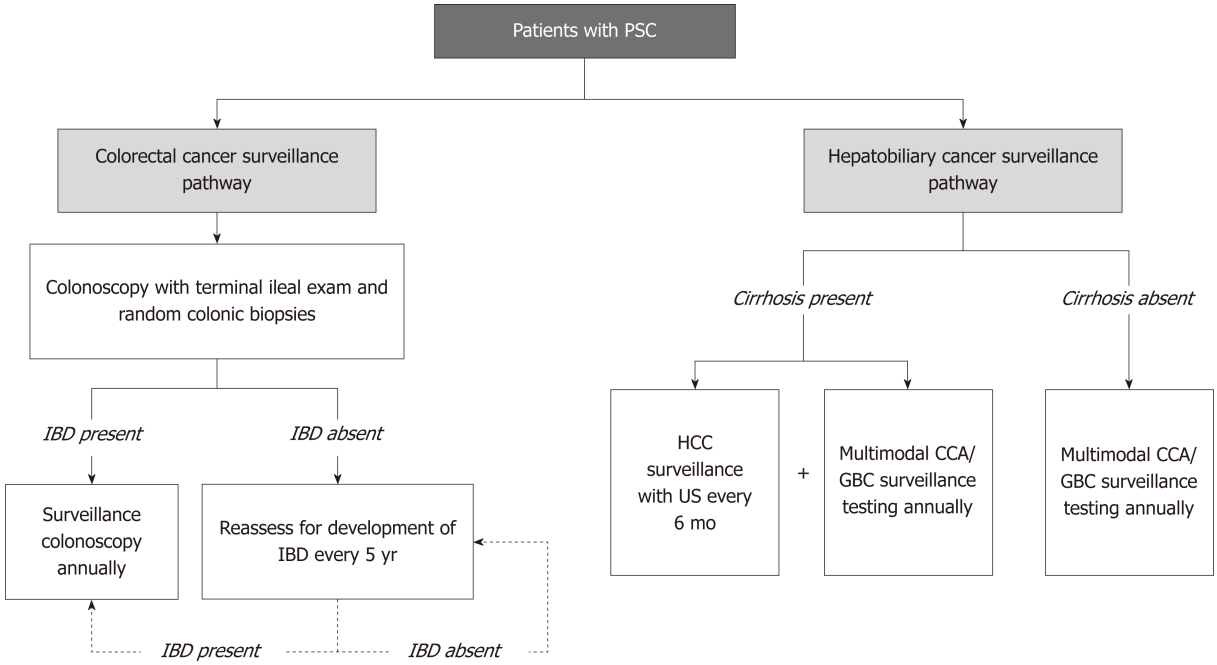

Figure 2 Overview of cancer surveillance in patients with primary sclerosing cholangitis, beginning at time of primary sclerosing cholangitis diagnosis. This overview is based on recommendations from the American Association for the Study of Liver Disease practice guidelines[44]. CCA: Cholangiocarcinoma; GBC: Gallbladder carcinoma; HCC: Hepatocellular carcinoma; IBD: Inflammatory bowel disease; US: Ultrasound; PSC: Primary sclerosing cholangitis.

offered only to selected patients with hilar CCA at highly specialized centers[89-92].

Surveillance for gallbladder carcinoma

In the general population, GBC is often diagnosed at late stages because of the paucity of symptoms at early stages. By the time a diagnosis is made, patients often have metastatic cancer and a 5-year survival rate of less than 5%[93]. However, if detected incidentally or at an early stage (T1), 5-year survival after simple cholecystectomy is near 100%[94]. The same analogy can be made for patients with PSC; however, patients with PSC are much more likely to have gallbladder neoplasms (polyps, masses) than the general population, as mentioned earlier, and a high proportion of such lesions harbor malignancy in PSC[41]. Given these considerations, both the AASLD and EASL recommend yearly abdominal ultrasound in patients with PSC[44,45]. Although ultrasound is the preferred modality due to its high accuracy, availability, and cost-effectiveness, GBC surveillance can also be performed with MRI/MRCP (*e.g.*, if used to concurrently surveil for CCA)[48]. As discussed earlier in this review, all patients with PSC with gallbladder polyps greater than 8 mm in size or gallbladder masses of any size should be evaluated for cholecystectomy[19,44-46]; while smaller lesions may be observed[47].

Surveillance for hepatocellular carcinoma

Historically, patients with PSC have been considered to have a relatively low risk for developing HCC, with an estimated lifetime incidence below 1.5%, a cut off established to justify regular HCC surveillance strategies based on cost-benefit analysis[95]. However, reports on the incidence of PSC have been limited and vary considerably. In a retrospective study of 119 patients with PSC and cirrhosis, no patients developed HCC[96]. Conversely, in a more recent study of 830 patients with PSC, 2.8% (n = 23) were found to have HCC, all of whom had underlying cirrhosis[51]. Therefore, it is unclear whether HCC surveillance is indicated for all patients with PSC[97]. At this time, the AASLD, EASL, and ACG do not provide specific recommendations on screening for HCC in patients with PSC, in part due to the fact that many patients with PSC do not (yet) have cirrhosis. Our practice is to conduct HCC surveillance with imaging every 6 mo for all patients with PSC-related cirrhosis, as is done for patients with cirrhosis due to other diseases[98,99]. For patients without cirrhosis, surveillance for HCC is effectively a byproduct of routine CCA surveillance.

Surveillance for colorectal cancer

Patients with PSC are at increased risk for CRC[16,18,55,57], and the risk is considered to be increased at time of initial PSC diagnosis[64]. Furthermore, the risk of CRC does not decrease after LT and can even increase further compared to pre-transplantation

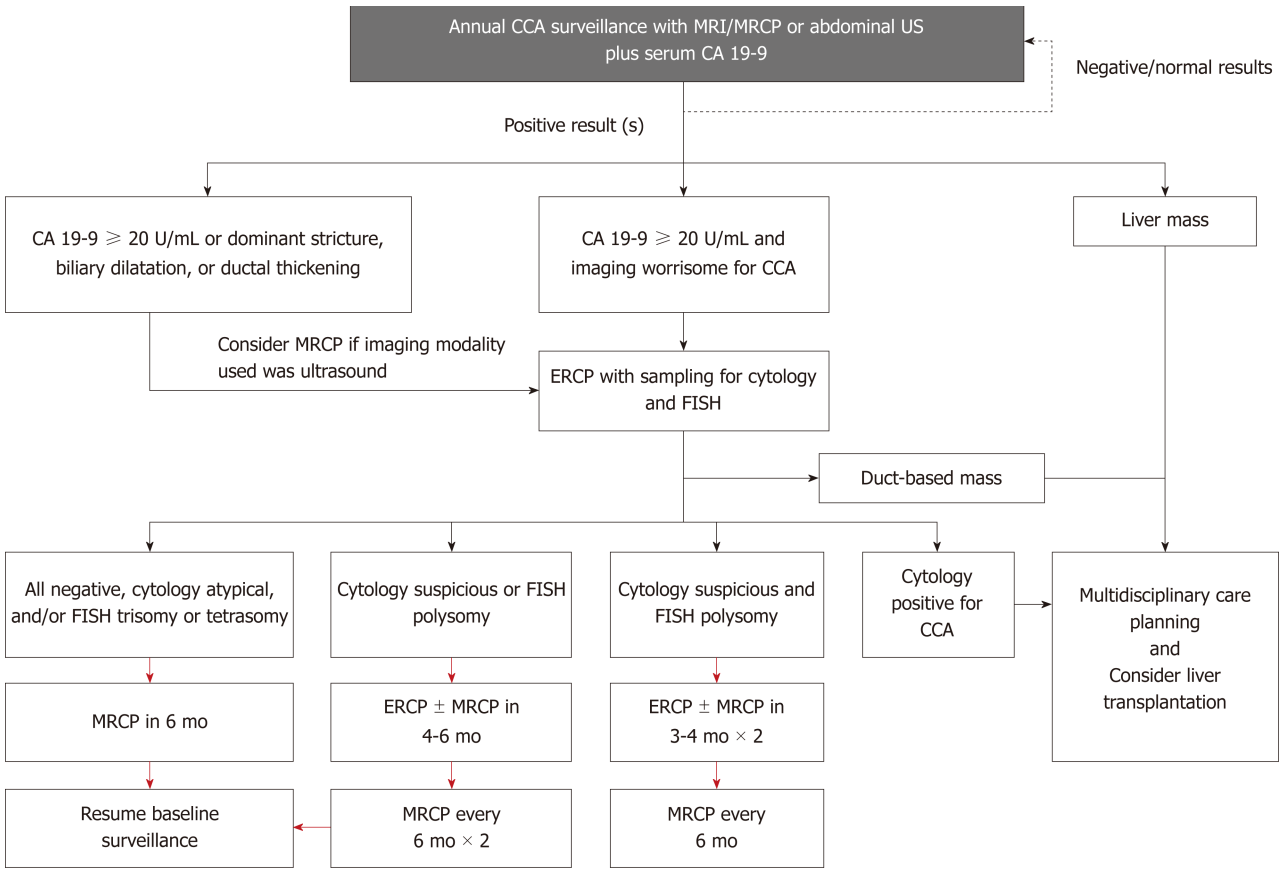

Figure 3 Suggested cholangiocarcinoma surveillance in patients with primary sclerosing cholangitis. Adapted from Tabibian *et al*[103], with permission. Red arrows represent assumes stable findings; CA 19-9: Carbohydrate antigen 19-9; CCA: Cholangiocarcinoma; ERC: Endoscopic retrograde cholangiography; GB: Gallbladder; GBC: Gallbladder cancer; FISH: Fluorescence *in situ* hybridization; HCC: Hepatocellular carcinoma; MRCP: Magnetic resonance cholangiopancreatography; US: Ultrasound; ERCP: Endoscopic retrograde cholangiopancreatography; MRI: Magnetic resonance imaging.

risk[66]. Thus, surveillance for CRC in patients with PSC pre- and post-transplantation is extremely important, with proven CRC-related survival benefit[5]. All leading societies recommend a full colonoscopy with biopsies in patients with a new diagnosis of PSC[44-46]. In patients with PSC and IBD, surveillance colonoscopy with biopsies should be performed at 1-2 year intervals from the time of diagnosis of PSC due to the high risk of CRC in patients with PSC-IBD[16,44,45] as well as the frequent lack of symptoms at diagnosis[54,60]. For patients without IBD, some experts advocate repeating a colonoscopy at 3-5 year intervals[46]. Of note, the use of chromoendoscopy with targeted biopsies has been recommended for surveillance of patients with IBD, though its value in unselected patients over high-definition colonoscopy is debatable, particularly considering the increased time and resources required for chromoendoscopy. Most providers thus tend to rely on high-definition colonoscopy with random colonic biopsies as first-line surveillance and reserve chromoendoscopy for patients known or believed to be at particularly increased risk for CRC (*e.g.*, those with longstanding extensive colitis, family history of colon cancer, and concomitant PSC)[100-102].

Surveillance in children

PSC appears relatively infrequently in children compared to adults[17]. Pediatric PSC also presents differently than PSC in adults and has a variable natural history[44,46]. Given the rarity of CCA and GBC in children and the differences in pediatric compared to adult PSC, routine surveillance for these malignancies is not recommended[44,46]. However, similar to PSC in adults, IBD is frequently identified in pediatric PSC; therefore, it may be reasonable to consider colonoscopy with biopsies in children who are newly diagnosed with PSC[44].

CONCLUSION

Patients with PSC have a significantly increased risk of developing hepatobiliary and

colorectal cancers, particularly the subset of patients with PSC-IBD. Currently, no proven pharmacological agents for prevention of carcinogenesis in patients with PSC exist. Leading national and international societies have published guidelines for CRC and GBC surveillance in patients with PSC, but surveillance strategies for CCA and HCC have not been well studied or data-proven. On the basis of a recent large study of patients with PSC, CCA surveillance appears to be associated with improved outcomes and should be performed once PSC has been diagnosed. The risk of HCC appears to be comparably lower and only present once PSC has progressed to cirrhosis. One common and (recent) evidence-based CCA surveillance strategy in patients with PSC is yearly cross-sectional imaging (US or MRI/MRCP) combined with serum tumor marker CA 19-9. Additional longitudinal, multicenter studies are needed to better evaluate the role, techniques, and impact of surveillance for CCA and other malignancies in patients with PSC.

REFERENCES

1 **Lazaridis KN**, LaRusso NF. Primary Sclerosing Cholangitis. *N Engl J Med* 2016; **375**: 1161-1170 [PMID: 27653566 DOI: 10.1056/NEJMra1506330]
2 **Tabibian JH**, Lindor KD. Primary sclerosing cholangitis: A review and update on therapeutic developments. *Expert Rev Gastroenterol Hepatol* 2013; **7**: 103-114 [PMID: 23363260 DOI: 10.1586/egh.12.80]
3 **O'Hara SP**, Tabibian JH, Splinter PL, LaRusso NF. The dynamic biliary epithelia: Molecules, pathways, and disease. *J Hepatol* 2013; **58**: 575-582 [PMID: 23085249 DOI: 10.1016/j.jhep.2012.10.011]
4 **Porayko MK**, Wiesner RH, LaRusso NF, Ludwig J, MacCarty RL, Steiner BL, Twomey CK, Zinsmeister AR. Patients with asymptomatic primary sclerosing cholangitis frequently have progressive disease. *Gastroenterology* 1990; **98**: 1594-1602 [PMID: 2338198 DOI: 10.1016/0016-5085(90)91096-O]
5 **Boonstra K**, Weersma RK, van Erpecum KJ, Rauws EA, Spanier BW, Poen AC, van Nieuwkerk KM, Drenth JP, Witteman BJ, Tuynman HA, Naber AH, Kingma PJ, van Buuren HR, van Hoek B, Vleggaar FP, van Geloven N, Beuers U, Ponsioen CY; EpiPSCPBC Study Group. Population-based epidemiology, malignancy risk, and outcome of primary sclerosing cholangitis. *Hepatology* 2013; **58**: 2045-2055 [PMID: 23775876 DOI: 10.1002/hep.26565]
6 **Takakura WR**, Tabibian JH, Bowlus CL. The evolution of natural history of primary sclerosing cholangitis. *Curr Opin Gastroenterol* 2017; **33**: 71-77 [PMID: 28030370 DOI: 10.1097/MOG.0000000000000333]
7 **Boonstra K**, Beuers U, Ponsioen CY. Epidemiology of primary sclerosing cholangitis and primary biliary cirrhosis: A systematic review. *J Hepatol* 2012; **56**: 1181-1188 [PMID: 22245904 DOI: 10.1016/j.jhep.2011.10.025]
8 **Molodecky NA**, Kareemi H, Parab R, Barkema HW, Quan H, Myers RP, Kaplan GG. Incidence of primary sclerosing cholangitis: A systematic review and meta-analysis. *Hepatology* 2011; **53**: 1590-1599 [PMID: 21351115 DOI: 10.1002/hep.24247]
9 **Tsaitas C**, Semertzidou A, Sinakos E. Update on inflammatory bowel disease in patients with primary sclerosing cholangitis. *World J Hepatol* 2014; **6**: 178-187 [PMID: 24799986 DOI: 10.4254/wjh.v6.i4.178]
10 **Silveira MG**, Mendes FD, Diehl NN, Enders FT, Lindor KD. Thyroid dysfunction in primary biliary cirrhosis, primary sclerosing cholangitis and non-alcoholic fatty liver disease. *Liver Int* 2009; **29**: 1094-1100 [PMID: 19291181 DOI: 10.1111/j.1478-3231.2009.02003.x]
11 **Lamberts LE**, Janse M, Haagsma EB, van den Berg AP, Weersma RK. Immune-mediated diseases in primary sclerosing cholangitis. *Dig Liver Dis* 2011; **43**: 802-806 [PMID: 21700515 DOI: 10.1016/j.dld.2011.05.009]
12 **Rupp C**, Mummelthei A, Sauer P, Weiss KH, Schirmacher P, Stiehl A, Stremmel W, Gotthardt DN. Non-IBD immunological diseases are a risk factor for reduced survival in PSC. *Liver Int* 2013; **33**: 86-93 [PMID: 23157607 DOI: 10.1111/liv.12028]
13 **Folseraas T**, Boberg KM. Cancer Risk and Surveillance in Primary Sclerosing Cholangitis. *Clin Liver Dis* 2016; **20**: 79-98 [PMID: 26593292 DOI: 10.1016/j.cld.2015.08.014]
14 **Gulamhusein AF**, Eaton JE, Tabibian JH, Atkinson EJ, Juran BD, Lazaridis KN. Duration of Inflammatory Bowel Disease Is Associated With Increased Risk of Cholangiocarcinoma in Patients With Primary Sclerosing Cholangitis and IBD. *Am J Gastroenterol* 2016; **111**: 705-711 [PMID: 27002801 DOI: 10.1038/ajg.2016.55]
15 **Bergquist A**, Ekbom A, Olsson R, Kornfeldt D, Lööf L, Danielsson A, Hultcrantz R, Lindgren S, Prytz H, Sandberg-Gertzén H, Almer S, Granath F, Broomé U. Hepatic and extrahepatic malignancies in primary sclerosing cholangitis. *J Hepatol* 2002; **36**: 321-327 [PMID: 11867174 DOI: 10.1016/S0168-8278(01)00288-4]
16 **Claessen MM**, Vleggaar FP, Tytgat KM, Siersema PD, van Buuren HR. High lifetime risk of cancer in primary sclerosing cholangitis. *J Hepatol* 2009; **50**: 158-164 [PMID: 19012991 DOI: 10.1016/j.jhep.2008.08.013]
17 **Card TR**, Solaymani-Dodaran M, West J. Incidence and mortality of primary sclerosing cholangitis in the UK: A population-based cohort study. *J Hepatol* 2008; **48**: 939-944 [PMID: 18433916 DOI: 10.1016/j.jhep.2008.02.017]
18 **Zheng HH**, Jiang XL. Increased risk of colorectal neoplasia in patients with primary sclerosing cholangitis and inflammatory bowel disease: A meta-analysis of 16 observational studies. *Eur J Gastroenterol Hepatol* 2016; **28**: 383-390 [PMID: 26938805 DOI: 10.1097/MEG.0000000000000576]
19 **Said K**, Glaumann H, Bergquist A. Gallbladder disease in patients with primary sclerosing cholangitis. *J Hepatol* 2008; **48**: 598-605 [PMID: 18222013 DOI: 10.1016/j.jhep.2007.11.019]
20 **Fevery J**, Verslype C, Lai G, Aerts R, Van Steenbergen W. Incidence, diagnosis, and therapy of cholangiocarcinoma in patients with primary sclerosing cholangitis. *Dig Dis Sci* 2007; **52**: 3123-3135 [PMID: 17431781 DOI: 10.1007/s10620-006-9681-4]
21 **Weismüller TJ**, Trivedi PJ, Bergquist A, Imam M, Lenzen H, Ponsioen CY, Holm K, Gotthardt D,

Färkkilä MA, Marschall HU, Thorburn D, Weersma RK, Fevery J, Mueller T, Chazouillères O, Schulze K, Lazaridis KN, Almer S, Pereira SP, Levy C, Mason A, Naess S, Bowlus CL, Floreani A, Halilbasic E, Yimam KK, Milkiewicz P, Beuers U, Huynh DK, Pares A, Manser CN, Dalekos GN, Eksteen B, Invernizzi P, Berg CP, Kirchner GI, Sarrazin C, Zimmer V, Fabris L, Braun F, Marzioni M, Juran BD, Said K, Rupp C, Jokelainen K, Benito de Valle M, Saffioti F, Cheung A, Trauner M, Schramm C, Chapman RW, Karlsen TH, Schrumpf E, Strassburg CP, Manns MP, Lindor KD, Hirschfield GM, Hansen BE, Boberg KM; International PSC Study Group. Patient Age, Sex, and Inflammatory Bowel Disease Phenotype Associate With Course of Primary Sclerosing Cholangitis. *Gastroenterology* 2017; **152**: 1975-1984.e8 [PMID: 28274849 DOI: 10.1053/j.gastro.2017.02.038]

22 **Burak K**, Angulo P, Pasha TM, Egan K, Petz J, Lindor KD. Incidence and risk factors for cholangiocarcinoma in primary sclerosing cholangitis. *Am J Gastroenterol* 2004; **99**: 523-526 [PMID: 15056096 DOI: 10.1111/j.1572-0241.2004.04067.x]

23 **Ahrendt SA**, Pitt HA, Nakeeb A, Klein AS, Lillemoe KD, Kalloo AN, Cameron JL. Diagnosis and management of cholangiocarcinoma in primary sclerosing cholangitis. *J Gastrointest Surg* 1999; **3**: 357-67; discussion 367-8 [PMID: 10482687 DOI: 10.1016/S1091-255X(99)80051-1]

24 **Blechacz B**. Cholangiocarcinoma: Current Knowledge and New Developments. *Gut Liver* 2017; **11**: 13-26 [PMID: 27928095 DOI: 10.5009/gnl15568]

25 **Bergquist A**, Glaumann H, Persson B, Broomé U. Risk factors and clinical presentation of hepatobiliary carcinoma in patients with primary sclerosing cholangitis: A case-control study. *Hepatology* 1998; **27**: 311-316 [PMID: 9462625 DOI: 10.1002/hep.510270201]

26 **Ghouri YA**, Mian I, Blechacz B. Cancer review: Cholangiocarcinoma. *J Carcinog* 2015; **14**: 1 [PMID: 25788866 DOI: 10.4103/1477-3163.151940]

27 **Chapman MH**, Webster GJ, Bannoo S, Johnson GJ, Wittmann J, Pereira SP. Cholangiocarcinoma and dominant strictures in patients with primary sclerosing cholangitis: A 25-year single-centre experience. *Eur J Gastroenterol Hepatol* 2012; **24**: 1051-1058 [PMID: 22653260 DOI: 10.1097/MEG.0b013e3283554bbf]

28 **DeOliveira ML**, Cunningham SC, Cameron JL, Kamangar F, Winter JM, Lillemoe KD, Choti MA, Yeo CJ, Schulick RD. Cholangiocarcinoma: Thirty-one-year experience with 564 patients at a single institution. *Ann Surg* 2007; **245**: 755-762 [PMID: 17457168 DOI: 10.1097/01.sla.0000251366.62632.d3]

29 **Lee WJ**, Lim HK, Jang KM, Kim SH, Lee SJ, Lim JH, Choo IW. Radiologic spectrum of cholangiocarcinoma: emphasis on unusual manifestations and differential diagnoses. *Radiographics* 2001; **21** Spec No: S97-S116 [PMID: 11598251 DOI: 10.1148/radiographics.21.suppl_1.g01oc12s97]

30 **Fevery J**, Verslype C. An update on cholangiocarcinoma associated with primary sclerosing cholangitis. *Curr Opin Gastroenterol* 2010; **26**: 236-245 [PMID: 20216413 DOI: 10.1097/MOG.0b013e328337b311]

31 **Karlsen TH**, Folseraas T, Thorburn D, Vesterhus M. Primary sclerosing cholangitis - a comprehensive review. *J Hepatol* 2017; **67**: 1298-1323 [PMID: 28802875 DOI: 10.1016/j.jhep.2017.07.022]

32 **Hilscher MB**, Tabibian JH, Carey EJ, Gostout CJ, Lindor KD. Dominant strictures in primary sclerosing cholangitis: A multicenter survey of clinical definitions and practices. *Hepatol Commun* 2018; **2**: 836-844 [PMID: 30027141 DOI: 10.1002/hep4.1194]

33 **Lazaridis KN**, Gores GJ. Primary sclerosing cholangitis and cholangiocarcinoma. *Semin Liver Dis* 2006; **26**: 42-51 [PMID: 16496232 DOI: 10.1055/s-2006-933562]

34 **Mouchli MA**, Singh S, Loftus EV, Boardman L, Talwalkar J, Rosen CB, Heimbach JK, Wiesner RH, Hasan B, Poterucha JJ, Kymberly WD. Risk Factors and Outcomes of De Novo Cancers (Excluding Nonmelanoma Skin Cancer) After Liver Transplantation for Primary Sclerosing Cholangitis. *Transplantation* 2017; **101**: 1859-1866 [PMID: 28272287 DOI: 10.1097/TP.0000000000001725]

35 **Khorsandi SE**, Salvans S, Zen Y, Agarwal K, Jassem W, Heaton N. Cholangiocarcinoma complicating recurrent primary sclerosing cholangitis after liver transplantation. *Transpl Int* 2011; **24**: e93-e96 [PMID: 21884553 DOI: 10.1111/j.1432-2277.2011.01324.x]

36 **Watt KD**, Pedersen RA, Kremers WK, Heimbach JK, Sanchez W, Gores GJ. Long-term probability of and mortality from de novo malignancy after liver transplantation. *Gastroenterology* 2009; **137**: 2010-2017 [PMID: 19766646 DOI: 10.1053/j.gastro.2009.08.070]

37 **Landaverde C**, Ng V, Sato A, Tabibian J, Durazo F, Busuttil R. De-novo cholangiocarcinoma in native common bile duct remnant following OLT for primary sclerosing cholangitis. *Ann Hepatol* 2009; **8**: 379-383 [PMID: 20009140 DOI: 10.1152/ajpgi.90631.2008]

38 **Heneghan MA**, Tuttle-Newhall JE, Suhocki PV, Muir AJ, Morse M, Bornstein JD, Sylvestre PB, Collins B, Kuo PC, Rockey DC. De-novo cholangiocarcinoma in the setting of recurrent primary sclerosing cholangitis following liver transplant. *Am J Transplant* 2003; **3**: 634-638 [PMID: 12752322 DOI: 10.1034/j.1600-6143.2003.00110.x]

39 **Tabibian JH**, Bowlus CL. Primary sclerosing cholangitis: A review and update. *Liver Res* 2017; **1**: 221-230 [PMID: 29977644 DOI: 10.1016/j.livres.2017.12.002]

40 **Tabibian J**, Lazaridis K, LaRusso N, Jarnagin W. Primary Sclerosing Cholangitis. Jarnagin W. *Blumgart's Surgery of the Liver, Biliary Tract and Pancreas*. Philadelphia, PA, United States: Elsevier; 2017; 663-674

41 **Karlsen TH**, Schrumpf E, Boberg KM. Gallbladder polyps in primary sclerosing cholangitis: Not so benign. *Curr Opin Gastroenterol* 2008; **24**: 395-399 [PMID: 18408471 DOI: 10.1097/MOG.0b013e3282f5727a]

42 **Buckles DC**, Lindor KD, Larusso NF, Petrovic LM, Gores GJ. In primary sclerosing cholangitis, gallbladder polyps are frequently malignant. *Am J Gastroenterol* 2002; **97**: 1138-1142 [PMID: 12014717 DOI: 10.1111/j.1572-0241.2002.05677.x]

43 **Sandrasegaran K**, Menias CO. Imaging and Screening of Cancer of the Gallbladder and Bile Ducts. *Radiol Clin North Am* 2017; **55**: 1211-1222 [PMID: 28991561 DOI: 10.1016/j.rcl.2017.06.005]

44 **Chapman R**, Fevery J, Kalloo A, Nagorney DM, Boberg KM, Shneider B, Gores GJ; American Association for the Study of Liver Diseases. Diagnosis and management of primary sclerosing cholangitis. *Hepatology* 2010; **51**: 660-678 [PMID: 20101749 DOI: 10.1002/hep.23294]

45 **European Association for the Study of the Liver**. EASL Clinical Practice Guidelines: Management of cholestatic liver diseases. *J Hepatol* 2009; **51**: 237-267 [PMID: 19501929 DOI: 10.1016/j.jhep.2009.04.009]

46 **Lindor KD**, Kowdley KV, Harrison ME; American College of Gastroenterology. ACG Clinical Guideline: Primary Sclerosing Cholangitis. *Am J Gastroenterol* 2015; **110**: 646-59; quiz 660 [PMID: 25869391 DOI: 10.1038/ajg.2015.112]

47 **Eaton JE**, Thackeray EW, Lindor KD. Likelihood of malignancy in gallbladder polyps and outcomes

following cholecystectomy in primary sclerosing cholangitis. *Am J Gastroenterol* 2012; **107**: 431-439 [PMID: 22031356 DOI: 10.1038/ajg.2011.361]
48 **Razumilava N**, Gores GJ, Lindor KD. Cancer surveillance in patients with primary sclerosing cholangitis. *Hepatology* 2011; **54**: 1842-1852 [PMID: 21793028 DOI: 10.1002/hep.24570]
49 **Harnois DM**, Gores GJ, Ludwig J, Steers JL, LaRusso NF, Wiesner RH. Are patients with cirrhotic stage primary sclerosing cholangitis at risk for the development of hepatocellular cancer? *J Hepatol* 1997; **27**: 512-516 [PMID: 9314129 DOI: 10.1016/S0168-8278(97)80356-X]
50 **Leidenius M**, Höckersted K, Broomé U, Ericzon BG, Friman S, Olausson M, Schrumpf E. Hepatobiliary carcinoma in primary sclerosing cholangitis: A case control study. *J Hepatol* 2001; **34**: 792-798 [PMID: 11451160 DOI: 10.1016/S0168-8278(01)00042-3]
51 **Ali AH**, Tabibian JH, Nasser-Ghodsi N, Lennon RJ, DeLeon T, Borad MJ, Hilscher M, Silveira MG, Carey EJ, Lindor KD. Surveillance for hepatobiliary cancers in patients with primary sclerosing cholangitis. *Hepatology* 2018; **67**: 2338-2351 [PMID: 29244227 DOI: 10.1002/hep.29730]
52 **Francescone R**, Hou V, Grivennikov SI. Cytokines, IBD, and colitis-associated cancer. *Inflamm Bowel Dis* 2015; **21**: 409-418 [PMID: 25563695 DOI: 10.1097/MIB.0000000000000236]
53 **de Vries AB**, Janse M, Blokzijl H, Weersma RK. Distinctive inflammatory bowel disease phenotype in primary sclerosing cholangitis. *World J Gastroenterol* 2015; **21**: 1956-1971 [PMID: 25684965 DOI: 10.3748/wjg.v21.i6.1956]
54 **Loftus EV**, Harewood GC, Loftus CG, Tremaine WJ, Harmsen WS, Zinsmeister AR, Jewell DA, Sandborn WJ. PSC-IBD: A unique form of inflammatory bowel disease associated with primary sclerosing cholangitis. *Gut* 2005; **54**: 91-96 [PMID: 15591511 DOI: 10.1136/gut.2004.046615]
55 **Broomé U**, Löfberg R, Veress B, Eriksson LS. Primary sclerosing cholangitis and ulcerative colitis: Evidence for increased neoplastic potential. *Hepatology* 1995; **22**: 1404-1408 [PMID: 7590655 DOI: 10.1002/hep.1840220511]
56 **Soetikno RM**, Lin OS, Heidenreich PA, Young HS, Blackstone MO. Increased risk of colorectal neoplasia in patients with primary sclerosing cholangitis and ulcerative colitis: A meta-analysis. *Gastrointest Endosc* 2002; **56**: 48-54 [PMID: 12085034 DOI: 10.1067/mge.2002.125367]
57 **Braden B**, Halliday J, Aryasingha S, Sharifi Y, Checchin D, Warren BF, Kitiyakara T, Travis SP, Chapman RW. Risk for colorectal neoplasia in patients with colonic Crohn's disease and concomitant primary sclerosing cholangitis. *Clin Gastroenterol Hepatol* 2012; **10**: 303-308 [PMID: 22037429 DOI: 10.1016/j.cgh.2011.10.020]
58 **Lindström L**, Lapidus A, Ost A, Bergquist A. Increased risk of colorectal cancer and dysplasia in patients with Crohn's colitis and primary sclerosing cholangitis. *Dis Colon Rectum* 2011; **54**: 1392-1397 [PMID: 21979184 DOI: 10.1097/DCR.0b013e31822bbcc1]
59 **Ricciuto A**, Kamath BM, Griffiths AM. The IBD and PSC Phenotypes of PSC-IBD. *Curr Gastroenterol Rep* 2018; **20**: 16 [PMID: 29594739 DOI: 10.1007/s11894-018-0620-2]
60 **Broomé U**, Bergquist A. Primary sclerosing cholangitis, inflammatory bowel disease, and colon cancer. *Semin Liver Dis* 2006; **26**: 31-41 [PMID: 16496231 DOI: 10.1055/s-2006-933561]
61 **Shah SC**, Ten Hove JR, Castaneda D, Palmela C, Mooiweer E, Colombel JF, Harpaz N, Ullman TA, van Bodegraven AA, Jansen JM, Mahmmod N, van der Meulen-de Jong AE, Ponsioen CY, van der Woude CJ, Oldenburg B, Itzkowitz SH, Torres J. High Risk of Advanced Colorectal Neoplasia in Patients With Primary Sclerosing Cholangitis Associated With Inflammatory Bowel Disease. *Clin Gastroenterol Hepatol* 2018; **16**: 1106-1113.e3 [PMID: 29378311 DOI: 10.1016/j.cgh.2018.01.023]
62 **Brackmann S**, Andersen SN, Aamodt G, Langmark F, Clausen OP, Aadland E, Fausa O, Rydning A, Vatn MH. Relationship between clinical parameters and the colitis-colorectal cancer interval in a cohort of patients with colorectal cancer in inflammatory bowel disease. *Scand J Gastroenterol* 2009; **44**: 46-55 [PMID: 18609187 DOI: 10.1080/00365520801977568]
63 **Claessen MM**, Lutgens MW, van Buuren HR, Oldenburg B, Stokkers PC, van der Woude CJ, Hommes DW, de Jong DJ, Dijkstra G, van Bodegraven AA, Siersema PD, Vleggaar FP. More right-sided IBD-associated colorectal cancer in patients with primary sclerosing cholangitis. *Inflamm Bowel Dis* 2009; **15**: 1331-1336 [PMID: 19229982 DOI: 10.1002/ibd.20886]
64 **Navaneethan U**, Kochhar G, Venkatesh PG, Lewis B, Lashner BA, Remzi FH, Shen B, Kiran RP. Duration and severity of primary sclerosing cholangitis is not associated with risk of neoplastic changes in the colon in patients with ulcerative colitis. *Gastrointest Endosc* 2012; **75**: 1045-1054.e1 [PMID: 22405258 DOI: 10.1016/j.gie.2012.01.015]
65 **Thackeray EW**, Charatcharoenwitthaya P, Elfaki D, Sinakos E, Lindor KD. Colon neoplasms develop early in the course of inflammatory bowel disease and primary sclerosing cholangitis. *Clin Gastroenterol Hepatol* 2011; **9**: 52-56 [PMID: 20920596 DOI: 10.1016/j.cgh.2010.09.020]
66 **Rao BB**, Lashner B, Kowdley KV. Reviewing the Risk of Colorectal Cancer in Inflammatory Bowel Disease After Liver Transplantation for Primary Sclerosing Cholangitis. *Inflamm Bowel Dis* 2018; **24**: 269-276 [PMID: 29361103 DOI: 10.1093/ibd/izx056]
67 **Fevery J**, Henckaerts L, Van Oirbeek R, Vermeire S, Rutgeerts P, Nevens F, Van Steenbergen W. Malignancies and mortality in 200 patients with primary sclerosering cholangitis: A long-term single-centre study. *Liver Int* 2012; **32**: 214-222 [PMID: 21745316 DOI: 10.1111/j.1478-3231.2011.02575.x]
68 **Pardi DS**, Loftus EV, Kremers WK, Keach J, Lindor KD. Ursodeoxycholic acid as a chemopreventive agent in patients with ulcerative colitis and primary sclerosing cholangitis. *Gastroenterology* 2003; **124**: 889-893 [PMID: 12671884 DOI: 10.1053/gast.2003.50156]
69 **Tung BY**, Emond MJ, Haggitt RC, Bronner MP, Kimmey MB, Kowdley KV, Brentnall TA. Ursodiol use is associated with lower prevalence of colonic neoplasia in patients with ulcerative colitis and primary sclerosing cholangitis. *Ann Intern Med* 2001; **134**: 89-95 [PMID: 11177311 DOI: 10.7326/0003-4819-134-2-200101160-00008]
70 **Lindström L**, Boberg KM, Wikman O, Friis-Liby I, Hultcrantz R, Prytz H, Sandberg-Gertzén H, Sangfelt P, Rydning A, Folvik G, Gangsøy-Kristiansen M, Danielsson A, Bergquist A. High dose ursodeoxycholic acid in primary sclerosing cholangitis does not prevent colorectal neoplasia. *Aliment Pharmacol Ther* 2012; **35**: 451-457 [PMID: 22221173 DOI: 10.1111/j.1365-2036.2011.04966.x]
71 **Eaton JE**, Silveira MG, Pardi DS, Sinakos E, Kowdley KV, Luketic VA, Harrison ME, McCashland T, Befeler AS, Harnois D, Jorgensen R, Petz J, Lindor KD. High-dose ursodeoxycholic acid is associated with the development of colorectal neoplasia in patients with ulcerative colitis and primary sclerosing cholangitis. *Am J Gastroenterol* 2011; **106**: 1638-1645 [PMID: 21556038 DOI: 10.1038/ajg.2011.156]
72 **Lindor KD**, Kowdley KV, Luketic VA, Harrison ME, McCashland T, Befeler AS, Harnois D, Jorgensen R, Petz J, Keach J, Mooney J, Sargeant C, Braaten J, Bernard T, King D, Miceli E, Schmoll J, Hoskin T,

Thapa P, Enders F. High-dose ursodeoxycholic acid for the treatment of primary sclerosing cholangitis. *Hepatology* 2009; **50**: 808-814 [PMID: 19585548 DOI: 10.1002/hep.23082]
73 **de Chambrun GP**, Nachury M, Funakoshi N, Gerard R, Bismuth M, Valats JC, Panaro F, Navarro F, Desreumaux P, Pariente B, Blanc P. Oral vancomycin induces sustained deep remission in adult patients with ulcerative colitis and primary sclerosing cholangitis. *Eur J Gastroenterol Hepatol* 2018; **30**: 1247-1252 [PMID: 30052539 DOI: 10.1097/MEG.0000000000001223]
74 **Tan LZ**, Reilly CR, Steward-Harrison LC, Balouch F, Muir R, Lewindon PJ. Oral vancomycin induces clinical and mucosal remission of colitis in children with primary sclerosing cholangitis-ulcerative colitis. *Gut* 2018; **pii**: gutjnl-2018-316599 [PMID: 30131321 DOI: 10.1136/gutjnl-2018-316599]
75 **Davies YK**, Tsay CJ, Caccamo DV, Cox KM, Castillo RO, Cox KL. Successful treatment of recurrent primary sclerosing cholangitis after orthotopic liver transplantation with oral vancomycin. *Case Rep Transplant* 2013; **2013**: 314292 [PMID: 23509657 DOI: 10.1155/2013/314292]
76 **Lindor K**. Vancomycin for Primary Sclerosing Cholangitis. [accessed 2018-10-22] In: ClinicalTrials.gov [Internet]. Bethesda (MD): U.S. National Library of Medicine. ClinicalTrials.gov Identifier: NCT03710122. Available from: https://clinicaltrials.gov/ct2/show/NCT03710122
77 **Hu RW**, Carey EJ, Lindor KD, Tabibian JH. Curcumin in Hepatobiliary Disease: Pharmacotherapeutic Properties and Emerging Potential Clinical Applications. *Ann Hepatol* 2017; **16**: 835-841 [PMID: 29055920 DOI: 10.5604/01.3001.0010.5273]
78 **Eaton JE**. A Study Evaluating the Safety and Efficacy of Curcumin in Patients With Primary Sclerosing Cholangitis. [accessed 2018-10-20] In: ClinicalTrials.gov [Internet]. Bethesda (MD): U.S. National Library of Medicine. ClinicalTrials.gov Identifier: NCT02978339. Available from: https://clinicaltrials.gov/ct2/show/NCT02978339
79 **Chalasani N**, Baluyut A, Ismail A, Zaman A, Sood G, Ghalib R, McCashland TM, Reddy KR, Zervos X, Anbari MA, Hoen H. Cholangiocarcinoma in patients with primary sclerosing cholangitis: A multicenter case-control study. *Hepatology* 2000; **31**: 7-11 [PMID: 10613720 DOI: 10.1002/hep.510310103]
80 **Schramm C**, Eaton J, Ringe KI, Venkatesh S, Yamamura J, MRI working group of the IPSCSG. Recommendations on the use of magnetic resonance imaging in PSC-A position statement from the International PSC Study Group. *Hepatology* 2017; **66**: 1675-1688 [PMID: 28555945 DOI: 10.1002/hep.29293]
81 **Charatcharoenwitthaya P**, Enders FB, Halling KC, Lindor KD. Utility of serum tumor markers, imaging, and biliary cytology for detecting cholangiocarcinoma in primary sclerosing cholangitis. *Hepatology* 2008; **48**: 1106-1117 [PMID: 18785620 DOI: 10.1002/hep.22441]
82 **Wannhoff A**, Gotthardt DN. Recent developments in the research on biomarkers of cholangiocarcinoma in primary sclerosing cholangitis. *Clin Res Hepatol Gastroenterol* 2018; **pii**: S2210-7401(18)30177-3 [PMID: 30266579 DOI: 10.1016/j.clinre.2018.08.013]
83 **Cuenco J**, Wehnert N, Blyuss O, Kazarian A, Whitwell HJ, Menon U, Dawnay A, Manns MP, Pereira SP, Timms JF. Identification of a serum biomarker panel for the differential diagnosis of cholangiocarcinoma and primary sclerosing cholangitis. *Oncotarget* 2018; **9**: 17430-17442 [PMID: 29707118 DOI: 10.18632/oncotarget.24732]
84 **Navaneethan U**, Parsi MA, Lourdusamy V, Bhatt A, Gutierrez NG, Grove D, Sanaka MR, Hammel JP, Stevens T, Vargo JJ, Dweik RA. Volatile organic compounds in bile for early diagnosis of cholangiocarcinoma in patients with primary sclerosing cholangitis: A pilot study. *Gastrointest Endosc* 2015; **81**: 943-9.e1 [PMID: 25500329 DOI: 10.1016/j.gie.2014.09.041]
85 **Trikudanathan G**, Navaneethan U, Njei B, Vargo JJ, Parsi MA. Diagnostic yield of bile duct brushings for cholangiocarcinoma in primary sclerosing cholangitis: A systematic review and meta-analysis. *Gastrointest Endosc* 2014; **79**: 783-789 [PMID: 24140129 DOI: 10.1016/j.gie.2013.09.015]
86 **Kipp BR**, Stadheim LM, Halling SA, Pochron NL, Harmsen S, Nagorney DM, Sebo TJ, Therneau TM, Gores GJ, de Groen PC, Baron TH, Levy MJ, Halling KC, Roberts LR. A comparison of routine cytology and fluorescence in situ hybridization for the detection of malignant bile duct strictures. *Am J Gastroenterol* 2004; **99**: 1675-1681 [PMID: 15330900 DOI: 10.1111/j.1572-0241.2004.30281.x]
87 **Bangarulingam SY**, Bjornsson E, Enders F, Barr Fritcher EG, Gores G, Halling KC, Lindor KD. Long-term outcomes of positive fluorescence in situ hybridization tests in primary sclerosing cholangitis. *Hepatology* 2010; **51**: 174-180 [PMID: 19877179 DOI: 10.1002/hep.23277]
88 **Bangarulingam SY**, Gossard AA, Petersen BT, Ott BJ, Lindor KD. Complications of endoscopic retrograde cholangiopancreatography in primary sclerosing cholangitis. *Am J Gastroenterol* 2009; **104**: 855-860 [PMID: 19259076 DOI: 10.1038/ajg.2008.161]
89 **Zamora-Valdes D**, Heimbach JK. Liver Transplant for Cholangiocarcinoma. *Gastroenterol Clin North Am* 2018; **47**: 267-280 [PMID: 29735023 DOI: 10.1016/j.gtc.2018.01.002]
90 **Stremitzer S**, Jones RP, Quinn LM, Fenwick SW, Diaz-Nieto R, Poston GJ, Malik HZ. Clinical outcome after resection of early-stage hilar cholangiocarcinoma. *Eur J Surg Oncol* 2018; **pii**: S0748-7983(18)31427-6 [PMID: 30360988 DOI: 10.1016/j.ejso.2018.09.008]
91 **De Vreede I**, Steers JL, Burch PA, Rosen CB, Gunderson LL, Haddock MG, Burgart L, Gores GJ. Prolonged disease-free survival after orthotopic liver transplantation plus adjuvant chemoirradiation for cholangiocarcinoma. *Liver Transpl* 2000; **6**: 309-316 [PMID: 10827231 DOI: 10.1053/lv.2000.6143]
92 **Darwish Murad S**, Kim WR, Harnois DM, Douglas DD, Burton J, Kulik LM, Botha JF, Mezrich JD, Chapman WC, Schwartz JJ, Hong JC, Emond JC, Jeon H, Rosen CB, Gores GJ, Heimbach JK. Efficacy of neoadjuvant chemoradiation, followed by liver transplantation, for perihilar cholangiocarcinoma at 12 US centers. *Gastroenterology* 2012; **143**: 88-98.e3; quiz e14 [PMID: 22504095 DOI: 10.1053/j.gastro.2012.04.008]
93 **Vijayakumar A**, Vijayakumar A, Patil V, Mallikarjuna MN, Shivaswamy BS. Early diagnosis of gallbladder carcinoma: An algorithm approach. *ISRN Radiol* 2012; **2013**: 239424 [PMID: 24959553 DOI: 10.5402/2013/239424]
94 **Shirai Y**, Yoshida K, Tsukada K, Muto T. Inapparent carcinoma of the gallbladder. An appraisal of a radical second operation after simple cholecystectomy. *Ann Surg* 1992; **215**: 326-331 [PMID: 1558412]
95 **Bruix J**, Sherman M; Practice Guidelines Committee, American Association for the Study of Liver Diseases. Management of hepatocellular carcinoma. *Hepatology* 2005; **42**: 1208-1236 [PMID: 16250051 DOI: 10.1002/hep.20933]
96 **Zenouzi R**, Weismüller TJ, Hübener P, Schulze K, Bubenheim M, Pannicke N, Weiler-Normann C, Lenzen H, Manns MP, Lohse AW, Schramm C. Low risk of hepatocellular carcinoma in patients with primary sclerosing cholangitis with cirrhosis. *Clin Gastroenterol Hepatol* 2014; **12**: 1733-1738 [PMID: 24530461 DOI: 10.1016/j.cgh.2014.02.008]

97 **Gossard AA**, Lindor KD. Hepatocellular carcinoma: Low risk of HCC in patients who have PSC and cirrhosis. *Nat Rev Gastroenterol Hepatol* 2014; **11**: 276-277 [PMID: 24686269 DOI: 10.1038/nrgastro.2014.47]

98 **Khaderi SA**, Sussman NL. Screening for malignancy in primary sclerosing cholangitis (PSC). *Curr Gastroenterol Rep* 2015; **17**: 17 [PMID: 25786901 DOI: 10.1007/s11894-015-0438-0]

99 **Ayuso C**, Rimola J, Vilana R, Burrel M, Darnell A, García-Criado Á, Bianchi L, Belmonte E, Caparroz C, Barrufet M, Bruix J, Brú C. Diagnosis and staging of hepatocellular carcinoma (HCC): Current guidelines. *Eur J Radiol* 2018; **101**: 72-81 [PMID: 29571804 DOI: 10.1016/j.ejrad.2018.01.025]

100 **Moussata D**, Allez M, Cazals-Hatem D, Treton X, Laharie D, Reimund JM, Bertheau P, Bourreille A, Lavergne-Slove A, Brixi H, Branche J, Gornet JM, Stefanescu C, Moreau J, Marteau P, Pelletier AL, Carbonnel F, Seksik P, Simon M, Flé, jou JF, Colombel JF, Charlois AL, Roblin X, Nancey S, Bouhnik Y, Berger F, Flourié, B, the GETAID. Are random biopsies still useful for the detection of neoplasia in patients with IBD undergoing surveillance colonoscopy with chromoendoscopy? *Gut* 2018; **67**: 616-624 [PMID: 28115492 DOI: 10.1136/gutjnl-2016-311892]

101 **van den Broek FJ**, Stokkers PC, Reitsma JB, Boltjes RP, Ponsioen CY, Fockens P, Dekker E. Random biopsies taken during colonoscopic surveillance of patients with longstanding ulcerative colitis: Low yield and absence of clinical consequences. *Am J Gastroenterol* 2014; **109**: 715-722 [PMID: 21427710 DOI: 10.1038/ajg.2011.93]

102 **Navaneethan U**, Kochhar G, Venkatesh PG, Bennett AE, Rizk M, Shen B, Kiran RP. Random biopsies during surveillance colonoscopy increase dysplasia detection in patients with primary sclerosing cholangitis and ulcerative colitis. *J Crohns Colitis* 2013; **7**: 974-981 [PMID: 23523416 DOI: 10.1016/j.crohns.2013.02.009]

103 **Tabibian JH**, Ali AH, Lindor KD. Primary Sclerosing Cholangitis, Part 2: Cancer Risk, Prevention, and Surveillance. *Gastroenterol Hepatol (NY)* 2018; **14**: 427-432 [PMID: 30166959 DOI: 10.6000/1927-7229.2012.01.01.7]

P- Reviewer: Bove A, Kapoor S, Perini MV

S- Editor: Yan JP **L- Editor:** A **E- Editor:** Yin SY

World Journal of Gastroenterology

Submit a Manuscript: https://www.f6publishing.com

World J Gastroenterol 2019 February 14; 25(6): 672-682

DOI: 10.3748/wjg.v25.i6.672

ISSN 1007-9327 (print) ISSN 2219-2840 (online)

MINIREVIEWS

Artificial intelligence in medical imaging of the liver

Li-Qiang Zhou, Jia-Yu Wang, Song-Yuan Yu, Ge-Ge Wu, Qi Wei, You-Bin Deng, Xing-Long Wu, Xin-Wu Cui, Christoph F Dietrich

ORCID number: Li-Qiang Zhou (0000-0002-6025-2694); Jia-Yu Wang (0000-0001-9902-0666); Song-Yuan Yu (0000-0003-3563-1884); Ge-Ge Wu (0000-0002-7159-2483); Qi Wei (0000-0002-7955-406X); You-Bin Deng (0000-0001-8002-5109); Xing-Long Wu (0000-0001-9778-0864); Xin-Wu Cui (0000-0003-3890-6660); Christoph F Dietrich (0000-0001-6015-6347).

Author contributions: Cui XW established the design and conception of the paper; Zhou LQ, Wang JY, Yu SY, Wu GG, Wei Q, Deng YB, Wu XL, Cui XW, and Dietrich CF explored the literature data; Zhou LQ provided the first draft of the manuscript, which was discussed and revised critically for intellectual content by Zhou LQ, Wang JY, Yu SY, Wu GG, Wei Q, Deng YB, Wu XL, Cui XW, and Dietrich CF; all authors discussed the statement and conclusions and approved the final version to be published.

Conflict-of-interest statement: There is no conflict of interest associated with any of the senior author or other coauthors who contributed their efforts in this manuscript.

Li-Qiang Zhou, Jia-Yu Wang, Ge-Ge Wu, Qi Wei, You-Bin Deng, Xin-Wu Cui, Christoph F Dietrich, Sino-German Tongji-Caritas Research Center of Ultrasound in Medicine, Department of Medical Ultrasound, Tongji Hospital, Tongji Medical College, Huazhong University of Science and Technology, Wuhan 430030, Hubei Province, China

Song-Yuan Yu, Department of Ultrasound, Tianyou Hospital Affiliated to Wuhan University of Technology, Wuhan 430030, Hubei Province, China

Xing-Long Wu, School of Mathematics and Computer Science, Wuhan Textitle University, Wuhan 430200, Hubei Province, China

Christoph F Dietrich, Medical Clinic 2, Caritas-Krankenhaus Bad Mergentheim, Academic Teaching Hospital of the University of Würzburg, Würzburg 97980, Germany

Corresponding author: Xin-Wu Cui, MD, PhD, Professor of Medicine, Sino-German Tongji-Caritas Research Center of Ultrasound in Medicine, Department of Medical Ultrasound, Tongji Hospital, Tongji Medical College, Huazhong University of Science and Technology, No. 1095, Jiefang Avenue, Wuhan 430030, Hubei Province, China. cuixinwu@live.cn
Telephone: +86-15927103161
Fax: +86-27-83662640

Abstract

Artificial intelligence (AI), particularly deep learning algorithms, is gaining extensive attention for its excellent performance in image-recognition tasks. They can automatically make a quantitative assessment of complex medical image characteristics and achieve an increased accuracy for diagnosis with higher efficiency. AI is widely used and getting increasingly popular in the medical imaging of the liver, including radiology, ultrasound, and nuclear medicine. AI can assist physicians to make more accurate and reproductive imaging diagnosis and also reduce the physicians' workload. This article illustrates basic technical knowledge about AI, including traditional machine learning and deep learning algorithms, especially convolutional neural networks, and their clinical application in the medical imaging of liver diseases, such as detecting and evaluating focal liver lesions, facilitating treatment, and predicting liver treatment response. We conclude that machine-assisted medical services will be a promising solution for future liver medical care. Lastly, we discuss the challenges and future directions of clinical application of deep learning techniques.

Key words: Liver; Imaging; Ultrasound; Artificial intelligence; Machine learning; Deep learning

Manuscript source: Invited manuscript

Received: November 25, 2018
Peer-review started: November 26, 2018
First decision: December 12, 2018
Revised: December 24, 2018
Accepted: January 9, 2019
Article in press: January 9, 2019
Published online: February 14, 2019

Core tip: Artificial intelligence (AI) is widely used and gaining in popularity in the medical imaging of the liver. AI can achieve an increased accuracy for diagnosis with higher efficiency and greatly reduce the physicians' workload. This article illustrates basic technical knowledge about AI, including traditional machine learning algorithms and deep learning algorithms, especially convolutional neural networks, and their clinical application in the medical imaging of liver diseases. Lastly, we discuss the challenges and future directions of clinical application of deep learning techniques.

Citation: Zhou LQ, Wang JY, Yu SY, Wu GG, Wei Q, Deng YB, Wu XL, Cui XW, Dietrich CF. Artificial intelligence in medical imaging of the liver. *World J Gastroenterol* 2019; 25(6): 672-682
URL: https://www.wjgnet.com/1007-9327/full/v25/i6/672.htm
DOI: https://dx.doi.org/10.3748/wjg.v25.i6.672

INTRODUCTION

In the past few decades, many medical imaging techniques have played a pivotal role in the early detection, diagnosis, and treatment of diseases, such as computed tomography (CT), magnetic resonance imaging (MRI), ultrasound, positron emission tomography (PET), mammography, and X-ray[1]. In clinical work, the interpretation and analysis of medical images are mainly done by human experts. Recently, medical doctors have begun to benefit from the help of computer-aided diagnosis. Artificial intelligence (AI) is intelligence applied by machines, in contrast to the natural intelligence displayed by humans. In computer science, AI research is defined as the study of "intelligent agents": any device that perceives its environment and takes actions that maximize its chance of successfully achieving its goals[2], which provides the version that is used in this article. Note that they use the term "computational intelligence" as a synonym for artificial intelligence. Russell & Norvig who prefer the term "rational agent" write "The whole-agent view is now widely accepted in the field"[3]. AI has made significant progress which allows machines to automatically represent and explain complicated data[4]. It is widely applied in the medical field, especially some domains that need imaging data analysis, such as radiology[5], ultrasound[6], pathology[7], dermatology[8], and ophthalmology[9]. The emergence of AI can meet the desire of healthcare professionals for better efficacy and higher efficiency in clinical work.

In liver medical imaging, physicians usually detect, characterize, and monitor diseases by assessing liver medical images visually. Sometimes, such visual assessment, which is based on expertise and experience, may be personal and inaccurate. AI can make a quantitative assessment by recognizing imaging information automatically instead of such qualitative reasoning[10]. Therefore, AI can assist physicians to make more accurate and reproductive imaging diagnosis and greatly reduce the physicians' workload. There are two kinds of AI methods widely used in medical imaging currently, one is traditional machine learning algorithms, and the other one is deep learning algorithms.

In the present paper, we discuss the basic principle of AI and current AI technologies about liver diseases in medical imaging domain for improved accurate diagnosis and evaluation (Table 1). In addition, we discuss the challenges and directions of clinical application of deep learning techniques in the future.

TRADITIONAL MACHINE LEARNING ALGORITHMS

Traditional machine learning algorithms rely mainly on the predefined engineered features that well describe the regular patterns inherent in data extracted from regions of interest (ROI) with explicit parameters on the basis of expert knowledge. The meaningful or task-related features are defined in line with mathematical equations so as to be quantified by computer programs[11]. These features can then be used to further quantify other medical imaging characteristics, such as different lesion density, shape, and echo. Statistical machine learning models, like support vector

Table 1 Clinical application of artificial intelligence

n	Task	Type	Accuracy	Sensitivity	Specificity	Ref.
1	Detecting fatty liver disease and making risk stratification	Deep learning based on US	100%	100%	100%	[42]
2	Detecting and distinguishing different focal liver lesions	Deep learning based on US	97.2%	98%	95.7%	[43]
3	Evaluating liver steatosis	Deep learning based on US	96.3%	100%	88.2%	[49]
4	Evaluating chronic liver disease	Machine learning algorithm based on SWE	87.3%	93.5%	81.2%	[12]
5	Discriminating liver tumors	DCCA-MKL framework based on US	90.41%	93.56%	86.89%	[50]
6	Predicting treatment response	Machine learning algorithm based on MRI	78%	62.5%	82.1%	[58]

DCCA-MKL: Deep canonical correlation analysis-multiple kernel learning; MRI: Magnetic resonance imaging; US: Ultrasound.

machines (SVM) or random forests, are fit to the most typical features to identify relevant imaging-based biomarkers. Gatos *et al*[12] have attempted to employ traditional machine learning algorithms to support the liver fibrosis diagnosis by ultrasound image. However, the predefined features usually do not have the ability to adapt to the imaging modality changes and their associated signal-to-noise ratio.

DEEP LEARNING ALGORITHMS

As a subset of machine learning, deep learning is based on a neural network structure inspired by the human brain. In terms of feature selection and extraction, deep learning algorithms do not have to pre-define features[13,14] and do not necessarily require placing complexly shaped ROI on images. They can directly learn feature representations by navigating the data space, and carry out image classification and task procession. This data-driven mode makes it more informative and practical. Today, convolutional neural networks (CNNs) are the most popular type of deep learning architecture in the medical image analysis field[15]. CNNs usually perform end-to-end supervised learning through tagging data, while other architectures conduct unsupervised learning tasks through untagged data. CNNs consist of quite a few layers and the 'hidden layer' among them can complete feature extraction and aggregation by convolution and pooling operations. The fully connected layers can perform high-level reasoning before the final output outcomes. Some studies have found that deep learning methods have excellent performance on staging tasks in computed tomography (CT)[16], segmentation tasks in MRI[17], and detection tasks in ultrasound[18].

INPUT DATA AND TEACHING DATA

The input data and teaching date need to be prepared before the deep learning process. Collecting as many training data as possible can help reduce the risk of overfitting. For gray-scale ultrasound images and red-green-blue (RGB) color ultrasound images, such as color Doppler and shear wave elastography images (SWE), the channel of input data is one and three, respectively. Some researchers concatenated several types of images as one image and used the concatenated images as input data[12,19]. The data volume of input images is associated with the number of CNN parameters. More calculations and longer time are needed to train the large CNNs. Cropped images or resized images can be used to solve this problem. It is necessary for training data to perform image augmentation (such as mirrored images and rotated images) so as to reduce the risk of the overfitting problem, because a slight difference in position may lead to the inconsistency between examinations. For supervised learning, teaching data need to be prepared. The data which researchers want to predict from the input data can be used as teaching data, such as clinical diagnosis data and pathological diagnosis data. The form of output layer should be in the same form as the teaching data. The type of teaching data includes nominal variables, ordinal variables, continuous variables, and images.

CNN

In 2006, Hinton *et al*[20] published a paper on "Science" that proposed an artificial neural network (ANN) with multiple hidden layers with excellent feature learning ability, which led to the study of deep learning. In 2012, Săftoiu *et al*[21] performed a study of the diagnosis of focal pancreatic lesions using ANN-assisted real-time endoscopic ultrasound (EUS) elastography and acquired ideal results. ANN is the main algorithm for driving deep learning and CNN is the most commonly used ANN for deep learning. In fact, as early as in the 1980s and 1990s, CNN performed with excellent results in several pattern recognition areas, especially handwritten digit recognition[22,23]. However, it is only suitable for the recognition of small pictures. Since the extended CNN achieved the best classification effect in ImageNet Large Scale Visual Recognition Challenge (LSVRC) in 2012, more researchers have begun to pay attention to it. CNN consists of input layer, hidden layer, and output layer. The hidden layer includes convolutional layers, pooling layers, and fully connected layers. Generally, a CNN model has many convolutional layers and pooling layers. The convolutional layer and the pooling layer are alternately set.

The convolution layer is composed of a plurality of feature maps, each feature map consists of many neurons, and each neuron is connected to a local region of the upper feature map through the convolution kernel which is a weight matrix[4]. The local weighted sum is then passed to a nonlinear function to obtain the output value of each neuron in the convolutional layer. The convolutional layers in CNN implement weight sharing in the same input and output feature map. This method can reduce the number of trainable parameters in the network and the complexity of the network model and make the network easier to train. The convolutional layer extracts various local features of its previous layer through the convolution operation. The first layer of convolution layer extracts low-level features and higher layers of convolutional layers extract more sophisticated features[24]. Increasing the depth of the network and the number of feature faces can improve the ability of deep learning, but it can easily lead to overfitting.

The pooled layer follows the convolutional layer and performs feature extraction again. Its role is mainly to semantically combine similar features and make the features robust to noise and deformation through pooling operations[4]. It is also composed of several feature maps. A feature map of the convolutional layer uniquely corresponds to a feature map of the pooled layer. The neurons in the pooled layer are connected to the local accepted domain of the convolutional layer, and the local accepted domains of different neurons do not overlap. The pooling layer obtains spatially invariant features by reducing the resolution of the feature map[25]. Common pooling methods include maximum pooling, mean pooling, and random pooling[26]. Maximum pooling methods are commonly used in recent studies. When the classification layer adopts linear classifiers, the maximum pooling method can achieve a better classification performance than the mean pooling[27]. Random pooling has the advantage of maximum pooling, and it avoids overfitting due to randomness.

The fully connected layer follows the pooled layer and the convolutional layer. Each neuron in the fully connected layer is fully connected to all neurons in the previous layer. The fully connected layer can integrate local information with class discrimination from the convolutional layer or the pooled layer[28]. The activation function of each neuron generally uses the rectified linear unit (ReLU) function[29,30]. The output value of the fully connected layer is passed to the output layer. The output layer performs regression tasks and multiple classification tasks by a softmax function. In order to reduce the risk of over-fitting of training, the dropout technique is often used in the fully connected layer[31]. Nodes within the CNNs which are dropped out with a certain probability at the training phase can prevent units from adopting too much. At present, the classification research on CNN mostly adopts ReLU function and dropout technique, and has obtained a good classification ability[28,31].

A prospective multicentre study aimed to evaluate liver fibrosis stages based on 2D-SWE images adopted a CNN model[32]. All the 2D-SWE images with the size of 250 × 250 pixels were used as the input data and then the CNN model was triggered. This CNN model had four hidden layers and each convolutional layer followed with a max pooling layer. The first hidden layer contained 16 feature maps, and the remaining three hiden layers each contained 32 feature maps. These feature maps were obtained by applying 16 or 32 convolution filters (3 × 3 pixels) to the previous layer. A fully connected layer with 32 nodes was used to connect every neuron in the last fourth pooling layer so as to output the result of binary classification in the form of probabilities.

TRAINING AND TESTING WITH CNN

During the training phase, output data from CNNs and teaching data are fed to an error function. The errors are backpropagated to CNNs and force CNNs to adjust inner parameters to make the errors smaller. For multiple classification tasks, softmax cross entropy is commonly used as the error function. Different kinds of optimizers are used to adjust parameters within CNNs, such as stochastic gradient descent, AdaGrad[33], and Adam[34]. The learning processes are iterated with units of single input data, groups of input data, or all the input data. At present, minibatch learning is more popular than batch learning for the reason that the amount of calculations for batch learning process is very large. With minibatch learning, data are usually shuffled and assigned to different groups for each epoch. Repeating epochs result in decreased errors for the training phase and the testing phase. Sometimes, repeat of epochs would not necessarily result in a decrease of errors, due to the overfitting problem. In such a situation, early stopping technique might be useful to mitigate this problem. During the testing phase, output values from the trained CNN are compared with teaching data. Methods for evaluating the performance of model include sensitivity, specificity, area under the receiver operating characteristic curve (AUC), and other parameters.

CLINICAL APPLICATIONS

Focal liver lesion detection

Deep learning algorithms combined with multiple image modalities have been widely used in the detection of focal liver lesions (Table 2). The combination of deep learning methods with CNNs and CT for liver disease diagnosis has gained wide attention[35]. Compared with the visual assessment, this strategy may capture more detailed lesion features and make more accurate diagnosis. According to Vivantil *et al* by using deep learning models based on longitudinal liver CT studies, new liver tumors could be detected automatically with a true positive rate of 86%, while the stand-alone detection rate was only 72% and this method achieved a precision of 87% and an improvement of 39% over the traditional SVM mode[36]. Some studies[37-39] have also used CNNs based on CT to detect liver tumors automatically, but these machine learning methods may not reliably detect new tumors because of the insufficient representativeness of small new tumors in the training data. Ben-Cohen *et al* developed a CNN model predicting the primary origin of liver metastasis among four sites (melanoma, colorectal cancer, pancreatic cancer, and breast cancer) with CT images[40]. In the task of automatic multiclass categorization of liver metastatic lesions, the automated system was able to achieve a 56% accuracy for the primary sites. If the prediction was made as top-2 and top-3 classification tasks, the accuracy could be up to 0.83 and 0.99, respectively. These automated systems may provide favorable decision support for physicians to achieve more efficient treatment.

CNN models which use ultrasound images to detect liver lesions were also developed. According to Liu *et al* by using a CNN model based on liver ultrasound images, the proposed method can effectively extract the liver capsules and accurately diagnose liver cirrhosis, with the diagnostic AUC being able to reach 0.968. Compared with two kinds of low level feature extraction method histogram of oriented gradients (HOG) and local binary pattern (LBP), whose mean accuracy rates were 83.6% and 81.4%, respectively, the deep learning method achieved a better classification accuracy of 86.9%[41]. It was reported that deep learning system using CNN showed a superior performance for fatty liver disease detection and risk stratification compared to conventional machine learning systems with the detection and risk stratification accuracy of 100%[42]. Hassan *et al* used the sparse auto encoder to access the representation of the liver ultrasound image and utilized the softmax layer to detect and distinguish different focal liver diseases. They found that the deep learning method achieved an overall accuracy of 97.2% compared with the accuracy rates of multi-SVM, KNN(K-Nearest Neighbor), and naive Bayes, which were 96.5, 93.6, and 95.2%, respectively[43].

An ANN based on ^{18}F-FDG PET/CT scan, demographic, and laboratory data showed a high sensitivity and specificity to detect liver malignancy and had a highly significant correlation with MR imaging findings which served as the reference standard[44]. The AUCs of lesion-dependent network and lesion-independent network were 0.905 (standard error, 0.0370) and 0.896 (standard error, 0.0386), respectively. The automated neural network could help identify nonvisually apparent focal FDG uptake in the liver, which was possibly positive for liver malignancy, and serve as a clinical adjunct to aid in interpretation of PET images of the liver.

Diffuse liver disease staging

Table 2 Liver leision detection

n	Task	Type	Accuracy	Ref.
1	Detecting liver new tumors	Deep learning based on CT	86%	[36]
2	Predicting the primary origin of liver metastasis	Deep learning based on CT	56%	[40]
3	Detecting cirrhosis with liver capsules	Deep learning based on ultrasound	96.8%	[41]
4	Detecting fatty liver disease and making risk stratification	Deep learning based on ultrasound	100%	[42]
5	Detecting and distinguishing different focal liver lesions.	Deep learning based on ultrasound	97.2%	[43]
6	Detecting metastatic liver malignancy	Deep learning based on PET/CT	90.5%	[44]

CT: Computed tomography; PET: Positron emission tomography.

There are many medical imaging methods combined with deep learning for staging of liver fibrosis diseases (Table 3). Yasaka *et al*[45] performed a retrospective study to investigate the performance of a deep CNN (DCNN) model with gadoxetic acid-enhanced hepatobiliary phase MR images in the staging of liver fibrosis and found that the fibrosis score obtained through deep learning (F_{DL} score) was correlated significantly with pathologically evaluated fibrosis stage (Spearman's correlation coefficient = 0.63, $P < 0.001$). The AUCs for diagnosing fibrosis stages cirrhosis (F4), advanced fibrosis (≥ F3), and significant fibrosis (≥ F2) were 0.84, 0.84, and 0.85, respectively. They made a similar study to predict liver fibrosis stage by using a deep learning model based on dynamic contrast-enhanced portal phase CT images and found that the fibrosis score acquired from deep learning based on CT images (F_{DLCT} score) had a strong correlation with pathologically evaluated liver fibrosis stage (Spearman's correlation coefficient = 0.48, $P < 0.001$). The prediction of F4, ≥ F3, and ≥ F2 could be possible by using the F_{DLCT} score with AUCs of 0.73 (0.62-0.84), 0.76 (0.66-0.85), and 0.74 (0.64-0.85), respectively[46]. Comparing the two models, the performance of the DCNN model based on CT images was not high, and the reason may be the difference in imaging modality's ability to capture the features of liver parenchyma. However, CT is more readily available than MRI in clinical settings and the performance is expected to be improved by applying new technologies or using high-performance computers in the future. Wang *et al*[32] conducted a prospective multicenter study to evaluate the performance of the innovatively developed deep learning radiomics of elastography (DLRE), which could achieve quantitative analysis of the heterogeneity in two-dimensional shear wave elastography images for assessing liver fibrosis stages in chronic hepatitis B. In the training cohort, AUCs of DLRE for F4, ≥ F3, and ≥ F2 were 1.00 (0.99-1.00), 0.99 (0.97-1.00), and 0.99 (0.97-1.00), respectively, which were 0.13, 0.18, and 0.25 higher than those of 2D-SWE. This strategy showed an excellent diagnostic performance in predicting liver fibrosis stages compared with 2D-SWE. It is valuable and practical that the noninvasive techniques can provide an alternative to invasive liver biopsy and make accurate diagnosis of liver fibrosis stages.

Focal liver lesion evaluation

The CNN is also greatly useful in evaluation of liver lesions. By using CNN models based on dynamic contrast-enhanced CT images in unenhanced, arterial phase, and delayed phase, a clinical retrospective study[47] investigated the diagnostic performance for the differentiation of liver masses. Masses were diagnosed according to five categories [category A, classic hepatocellular carcinomas (HCCs); category B, malignant liver tumors other than classic and early HCCs; category C, indeterminate masses or mass-like lesions (including early HCCs and dysplastic nodules) and rare benign liver masses other than hemangiomas and cysts; category D, hemangiomas; and category E, cysts] with a sensitivity of 0.71, 0.33, 0.94, 0.90, and 1.00, respectively. Median accuracy of the CNN model with dynamic CT for categorizing liver masses was 0.84. Median AUC for differentiating categories A-B from C-E was 0.92.

A new method[36] to automatically evaluate tumor burden in longitudinal liver CT studies by using a CNN model was developed and the tumor burden volume overlap error was 16%. This work is of great importance with the reason that the tumor burden can be used to evaluate the progression of disease and the response to therapy. The authors also performed liver tumor volumetric measurements to evaluate disease progression and response to treatment by tumor delineation with global and patient specific CNNs trained on a small annotated database of delineated images in longitudinal CT follow-up[48]. This method can automatically select the most appropriate CNN model for the unseen input CT scan and obviously improve the

Table 3 Diffuse liver disease staging

n	Type	AUCs	Ref.
1	Deep learning based on MRI	F4: 0.84; ≥ F3: 0.84; ≥ F2: 0.85	[45]
2	Deep learning based on CT	F4: 0.73; ≥ F3: 0.76; ≥ F2: 0.74	[46]
3	Deep learning based on SWE	F4: 0.97; ≥ F3: 0.98; ≥ F2: 0.85	[32]

AUC: Area under the receiver operating characteristic curve; MRI: Magnetic resonance imaging; CT: Computed tomography; SWE: Shear wave elastography.

robustness from 67% for stand-alone global CNN segmentation to 100% in liver tumor delineation.

Byra *et al* proposed a deep CNN model with transfer learning for liver steatosis assessment in B-mode ultrasound images[49]. The pre-trained deep CNN on the ImageNet dataset extracted high-level features first, and then the SVM algorithm classified images. The steatosis level was evaluated by the features and the Lasso regression method. Compared with the hepatorenal index and the gray-level co-occurrence matrix algorithm, whose accuracy rates were 90.9% and 85.4%, the CNN-based approach achieved significantly better results, with an AUC of 0.977, sensitivity of 100%, specificity of 88.2%, and accuracy of 96.3%.

A machine-learning algorithm that quantifies color information in terms of stiffness values from ultrasound shear wave elastography (SWE) images and discriminates chronic liver diseases (CLD) from healthy cases was introduced[12]. The highest accuracy of SVM model in the differentiation of healthy persons from CLD patients was 87.3%, and the sensitivity and specificity values were 93.5% and 81.2%, respectively. The present study provided novel objective parameters and criteria for CLD diagnosis through SWE images.

A novel two-stage multi-view artificial intelligence learning framework based on contrast-enhanced ultrasound (CEUS) for discriminating benign and malignant liver tumors achieved the best performance[50]. This method conducted deep canonical correlation analysis (DCCA) on three image pairs and generated total six-view features. A multiple kernel learning (MKL) classification algorithm then yielded the diagnosis result by these multi-view features. The mean classification accuracy, sensitivity, and specificity of DCCA-MKL framework were 90.41 ± 5.80%, 93.56 ± 5.90%, and 86.89 ± 9.38%, respectively. DCCA-MKL achieved 17.31%, 10.45%, 24.00%, 34.44%, 24.00%, and 10.45% improvements over A-P-SVM, on classification accuracy, sensitivity, specificity, Youden index, false positive rate, and false negative rate, respectively. The proposed DCCA-MKL framework based on liver CEUS has high evaluation and prediction performance for liver tumors. In future work, multi-modal deep neural network algorithm deserves to be investigated and this deep learning algorithm may more effectively fuse and learn feature representation of three-phase CEUS images.

Segmentation

Segmentation of the liver or liver vasculature with CT is of great importance in the diagnosis of vascular disease, radiotherapy planning, liver vascular surgeries, liver transplantation planning, tumor vascularization analysis, *etc*. Manual segmentation is time-consuming and prone to human errors. The application of deep learning models with the process to achieve automation was studied by some investigators. By using CNN, Bulat *et al* achieved accurate segmentation of the portal vein automatically from CT images with a Dice similarity coefficient of 0.83 for patients scheduled for liver stereotactic body radiation therapy[51]. Lu *et al*[52] reported that the liver could be located and segmented automatically *via* CNN from CT scans for patients planned for living donor liver transplant surgery or volume measurement with high accuracy and efficiency. Li *et al*[39] described a stand-alone liver tumor segmentation method based on a seven-layer CNN from CT images and achieved a 82.67% ± 1.43% precision. The CNN method has better performance than other machine learning algorithms. In addition, a novel, fully automatic approach to segment liver tumors from contrast-enhanced CT images based on a multi-channelfully convolutional network (MC-FCN) was presented. The MC-FCN model provided greater accuracy and robustness than previous methods[53]. These automated segmentation solutions show the potentials of using deep learning to facilitate clinical therapy and achieve more precise medical care.

Liver image quality (IQ) evaluation

Automatical qualitative IQ evaluation based on a classification task (diagnostic *vs* nondiagnostic IQ) is greatly necessary and useful, because liver MRI as a powerful tool to evaluate chronic liver diseases and to detect focal liver lesions has many limitations, such as inconsistent image quality and decreased robustness related to long acquisition time, motion artifact, and multiple breath-holds, especially T_2-weighted sequences(T2WI) are more easily affected by suboptimal image quality[54,55]. Steven *et al* developed and tested a deep learning approach using CNN for automated task-based IQ evaluation of liver T_2WI. They found that the CNN algorithm yielded a high negative predictive value when screening for nondiagnostic T_2WI of the liver[56]. The ability of real-time marking low-quality images allows the technologist to make timely adjustments and improve image quality by altering technical parameters, re-running a sequence, or running additional sequences.

Treatment response prediction

Automatical prediction of an HCC patient's possible response to transarterial chemoembolization before treatment by an accurate method is significant and worthwhile. It could minimize patient harm, reduce unnecessary interventions, lower health care costs and so on. Abajian *et al* reported that transarterial chemoembolization outcomes in HCC patients could be accurately predicted by combining clinical data and baseline MR imaging based on ML models. The overall accuracy of logistic regression (LR) and random forest (RF) models to predict treatment response was 78% (sensitivity 62.5%, specificity 82.1%, positive predictive value 50.0%, and negative predictive value 88.5%)[57]. This strategy can assist physicians to make optimal treatment selection in HCC patients.

In addition to predicting chemotherapy response, deep learning CNN models are also utilized for the prediction of radiotherapy toxicity. Ibragimov *et al* proposed a novel method to predict hepatobiliary toxicities after liver stereotactic body radiation therapies by using CNNs with transfer learning based on 3D CT. The CNNs were applied to find the consistent patterns in toxicity-related 3D dose plans and numerical pre-treatment features were inputted into the fully-connected neural network for more comprehensive prediction. The AUC of CNNs for 3D dose planned analysis to achieve hepatobiliary toxicity prediction was 0.79, and when combined with some pre-treatment features analysis, the AUC can reach 0.85[58]. This framework can implement accurate prediction of radiation toxicity and greatly helps in the progress of radiotherapy.

CONCLUSION

AI, especially deep learning, is rapidly becoming an extremely promising aid in liver image tasks, leading to improved performance in detecting and evaluating liver lesions, facilitating liver clinical therapy, and predicting liver treatment response. In the future, the development of AI is inseparable from physicians and the work of physicians will be closely linked with AI. Machine-assisted medical services will be the optimal solution for future liver medical care. We need to determine which specific radiology tasks are most likely to benefit from the deep learning algorithm, taking into account the strengths and limitations of these algorithms. In the context of the rapid development of AI technology, physicians must keep pace with the times and apply technology rigorously in order to become a technology driver and better serve patients.

CHALLENGES AND FUTURE PERSPECTIVES

There is considerable controversy about the time needed to implement fully automated clinical tasks by deep learning methods[59]. The debated time ranges from a few years to decades. The automated solutions based on deep learning aim to solve the most common clinical problems which demand a lot of long-term accumulation of expertise or are much too complicated for human readers, for example, lung screening CT, mammograms and so on. Next, researchers need to develop more advanced deep learning algorithms to solve more complex medical imaging problems, such as ultrasound or PET. At present, a common shortage of AI tools is that they cannot resolve multiple tasks. There is currently no comprehensive AI system capable of detecting multiple abnormalities throughout the human body.

A great amount of medical data which are electronically organized and amassed in a systematic style facilitate access and retrieval by researchers. However, the lack of curation of the training data is a major drawback in learning any AI model. To select

relevant patient cohort for specific AI task or make segmentation within images is essential and helpful. Some segmentation algorithms using AI[60] are not perfect to curate data, as they always need human experts to verify accuracy. Unsupervised learning which includes generative adversarial networks[61] and variational autoencoders[62] may achieve automated data curation by learning discriminatory features without explicit labeling. Many studies have explored the possibilities of unsupervised learning application in brain MRI[63] and mammography[64] and more field applications of this state of the art method are needed.

It is of great significance to indicate that AI is different from human intelligence in numerous ways. Although various forms of AI have exceeded human performance, they lacked higher-level background knowledge and failed to establish associations like the human brain. In addition, AI is trained for one task only. The AI field of medical imaging is still in its infancy, especially in the ultrasound field. It is almost impossible for AI to replace radiologists in the coming decades, but radiologists using AI will inevitably replace radiologists who do not. With the advancement of AI technology, radiologists will achieve an increased accuracy with higher efficiency. We also need to call for advocacy for creating interconnected networks of identifying patient data from around the world and training AI on a large scale according to different patient demographics, geographic areas, diseases, *etc*. Only in this way can we create an AI that is socially responsible and benefits more people.

REFERENCES

1 **Brody H**. Medical imaging. *Nature* 2013; **502**: S81 [PMID: 24187698 DOI: 10.1038/502S81a]
2 **Poole D**, Mackworth A, Goebel R. Computational Intelligence: A Logical Approach. New York: Oxford University Press, 1998.
3 **Russell SJ**, Norvig P. Artificial Intelligence: A Modern Approach 2nd. Upper Saddle River, New Jersey: Prentice Hall/Pearson Education. 2003.
4 **LeCun Y**, Bengio Y, Hinton G. Deep learning. *Nature* 2015; **521**: 436-444 [PMID: 26017442 DOI: 10.1038/nature14539]
5 **Hosny A**, Parmar C, Quackenbush J, Schwartz LH, Aerts HJWL. Artificial intelligence in radiology. *Nat Rev Cancer* 2018; **18**: 500-510 [PMID: 29777175 DOI: 10.1038/s41568-018-0016-5]
6 **Huang Q**, Zhang F, Li X. Machine Learning in Ultrasound Computer-Aided Diagnostic Systems: A Survey. *Biomed Res Int* 2018; **2018**: 5137904 [PMID: 29687000 DOI: 10.1155/2018/5137904]
7 **Wong STC**. Is pathology prepared for the adoption of artificial intelligence? *Cancer Cytopathol* 2018; **126**: 373-375 [PMID: 29663732 DOI: 10.1002/cncy.21994]
8 **Esteva A**, Kuprel B, Novoa RA, Ko J, Swetter SM, Blau HM, Thrun S. Dermatologist-level classification of skin cancer with deep neural networks. *Nature* 2017; **542**: 115-118 [PMID: 28117445 DOI: 10.1038/nature21056]
9 **Gulshan V**, Peng L, Coram M, Stumpe MC, Wu D, Narayanaswamy A, Venugopalan S, Widner K, Madams T, Cuadros J, Kim R, Raman R, Nelson PC, Mega JL, Webster DR. Development and Validation of a Deep Learning Algorithm for Detection of Diabetic Retinopathy in Retinal Fundus Photographs. *JAMA* 2016; **316**: 2402-2410 [PMID: 27898976 DOI: 10.1001/jama.2016.17216]
10 **Ambinder EP**. A history of the shift toward full computerization of medicine. *J Oncol Pract* 2005; **1**: 54-56 [PMID: 20871680 DOI: 10.1200/JOP.2005.1.2.54]
11 **Castellino RA**. Computer aided detection (CAD): an overview. *Cancer Imaging* 2005; **5**: 17-19 [PMID: 16154813 DOI: 10.1102/1470-7330.2005.0018]
12 **Gatos I**, Tsantis S, Spiliopoulos S, Karnabatidis D, Theotokas I, Zoumpoulis P, Loupas T, Hazle JD, Kagadis GC. A Machine-Learning Algorithm Toward Color Analysis for Chronic Liver Disease Classification, Employing Ultrasound Shear Wave Elastography. *Ultrasound Med Biol* 2017; **43**: 1797-1810 [PMID: 28634041 DOI: 10.1016/j.ultrasmedbio.2017.05.002]
13 **Miotto R**, Wang F, Wang S, Jiang X, Dudley JT. Deep learning for healthcare: review, opportunities and challenges. *Brief Bioinform* 2018; **19**: 1236-1246 [PMID: 28481991 DOI: 10.1093/bib/bbx044]
14 **Shen D**, Wu G, Suk HI. Deep Learning in Medical Image Analysis. *Annu Rev Biomed Eng* 2017; **19**: 221-248 [PMID: 28301734 DOI: 10.1146/annurev-bioeng-071516-044442]
15 **Litjens G**, Kooi T, Bejnordi BE, Setio AAA, Ciompi F, Ghafoorian M, van der Laak JAWM, van Ginneken B, Sánchez CI. A survey on deep learning in medical image analysis. *Med Image Anal* 2017; **42**: 60-88 [PMID: 28778026 DOI: 10.1016/j.media.2017.07.005]
16 **González G**, Ash SY, Vegas-Sánchez-Ferrero G, Onieva Onieva J, Rahaghi FN, Ross JC, Díaz A, San José Estépar R, Washko GR; COPDGene and ECLIPSE Investigators. Disease Staging and Prognosis in Smokers Using Deep Learning in Chest Computed Tomography. *Am J Respir Crit Care Med* 2018; **197**: 193-203 [PMID: 28892454 DOI: 10.1164/rccm.201705-0860OC]
17 **Ghafoorian M**, Karssemeijer N, Heskes T, van Uden IWM, Sanchez CI, Litjens G, de Leeuw FE, van Ginneken B, Marchiori E, Platel B. Location Sensitive Deep Convolutional Neural Networks for Segmentation of White Matter Hyperintensities. *Sci Rep* 2017; **7**: 5110 [PMID: 28698556 DOI: 10.1038/s41598-017-05300-5]
18 **Metaxas D**, Axel L, Fichtinger G, Szekely G. Medical image computing and computer-assisted intervention--MICCAI2008. Preface. *Med Image Comput Comput Assist Interv* 2008; **11**: V-VII [PMID: 18979724]
19 **Nakao T**, Hanaoka S, Nomura Y, Sato I, Nemoto M, Miki S, Maeda E, Yoshikawa T, Hayashi N, Abe O. Deep neural network-based computer-assisted detection of cerebral aneurysms in MR angiography. *J Magn Reson Imaging* 2018; **47**: 948-953 [PMID: 28836310 DOI: 10.1002/jmri.25842]
20 **Hinton GE**, Salakhutdinov RR. Reducing the dimensionality of data with neural networks. *Science* 2006; **313**: 504-507 [PMID: 16873662 DOI: 10.1126/science.1127647]
21 **Săftoiu A**, Vilmann P, Gorunescu F, Janssen J, Hocke M, Larsen M, Iglesias-Garcia J, Arcidiacono P,

Will U, Giovannini M, Dietrich CF, Havre R, Gheorghe C, McKay C, Gheonea DI, Ciurea T; European EUS Elastography Multicentric Study Group. Efficacy of an artificial neural network-based approach to endoscopic ultrasound elastography in diagnosis of focal pancreatic masses. *Clin Gastroenterol Hepatol* 2012; **10**: 84-90.e1 [PMID: 21963957 DOI: 10.1016/j.cgh.2011.09.014]

22 **Lawrence S**, Giles CL, Tsoi AC, Back AD. Face recognition: a convolutional neural-network approach. *IEEE Trans Neural Netw* 1997; **8**: 98-113 [PMID: 18255614 DOI: 10.1109/72.554195]

23 **Nebauer C**. Evaluation of convolutional neural networks for visual recognition. *IEEE Trans Neural Netw* 1998; **9**: 685-696 [PMID: 18252491 DOI: 10.1109/72.701181]

24 **Suzuki K**. Overview of deep learning in medical imaging. *Radiol Phys Technol* 2017; **10**: 257-273 [PMID: 28689314 DOI: 10.1007/s12194-017-0406-5]

25 **Yamashita R**, Nishio M, Do RKG, Togashi K. Convolutional neural networks: an overview and application in radiology. *Insights Imaging* 2018 [PMID: 29934920 DOI: 10.1007/s13244-018-0639-9]

26 **Voulodimos A**, Doulamis N, Doulamis A, Protopapadakis E. Deep Learning for Computer Vision: A Brief Review. *Comput Intell Neurosci* 2018; **2018**: 7068349 [PMID: 29487619 DOI: 10.1155/2018/7068349]

27 **Gokmen T**, Onen M, Haensch W. Training Deep Convolutional Neural Networks with Resistive Cross-Point Devices. *Front Neurosci* 2017; **11**: 538 [PMID: 29066942 DOI: 10.3389/fnins.2017.00538]

28 **Sainath TN**, Kingsbury B, Saon G, Soltau H, Mohamed AR, Dahl G, Ramabhadran B. Deep Convolutional Neural Networks for large-scale speech tasks. *Neural Netw* 2015; **64**: 39-48 [PMID: 25439765 DOI: 10.1016/j.neunet.2014.08.005]

29 **Nair V**, Hinton GE. Rectified linear units improve restricted boltzmann machines. Proceedings of the International Conference on International Conference on Machine Learning; 2010: 807-814.

30 **O'Shea K**, Nash R. An Introduction to Convolutional Neural Networks. Computer Science 2015. Available from: URL: https://arxiv.org/abs/1511.08458.

31 **Srivastava N**, Hinton G, Krizhevsky A, Sutskever I, Salakhutdinov R. Dropout: a simple way to prevent neural networks from overfitting. *J Mach Learn Res* 2014; **15**: 1929-1958

32 **Wang K**, Lu X, Zhou H, Gao Y, Zheng J, Tong M, Wu C, Liu C, Huang L, Jiang T, Meng F, Lu Y, Ai H, Xie XY, Yin LP, Liang P, Tian J, Zheng R. Deep learning Radiomics of shear wave elastography significantly improved diagnostic performance for assessing liver fibrosis in chronic hepatitis B: a prospective multicentre study. *Gut* 2018; Epub ahead of print [PMID: 29730602 DOI: 10.1136/gutjnl-2018-316204]

33 **Duchi J**, Hazan E, Singer Y. Adaptive Subgradient Methods for Online Learning and Stochastic Optimization. *J Mach Learn Res* 2011; **12**: 2121-2159

34 **Kingma DP**, Ba J. Adam: A Method for Stochastic Optimization. Computer Science 2014. Available from: URL: https://arxiv.org/abs/1412.6980.

35 **Kahn CE**. From Images to Actions: Opportunities for Artificial Intelligence in Radiology. *Radiology* 2017; **285**: 719-720 [PMID: 29155645 DOI: 10.1148/radiol.2017171734]

36 **Vivanti R**, Szeskin A, Lev-Cohain N, Sosna J, Joskowicz L. Automatic detection of new tumors and tumor burden evaluation in longitudinal liver CT scan studies. *Int J Comput Assist Radiol Surg* 2017; **12**: 1945-1957 [PMID: 28856515 DOI: 10.1007/s11548-017-1660-z]

37 **Ben-Cohen A**, Diamant I, Klang E, Amitai M, Greenspan H. *Fully convolutional network for liver segmentation and lesions detection. Springer International Publishing*. 2016; 77-85 [DOI: 10.1007/978-3-319-46976-89]

38 **Christ PF**, Elshaer ME, Ettlinger F, Tatavarty S, Bickel M, Bilic P, Rempfler M, Armbruster M, Hofmann F, D'Anastasi M, Sommer WH, Ahmadi SA, Menze BH. Automatic Liver and Lesion Segmentation in CT Using Cascaded Fully Convolutional Neural Networks and 3D Conditional Random Fields. Computer Science 2016. Available from: URL: https://arxiv.org/abs/1610.02177.

39 **Li W**, Jia F, Hu Q. Automatic segmentation of liver tumors in CT images with deep convolutional neural networks. *J Comput Commun* 2015; **3**: 146-151 [DOI: 10.4236/jcc.2015.311023]

40 **Ben-Cohen A**, Klang E, Diamant I, Rozendorn N, Raskin SP, Konen E, Amitai MM, Greenspan H. CT Image-based Decision Support System for Categorization of Liver Metastases Into Primary Cancer Sites: Initial Results. *Acad Radiol* 2017; **24**: 1501-1509 [PMID: 28778512 DOI: 10.1016/j.acra.2017.06.008]

41 **Liu X**, Song JL, Wang SH, Zhao JW, Chen YQ. Learning to Diagnose Cirrhosis with Liver Capsule Guided Ultrasound Image Classification. *Sensors (Basel)* 2017; **17** [PMID: 28098774 DOI: 10.3390/s17010149]

42 **Biswas M**, Kuppili V, Edla DR, Suri HS, Saba L, Marinhoe RT, Sanches JM, Suri JS. Symtosis: A liver ultrasound tissue characterization and risk stratification in optimized deep learning paradigm. *Comput Methods Programs Biomed* 2018; **155**: 165-177 [PMID: 29512496 DOI: 10.1016/j.cmpb.2017.12.016]

43 **Hassan TM**, Elmogy M, Sallam ES. Diagnosis of Focal Liver Diseases Based on Deep Learning Technique for Ultrasound Images. *Arab J Sci Eng* 2017; **42**: 3127-3140 [DOI: 10.1007/s13369-016-2387-9]

44 **Preis O**, Blake MA, Scott JA. Neural network evaluation of PET scans of the liver: a potentially useful adjunct in clinical interpretation. *Radiology* 2011; **258**: 714-721 [PMID: 21339347 DOI: 10.1148/radiol.10100547]

45 **Yasaka K**, Akai H, Kunimatsu A, Abe O, Kiryu S. Liver Fibrosis: Deep Convolutional Neural Network for Staging by Using Gadoxetic Acid-enhanced Hepatobiliary Phase MR Images. *Radiology* 2018; **287**: 146-155 [PMID: 29239710 DOI: 10.1148/radiol.2017171928]

46 **Yasaka K**, Akai H, Kunimatsu A, Abe O, Kiryu S. Deep learning for staging liver fibrosis on CT: a pilot study. *Eur Radiol* 2018; Epub ahead of print [PMID: 29761358 DOI: 10.1007/s00330-018-5499-7]

47 **Yasaka K**, Akai H, Abe O, Kiryu S. Deep Learning with Convolutional Neural Network for Differentiation of Liver Masses at Dynamic Contrast-enhanced CT: A Preliminary Study. *Radiology* 2018; **286**: 887-896 [PMID: 29059036 DOI: 10.1148/radiol.2017170706]

48 **Vivanti R**, Joskowicz L, Lev-Cohain N, Ephrat A, Sosna J. Patient-specific and global convolutional neural networks for robust automatic liver tumor delineation in follow-up CT studies. *Med Biol Eng Comput* 2018; **56**: 1699-1713 [PMID: 29524116 DOI: 10.1007/s11517-018-1803-6]

49 **Byra M**, Styczynski G, Szmigielski C, Kalinowski P, Michałowski Ł, Paluszkiewicz R, Ziarkiewicz-Wróblewska B, Zieniewicz K, Sobieraj P. Transfer learning with deep convolutional neural network for liver steatosis assessment in ultrasound images. *Int J Comput Assist Radiol Surg* 2018; **13**: 1895-1903 [PMID: 30094778 DOI: 10.1007/S11548-018-1843-2]

50 **Guo LH**, Wang D, Qian YY, Zheng X, Zhao CK, Li XL, Bo XW, Yue WW, Zhang Q, Shi J, Xu HX. A two-stage multi-view learning framework based computer-aided diagnosis of liver tumors with contrast enhanced ultrasound images. *Clin Hemorheol Microcirc* 2018; **69**: 343-354 [PMID: 29630528 DOI:

10.3233/CH-170275]
51 **Ibragimov B**, Toesca D, Chang D, Koong A, Xing L. Combining deep learning with anatomical analysis for segmentation of the portal vein for liver SBRT planning. *Phys Med Biol* 2017; **62**: 8943-8958 [PMID: 28994665 DOI: 10.1088/1361-6560/aa9262]
52 **Lu F**, Wu F, Hu P, Peng Z, Kong D. Automatic 3D liver location and segmentation via convolutional neural network and graph cut. *Int J Comput Assist Radiol Surg* 2017; **12**: 171-182 [PMID: 27604760 DOI: 10.1007/s11548-016-1467-3]
53 **Sun C**, Guo S, Zhang H, Li J, Chen M, Ma S, Jin L, Liu X, Li X, Qian X. Automatic segmentation of liver tumors from multiphase contrast-enhanced CT images based on FCNs. *Artif Intell Med* 2017; **83**: 58-66 [PMID: 28347562 DOI: 10.1016/j.artmed.2017.03.008]
54 **Hecht EM**, Holland AE, Israel GM, Hahn WY, Kim DC, West AB, Babb JS, Taouli B, Lee VS, Krinsky GA. Hepatocellular carcinoma in the cirrhotic liver: gadolinium-enhanced 3D T1-weighted MR imaging as a stand-alone sequence for diagnosis. *Radiology* 2006; **239**: 438-447 [PMID: 16641353 DOI: 10.1148/radiol.2392050551]
55 **Tsurusaki M**, Semelka RC, Zapparoli M, Elias J, Altun E, Pamuklar E, Sugimura K. Quantitative and qualitative comparison of 3.0T and 1.5T MR imaging of the liver in patients with diffuse parenchymal liver disease. *Eur J Radiol* 2009; **72**: 314-320 [PMID: 18789840 DOI: 10.1016/j.ejrad.2008.07.027]
56 **Esses SJ**, Lu X, Zhao T, Shanbhogue K, Dane B, Bruno M, Chandarana H. Automated image quality evaluation of T_2-weighted liver MRI utilizing deep learning architecture. *J Magn Reson Imaging* 2018; **47**: 723-728 [PMID: 28577329 DOI: 10.1002/jmri.25779]
57 **Abajian A**, Murali N, Savic LJ, Laage-Gaupp FM, Nezami N, Duncan JS, Schlachter T, Lin M, Geschwind JF, Chapiro J. Predicting Treatment Response to Intra-arterial Therapies for Hepatocellular Carcinoma with the Use of Supervised Machine Learning-An Artificial Intelligence Concept. *J Vasc Interv Radiol* 2018; **29**: 850-857.e1 [PMID: 29548875 DOI: 10.1016/j.jvir.2018.01.769]
58 **Ibragimov B**, Toesca D, Chang D, Yuan Y, Koong A, Xing L. Development of deep neural network for individualized hepatobiliary toxicity prediction after liver SBRT. *Med Phys* 2018; **45**: 4763-4774 [PMID: 30098025 DOI: 10.1002/mp.13122]
59 **Lee JG**, Jun S, Cho YW, Lee H, Kim GB, Seo JB, Kim N. Deep Learning in Medical Imaging: General Overview. *Korean J Radiol* 2017; **18**: 570-584 [PMID: 28670152 DOI: 10.3348/kjr.2017.18.4.570]
60 **Sharma N**, Aggarwal LM. Automated medical image segmentation techniques. *J Med Phys* 2010; **35**: 3-14 [PMID: 20177565 DOI: 10.4103/0971-6203.58777]
61 **Zhang MM**, Ma KT, Lim J, Zhao Q, Feng JS. Anticipating Where People Will Look Using Adversarial Networks. IEEE Trans Pattern Anal Mach Intell 2018. [DOI: 10.1109/TPAMI.2018.2871688]
62 **Kingma DP**, Welling M. Auto-Encoding Variational Bayes. 2013.
63 **Kamnitsas K**, Ledig C, Newcombe VFJ, Simpson JP, Kane AD, Menon DK, Rueckert D, Glocker B. Efficient multi-scale 3D CNN with fully connected CRF for accurate brain lesion segmentation. *Med Image Anal* 2017; **36**: 61-78 [PMID: 27865153 DOI: 10.1016/j.media.2016.10.004]
64 **Kallenberg M**, Petersen K, Nielsen M, Ng AY, Pengfei Diao, Igel C, Vachon CM, Holland K, Winkel RR, Karssemeijer N, Lillholm M, . Unsupervised Deep Learning Applied to Breast Density Segmentation and Mammographic Risk Scoring. *IEEE Trans Med Imaging* 2016; **35**: 1322-1331 [PMID: 26915120 DOI: 10.1109/TMI.2016.2532122]

P- Reviewer: Khalek Abdel Razek AA, Pompili M, Ooi L
S- Editor: Gong ZM **L- Editor:** Wang TQ **E- Editor:** Yin SY

World Journal of Gastroenterology

Submit a Manuscript: https://www.f6publishing.com

World J Gastroenterol 2019 February 14; 25(6): 683-695

DOI: 10.3748/wjg.v25.i6.683

ISSN 1007-9327 (print) ISSN 2219-2840 (online)

ORIGINAL ARTICLE

Basic Study

Effect of Sheng-jiang powder on multiple-organ inflammatory injury in acute pancreatitis in rats fed a high-fat diet

Yi-Fan Miao, Hong-Xin Kang, Juan Li, Yu-Mei Zhang, Hong-Yu Ren, Lv Zhu, Huan Chen, Ling Yuan, Hang Su, Mei-Hua Wan, Wen-Fu Tang

ORCID number: Yi-Fan Miao (0000-0002-3483-2345); Hong-Xin Kang (0000-0001-8212-0134); Juan Li (0000-0002-5775-9355); Yu-Mei Zhang (0000-0001-9802-776X); Hong-Yu Ren (0000-0002-9665-0782); Lv Zhu (0000-0002-4302-3339); Huan Chen (0000-0002-4763-6730); Ling Yuan (0000-0002-0921-713X); Hang Su (0000-0003-2468-557X); Mei-Hua Wan (0000-0002-1237-9455); Wen-Fu Tang (0000-0001-9294-6634).

Author contributions: Tang WF and Li J designed the research; Miao YF, Kang HX, Li J, Zhang YM, Ren HY, Zhu L, Chen H, Yuan L, and Su H performed the research; Miao YF, Kang HX, and Li J analyzed the data; Wan MH contributed new reagents or analytic tools; Miao YF and Kang HX wrote the paper.

Supported by the National Natural Science Foundation of China, No. 81603519 and No. 81573857.

Institutional review board statement: This study was reviewed and approved by the Institutional Animal Care and Use Committee of West China Hospital of Sichuan University.

Institutional animal care and use committee statement: All rats were handled according to the University Guidelines and the Animal Care Committee Guidelines of West China Hospital (Chengdu, China) (protocol number, 2017052A).

Conflict-of-interest statement: None of the authors have any

Yi-Fan Miao, Hong-Xin Kang, Juan Li, Yu-Mei Zhang, Hong-Yu Ren, Lv Zhu, Huan Chen, Ling Yuan, Hang Su, Mei-Hua Wan, Wen-Fu Tang, Department of Integrative Medicine, West China Hospital, Sichuan University, Chengdu 610041, Sichuan Province, China

Corresponding author: Wen-Fu Tang, PhD, Professor, Department of Integrative Medicine, West China Hospital, Sichuan University, No. 37, Guoxue Lane, Wuhou District, Chengdu 610041, Sichuan Province, China. tangwf@scu.edu.cn
Telephone: +86-28-85423546
Fax: +86-28-85423373

Abstract

BACKGROUND

Obesity worsens inflammatory organ injury in acute pancreatitis (AP), but there is no effective preventive strategy. Sheng-jiang powder (SJP) has been shown to alleviate multiple-organ inflammatory injury in rats with high-fat diet-induced obesity. Hence, SJP is supposed to have an effect on multiple-organ inflammatory injury in AP in rats fed a high-fat diet.

AIM

To explore how obesity may contribute to aggravating inflammatory organ injury in AP in rats and observe the effect of SJP on multiple-organ inflammatory injury in AP in rats fed a high-fat diet.

METHODS

Rats were randomly assigned to a control group (CG), an obese group (OG), and an SJP treatment group (SG), with eight rats per group. The rats in the OG and SG were fed a high-fat diet. From the third week, the rats in the SG were given oral doses of SJP (5 g/kg of body weight). After 12 wk, AP was induced in the three groups. Serum amylase level, body weight, Lee's index, serum biochemistry parameters, and serum inflammatory cytokine and tissue cytokine levels were assessed, and the tissue histopathological scores were evaluated and compared.

RESULTS

Compared with the CG, serum triglyceride, total cholesterol, interleukin-6, and interleukin-10 levels were significantly higher in the OG, and serum high-density lipoprotein cholesterol level was significantly lower in the OG. Moreover, enhanced oxidative damage was observed in the pancreas, heart, spleen, lung, intestine, liver, and kidney. Evidence of an imbalanced antioxidant defense system, especially in the pancreas, spleen, and intestine, was observed in the

conflicts of interest to declare.

Data sharing statement: No additional data are available.

ARRIVE guidelines statement: The authors have read the ARRIVE guidelines, and the manuscript was prepared and revised according to the ARRIVE guidelines.

Manuscript source: Unsolicited manuscript

Received: November 14, 2018
Peer-review started: November 14, 2018
First decision: December 28, 2018
Revised: January 10, 2019
Accepted: January 20, 2019
Article in press: January 21, 2019
Published online: February 14, 2019

obese AP rats. Compared with the OG, serum high-density lipoprotein cholesterol, interleukin-10, and superoxide dismutase expression levels in the pancreas, spleen, and intestine were increased in the SG. Additionally, SJP intervention led to a decrease in the following parameters: body weight; Lee's index; serum triglyceride levels; serum total cholesterol levels; malondialdehyde expression levels in the pancreas, heart, spleen, lung, and liver; myeloperoxidase expression levels in the lung; and pathological scores in the liver.

CONCLUSION
Obesity may aggravate the inflammatory reaction and pathological multiple-organ injury in AP rats, and SJP may alleviate multiple-organ inflammatory injury in AP in rats fed a high-fat diet.

Key words: Obesity; Acute pancreatitis; Sheng-jiang powder; Multiple-organ inflammatory injury; Oxidative stress

Core tip: Obesity worsens inflammatory organ injury in acute pancreatitis (AP), but there is no effective strategy. Sheng-jiang powder (SJP) has been shown to alleviate obesity-induced multiple-organ inflammatory injury. This study demonstrates that obesity may aggravate the inflammatory reaction and pathological injury in multiple organs in AP rats and that SJP may alleviate multiple-organ inflammatory injury in AP in rats fed a high-fat diet.

Citation: Miao YF, Kang HX, Li J, Zhang YM, Ren HY, Zhu L, Chen H, Yuan L, Su H, Wan MH, Tang WF. Effect of Sheng-jiang powder on multiple-organ inflammatory injury in acute pancreatitis in rats fed a high-fat diet. *World J Gastroenterol* 2019; 25(6): 683-695
URL: https://www.wjgnet.com/1007-9327/full/v25/i6/683.htm
DOI: https://dx.doi.org/10.3748/wjg.v25.i6.683

INTRODUCTION

The prevalence and incidence of obesity have sharply increased worldwide over the past 40 years[1]. Several studies have shown that obesity has contributed to the increased incidence[2] and severity[3,4] of acute pancreatitis (AP), specifically by increasing the risk of multisystem organ failure[5]. Although increasing evidence has confirmed the adverse effects of obesity on the course and prognosis of AP, the mechanism by which obesity influences AP has not been elucidated to date. There is no effective strategy to prevent AP from causing organ deterioration in obesity; thus, the current management standard is supportive care and the management of complications as they occur[6].

The most common mechanisms underlying the obesity-related increase in AP severity include visceral fat-induced acute lipotoxicity and the inflammatory response[7,8]. An increase in obesity-associated intrapancreatic fat and peripancreatic fat enables the unregulated lipolysis of visceral fat enriched in triglycerides, resulting in systemic unsaturated fatty acid (UFA) release, pancreatic necrosis, and respiratory, cardiovascular, and renal failure[3]. In addition to visceral fat-induced acute lipotoxicity, an obesity-induced imbalance between pro- and anti-inflammatory reactions is another mechanism involved in the exacerbation of AP in obesity. Adipose tissue leads to abundant macrophage infiltration, followed by increased secretion of proinflammatory cytokines [*e.g.*, interleukin-6 (IL-6) and tumor necrosis factor alpha] and decreased production of anti-inflammatory cytokines [*e.g.*, interleukin-10 (IL-10) and adiponectin], promoting inflammation, impairing insulin sensitivity, and dysregulating lipid metabolism[9]. Moreover, in obese AP rats, oxidative stress occurs locally and systemically along with the upregulation of proinflammatory cytokines and exacerbation of lipid peroxidation[10]. Our previous studies have demonstrated that high-fat diet-induced obesity can cause extensive inflammatory damage, especially multiple-organ inflammatory injury, in rats[11-13]. More importantly, obese individuals have an increased risk of developing multisystem organ failure in AP[5]. However, the mechanism of this effect is still

unknown. Therefore, in this study, we focused on inflammatory organ injury differences in AP between obese and lean rats.

According to traditional Chinese medicine (TCM) theory, obesity belongs to the category of "Turbidity"[14]. Sheng-Jiang powder (SJP), which is composed of Jiangchan (*Bombyx batryticatus*), Chantui (*Periostracum cicada*), Jianghuang (*Curcuma longa L.*), and Dahuang (*Rheum palmatum L.*)[15], has been widely used for the treatment of "Turbidity" for hundreds of years in China. SJP has been reported to exhibit diverse biological properties, including anti-inflammatory, lipid-lowering, and immune regulatory characteristics[16]. Our previous studies have demonstrated that SJP can ameliorate the inflammatory response and histopathological lesions in multiple organs in obese rats[11-13]. In addition, a previous study reported that SJP can reduce the inflammatory response and improve the clinical symptoms and prognosis of patients with AP[17]. Could SJP alleviate multiple-organ inflammatory injury in AP by preventing obesity in rats? To address this question, we aimed to explore how obesity may contribute to aggravating inflammatory organ injury in AP in rats and observe the effect of SJP on multiple-organ inflammatory injury in AP in rats fed a high-fat diet.

MATERIALS AND METHODS

SJP preparation

Dahuang (batch No. 16110150), Jianghuang (batch No. 16080008), Jiangchan (batch No. 16100147), and Chantui (batch No. 16080020) spray-dried drug powders were purchased from the Affiliated Hospital of Chengdu University of TCM (Chengdu, China) and authenticated by Professor Wang WM (Department of Herbal Pharmacy, West China Hospital, Sichuan University, China) according to the Chinese Pharmacopoeia (The Pharmacopoeia Commission of People's Republic of China, 2010). Voucher specimens were deposited in our laboratory. The spray-dried drug powders were mixed and reconstituted with sterile double-distilled water (concentration: 1 g/mL) according to the standard proportion of 4:3:2:1 based on *Wan-Bing-Hui-Chun*, which is a famous, classic TCM book[14]. This SJP solution was stored at 4 °C until use and administered orally to the rats at a dose of 5 mL/kg of body weight.

Animals

Male Sprague-Dawley rats (n = 24) weighing 60-80 g (3-4 wk of age) were purchased from Chengdu Dashuo Experimental Animal Co., Ltd. (Chengdu, China). The rats were acclimatized to the laboratory conditions (22 ± 2°C, 65% ± 10% relative humidity, 12-h light/dark cycle, and *ad libitum* access to water and food) for one week prior to the special feeding and fasted for 12 h prior to the induction of the AP model. The protocol was approved by the Institution Animal Care and Use Committee of Sichuan University (Chengdu, China) (protocol number, 2017052A).

Induction of obesity and AP, treatment, and sample collection

The rats were randomly selected and assigned to three groups (eight rats per group) according to the type of diet and treatment. As shown in Table 1, a control group (CG) was fed a control diet (#LAD3001G; Trophic Animal Feed High-Tech Co., Ltd., Nantong, China) and treated with normal saline; an obese group (OG) was fed a high-fat diet (#TP23300; Trophic Animal Feed High-Tech Co., Ltd.) and treated with normal saline; and an SJP treatment group (SG) was fed a high-fat diet and treated with SJP (5 g/kg of body weight). AIN93G is a type of diet that has been extensively used worldwide and designed for growing rodents[18], and the composition of the control diet (Table 2) used in this study is similar to that of AIN93G. The high-fat diet, in which approximately 33% of the calories are derived from fat, primarily lard (Table 2), was appropriate for inducing an obesity rodent model[19]. All rats were acclimatized to the respective diets for 2 wk before the experiment started. Then, the rats were orally treated with SJP/normal saline once a day for 10 wk.

After 12 weeks, the rats were fasted for 12 h. After performing intraperitoneal anesthesia with 2% sodium pentobarbital at 40 mg/kg of body weight, blood from the tail vein was collected for amylase detection, and an AP model was induced by a retrograde injection of 3.5% sodium taurocholate (Sigma, St. Louis, MO, United States; 1 mL/kg of body weight) with a microinfusion pump at a rate of 0.2 mL/min into the biliopancreatic ducts of the rats in each group. Twenty-four hours after the AP induction, the rats were anesthetized (2% sodium pentobarbital, intraperitoneal injection, 40 mg/kg of body weight), and blood samples were collected from each rat into tubes using cardiac puncture to test the levels of serum biochemistry parameters

Table 1 Feeding schedules used in the present study

Group	Rats (*n*)	Food	Treatment (oral administration for 10 wk)
CG	8	Control diet	Equal volumes of normal saline.
OG	8	High-fat diet	Equal volumes of normal saline.
SG	8	High-fat diet	Sheng-jiang powder (5 g/kg of body weight)

CG: Control group; OG: Obese group; SG: Sheng-jiang powder treatment group.

and cytokines (IL-6 and IL-10). Lee's index, which is a rapid means of determining obesity in rats, was calculated by using the following formula[20]:

Lee's index = [body weight (g)]$^{1/3}$ × 10^3/naso - anal length (cm).

Pancreas, liver, heart, spleen, lung, kidney, and intestinal tissue samples were collected after euthanizing the rats (2% sodium pentobarbital, intraperitoneal injection, 200 mg/kg of body weight) for the pathological and tissue cytokine analyses.

Biochemical assays

The blood samples were centrifuged at 2500 rpm for 5 min to collect the supernatants for analysis. The levels of triglycerides, total cholesterol, high-density lipoprotein cholesterol (HDL-c), low-density lipoprotein cholesterol (LDL-c), and amylase were measured using a HITACHI automatic biochemical analyzer (7170A, HITACHI, Tokyo, Japan) at the Affiliated Hospital of Chengdu University of TCM (Chengdu, China).

Measurement of serum IL-6 and IL-10 levels

The blood samples were centrifuged at 2500 rpm for 5 min to collect the supernatants for analysis. The levels of IL-6 and IL-10 were measured by enzyme-linked immunosorbent assay (ELISA) using a Rat IL-6 ELISA kit (EKT24498, Friendbio, Wuhan, China) and a Rat IL-10 ELISA kit (EKT25325, Friendbio, Wuhan, China), respectively. According to the manufacturer's protocol, the absorbance was measured at 450 nm with a High-Throughput Universal Microplate Assay. Then, the sample values were read based on the standard curve, and the relative concentrations were calculated.

Histopathological analysis

Fresh tissue samples used for the pathological analysis were fixed in 4% paraformaldehyde (AR1068, BOSTER, Wuhan, China), embedded in paraffin, sectioned into 5-μm sections, and stained with hematoxylin and eosin. All histopathological sections were observed and scored by two independent blinded pathologists. The total histopathology score represents the mean of the combined scores of each parameter assigned by the two investigators. The histopathological severity of pancreatitis was determined according to Kusske *et al*[21] (points 0-4, edema, inflammation, hemorrhage, and necrosis). The scoring system described by Mikawa *et al*[22] (points 0-4: alveolar congestion, hemorrhage, infiltration or aggregation of neutrophils in the airspace or the vessel wall, and thickness of the alveolar wall/hyaline membrane formation) was used to score acute lung injury. Inflammation-associated histological alterations in the intestinal mucosa were graded using a scoring system according to Wirtz *et al*[23]. The liver, heart, spleen, and kidney sections were examined for signs of edema, inflammatory infiltration, fat necrosis, parenchymal necrosis, and hemorrhage.

Tissue cytokine analysis

Tissue samples were homogenized, sonicated, and centrifuged at 10000 rpm for 10 min at 4 °C. The supernatants were collected for the cytokine analysis. Malondialdehyde (MDA), superoxide dismutase (SOD), glutathione peroxidase (GSH-Px), reactive oxygen species (ROS), and myeloperoxidase (MPO) levels were determined using the following reagent kits according to the manufacturer's protocols: rat MDA ELISA assay kit (EKT2065-75-0), SOD ELISA assay kit (EKT2486), GSH-Px ELISA assay kit (EKT2876), ROS ELISA assay kit (EKT25346), and MPO ELISA assay kit (EKT303413) (obtained from Friendbio Biotechnology Co., Ltd., Wuhan, China). Briefly, the absorbance was measured at 450 nm with a High-Throughput Universal Microplate Assay. Then, the sample values were read based on the standard curve, and the relative concentrations were calculated.

Table 2 Compositions of the experimental diet

Ingredient	Control diet (LAD3001G)		High-fat diet (TP23300)	
	g	kcal	g	kcal
Casein	200	753.20	267	1335
Corn starch	397	1495.10	0	0
Maltodextrin	132	497.11	157	785
Sucrose	100	376.60	89	445
Soybean oil	70	263.62	33	165
Lard	0	0.00	301	1505
Cellulose	50	188.30	67	335
Mineral mixture	35	131.81	66	330
Vitamin mixture	10	37.66	13	65
L-cystine	3	11.30	4	20
Choline bitartrate	0	0.00	3	15
Choline chloride	3	11.30	0	0
Total	1000	3766	1000	5000

Statistical analysis

The statistical methods used in this study were reviewed by Dr. Hai Niu from the College of Mathematics, Sichuan University. Normality was assessed by the Shapiro-Wilk normality test, and homogeneity of variance was assessed by the Bartlett's test. In this study, all data, which are expressed as the mean ± standard deviation, passed the normality test. If the variances of the three experimental groups were equal, two-sided one-way analysis of variance (followed by multiple pairwise comparisons using the Dunnett-*t* test) was used to discover the differences among the groups; if the variances were unequal, the Kruskal-Wallis test was used. In addition, Student's *t*-test was used to compare the difference in the amylase levels between the CG and CG′ (CG before AP induction). Statistical analyses were performed using GraphPad Prism 6.01 software (GraphPad Software Inc., San Diego, CA, United States). Statistical significance is expressed as $^{a}P < 0.05$, $^{b}P < 0.01$ *vs* CG; $^{c}P < 0.05$, $^{d}P < 0.01$ *vs* OG; or $^{e}P < 0.01$ *vs* CG′.

RESULTS

Body weight, Lee's index, and serum biochemistry parameters of the rats

At the end of the experiment, compared with the CG, the body weight of the rats in the OG increased by 26.67% ($P < 0.01$; Table 3); furthermore, Lee's index also increased by 10.45% in the OG ($P < 0.05$; Table 3). The levels of serum triglyceride and total cholesterol in the OG were significantly higher than those in the CG ($P < 0.01$; Table 3). SJP treatment significantly reduced the above four parameters in the rats fed a high-fat diet ($P < 0.01$ or $P < 0.05$; Table 3). In addition, serum HDL-c level in the OG was significantly lower than that in the CG ($P < 0.01$; Table 3), and SJP treatment significantly improved the low levels of serum HDL-c in the rats fed a high-fat diet ($P < 0.05$; Table 3). However, serum LDL-c values did not significantly differ among the experimental groups.

Serum amylase levels in the rats

Sodium taurocholate treatment led to a significant increase in serum amylase levels in the rats in the CG′ ($P < 0.01$; Figure 1). However, serum amylase levels only slightly changed among the three groups after AP induction (Figure 1).

SJP increases serum levels of IL-10 but not IL-6

Compared with the CG group, serum levels of IL-6 and IL-10 in the OG group were increased ($P < 0.01$, Figure 2). Serum IL-10 level in the SG group was significantly higher than that in the OG group ($P < 0.01$, Figure 2).

SJP suppresses oxidative stress in multiple organs

MDA levels in the pancreas, heart, spleen, liver, lung, and kidney from the obese rats with AP were higher than those in the lean rats with AP ($P < 0.05$ for the lung, $P <$

Table 3 Body weight, Lee's index, and serum biochemistry parameter levels of rats

Parameter	CG	OG	SG
Body weight (g)	480.10 ± 43.62	608.10 ± 36.96[b]	536.60 ± 46.77[d]
Lee's index	301.40 ± 23.36	332.90 ± 19.52[a]	307.30 ± 19.40[b]
TG (mmol/L)	1.35 ± 0.51	2.69 ± 0.86[b]	1.60 ± 0.60[d]
TC (mmol/L)	1.46 ± 0.32	1.97 ± 0.21[b]	1.68 ± 0.19[b]
HDL-c (mmol/L)	0.68 ± 0.11	0.46 ± 0.07[b]	0.59 ± 0.12[b]
LDL-c (mmol/L)	0.54 ± 0.13	0.49 ± 0.11	0.48 ± 0.11

The results are presented as the mean ± SD.
[a]$P < 0.05$.
[b]$P < 0.01$ *vs* the control group.
[c]$P < 0.05$.
[d]$P < 0.01$ *vs* the obese group.
CG: Control group; OG: Obese group; SG: Sheng-jiang powder treatment group; TG: Triglyceride; TC: Total cholesterol; HDL-c: High-density lipoprotein cholesterol; LDL-c: Low-density lipoprotein cholesterol.

0.01 for other tissues, Table 4). SOD levels in the pancreas, spleen, intestine, and liver from the obese rats with AP were lower than those in the lean rats with AP ($P < 0.01$, Table 4). In contrast, the SOD levels in the lung and kidney from the obese rats with AP were higher than those in the lean rats with AP ($P < 0.01$, Table 4). Similarly, the MPO level in the intestine from the obese rats with AP was also higher than that in the lean rats with AP ($P < 0.01$, Table 4). However, the ROS and GSH-Px levels in the liver and kidney from the rats showed minimal changes between the CG and OG. SJP markedly reduced the MDA levels in the pancreas, heart, spleen, lung, and liver ($P < 0.05$ for the spleen, $P < 0.01$ for other tissues, Table 4) and the MPO level in the lung ($P < 0.05$, Table 4). In contrast, SJP markedly increased the SOD levels in the pancreas, spleen, and intestine ($P < 0.01$, Table 4) and the GSH-Px level in the kidney ($P < 0.05$, Table 4).

SJP relieves liver pathological damage

Compared with the organs from the CG group rats, obesity exacerbated the pathological damage to the pancreas, liver, and heart, and more inflammatory cell infiltration, a large degree of severe tissue edema, more hemorrhage, and more necrosis were observed ($P < 0.01$, Figure 3A and B). However, SJP mitigated the hepatic pathological damage, and less inflammatory cell infiltration, mild tissue edema, and less necrosis were observed ($P < 0.05$, Figure 3A and B).

DISCUSSION

In the present study, serum triglyceride, total cholesterol, IL-6, and IL-10 levels in the obese AP rats were extremely high, and serum HDL-c level was significantly low. Enhanced oxidative damage was observed in the pancreas, heart, spleen, lung, intestine, liver, and kidney. Additionally, an imbalance in the antioxidant defense system, especially in the pancreas, spleen, intestine, and liver, was observed in the obese AP rats. Importantly, SJP treatment significantly increased serum HDL-c and IL-10 levels, decreased serum triglyceride and total cholesterol levels, induced oxidative stress in multiple organs, and ultimately ameliorated the pathological damage to the liver.

As one becomes more obese, more fat accumulates in and around the viscera, including the pancreas[3]. Fat in adipocytes is known to be composed of triglycerides, which are three free fatty acids hinged to a glycerol backbone, forming > 80% of the adipocyte mass[4]. More significantly, increased free fatty acids, particularly unsaturated fatty acids (UFAs), have been documented in serum from patients with severe AP[24], and serum triglyceride levels in AP patients are independently and proportionally correlated with persistent organ failure regardless of the etiology[25]. Furthermore, sufficient evidence suggests that UFAs are directly toxic to pancreatic acinar cells due to cytosolic calcium, largely causing extracellular release, decreased ATP levels, the inhibition of mitochondrial complexes I and V, and, ultimately, necrosis[3]. In AP associated with obesity, the expression levels of cytokines are significantly elevated in serum or organs involved in AP (pancreas, liver, and lungs)[26,27]. One study demonstrated that obesity reduces IL-10 expression in the spleen and that spleen-derived IL-10 protects against obesity-induced inflammatory

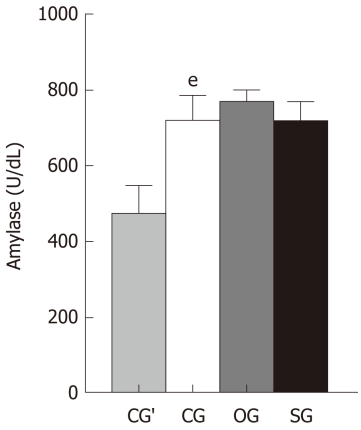

Figure 1 Serum amylase levels in rats. The results are presented as the mean ± SD. $^{e}P < 0.01$ *vs* the control group before acute pancreatitis induction. CG': Control group before acute pancreatitis induction; CG: Control group; OG: Obese group; SG: Sheng-jiang powder treatment group.

responses in the pancreas[28]. In addition, in obese mice, the levels of proinflammatory cytokines, including tumor necrosis factor alpha and IL-6, increased along with serum UFAs, but treatment with the triglyceride lipolysis inhibitor orlistat significantly reduced these cytokines and UFAs and prevented organ failure and mortality[29]. Hence, in addition to being directly responsible for necrosis, lipolysis is likely a contributor to the milieu of exaggerated inflammation characterizing AP. In this study, high-fat diet-induced obesity resulted in high serum levels of triglycerides, IL-6, and IL-10 in AP rats, but SJP prevented lipotoxicity and the systemic inflammatory response in obese AP rats. Moreover, previous studies have shown that SJP can reduce systemic inflammatory injury and downregulate the production of proinflammatory cytokines in mice and humans with sepsis[30].

Oxidative stress occurs when there is an imbalance between the production of reactive metabolites and the activity of antioxidant enzymes. Many studies have shown that oxidative stress is significantly increased in obese patients and animals and causes direct or indirect damage to various organs[31,32]. MDA is a toxic decomposition product of lipid peroxidation degradation, and the MDA content can reflect the degree of oxidative stress and cell damage[33]. During lipid peroxidation in pancreatitis, the MDA levels in plasma and ascites in obese animals are always higher than those in lean animals[34]. Hayam Ateyya *et al*[35] revealed that in rats with AP, the MDA levels are markedly increased when the SOD and glutathione levels are reduced in the pancreas and distant organs (*i.e.*, lung, liver, and kidney). In our study, we found similar results in multiple organs (*i.e.*, pancreas, liver, heart, spleen, lung, and kidney) from obese AP rats, suggesting that these organs might experience very serious conditions of oxidative stress and cell damage.

Various proinflammatory transcription factors can induce lipid peroxidation, causing the release of inflammatory cytokines and exacerbating oxidative stress, establishing a vicious circle[10]. Therefore, the synergistic effect of proinflammatory cytokines released during AP combined with the increased MDA levels in obese rats may aggravate the multiple-organ damage. ROS, which are chemical species containing oxygen, are byproducts of aerobic metabolism that play significant roles in cell signaling and homeostasis[36]. ROS levels can dramatically increase following oxidative stress in obesity, which may significantly damage the cell structure[36]. According to this study, ROS levels in the liver and kidney changed minimally between the obese and lean rats, but MDA levels in the obese rats were significantly increased. We speculate that this result may be due to the longer half-life of MDA compared with that of ROS, indicating that MDA is able to spread and reach distant intracellular and extracellular targets, thereby amplifying the effects of oxidative stress[37].

MPO is a characteristic enzyme of neutrophils, and its activity reflects the extent of neutrophil infiltration; sustained activation of MPO can cause tissue damage and aggravate inflammatory lesions[38]. Intestinal injury, which is considered a primary complication after AP onset, is well known to occur during early disease progression[39]. In addition, the intestine is considered an important target organ for obesity outcomes because of the effects of diet on this organ. An increase in intestinal ROS production and MPO activity was observed in rats fed a high-energy diet[40]. The increased MPO levels in the intestinal tissues in our study may suggest that obesity aggravates intestinal inflammatory injury in AP rats.

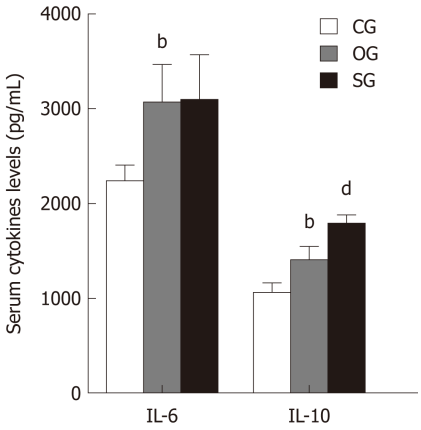

Figure 2 Serum inflammatory cytokine levels in rats. The results are presented as the mean ± SD. $^{b}P < 0.01$ *vs* the control group, $^{d}P < 0.01$ *vs* the obese group. CG: Control group; OG: Obese group; SG: Sheng-jiang powder treatment group; IL: Interleukin.

SOD, catalase, and GSH-Px are important antioxidant enzymes in organs and are involved in free-radical scavenging[41]. Erythrocyte SOD and GSH-Px activities are decreased in rats with AP[42]. Furthermore, low basal levels of pancreatic SOD activity are associated with increased mortality and tissue damage in rats with AP[43]. In the present work, SOD levels in the liver, pancreas, spleen, and intestinal tissues from the obese rats were lower than those from the lean animals, indicating that the antioxidant capacity in obese rats with AP may be lower than that in nonobese rats; this compromised antioxidant defense system may contribute to the increase in multiple-organ damage in obese rats with AP.

In China, SJP is widely used for the treatment of inflammatory diseases or syndromes, such as sepsis, pneumonia, and systemic inflammatory response syndrome; in addition, SJP has a positive effect on obesity-related glomerulopathy and obesity after contraception by subcutaneous Norplant implants (Supplementary material). Notably, our previous study showed that rhein and bisdemethoxycurcumin may be the potential active components of SJP for the treatment of AP[44]. Curcumin, an effective compound extracted from *Curcuma longa* L., exerts its ameliorative effects against AP by inhibiting oxidative stress and inflammation[45]. One study showed that curcumin administration reduces MDA levels in skeletal muscle to improve oxidative stress in high-fat diet-induced obese rats[46]. In contrast, curcumin is effective at countering the depletion of antioxidants. Kempaiah *et al*[47] reported that curcumin countered the depletion of GSH in erythrocytes and livers of high-fat diet-fed rats. Elevated hepatic SOD activity has also been found to be decreased by curcumin treatment. Moreover, emodin, which is derived from *Rheum palmatum* L., can prevent diet-induced obesity and associated metabolic syndrome by inhibiting the sterol regulatory element-binding protein pathway[48]. In this study, administration of SJP to obese rats reduced the activity of MPO in the lung; decreased the content of MDA in the pancreas, heart, spleen, lung, and liver; and increased the activity of SOD in the pancreas, spleen, and intestine. These results suggest that SJP can prevent AP from causing multiple-organ inflammatory injury-related deterioration in obese rats by reducing reactive oxygen free radicals, improving the activities of antioxidant enzymes, and alleviating the systemic inflammatory response.

However, there were some limitations to this study. First, SJP was not administered to obese rats, but it was administered at the time obesity was induced. According to the obesity and Lee's index results, SJP appears to largely prevent the development of obesity. Hence, the preventive effect of SJP on AP in obesity needs further exploration. Second, this study provided partial information about multiple-organ injuries in obese AP rats; however, the more specific mechanism needs further study. Third, the specific effective monomer components and tissue pharmacokinetics of SJP should be considered. Finally, studies investigating the effectiveness of SJP in obesity are limited to case reports and small-sample single-center randomized controlled trials in which SJP is always combined with other complementary or alternative medicine therapy (acupuncture or ear acupressure); hence, large sample multicenter randomized controlled trials should be considered.

In conclusion, obesity may aggravate the inflammatory reaction and pathological injury to multiple organs in AP rats, but SJP may alleviate multiple-organ inflammatory injury in AP in rats fed a high-fat diet. The results of this study may provide an experimental basis for clinical discoveries. Future research should

Table 4 Oxidative stress conditions of multiple organs

Organ	CG	OG	SG
Pancreas			
MDA (pmol/mL)	1048 ± 116	1584 ± 278[b]	1066 ± 156[d]
SOD (U/mL)	338 ± 31	244±21[b]	285 ± 18[d]
Heart			
MDA (pmol/mL)	1358 ± 199	1685 ± 87[b]	1297 ± 83[d]
SOD (U/mL)	313 ± 24	321 ± 42	351 ± 14
Spleen			
MDA (pmol/mL)	1247 ± 205	1748 ± 96[b]	1569 ± 185[b]
SOD (U/mL)	288 ± 17	214 ± 15[b]	322 ± 44[d]
Lung			
MDA (pmol/mL)	1359 ± 283	1745 ± 86[a]	1282 ± 140d
SOD (U/mL)	153 ± 31	268 ± 21[b]	241 ± 23
MPO (ng/mL)	77 ± 5	79 ± 12	56 ± 6[b]
Intestine			
MDA (pmol/mL)	1266 ± 141	1412 ± 325	1414 ± 235
SOD (U/mL)	347 ± 12	240 ± 19[b]	341 ± 29[d]
MPO (ng/mL)	46 ± 3	75 ± 9[b]	64 ± 3
Liver			
MDA (pmol/mL)	1285 ± 146	1549 ± 92[b]	1235 ± 160[d]
SOD (U/mL)	308 ± 47	229 ± 11[b]	231 ± 12
ROS (IU/mL)	718 ± 146	819 ± 96	730 ± 85
GSH-Px (mIU/mL)	86 ± 11	71 ± 20	80 ± 6
Kidney			
MDA (pmol/mL)	1077 ± 236	1519 ± 217[b]	1513 ± 223
SOD (U/mL)	240 ± 22	350 ± 22[b]	316 ± 55
ROS (IU/mL)	598 ± 85	677 ± 142	666 ± 49
GSH-Px (mIU/mL)	53 ± 7	66 ± 17	82 ± 13[b]

The results are presented as the mean ± SD.
[a]$P < 0.05$.
[b]$P < 0.01$ *vs* the control group; [c]$P < 0.05$.
[d]$P < 0.01$ *vs* the obese group.
CG: Control group; OG: Obese group; SG: Sheng-jiang powder treatment group; MDA: Malondialdehyde; SOD: Superoxide dismutase; MPO: Myeloperoxidase; ROS: Reactive oxygen species; GSH-Px: Glutathione peroxidase.

investigate the active components and mechanisms of action of SJP before it can be transformed into a potentially useful treatment in human trials (Supplementary Table 1).

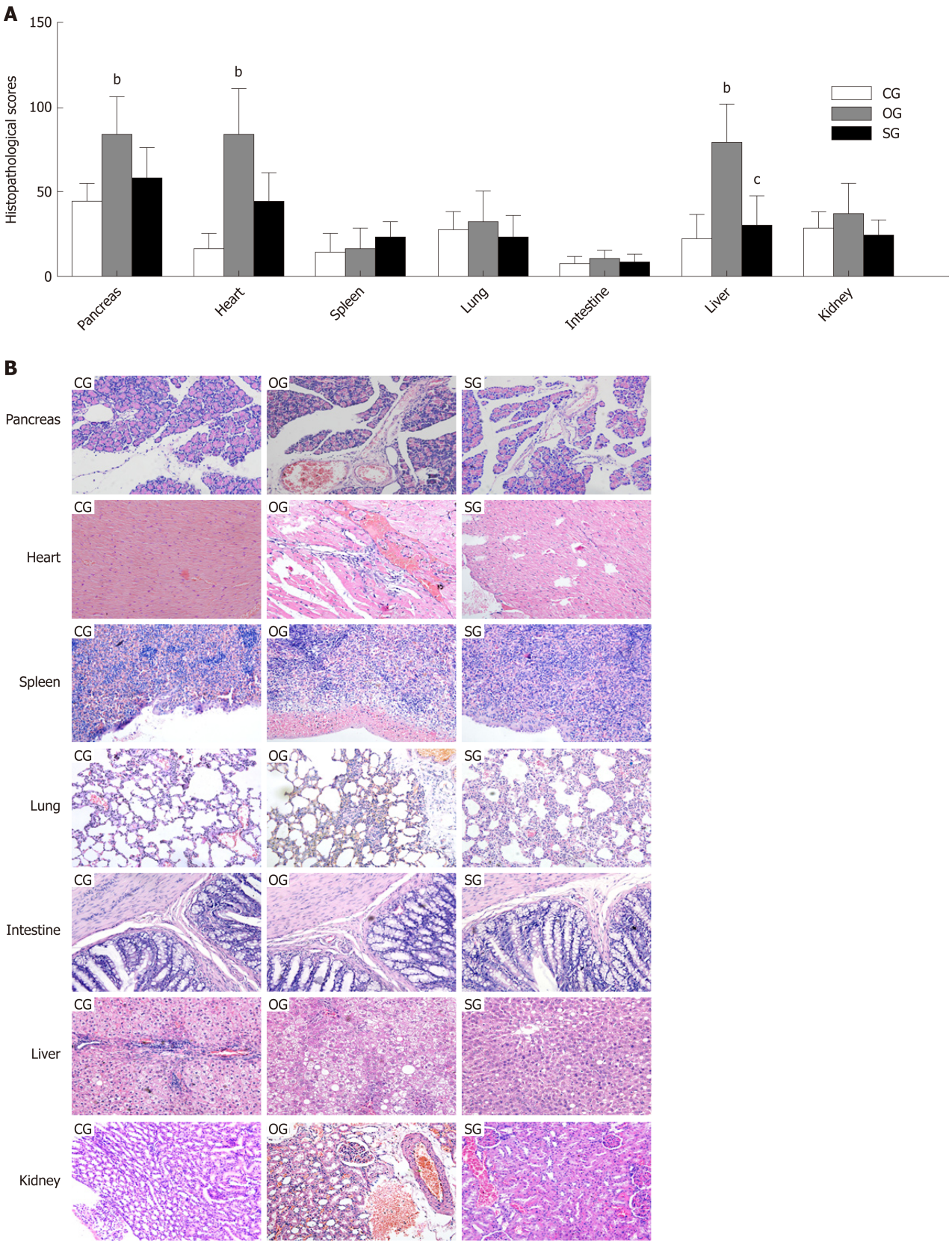

Figure 3 Histological scores and pathological images of multiple organs in rats. A: Histological scores of the pancreas, heart, spleen, lung, intestine, liver, and kidney. B: Pathological images of the pancreas, heart, spleen, lung, intestine, liver, and kidney (× 200). The results are presented as the mean ± SD. $^{b}P < 0.01$ *vs* the control group, $^{c}P < 0.05$ *vs* the obese group. CG: Control group; OG: Obese group; SG: Sheng-jiang powder treatment group.

ARTICLE HIGHLIGHTS

Research background

Obesity has contributed to the increased incidence and severity of acute pancreatitis (AP), specifically by increasing the risk of multisystem organ failure. However, the mechanism by which obesity influences AP has not been elucidated to date. There is no effective strategy for preventing AP from causing organ deterioration in obesity; thus, the current management standard is supportive and symptomatic. Therefore, investigations of how obesity may contribute to aggravating inflammatory organ injury in AP and identification of potential treatments are urgently required.

Research motivation

Our previous studies have demonstrated that high-fat diet-induced obesity can cause extensive inflammatory damage, especially multiple-organ inflammatory injury, in rats. However, the effect of high-fat diet-induced obesity on AP is still unknown. Sheng-jiang powder (SJP) is considered able to ameliorate the inflammatory response and histopathological lesions in multiple organs in obese rats. Could SJP alleviate multiple-organ inflammatory injury in AP by preventing obesity in rats? Therefore, this study aimed to explore the mechanisms of the effect of high-fat diet-induced obesity on inflammatory organ injury in AP rats and observe the effect of SJP on multiple-organ inflammatory injury in AP in rats fed a high-fat diet to provide an experimental basis for its clinical application in the future.

Research objectives

To explore how high-fat diet-induced obesity may contribute to aggravating inflammatory organ injury in AP rats and observe the effect of SJP on multiple-organ inflammatory injury in AP in rats fed a high-fat diet.

Research methods

In this study, an obese rat model was induced by high-fat diet feeding, which is widely accepted and used for the induction of obesity in rats. The AP rat model was induced by a retrograde injection of sodium taurocholate into the biliopancreatic ducts, which is widely used to induce AP in rats. The levels of serum biochemistry parameters [triglycerides, total cholesterol, high-density lipoprotein cholesterol (HDL-c), low-density lipoprotein cholesterol (LDL-c), and amylase] were measured using an HITACHI automatic biochemical analyzer (7170A, HITACHI, Tokyo, Japan). The levels of serum inflammatory cytokines (IL-6 and IL-10) and tissue oxidative stress cytokines [malondialdehyde (MDA), superoxide dismutase (SOD), glutathione peroxidase (GSH-Px), reactive oxygen species (ROS), and myeloperoxidase (MPO)] were measured by ELISA, which is a simple, rapid, accurate, and sensitive method. All histopathological sections were observed and scored by two independent blinded pathologists using different scoring systems specific to different tissues.

Statistical analyses were performed with GraphPad Prism 6.01 software. All data are expressed as the mean ± standard deviation and passed the normality test. Two-sided one-way analysis of variance (followed by multiple pairwise comparisons using the Dunnett-*t* test) or the Kruskal-Wallis test was used to discover the differences among the three groups. In addition, Student's *t*-test was used to compare the difference in the amylase levels between the control group (CG) and CG′ (CG before AP induction).

Research results

In the present study, serum triglyceride, total cholesterol, interleukin (IL)-6, and IL-10 levels in the obese AP rats were extremely high, and serum HDL-c level was significantly low. Enhanced oxidative damage was observed in the pancreas, heart, spleen, lung, intestine, liver, and kidney. Additionally, an imbalance in the antioxidant defense system, especially in the pancreas, spleen, intestine, and liver, was observed in the obese AP rats. Interestingly, SJP significantly increased serum HDL-c and IL-10 levels, decreased serum triglyceride and total cholesterol levels, induced oxidative stress in multiple organs, and ultimately ameliorated the pathological damage to the liver.

The preventive effect of SJP on AP in obesity remains to be determined. Moreover, this study provides partial information about multiple-organ injuries in obese AP rats, but the more specific mechanism needs further study. Finally, the specific effective monomer components and tissue pharmacokinetics of SJP should be considered to provide more systematic and comprehensive evidence for the clinical application of this Chinese decoction.

Research conclusions

This study demonstrates that high-fat diet-induced obesity may aggravate the inflammatory reaction and pathological injury to multiple organs, especially leading to a strong and extensive oxidative stress response in organs, in sodium taurocholate-induced AP rats. In addition, SJP may alleviate multiple-organ inflammatory injury in AP in rats fed a high-fat diet.

Research perspectives

As we observed that SJP may ameliorate multiple-organ inflammatory injury in AP in rats fed a high-fat diet by regulating the oxidative stress response, further investigation of the underlying molecular mechanism is urgently required to provide experimental evidence for wider clinical usage.

REFERENCES

1 **World Health Organization**. Obesity and overweight. Accessed November 2, 2018 Available from: http://www.who.int/mediacentre/factsheets/fs311/en/.
2 **Peery AF**, Crockett SD, Barritt AS, Dellon ES, Eluri S, Gangarosa LM, Jensen ET, Lund JL, Pasricha S, Runge T, Schmidt M, Shaheen NJ, Sandler RS. Burden of Gastrointestinal, Liver, and Pancreatic Diseases in the United States. *Gastroenterology* 2015; **149**: 1731-1741.e3 [PMID: 26327134 DOI: 10.1053/j.gastro.2015.08.045]
3 **Navina S**, Acharya C, DeLany JP, Orlichenko LS, Baty CJ, Shiva SS, Durgampudi C, Karlsson JM, Lee K, Bae KT, Furlan A, Behari J, Liu S, McHale T, Nichols L, Papachristou GI, Yadav D, Singh VP. Lipotoxicity causes multisystem organ failure and exacerbates acute pancreatitis in obesity. *Sci Transl Med* 2011; **3**: 107ra110 [PMID: 22049070 DOI: 10.1126/scitranslmed.3002573]
4 **Acharya C**, Navina S, Singh VP. Role of pancreatic fat in the outcomes of pancreatitis. *Pancreatology* 2014; **14**: 403-408 [PMID: 25278311 DOI: 10.1016/j.pan.2014.06.004]
5 **Papachristou GI**, Papachristou DJ, Avula H, Slivka A, Whitcomb DC. Obesity increases the severity of acute pancreatitis: performance of APACHE-O score and correlation with the inflammatory response. *Pancreatology* 2006; **6**: 279-285 [PMID: 16636600 DOI: 10.1159/000092689]
6 **Banks PA**, Freeman ML; Practice Parameters Committee of the American College of Gastroenterology. Practice guidelines in acute pancreatitis. *Am J Gastroenterol* 2006; **101**: 2379-2400 [PMID: 17032204 DOI: 10.1111/j.1572-0241.2006.00856.x]
7 **Sadr-Azodi O**, Orsini N, Andrén-Sandberg Å, Wolk A. Abdominal and total adiposity and the risk of acute pancreatitis: a population-based prospective cohort study. *Am J Gastroenterol* 2013; **108**: 133-139 [PMID: 23147519 DOI: 10.1038/ajg.2012.381]
8 **Yashima Y**, Isayama H, Tsujino T, Nagano R, Yamamoto K, Mizuno S, Yagioka H, Kawakubo K, Sasaki T, Kogure H, Nakai Y, Hirano K, Sasahira N, Tada M, Kawabe T, Koike K, Omata M. A large volume of visceral adipose tissue leads to severe acute pancreatitis. *J Gastroenterol* 2011; **46**: 1213-1218 [PMID: 21805069 DOI: 10.1007/s00535-011-0430-x]
9 **Zyromski NJ**, Mathur A, Pitt HA, Lu D, Gripe JT, Walker JJ, Yancey K, Wade TE, Swartz-Basile DA. A murine model of obesity implicates the adipokine milieu in the pathogenesis of severe acute pancreatitis. *Am J Physiol Gastrointest Liver Physiol* 2008; **295**: G552-G558 [PMID: 18583460 DOI: 10.1152/ajpgi.90278.2008]
10 **Bryan HK**, Olayanju A, Goldring CE, Park BK. The Nrf2 cell defence pathway: Keap1-dependent and -independent mechanisms of regulation. *Biochem Pharmacol* 2013; **85**: 705-717 [PMID: 23219527 DOI: 10.1016/j.bcp.2012.11.016]
11 **Li J**, Zhang YM, Li JY, Zhu L, Kang HX, Ren HY, Chen H, Yuan L, Miao YF, Wan MH, Tang WF. Effect of Sheng-Jiang Powder on Obesity-Induced Multiple Organ Injuries in Rats. *Evid Based Complement Alternat Med* 2017; **2017**: 6575276 [PMID: 29234419 DOI: 10.1155/2017/6575276]
12 **Miao YF**, Li J, Zhang YM, Zhu L, Chen H, Yuan L, Hu J, Yi XL, Wu QT, Wan MH, Tang WF. Sheng-jiang powder ameliorates obesity-induced pancreatic inflammatory injury *via* stimulating activation of the AMPK signalling pathway in rats. *World J Gastroenterol* 2018; **24**: 4448-4461 [PMID: 30356974 DOI: 10.3748/wjg.v24.i39.4448]
13 **Li J**, Zhu L, Zhang YM, Chen H, Miao YF, Kang HX, Ren HY, Wan MH, Long D, Tang WF. Sheng-Jiang Powder Ameliorates High Fat Diet Induced Nonalcoholic Fatty Liver Disease via Inhibiting Activation of Akt/mTOR/S6 Pathway in Rats. *Evid Based Complement Alternat Med* 2018; **2018**: 6190254 [PMID: 30402130 DOI: 10.1155/2018/6190254]
14 **Liu XM**, Tong XL, Wang PQ. Discussion on the theory of turbidity. *Shijie Zhongxiyi Jiehe Zazhi* 2009; **4**: 839-842 [DOI: 10.13935/j.cnki.sjzx.2009.12.002]
15 **Tian SX**, Li SM. Clinical application on the effect of Sheng-jiang powder. *Hebei Zhongxiyi Xuebao* 1994; **9**: 40-44 [DOI: 10.16370/j.cnki.13-1214/r.1994.01.012]
16 **Liu WJ**, Xue YX, Hu DP. Research Progress on Modern Pharmacological Mechanism of Sheng-Jiang Powder. *Beijing Zhongyiyao* 2012; **31**: 939-943 [DOI: 10.16025/j.1674-1307.2012.12.029]
17 **Gu WY**, Zhao L, Qian FH, Wu Y, Cao DF. Treatment of acute pancreatitis with Sheng-Jiang Powder. *Jilin Zhongyiyao* 2013; **33**: 1232-1234 [DOI: 10.13463/j.cnki.jlzyy.2013.12.011]
18 **Reeves PG**, Nielsen FH, Fahey GC. AIN-93 purified diets for laboratory rodents: final report of the American Institute of Nutrition ad hoc writing committee on the reformulation of the AIN-76A rodent diet. *J Nutr* 1993; **123**: 1939-1951 [PMID: 8229312 DOI: 10.1093/jn/123.11.1939]
19 **Wang H**, Storlien LH, Huang XF. Effects of dietary fat types on body fatness, leptin, and ARC leptin receptor, NPY, and AgRP mRNA expression. *Am J Physiol Endocrinol Metab* 2002; **282**: E1352-E1359 [PMID: 12006366 DOI: 10.1152/ajpendo.00230.2001]
20 **Li M**, Ye T, Wang XX, Li X, Qiang O, Yu T, Tang CW, Liu R. Effect of Octreotide on Hepatic Steatosis in Diet-Induced Obesity in Rats. *PLoS One* 2016; **11**: e0152085 [PMID: 27002331 DOI: 10.1371/journal.pone.0152085]
21 **Kusske AM**, Rongione AJ, Ashley SW, McFadden DW, Reber HA. Interleukin-10 prevents death in lethal necrotizing pancreatitis in mice. *Surgery* 1996; **120**: 284-8; discussion 289 [PMID: 8751594]
22 **Mikawa K**, Maekawa N, Nishina K, Takao Y, Yaku H, Obara H. Effect of lidocaine pretreatment on endotoxin-induced lung injury in rabbits. *Anesthesiology* 1994; **81**: 689-699 [PMID: 8092515]
23 **Wirtz S**, Neufert C, Weigmann B, Neurath MF. Chemically induced mouse models of intestinal inflammation. *Nat Protoc* 2007; **2**: 541-546 [PMID: 17406617 DOI: 10.1038/nprot.2007.41]
24 **Sztefko K**, Panek J. Serum free fatty acid concentration in patients with acute pancreatitis. *Pancreatology* 2001; **1**: 230-236 [PMID: 12120200 DOI: 10.1159/000055816]
25 **Nawaz H**, Koutroumpakis E, Easler J, Slivka A, Whitcomb DC, Singh VP, Yadav D, Papachristou GI. Elevated serum triglycerides are independently associated with persistent organ failure in acute pancreatitis. *Am J Gastroenterol* 2015; **110**: 1497-1503 [PMID: 26323188 DOI: 10.1038/ajg.2015.261]
26 **Segersvärd R**, Tsai JA, Herrington MK, Wang F. Obesity alters cytokine gene expression and promotes liver injury in rats with acute pancreatitis. *Obesity (Silver Spring)* 2008; **16**: 23-28 [PMID: 18223607 DOI: 10.1038/oby.2007.27]
27 **Park J**, Chang JH, Park SH, Lee HJ, Lim YS, Kim TH, Kim CW, Han SW. Interleukin-6 is associated with obesity, central fat distribution, and disease severity in patients with acute pancreatitis. *Pancreatology* 2015; **15**: 59-63 [PMID: 25434497 DOI: 10.1016/j.pan.2014.11.001]
28 **Gotoh K**, Inoue M, Shiraishi K, Masaki T, Chiba S, Mitsutomi K, Shimasaki T, Ando H, Fujiwara K, Katsuragi I, Kakuma T, Seike M, Sakata T, Yoshimatsu H. Spleen-derived interleukin-10 downregulates the severity of high-fat diet-induced non-alcoholic fatty pancreas disease. *PLoS One* 2012; **7**: e53154 [PMID: 23285260 DOI: 10.1371/journal.pone.0053154]

29 **Malecki EA**, Castellanos KJ, Cabay RJ, Fantuzzi G. Therapeutic administration of orlistat, rosiglitazone, or the chemokine receptor antagonist RS102895 fails to improve the severity of acute pancreatitis in obese mice. *Pancreas* 2014; **43**: 903-908 [PMID: 24632545 DOI: 10.1097/MPA.0000000000000115]

30 **Zhu L**, Zhao L, Qian FH, Qi LL, Xia YC, Qian YM Xi Y. Research on the Inhibition of Inflammatory Cytokines by Shengjiang San in Sepsis Mice. *Zhongguo Zhongyi Jizheng* 2015; **24**: 384-386 [DOI: 10.3969/j.issn.1004-745X.2015.03.003]

31 **Dimassi S**, Chahed K, Boumiza S, Canault M, Tabka Z, Laurant P, Riva C. Role of eNOS- and NOX-containing microparticles in endothelial dysfunction in patients with obesity. *Obesity (Silver Spring)* 2016; **24**: 1305-1312 [PMID: 27130266 DOI: 10.1002/oby.21508]

32 **Fu J**, Zeng C, Zeng Z, Wang B, Gong D. Cinnamomum camphora Seed Kernel Oil Ameliorates Oxidative Stress and Inflammation in Diet-Induced Obese Rats. *J Food Sci* 2016; **81**: H1295-H1300 [PMID: 27003858 DOI: 10.1111/1750-3841.13271]

33 **Tsikas D**. Assessment of lipid peroxidation by measuring malondialdehyde (MDA) and relatives in biological samples: Analytical and biological challenges. *Anal Biochem* 2017; **524**: 13-30 [PMID: 27789233 DOI: 10.1016/j.ab.2016.10.021]

34 **Pereda J**, Pérez S, Escobar J, Arduini A, Asensi M, Serviddio G, Sabater L, Aparisi L, Sastre J. Obese rats exhibit high levels of fat necrosis and isoprostanes in taurocholate-induced acute pancreatitis. *PLoS One* 2012; **7**: e44383 [PMID: 23028532 DOI: 10.1371/journal.pone.0044383]

35 **Ateyya H**, Wagih HM, El-Sherbeeny NA. Effect of tiron on remote organ injury in rats with severe acute pancreatitis induced by L-arginine. *Naunyn Schmiedebergs Arch Pharmacol* 2016; **389**: 873-885 [PMID: 27118662 DOI: 10.1007/s00210-016-1250-6]

36 **McMurray F**, Patten DA, Harper ME. Reactive Oxygen Species and Oxidative Stress in Obesity-Recent Findings and Empirical Approaches. *Obesity (Silver Spring)* 2016; **24**: 2301-2310 [PMID: 27804267 DOI: 10.1002/oby.21654]

37 **Rolo AP**, Teodoro JS, Palmeira CM. Role of oxidative stress in the pathogenesis of nonalcoholic steatohepatitis. *Free Radic Biol Med* 2012; **52**: 59-69 [PMID: 22064361 DOI: 10.1016/j.freeradbiomed.2011.10.003]

38 **Odobasic D**, Kitching AR, Yang Y, O'Sullivan KM, Muljadi RC, Edgtton KL, Tan DS, Summers SA, Morand EF, Holdsworth SR. Neutrophil myeloperoxidase regulates T-cell-driven tissue inflammation in mice by inhibiting dendritic cell function. *Blood* 2013; **121**: 4195-4204 [PMID: 23509155 DOI: 10.1182/blood-2012-09-456483]

39 **Tian R**, Tan JT, Wang RL, Xie H, Qian YB, Yu KL. The role of intestinal mucosa oxidative stress in gut barrier dysfunction of severe acute pancreatitis. *Eur Rev Med Pharmacol Sci* 2013; **17**: 349-355 [PMID: 23426538]

40 **Gil-Cardoso K**, Ginés I, Pinent M, Ardévol A, Terra X, Blay M. A cafeteria diet triggers intestinal inflammation and oxidative stress in obese rats. *Br J Nutr* 2017; **117**: 218-229 [PMID: 28132653 DOI: 10.1017/S0007114516004608]

41 **Czakó L**, Takács T, Varga IS, Tiszlavicz L, Hai DQ, Hegyi P, Matkovics B, Lonovics J. Oxidative stress in distant organs and the effects of allopurinol during experimental acute pancreatitis. *Int J Pancreatol* 2000; **27**: 209-216 [PMID: 10952403 DOI: 10.1385/IJGC:27:3:209]

42 **Tang QQ**, Su SY, Fang MY. Zinc supplement modulates oxidative stress and antioxidant values in rats with severe acute pancreatitis. *Biol Trace Elem Res* 2014; **159**: 320-324 [PMID: 24771310 DOI: 10.1007/s12011-014-9971-1]

43 **Ren J**, Luo Z, Tian F, Wang Q, Li K, Wang C. Hydrogen-rich saline reduces the oxidative stress and relieves the severity of trauma-induced acute pancreatitis in rats. *J Trauma Acute Care Surg* 2012; **72**: 1555-1561 [PMID: 22695421 DOI: 10.1097/TA.0b013e31824a7913]

44 **Zhu L**, Li JY, Zhang YM, Kang HX, Chen H, Su H, Li J, Tang WF. Pharmacokinetics and pharmacodynamics of Shengjiang decoction in rats with acute pancreatitis for protecting against multiple organ injury. *World J Gastroenterol* 2017; **23**: 8169-8181 [PMID: 29290653 DOI: 10.3748/wjg.v23.i46.8169]

45 **Shafik NM**, Abou-Fard GM. Ameliorative Effects of Curcumin on Fibrinogen-Like Protein-2 Gene Expression, Some Oxido-Inflammatory and Apoptotic Markers in a Rat Model of l-Arginine-Induced Acute Pancreatitis. *J Biochem Mol Toxicol* 2016; **30**: 302-308 [PMID: 26862043 DOI: 10.1002/jbt.21794]

46 **Maithilikarpagaselvi N**, Sridhar MG, Swaminathan RP, Sripradha R. Preventive effect of curcumin on inflammation, oxidative stress and insulin resistance in high-fat fed obese rats. *J Complement Integr Med* 2016; **13**: 137-143 [PMID: 26845728 DOI: 10.1515/jcim-2015-0070]

47 **Kempaiah RK**, Srinivasan K. Antioxidant status of red blood cells and liver in hypercholesterolemic rats fed hypolipidemic spices. *Int J Vitam Nutr Res* 2004; **74**: 199-208 [PMID: 15296079 DOI: 10.1024/0300-9831.74.3.199]

48 **Li J**, Ding L, Song B, Xiao X, Qi M, Yang Q, Yang Q, Tang X, Wang Z, Yang L. Emodin improves lipid and glucose metabolism in high fat diet-induced obese mice through regulating SREBP pathway. *Eur J Pharmacol* 2016; **770**: 99-109 [PMID: 26626587 DOI: 10.1016/j.ejphar.2015.11.045]

P- Reviewer: Negoi I, Neri V, Tao R, Venu RP, Yago MD

S- Editor: Ma RY **L- Editor:** Wang TQ **E- Editor:** Yin SY

World Journal of Gastroenterology

Submit a Manuscript: https://www.f6publishing.com

World J Gastroenterol 2019 February 14; 25(6): 696-706

DOI: 10.3748/wjg.v25.i6.696

ISSN 1007-9327 (print) ISSN 2219-2840 (online)

ORIGINAL ARTICLE

Retrospective Study

Preoperative rectosigmoid endoscopic ultrasonography predicts the need for bowel resection in endometriosis

Victor Desplats, René-Louis Vitte, Joseph du Cheyron, Gilles Roseau, Arnaud Fauconnier, Frédérick Moryoussef

ORCID number: Victor Desplats (0000-0001-6911-8718); René-Louis Vitte (0000-0002-7601-5183); Joseph du Cheyron (0000-0002-1296-4072); Gilles Roseau (0000-0003-0364-4541); Arnaud Fauconnier (0000-0003-0724-6831); Frederick Moryoussef (0000-0002-6985-0404).

Author contributions: Desplats V designed, performed the research and wrote the paper; du Cheyron J contributed to the analysis; Vitte RL, Roseau G and Fauconnier A provided clinical advice; Moryoussef F designed the research and supervised the report.

Institutional review board statement: The cohort used for this study had the approval of the local ethic committee of Centre Hospitalier Intercommunal Poissy Saint Germain.

Informed consent statement: All patients included in this retrospective analysis gave their prior informed consent for inclusion in the cohort.

Conflict-of-interest statement: We have no financial relationships to disclose.

Data sharing statement: No additional data are available.

Victor Desplats, René-Louis Vitte, Frédérick Moryoussef, Department of Hepato-gastro-enterology, Centre Hospitalier Intercommunal Poissy Saint Germain, Poissy 78300, France

Joseph du Cheyron, Department of Statistics, Centre Hospitalier Intercommunal Poissy Saint Germain, Poissy 78300, France

Gilles Roseau, Department of Gastroenterology, Hôpital Cochin, Paris 75014, France

Arnaud Fauconnier, Department of Obstetrics and Gynecology, Centre Hospitalier Intercommunal Poissy Saint Germain, University of Saint Quentin en Yvelines, Poissy 78300, France

Corresponding author: Victor Desplats, MD, Doctor, Medical Resident, Department of Hepato-gastro-enterology, Centre Hospitalier Intercommunal Poissy Saint Germain, 10 rue du Champ Gaillard, Poissy 78300, France. victor.desplats@aphp.fr
Telephone: +33-663185173

Abstract

BACKGROUND

Rectosigmoid endometriosis is an underdiagnosed disease responsible for abdominal pain, transit disorders and rectal bleeding. Two surgical approaches, rectosigmoid bowel resection (segmental or patch) or intramuscular layer dissection (shaving), are available.

AIM

To assess whether the lesion features observed *via* preoperative rectosigmoid endoscopic ultrasonography (RS-EUS) might predict the need for bowel resection.

METHODS

This multicentric retrospective study was conducted on patients with rectosigmoid endometriosis who underwent a curative surgical procedure, evaluated by RS-EUS performed by two trained operators, between January 2012 and March 2018. A univariate statistical analysis was performed on nodules' RS-EUS features (thickness, width, infiltration of the submucosae, presence of a bump into the digestive lumen and presence of multiple rectosigmoid localizations). A multivariate logistic regression was then performed on the significant results.

RESULTS

Manuscript source: Invited conference manuscripts

Received: December 7, 2018
Peer-review started: December 8, 2018
First decision: December 28, 2018
Revised: January 14, 2018
Accepted: January 18, 2019
Article in press: January 18, 2019
Published online: February 14, 2019

Of the 367 patients, 73 patients with rectosigmoid endometriosis were evaluated by RS-EUS and underwent rectosigmoid surgery. After the univariate analysis was completed, thickness, width and infiltration of the submucosae were identified as potential predictive factors for bowel resection. In a multivariate logistic regression model, only thickness appeared to be a significant [odds ratio (OR) = 1.49, 95% confidence interval (CI): 1.04-2.12, P = 0.028] predictive factor for bowel resection. Receiver operating characteristic analysis performed showed that a thickness over 5.20 mm might be used as cut-off with a sensitivity of 76%, a specificity of 81%, and an area under carve = 0.82. The cut-off values for 100% sensitivity and 100% specificity were 0.90 mm and 10.00 mm, respectively. A trend concerning width to predict the need for resection was also observed (OR 1.12, 95%CI: 1.00-1.26, P = 0.054)

CONCLUSION
The presence of a rectosigmoid nodule of endometriosis greater than 5.20 mm thick on RS-EUS might predict the need for bowel resection.

Key words: Endometriosis; Surgery; Endoscopy; Ultrasound; Bowel disease; Rectum and sigmoid

Core tip: Rectosigmoid endometriosis is an underdiagnosed disease responsible for abdominal pain, transit disorders and rectal bleeding. The treatment can be either medical or surgical. If a surgical resection of the bowel is needed, it must be performed by a multidisciplinary team. The aim of our study was to assess whether the lesion features observed *via* preoperative rectosigmoid endoscopic ultrasonography (RS-EUS), a key exam in this condition, might predict the need for bowel resection. We found that the presence of a rectosigmoid nodule of endometriosis greater than 5.20 mm thick on RS-EUS might predict the need for bowel resection.

Citation: Desplats V, Vitte RL, du Cheyron J, Roseau G, Fauconnier A, Moryoussef F. Preoperative rectosigmoid endoscopic ultrasonography predicts the need for bowel resection in endometriosis. *World J Gastroenterol* 2019; 25(6): 696-706
URL: https://www.wjgnet.com/1007-9327/full/v25/i6/696.htm
DOI: https://dx.doi.org/10.3748/wjg.v25.i6.696

INTRODUCTION

Endometriosis is a benign estrogen-dependent disease associated with pelvic pain and infertility, affecting 10% to 15% of women of childbearing age[1]. Intestinal endometriosis is the most common extra-gynecologic localization[2], affecting 3% to 38% of women with endometriosis; this condition can be responsible for rectal bleeding, transit disorders and dyschezia, leading to an altered quality of life[3]. The decision on whether endometriosis requires surgical treatment depends on many factors, such as age, clinical findings, reproductive expectations and sites affected by the disease[4]. Although medical treatment is effective for the control of symptoms, it has no impact on organ lesions, and a surgical treatment might be needed.

Two surgical approaches are available for rectosigmoid endometriosis: intramuscular layer dissection (shaving) or rectosigmoid bowel resection (segmental or patch). Shaving is a conservative technique with some advantages: shorter operative time, shorter hospitalization time, and fewer peroperative complications[5]. Moreover, resection techniques may lead to more postoperative digestive disabilities compared with shaving, such as unsuccessful evacuatory attempts, feeling of incomplete evacuation, abdominal pain and painful evacuation effort[6]. Choice is led by clinical and radiological factors. The shaving technique is preferred for single, nonsymptomatic lesions, whereas the resection technique appears to be more adequate for multiple or symptomatic lesions[7]. According to local recommendations, the first-line exam involves pelvic ultrasonography. Magnetic resonance imaging (MRI) and preoperative rectosigmoid endoscopic ultrasonography (RS-EUS) are only considered as second- and third-line exams, respectively, for the evaluation of deep

infiltrating lesions[8].

A recent study has shown that a pre-operative MRI-colonography might predict the need for bowel resection in recto-sigmoid endometriosis[9]. However, it has previously been demonstrated that RS-EUS exhibits better sensitivity and negative predictive value than MRI in the diagnosis of rectosigmoid endometriosis[10]. We therefore decided to conduct a study to assess whether the characteristics of endometriosis lesions evaluated on a preoperative rectosigmoid ultrasonography can predict the need for bowel resection in rectosigmoid endometriosis.

MATERIALS AND METHODS

Patients

We conducted a multicentric retrospective study in a cohort of patients including 367 patients followed for endometriosis between January 2012 and March 2018. In this cohort, data were collected prospectively when patients were suspected of having endometriosis. Patients were suspected of having endometriosis when they experienced chronic pelvic pain for a greater than six-month duration. This pain could be a severe dysmenorrhea, a deep dyspareunia, a cyclic pelvic pain and painful defecation with or without infertility. In this cohort, patients could have been explored with other radiological exams, such as MRI or endovaginal ultrasonography, at the discretion of the clinician. Endometriosis was finally diagnosed according to surgical and histological criteria.

In our study, the inclusion criteria were patients aged over 18 with rectosigmoid endometriosis who underwent a surgery after a RS-EUS. Age, body mass index (BMI), pregnancy, parity and preoperative medical treatment were recorded from the patients' files. In addition, the patients were asked to complete a questionnaire regarding their symptoms, including digestive symptoms. Each patient was asked to report whether the symptoms were never, sometimes, often, or always present. Patients were also asked whether these symptoms were exacerbated during their period. Symptoms that were not exacerbated during period were denoted as "none" to avoid confusion with other digestive conditions.

Rectosigmoid endoscopic ultrasonography

RS-EUS was performed by two well-trained ultrasonographists (RV and GR) in two different centers. The exam was divided into two different steps. The patients were in lateral decubitus position whenever it was possible. The first step involved endoscopic evaluation of the mucosae and the digestive lumen. The second step involved an ultrasonographic evaluation of the digestive wall. The device used was a flexible Pentax (Argenteuil, France) echoendoscope with radial probe. The normal rectosigmoid anatomy appears as follows on ultrasound 7.5 MHz (from the lumen to the serosa): Hypoechoic mucosa, hyperechoic submucosa, and hypoechoic muscular layer (Figure 1). Rectosigmoid endometriosis appears as a hypoechoic nodule infiltrating the muscular layer. Mucosal or submucosal invasion are characterized by an interruption of their hypoechogenic line (Figure 2). The evaluation criteria were thickness and width of the nodule, presence of a bump in the digestive lumen, presence of infiltration of the submucosae and presence of multiple lesions. The presence of a bump in the digestive lumen was evaluated during the endoscopic step of the exam and defined as a mucosal lesion or a narrowing of the digestive lumen.

Surgery

All the interventions were performed by the same gynecologic surgeon (AF) who was well trained in endometriosis surgery. Interventions were performed *via* open laparoscopy. According to the recommendations, surgery on the digestive tract could involve a shaving (intramuscular layer dissection), a patch or a segmental digestive resection (subtotal proctectomy, sigmoidectomy or both). Patch and segmental resection surgeries were performed by a multidisciplinary team including digestive surgeons. A shaving, or intramuscular layer dissection of the lesions, involves the excision of the nodule on the digestive tract without digestive tract opening.

The choice of the surgical procedure was made by the surgeon, and shaving was preferred any time it was possible based on the nodule characteristics. This procedure was typically performed on unique and small lesions without submucosae involvement.

Statistical analysis

Patients were analyzed in two different groups: Shaving and digestive resection (patch or segmental resection). Univariate analysis was first performed to evaluate the relation between each criterion and the need for digestive resection. For qualitative

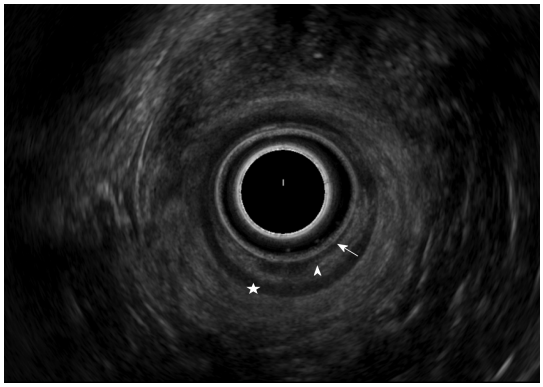

Figure 1 Normal view of the rectal wall with a radial probe in Rectosigmoid Endoscopic Ultrasonography. Arrow: Mucosae; Arrowhead: Muscular mucosa; Star: Submucosa; Disc: Muscular layer; Device: PENTAX EG-3670 URK ultrasound video-endoscope 7.5 MHz.

variables, including the presence of a bump, infiltration of the submucosae and presence of multiple lesions, a Fisher exact test was performed when one or more of the theoretical frequencies were less than five. A chi-square test was performed when all of the theoretical frequencies were greater than or equal to five. For quantitative variables, Student t-tests were performed. Second, we performed multivariate logistic regression with significant variables after univariate analysis. Every test was performed with a two-tailed alpha risk of 5%. A *P*-value less than 0.05 was considered statistically significant. The statistical review of the study was performed by a biomedical statistician. All statistics were performed with XLSTAT version 20.1 (Addinsoft, 33000, Bordeaux, France).

Patient disclosure

All patients included in this retrospective analysis gave their prior informed consent for inclusion in the cohort. The cohort had the approval of the local ethic committee for protection of people (Comité de Protection des Personnes, CPP) on the 20th of June 2013.

RESULTS

In total, 367 women were followed for endometriosis and included in the cohort between January 2012 and March 2018. Among them, 280 underwent a surgical procedure, 88 of whom had a need for bowel intervention. Two and three patients underwent an ileo-cecal surgery and appendectomy, respectively, and were therefore excluded from the analysis. An additional 10 women were excluded from the analysis because they did not undergo a preoperative RS-EUS (7 patients) or because the RS-EUS was not performed by well-trained ultrasonographists (3 patients). Finally, 73 patients were included in the analysis and separated in two different groups: shaving (36 patients) and bowel resection (37 patients) (Figure 3).

Concerning the study population, no differences in age, BMI, pregnancy, parity and preoperative medical treatment were noted between groups. No difference was found regarding digestive symptoms except dyschezia. Indeed, patients in the resection group exhibited significantly more severe dyschezia compared with the shaving group (P = 0,020) (Table 1).

In univariate analysis (Table 2), the mean thickness was 4.22 mm in the shaving group and 6.81 mm in the resection group, and the difference was statistically significant (P < 0.001). Regarding width, the mean measures were 13.43 and 19.34 mm in the shaving group and the resection group, respectively, and the difference was statistically significant (P < 0.001). Infiltration of the submucosae was observed in 5.6% (2/36) of the patients in the shaving group and 30% (11/35) in the resection group, leading to a significant difference (P = 0.007). No significant differences in the presence of a bump in the digestive lumen (5.6% in the shaving group *vs* 16% in the resection group, P = 0.261) and the presence of 2 or more lesions (2.8% in the shaving group *vs* 11% in the resection group, P = 0.358) were noted between the groups. No differences in classification in the shaving group and the resection group were noted between the two ultrasonographists (RV, GR) (P = 0.98) (See in Appendix).

In the multivariate model, thickness, width and submucosae infiltration were included in the analysis. After logistic regression, only thickness appeared to be

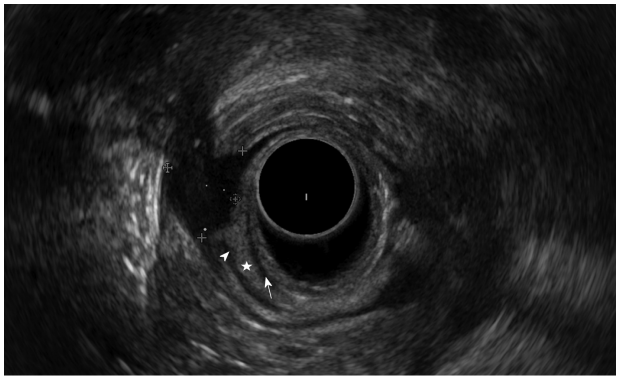

Figure 2 View with a radial probe of an endometriotic nodule in rectosigmoid endoscopic ultrasonography. This nodule is located in the front side of the upper rectum next to the torus and exhibits infiltration of the submucosa. Width: 11 mm; Thickness: 8.6 mm. Arrow: Mucosae; Star: Submucosa; Arrowhead: Muscular layer; Device: PENTAX EG-3670 URK ultrasound video-endoscope 7.5 MHz.

significant with an odds ratio (OR) = 1.49 [95% confidence interval (CI): 1.04–2.12, P = 0.028] (Table 3). Nevertheless, a sensible trend regarding width was identified. Specifically, width was increased in the resection group compared with the shaving group (OR 1.12, 95%CI : 1.00-1.26, P = 0.054).

Based on receiver operating characteristic (ROC) analysis, a thickness greater than 5.20 mm was the best threshold to determine the need for digestive resection with a sensitivity of 76%, a specificity of 81%, and a positive predictive value (PPV) and negative predictive value (NPV) of 0.80 and 0.76, respectively. Cut-off values for 100% sensitivity and 100% specificity were 0.9 and 10.0 mm, respectively (Table 4). The area under curve of the ROC curve was 0.82 (Figure 4).

DISCUSSION

We found that a rectosigmoid endometriosis nodule thickness greater than 5.20 mm measured by RS-EUS might be a predictive factor for the need for patch or segmental resection in rectosigmoid endometriosis with a sensitivity of 76% and a specificity of 81%. In addition, although the result was not significant, there was a trend for width to predict the need for resection. Further investigations with more patients should be conducted to confirm this finding, and width could appear as another independent predictive factor for resection.

It was previously demonstrated that RS-EUS exhibits good performance for detection and evaluation of rectosigmoid endometriosis with good sensitivity and negative predictive value[11]. However, RS-EUS remains a third-line exam, and its priority among examinations should be reevaluated. Other technics were also evaluated in detecting and characterizing deep infiltrating endometriosis nodules such as transvaginal ultrasonography, MRI and colonoscopy.

Nowadays, transvaginal ultrasonography has been well studied and experiences great performance in detecting and characterizing rectosigmoid endometriosis nodules and their digestive wall infiltration. In a study par Goncalves *et al*[4] this exam showed indeed sensitivity and a specificity of 97% and 100% respectively. Although, performance drops when detecting an infiltration of the submucosae with sensitivity between 62% and 83%[12]. This might explain why it has never been studied as a predictive factor for the surgery needed such as we did for RS-EUS.

Some new ultrasound techniques were also evaluated for the diagnosis of deep infiltrating endometriosis. Guerriero *et al*[13] compared the diagnostic accuracy of 2-Dimensions ultrasound (DUS) and 3-DUS in patients with deep infiltrating endometriosis confirmed surgically. They showed no significant difference regarding sensitivity, specificity, NPV and PPV between techniques for the intestinal location. Nevertheless, they used transvaginal ultrasound and, to our knowledge, there is no such study comparing the diagnostic accuracy of 2D and 3D RS-EUS. This could be the subject of further researches.

Another interesting study by Bergamini *et al*[14] compared the diagnostic accuracy of RS-EUS with Transvaginal Sonography with Water-Contrast in the Rectum (RWC-TVS) in the diagnosis of rectosigmoid endometriosis, confirmed by surgical and pathological findings. In this study RWC-TVS appeared to have better diagnostic performance than RS-EUS but the difference wasn't significant with sensitivity,

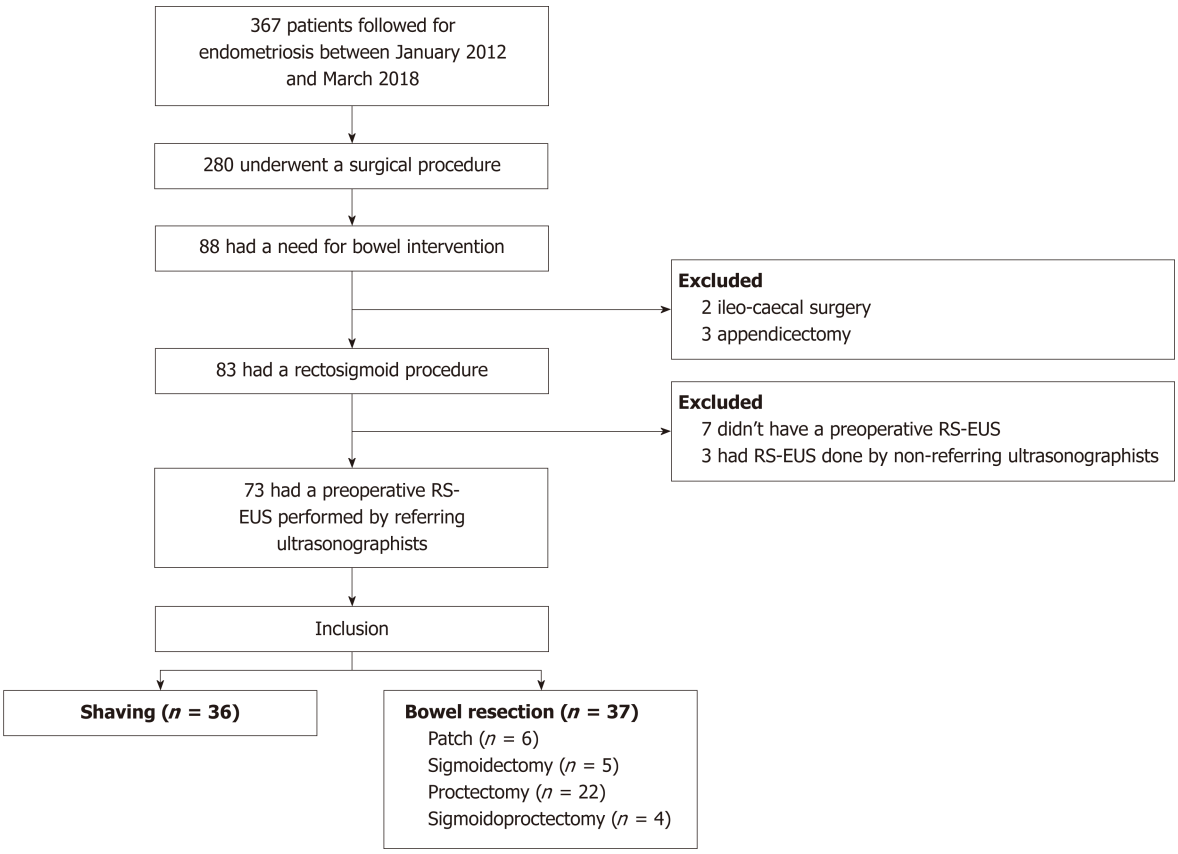

Figure 3 Flow chart. RS-EUS: Rectosigmoid endoscopic ultrasonography.

specificity, PPV and NPV of 96%, 90%, 98% and 81.8% and 88.2%, 80%, 95.7% and 57.1% respectively. However, this time again, they only studied the diagnostic accuracy of the exam and not its performance as a pretherapeutic test as we decided to do in our study. Similarly, this could be an interesting subject for further investigations.

Many other ultrasound techniques have also been studied in the diagnosis of intestinal endometriosis such as elastosonography[15], but none of them has been evaluated as a pretherapeutic test. Colonoscopy has also been studied but cannot be routinely performed for the diagnosis of intestinal endometriosis, giving poor outcomes to this exam with a sensitivity of 7% and a specificity of 85%, due to the paucity of lesions affecting the intestinal mucosa[16]. Regarding MRI, our study completes the recent findings concerning MRI measures of stenosis and long axis to predict the need for bowel resection In this study, a nodule's short axis of 11 mm or more was a predictor for bowel resection with a sensitivity and a specificity of 93% and 99% respectively. Similarly, a bowel stenosis of 30% or more experienced a sensitivity of 95% and a specificity of 99% in predicting the need for a bowel resection[9]. Nevertheless, MRI colonography was a required parameter of this study, and this technique is only available in a limited number of centers. In comparison, RS-EUS is a common, easily accessible exam and is currently well evaluated in the staging of deep infiltrating endometriosis with better sensitivity and negative predictive value compared with MRI[17]; this finding indicates that MRI exams do not detect nodules that are detectable by RS-EUS. More precisely, RS-EUS experiences better sensitivity (79% *vs* 47%) and negative predictive value (71% *vs* 63%) than MRI when detecting a mucosal or submucosal involvement[18]. Therefore, RS-EUS appears to be more adequate in the preoperative evaluation of rectosigmoid endometriosis.

Another study demonstrated the interest of the presence of an infiltration of the muscular layer to determine whether bowel resection was needed[19]. In this study, lesion and infiltration characteristics were analyzed retrospectively on the surgical piece. In our study, information on rectosigmoid endometriosis nodules was collected prospectively before the surgical procedure. As mentioned above, the choice of the surgical procedure is actually based on clinical findings and local conditions. Nevertheless, the place for clinical findings in the decision path remains unclear. Indeed, another study by Wattiez *et al*[20] did not take into account the clinical manifestations of the disease to select the surgical procedure. However, our study

Table 1 Patient characteristics

	Shaving (*n* = 36)	Resection (*n* = 37)	*P* value
Age			0.424[1]
n (%)	36 (100)	37 (100)	
Mean (SD)	32.42 (6.57)	33.54 (5.32)	
Body mass index			0.656[1]
n (%)	34 (94)	35 (95)	
Mean (SD)	23.83 (3.96)	24.31 (4.83)	
Pregnancy			0.914[3]
n (%)	36 (100)	35 (95)	
0 (*n*)	22	24	
1 (*n*)	5	5	
2 (*n*)	6	4	
≥ 3 (*n*)	3	2	
Parity			0.568[3]
n (%)	36 (100)	35 (95)	
0 (*n*)	25	26	
1 (*n*)	4	6	
2 (*n*)	6	3	
≥ 3 (*n*)	1	0	
Preoperative medical treatment			0.732[3]
n (%)	36 (100)	37 (100)	
None	1	3	
Progestin	16	16	
GnRH analog	20	18	
Estrogen	3	6	
≥ 2 treatments	4	6	
Symptoms of rectosigmoid endometriosis			
Dyschezia			0.020[2]
n (%)	29 (81)	34 (92)	
None to mild	16	9	
Moderate to severe	13	25	
Transit disorders			0.893[2]
n (%)	29 (81)	32 (86)	
None to mild	14	16	
Moderate to severe	15	16	
Vomiting			1.00[3]
n (%)	29 (81)	31 (84)	
None to mild	27	28	
Moderate to severe	2	3	
Rectal Bleeding			0.237[3]
n (%)	30 (83)	29 (78)	
None to mild	30	27	
Moderate to Severe	0	2	
Abdominal pain			0.943[2]
n (%)	32 (89)	33 (89)	
None to mild	8	8	
Moderate to severe	24	25	

[1]Student *t*-test.
[2]Chi-square test.
[3]Fisher exact test.

brings to light the possibility of some specific symptoms, such as dyschezia, to aid in the selection of the surgical procedure, and other studies should be performed to

Table 2 Univariate analysis for characteristics of the lesions on rectosigmoid endoscopic ultrasonography

	Shaving (*n* = 36)	Resection (*n* = 37)	*P* value
Thickness			< 0.0001[1]
n (%)	36(100)	37(100)	
Mean (SD)	4.22 (1.90)	6.81 (2.61)	
Width			< 0.0001[1]
n (%)	36 (100)	36 (97)	
Mean (SD)	13.70 (5.29)	19.10 (5.53)	
Bump			0.261[3]
n (%)	36 (100)	37 (100)	
Presence (%)	2 (5.6)	6 (16)	
Submucosae infiltration			0.007[2]
n (%)	36 (100)	37 (100)	
Presence (%)	2 (5.6)	11 (30)	
Multiple lesions			0.358[3]
n (%)	36 (100)	37 (100)	
Presence (%)	1 (2.8)	4 (11)	

[1]Student *t*-test.
[2]Chi-square test.
[3]Fisher exact test.

evaluate the accuracy of the physical examination in this situation. Currently, RS-EUS is a third-line exam in the evaluation of deep infiltrating endometriosis[8]. However, our study suggests the possible use of RS-EUS as one of the first exams performed. Indeed, RS-EUS is an easy access exam with good diagnostic performance in endometriosis. It is also now clear that RS-EUS provides some important information on the extent of the disease and the local conditions to select the correct surgical procedure.

Our study has some strengths. First, this is the first study to evaluate the accuracy of RS-EUS before surgical procedure in rectosigmoid endometriosis. Second, RS-EUS was performed by two expert ultrasonographists working in two different centers, reducing the risk of evaluation bias. Similarly, no classification bias was noted between the operators, highlighting the reproducibility of RS-EUS in the evaluation of rectosigmoid endometriosis. Finally, all surgical procedures were realized by the same trained surgeon (AF) familiar with endometriosis procedures and preoperative management. This study has also some limitations. This is a retrospective study with a small patient sample. Prospective, multicentric studies should be performed to confirm our results. We decided to classify patients who did not experience worsening symptoms during periods as "none". This system could have misclassified some patients with milder clinical manifestations and biased the results. Finally, our study has some implications as it reveals new interest in the realization of preoperative RS-EUS in deep infiltrating endometriosis. This information might help a surgeon to organize the procedure given that digestive resection must be performed by a multidisciplinary team. RS-EUS could also facilitate the transmission of appropriate information to the patient, defining the benefits and risks of the procedure.

In conclusion, in our retrospective study, we found that an endometriosis nodule greater than 5.20 mm thick might predict the need for bowel resection in rectosigmoid endometriosis. A trend concerning width to predict the need for resection was also observed. Further investigations, such as prospective studies, should be conducted to confirm these results.

Table 3 Logistic regression for significant variables after multiple imputation for missing data

	OR	95%CI	*P* value
Thickness	1.49	1.04-2.12	0.028
Width	1.12	1.00-1.26	0.054
Submucosae infiltration	1.97	0.31-12.66	0.475

OR: Odds ratio; CI: Confidence interval.

Table 4 Receiver operating characteristic analysis for thickness

Cut-off (mm)	Sensibility	Specificity	PPV	NPV	Overall accuracy
0.9	1.00	0.03	0.51	1.00	0.52
5.2	0.76	0.81	0.80	0.76	0.78
10.0	0.05	1.00	1.00	0.51	0.52

PPV: Positive predictive value; NPV: Negative predictive value.

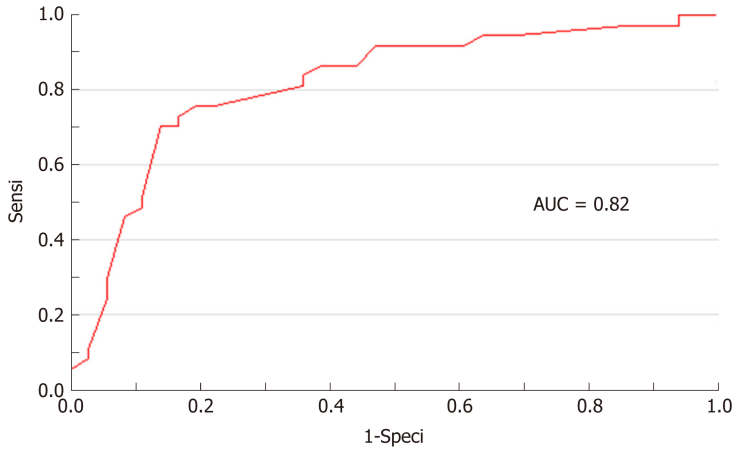

Figure 4 Receiver operating characteristic curve of nodule thickness. AUC: Area under curve.

ARTICLE HIGHLIGHTS

Research background

Rectosigmoid endometriosis is an underdiagnosed disease responsible for digestive disorders. Two surgical approaches, rectosigmoid bowel resection (segmental or patch) or intramuscular layer dissection (shaving), are available. Nowadays, the choice is led by a conjunction of clinical and radiological findings without strict criteria. A recent study has shown that a pre-operative magnetic resonance imaging (MRI) colonography might predict the need for bowel resection in rectosigmoid endometriosis. However, it has previously been demonstrated that rectosigmoid endoscopic ultrasonography (RS-EUS) exhibits better sensitivity and negative predictive value than MRI in the diagnosis of rectosigmoid endometriosis.

Research motivation

To assess whether the characteristics of endometriosis lesions evaluated on a preoperative RS-EUS could predict the need for bowel resection in rectosigmoid endometriosis for a better optimization of the preoperative management of the patient.

Research objectives

To assess whether the lesion features observed *via* preoperative RS-EUS might predict the need for bowel resection.

Research methods

This multicentric retrospective study was conducted on a cohort of patients with rectosigmoid endometriosis who underwent a curative surgical procedure, evaluated by RS-EUS performed by two trained operators, between January 2012 and March 2018. In this cohort, data were

collected prospectively when patients were suspected of having endometriosis. RS-EUS features evaluated were thickness, width, infiltration of the submucosae, presence of a bump into the digestive lumen and presence of multiple rectosigmoid localizations All the surgical interventions were performed by one well trained gynecologic surgeon *via* open laparoscopy. Shaving was preferred any time it was possible based on the nodule characteristics. This procedure was typically performed on unique and small lesions without submucosae involvement. A univariate statistical analysis was performed on nodules' RS-EUS features followed by multivariate logistic regression on significant results.

Research results

In total, 367 women were followed for endometriosis and included in the cohort between January 2012 and March 2018. 73 patients met the inclusion criteria and were included in the analysis, in two groups: Shaving (36 patients) and bowel resection (37 patients). In univariate analysis thickness ($P < 0.001$), width $P < 0.001$) and infiltration of the submucosae ($P = 0.007$) experienced significant results. After multivariate logistic regression only thickness appeared to be significant with an odds ratio (OR) = 1.49 [95% confidence interval (CI) 1.04-2.12, $P = 0.028$]. Nevertheless, a sensible trend regarding width was identified. Specifically, width was increased in the resection group compared with the shaving group (OR 1.12, CI95% 1.00-1.26, $P = 0.054$). Based on receiver operating characteristic analysis, a thickness greater than 5.20 mm was the best threshold to determine the need for digestive resection with a sensitivity of 76%, a specificity of 81%, and a positive predictive value and negative predictive value of 0.80 and 0.76, respectively.

Research conclusions

We found that an endometriosis nodule greater than 5.20 mm thick might predict the need for bowel resection in rectosigmoid endometriosis. This is the first study to evaluate the accuracy of RS-EUS before surgical procedure in rectosigmoid endometriosis. It has some implications as it reveals new interest in the realization of preoperative RS-EUS in deep infiltrating endometriosis. This information might help surgeons to organize procedures in a multidisciplinary team. Although, our work has also some limitations, mainly because of its retrospective design with small patient samples.

Research perspectives

Further investigations, such as prospective, multicentric studies, have to be conducted to confirm our results.

REFERENCES

1 **Giudice LC**, Kao LC. Endometriosis. *Lancet* 2004; **364**: 1789-1799 [PMID: 15541453 DOI: 10.1016/S0140-6736(04)17403-5]
2 **Williams TJ**, Pratt JH. Endometriosis in 1,000 consecutive celiotomies: Incidence and management. *Am J Obstet Gynecol* 1977; **129**: 245-250 [PMID: 900194 DOI: 10.1016/0002-9378(77)90773-6]
3 **Parasar P**, Ozcan P, Terry KL. Endometriosis: Epidemiology, Diagnosis and Clinical Management. *Curr Obstet Gynecol Rep* 2017; **6**: 34-41 [PMID: 29276652 DOI: 10.1007/s13669-017-0187-1]
4 **Goncalves MO**, Podgaec S, Dias JA, Gonzalez M, Abrao MS. Transvaginal ultrasonography with bowel preparation is able to predict the number of lesions and rectosigmoid layers affected in cases of deep endometriosis, defining surgical strategy. *Hum Reprod* 2010; **25**: 665-671 [PMID: 20023291 DOI: 10.1093/humrep/dep433]
5 **Canon B**, Collinet P, Piessen G, Rubod C. Résection rectale segmentaire et shaving rectal laparoscopiques pour endométriose: Morbidité péri-opératoire. *Gynécologie Obstétrique Fertil* 2013; **41**: 275-281 [DOI: 10.1016/j.gyobfe.2013.02.005]
6 **Roman H**, Vassilieff M, Tuech JJ, Huet E, Savoye G, Marpeau L, Puscasiu L. Postoperative digestive function after radical versus conservative surgical philosophy for deep endometriosis infiltrating the rectum. *Fertil Steril* 2013; **99**: 1695-1704 [PMID: 23465818 DOI: 10.1016/j.fertnstert.2013.01.131]
7 **Donnez O**, Roman H. Choosing the right surgical technique for deep endometriosis: Shaving, disc excision, or bowel resection? *Fertil Steril* 2017; **108**: 931-942 [PMID: 29202966 DOI: 10.1016/j.fertnstert.2017.09.006]
8 Prise en charge de l'endométriose - Recommandations HAS France. In: Haute Autorité de Santé [Internet]. Available from: https://www.has-sante.fr/portail/plugins/ModuleXitiKLEE/types/FileDocument/doXiti.jsp?id=c_2820459.
9 **Scardapane A**, Lorusso F, Francavilla M, Bettocchi S, Fascilla FD, Angelelli G, Scioscia M. Magnetic Resonance Colonography May Predict the Need for Bowel Resection in Colorectal Endometriosis. *Biomed Res Int* 2017; **2017**: 5981217 [PMID: 29147655 DOI: 10.1155/2017/5981217]
10 **Alborzi S**, Rasekhi A, Shomali Z, Madadi G, Alborzi M, Kazemi M, Hosseini Nohandani A. Diagnostic accuracy of magnetic resonance imaging, transvaginal, and transrectal ultrasonography in deep infiltrating endometriosis. *Medicine (Baltimore)* 2018; **97**: e9536 [PMID: 29465552 DOI: 10.1097/MD.0000000000009536]
11 **Delpy R**, Barthet M, Gasmi M, Berdah S, Shojai R, Desjeux A, Boubli L, Grimaud JC. Value of endorectal ultrasonography for diagnosing rectovaginal septal endometriosis infiltrating the rectum. *Endoscopy* 2005; **37**: 357-361 [PMID: 15824947 DOI: 10.1055/s-2005-861115]
12 **Hudelist G**, Tuttlies F, Rauter G, Pucher S, Keckstein J. Can transvaginal sonography predict infiltration depth in patients with deep infiltrating endometriosis of the rectum? *Hum Reprod* 2009; **24**: 1012-1017 [PMID: 19221097 DOI: 10.1093/humrep/dep014]
13 **Guerriero S**, Alcázar JL, Pascual MA, Ajossa S, Perniciano M, Piras A, Mais V, Piras B, Schirru F, Benedetto MG, Saba L. Deep Infiltrating Endometriosis: Comparison Between 2-Dimensional Ultrasonography (US), 3-Dimensional US, and Magnetic Resonance Imaging. *J Ultrasound Med* 2018; **37**: 1511-1521 [PMID: 29193230 DOI: 10.1002/jum.14496]

14 **Bergamini V**, Ghezzi F, Scarperi S, Raffaelli R, Cromi A, Franchi M. Preoperative assessment of intestinal endometriosis: A comparison of transvaginal sonography with water-contrast in the rectum, transrectal sonography, and barium enema. *Abdom Imaging* 2010; **35**: 732-736 [PMID: 20364253 DOI: 10.1007/s00261-010-9610-z]

15 **Mezzi G**, Ferrari S, Arcidiacono PG, Di Puppo F, Candiani M, Testoni PA. Endoscopic rectal ultrasound and elastosonography are useful in flow chart for the diagnosis of deep pelvic endometriosis with rectal involvement. *J Obstet Gynaecol Res* 2011; **37**: 586-590 [PMID: 21159047 DOI: 10.1111/j.1447-0756.2010.01413.x]

16 **Milone M**, Mollo A, Musella M, Maietta P, Sosa Fernandez LM, Shatalova O, Conforti A, Barone G, De Placido G, Milone F. Role of colonoscopy in the diagnostic work-up of bowel endometriosis. *World J Gastroenterol* 2015; **21**: 4997-5001 [PMID: 25945014 DOI: 10.3748/wjg.v21.i16.4997]

17 **Roseau G**. Recto-sigmoid endoscopic-ultrasonography in the staging of deep infiltrating endometriosis. *World J Gastrointest Endosc* 2014; **6**: 525-533 [PMID: 25400866 DOI: 10.4253/wjge.v6.i11.525]

18 **Kim A**, Fernandez P, Martin B, Palazzo L, Ribeiro-Parenti L, Walker F, Bucau M, Collinot H, Luton D, Koskas M. Magnetic Resonance Imaging Compared with Rectal Endoscopic Sonography for the Prediction of Infiltration Depth in Colorectal Endometriosis. *J Minim Invasive Gynecol* 2017; **24**: 1218-1226 [PMID: 28802956 DOI: 10.1016/j.jmig.2017.07.026]

19 **Abrão MS**, Podgaec S, Dias JA, Averbach M, Silva LF, Marino de Carvalho F. Endometriosis lesions that compromise the rectum deeper than the inner muscularis layer have more than 40% of the circumference of the rectum affected by the disease. *J Minim Invasive Gynecol* 2008; **15**: 280-285 [PMID: 18439498 DOI: 10.1016/j.jmig.2008.01.006]

20 **Wattiez A**, Puga M, Albornoz J, Faller E. Surgical strategy in endometriosis. *Best Pract Res Clin Obstet Gynaecol* 2013; **27**: 381-392 [PMID: 23340291 DOI: 10.1016/j.bpobgyn.2012.12.003]

P- Reviewer: Jiang QP, Milone M, Richardson WS, Santoro GA

S- Editor: Yan JP **L- Editor:** A **E- Editor:** Yin SY

World Journal of Gastroenterology

Submit a Manuscript: https://www.f6publishing.com

World J Gastroenterol 2019 February 14; 25(6): 707-718

DOI: 10.3748/wjg.v25.i6.707

ISSN 1007-9327 (print) ISSN 2219-2840 (online)

ORIGINAL ARTICLE

Retrospective Study

Short- and long-term outcomes of endoscopically treated superficial non-ampullary duodenal epithelial tumors

Yuko Hara, Kenichi Goda, Akira Dobashi, Tomohiko Richard Ohya, Masayuki Kato, Kazuki Sumiyama, Takehiro Mitsuishi, Shinichi Hirooka, Masahiro Ikegami, Hisao Tajiri

ORCID number: Yuko Hara (0000-0001-8288-7730); Kenichi Goda (0000-0002-0350-3151); Akira Dobashi (0000-0002-4882-3220); Tomohiko Richard Ohya (0000-0002-4106-0355); Masayuki Kato (0000-0002-9715-2902); Kazuki Sumiyama (0000-0002-7976-6070); Takehiro Mitsuishi (0000-0002-3679-6616); Shinichi Hirooka (0000-0002-0721-5704); Masahiro Ikegami (0000-0002-0036-4109); Hisao Tajiri (0000-0002-5175-8685).

Author contributions: All authors helped to perform the research; Hara Y, Goda K, Dobashi A, and Ohya TR performed the endoscopic procedure; Hara Y and Kato M analyzed and interpreted the data; Hara Y drafted the article; Goda K designed the research; Dobashi A, Ohya TR, Mistuishi T and Hirooka S collected the data; Mistuishi T and Hirooka S performed the pathological diagnosis; Hara Y, Goda K, Sumiyama K, Ikegami M and Tajiri H contributed to critical revision of the article for important intellectual content; Tajiri H provided the final approval for this article.

Institutional review board statement: This study protocol was approved by the Institutional Review Board of the Jikei University School of Medicine, Tokyo, Japan, for clinical research [Registration No.: 29-079 (8695)].

Informed consent statement: This study was a retrospective observational study and carried

Yuko Hara, Akira Dobashi, Tomohiko Richard Ohya, Kazuki Sumiyama, Department of Endoscopy, The Jikei University School of Medicine, Tokyo 105-8461, Japan

Kenichi Goda, Department of Gastroenterology, Dokkyo Medical University, Tochigi 321-0293, Japan

Masayuki Kato, Department of Endoscopy, The Jikei University Katsushika Medical Center, Tokyo 125-8506, Japan

Takehiro Mitsuishi, Shinichi Hirooka, Masahiro Ikegami, Department of Pathology, The Jikei University School of Medicine, Tokyo 105-8461, Japan

Hisao Tajiri, Department of Innovative Interventional Endoscopy Research, The Jikei University School of Medicine, Tokyo 105-8461, Japan

Corresponding author: Yuko Hara, MD, Research Associate, Department of Endoscopy, The Jikei University School of Medicine, 3-25-8 Nishi Shinbashi, Minato-ku, Tokyo 105-8461, Japan. yukohara0526@yahoo.co.jp
Telephone: +81-3-34331111-3181
Fax: +81-3-34594524

Abstract

BACKGROUND

It is widely recognized that endoscopic resection (ER) of superficial non-ampullary duodenal epithelial tumors (SNADETs) is technically challenging and may carry high risks of intraoperative and delayed bleeding and perforation. These adverse events could be more critical than those occurring in other levels of the gastrointestinal tract. Because of the low prevalence of the disease and the high risks of severe adverse events, the curability including short- and long-term outcomes have not been standardized yet.

AIM

To investigate the curability including short- and long-term outcomes of ER for SNADETs in a large case series.

METHODS

This retrospective study included cases that underwent ER for SNADETs at our university hospital between March 2004 and July 2017. Short-term outcomes of ER were measured based on *en bloc* and R0 resection rates as well as adverse events. Long-term outcomes included local recurrence detected on endoscopic

out by the opt-out method to post a purpose in the Jikei University School of Medicine. Patients were not required to give informed consent for the study because the analysis used anonymous clinical data that were obtained after each patient agreed to treatment by written consent. For full disclosure, the details of the study are mentioned in the opt-put document in the Jikei University School of Medicine.

Conflict-of-interest statement: All authors declare no conflicts of interest related to this article.

Data sharing statement: No additional data are available.

Manuscript source: Unsolicited manuscript

Received: October 13, 2018
Peer-review started: October 14, 2018
First decision: November 7, 2018
Revised: December 31, 2018
Accepted: January 9, 2019
Article in press: January 9, 2019
Published online: February 14, 2019

surveillance and disease-specific mortality in patients followed up for ≥ 12 mo after ER.

RESULTS

In the study, 131 patients with 147 SNADETs were analyzed. The 147 ERs consisted of 136 endoscopic mucosal resections (EMRs) (93%) and 11 endoscopic submucosal dissections (ESDs) (7%). The median tumor diameter was 10 mm. The pathology diagnosis was adenocarcinoma (56/147, 38%), high-grade intraepithelial neoplasia (44/147, 30%), or low-grade intraepithelial neoplasia (47/147, 32%). The R0 resection rate was 68% (93/136) in the EMR group and 73% (8/11) in the ESD group, respectively. Cap-assisted EMR (known as EMR-C) showed a higher rate of R0 resection compared to the conventional method of EMR using a snare (78% *vs* 62%, $P = 0.06$). No adverse event was observed in the EMR group, whereas delayed bleeding, intraoperative perforation, and delayed perforation in 3, 3, and 5 patients occurred in the ESD group, respectively. One patient with perforation required emergency surgery. In the 43 mo median follow-up period, local recurrence was found in four EMR cases and all cases were treated endoscopically. No patient died due to tumor recurrence.

CONCLUSION

Our findings suggest that ER provides good long-term outcomes in the patients with SNADETs. EMR is likely to become the safe and reliable treatment for small SNADETs.

Key words: Duodenal adenoma; Duodenal cancer; Endoscopic resection; Endoscopic submucosal dissection; Long-term outcome

Core tip: Endoscopic resection (ER) in the duodenum remains a challenging technique owing to the anatomical peculiarity associated with the procedure and the high frequency of adverse events. This study aimed to investigate the curability, including long-term outcomes, related to ER for superficial non-ampullary duodenal epithelial tumors (SNADETs) in a large case series. In contrast to endoscopic submucosal dissection (ESD), endoscopic mucosal resection (EMR) was not associated with any adverse events. Nevertheless, ER is expected to provide good long-term outcomes in patients with SNADETs. In conclusion, EMR should be considered as standard treatment for small lesions of SNADETs; however, ESD remains challenging.

Citation: Hara Y, Goda K, Dobashi A, Ohya TR, Kato M, Sumiyama K, Mitsuishi T, Hirooka S, Ikegami M, Tajiri H. Short- and long-term outcomes of endoscopically treated superficial non-ampullary duodenal epithelial tumors. *World J Gastroenterol* 2019; 25(6): 707-718
URL: https://www.wjgnet.com/1007-9327/full/v25/i6/707.htm
DOI: https://dx.doi.org/10.3748/wjg.v25.i6.707

INTRODUCTION

Primary duodenal cancer is one of the gastrointestinal tumors with a low frequency of occurrence. Its prevalence rate in necropsy cases is reported to be 0.02%-0.5%[1]. Precancerous lesions, duodenal adenomas, are also rare and reported in approximately 0.1%-0.4% of patients who have undergone an esophagogastroduodenoscopy[2,3]. Previous studies showed that the 5-yr survival rate of patients with duodenal cancer was less than 30%[4]. Duodenal cancer has the poorest prognosis among cancers of all parts of the small intestine because most cases are detected at a far-advanced stage[4]. Additionally, since the duodenum is adjacent to important organs, such as the pancreas, gallbladder and liver, invasion or spread to these organs will be a factor of poor prognosis. Early detection and treatment of duodenal cancer will be necessary to improve patient prognosis. It, however, remains unknown about the clinical course of those patients who have early-stage cancer and adenomas in the duodenum.

Among duodenal tumors, epithelial tumors located at the ampullary site are

classified as biliary tract tumors[5]. The ampullary tumors are different from non-ampullary tumors in endoscopic diagnosis and treatment. In the previous study, superficial non-ampullary duodenal epithelial tumors (SNADETs; as adenoma or mucosal/submucosal carcinoma located outside the ampullary region) are considered an indication of endoscopic resection (ER) because of a low risk of lymph node metastasis[6-8].

ER for SNADET is a challenging technique compared to other gastrointestinal tracts because of the following reasons. First, the anatomical features, a narrow lumen and precipitous curvature of the duodenum, can provide inadequate view and make it difficult to maintain stable view of the endoscope. Second, Brunner's glands in the submucosal layer can stiffen the duodenal wall; therefore, mucosal lifting is poor at submucosal injection, making ER more difficult, especially for the macroscopically depressed type of tumors. The muscular layer of the duodenum is very thin and this increases the risk of perforation[9].

Due to the rarity of SNADETs and the difficulty of ER, there have been few large-scale studies including more than 100 cases conducted to evaluate treatment outcomes of ER in patients with SNADETs. Therefore, this study aimed to investigate the short- and long-term outcomes of ER with more than 100 cases of SNADET to evaluate the safety, efficacy, and curability of the endoscopic treatment.

MATERIALS AND METHODS

This retrospective study included the patients who underwent ER for SNADETs in a single-center at Jikei University Hospital between March 2004 and April 2017, and who met the following criteria: (1) newly diagnosed SNADET that included adenomas of low/high-grade intraepithelial neoplasia (LGIN/HGIN) and superficial adenocarcinomas in which invasion was confined to the submucosal layer; and (2) no lymph node or distant organ metastasis. This study protocol was approved by the Institutional Review Board of the Jikei University School of Medicine, Tokyo, Japan, for clinical research [Registration No.: 29-079 (8695)]. This study was conducted in compliance with the revised Helsinki Declaration (1989).

Indications for ER

Indications for ER were defined as follows: (1) histologically diagnosed as adenoma with HGIN or adenocarcinoma by endoscopic biopsy; and (2) tumor lesions of macroscopic type 0-I and 0-IIa > 10 mm or type 0-IIc > 5 mm in diameter, which were endoscopically suspected as HGIN or superficial adenocarcinoma based on results of our previous study[6,10,11]. Lesions were suspected as HGIN or superficial adenocarcinoma when they showed a reddish area on white light endoscopy or an obscure mucosal pattern or network vascular pattern on magnifying endoscopy with narrow-band imaging[6,11].

Endoscopic procedures

Endoscopic submucosal dissection (ESD) was mainly performed for lesions ≥ 20 mm in diameter, and endoscopic mucosal resection (EMR) was performed for lesions < 20 mm in diameter. EMR was performed under conscious sedation using pethidine hydrochloride (Takeda Pharmaceutical Co., Ltd., Osaka, Japan) and flunitrazepam (Eisai Co., Ltd., Tokyo, Japan) and ESD was performed under general anesthesia. When performing EMR, 10% glycerin solution (Glycerol; Chugai Pharmaceutical Co., Ltd., Tokyo, Japan) with a minute amount of indigo carmine dye was used for submucosal injection to lift up the superficial lesion. When performing ESD, 0.4% sodium hyaluronate (MucoUp; Boston Scientific Japan Co., Tokyo, Japan) was injected into the submucosal layer to obtain adequate and sustained submucosal elevation.

Two types of EMR were performed. Basically, a conventional method of EMR was performed using a snare (EMR-S) mainly for elevated lesions, and "EMR-C" method was performed mainly for depressed-type lesions. EMR-C is an aspiration resection method using a medium-sized transparent plastic cap (MAJ-296, 16.1 mm; Olympus, Tokyo, Japan). A "suck and shake" method was used for this procedure to avoid perforation, as shown in Figure 1. If *en bloc* resection was not achieved in the initial resection, additional resection using the snare was performed to remove the residual portion of the lesion. Otherwise, coagulation method using either hot-biopsy forceps (Olympus, Tokyo, Japan) or argon plasma coagulation (VIO300D; ERBE Elektromedizin, Tubingen, Germany) was occasionally carried out when minute tumor remained[12,13]. A dual knife and hook knife (KD-650L and KD-620LR, respectively; Olympus) were used for ESD (Figure 2). We tried to completely close or cover mucosal defects by clip closure or tissue shielding methods in all EMR and ESD cases to prevent delayed bleeding and delayed perforation[14,15].

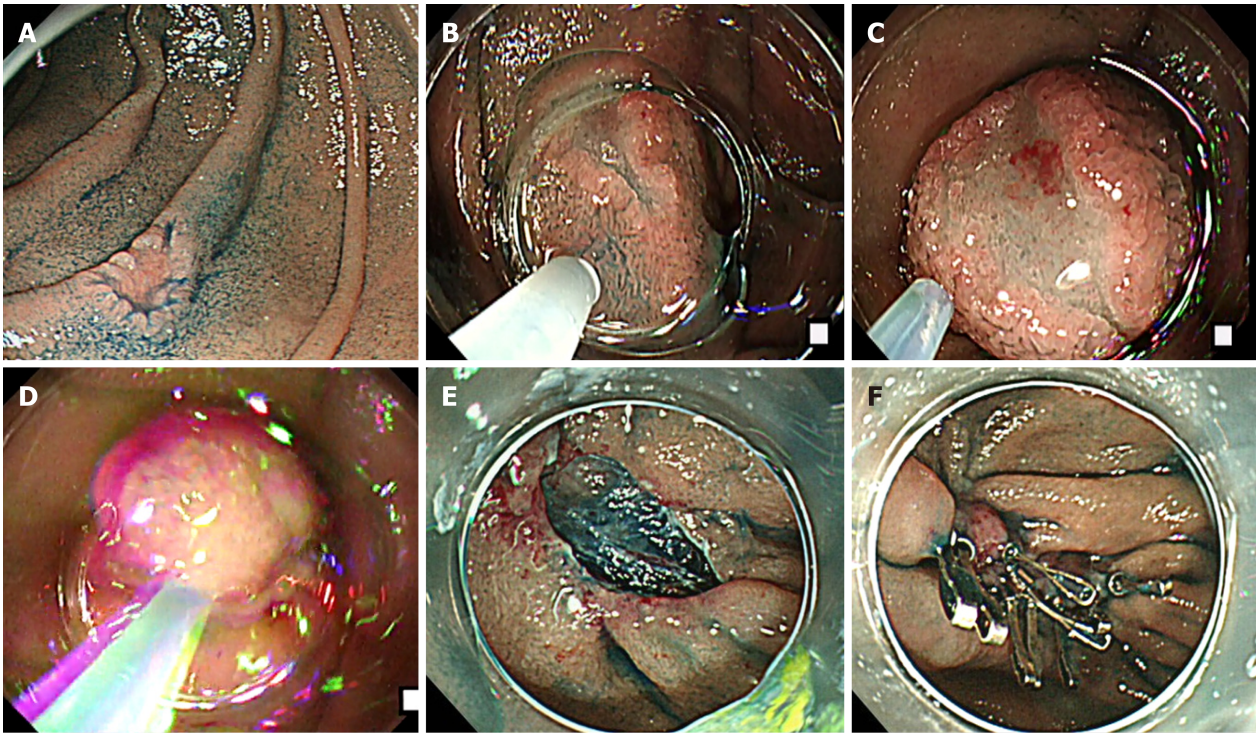

Figure 1 The cap-assisted endoscopic mucosal resection method of superficial non-ampullary duodenal epithelial tumor. This is the "suck and shake" technique. Type 0-IIc lesion, 10 mm × 5 mm, mucosal carcinoma, cut-end negative. A: Indigo carmine spraying view. Depressed-type lesion was located in the second portion of the duodenum; B: Injecting the glycerol into submucosal layer; C: Sucking the lesion; D: Shaking the lesion to prevent muscle layer involvement; E: Ulcer findings just after lesion removal. The lesion was resected *en bloc*, and there was no bleeding or perforation in the ulcer just after the procedure; F: Closing the ulcer floor completely by clip to prevent delayed bleeding and perforation.

All patients were admitted to our hospital and remained nil per os for 48 h. On day 2, patients were provided with a liquid diet and patients with an unremarkable postoperative course were discharged from the hospital on day 7 after ER.

Adverse events

Delayed bleeding was defined as a postoperative decrease in hemoglobin level of > 2.0 g/dL[16]. Delayed perforation was defined by the presence of free air on postoperative computed tomography (CT), with severe abdominal pain in patients without intraoperative macroscopic perforation.

Surveillance after ER

Patients underwent an initial follow-up endoscopy at 2 mo after ER. Thereafter, endoscopic surveillance was performed at 6 mo or 12 mo intervals. If a residual tumor was suspected, a biopsy was performed and the tissue obtained was examined histologically. We conducted a CT at 12 mo interval to detect metastasis in the patients with mucosal adenocarcinoma. If the pathology diagnosis was submucosal carcinoma (SMC), additional surgical local resection of duodenum was performed. If a patient was referred to another hospital after ER, a telephone survey with the referred physician was conducted to ascertain the date of the last endoscopic follow-up, tumor recurrence status, and survival status.

Pathology diagnosis

Pathology diagnosis was established by two expert gastrointestinal pathologists (SH, TM) who were blinded to the endoscopic finding. As aforementioned, SNADETs were histologically defined as adenoma and superficial adenocarcinoma consisting of mucosal carcinoma (MC) and SMC. The grade of atypia of all tumors was estimated in the highest atypical region and was categorized according to the World Health Organization (commonly known as WHO) 2010 classification[17], consisting of LGIN, HGIN, MC, and SMC[18]. The final diagnosis was established with endoscopically or surgically resected specimens when the diagnosis of resected specimens was different from that of preoperatively biopsied specimens[6].

Outcomes

The primary endpoint was the long-term outcome of endoscopically treated

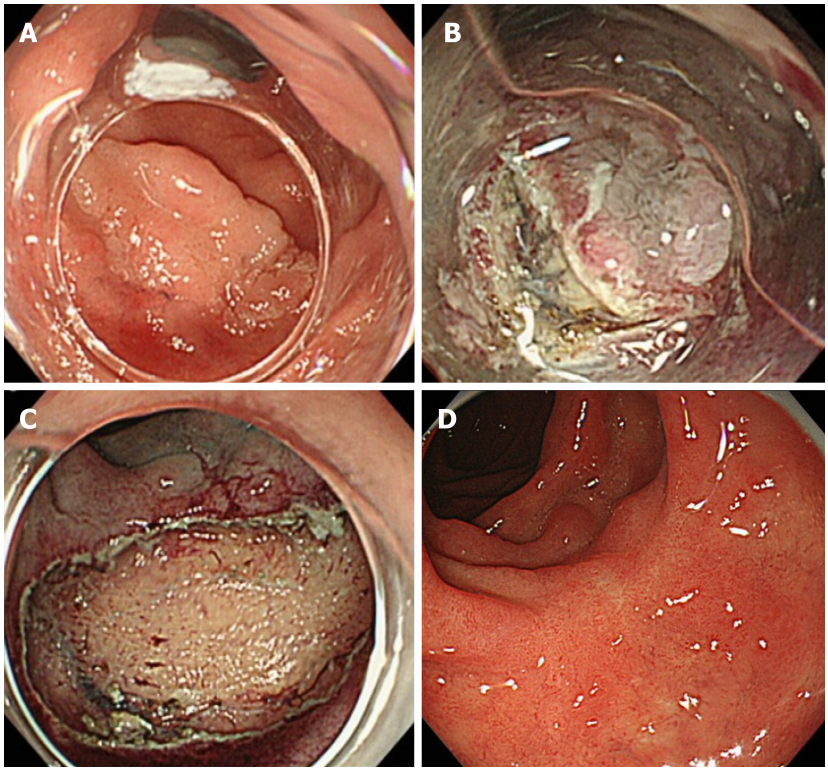

Figure 2 The endoscopic submucosal dissection method of superficial non-ampullary duodenal epithelial tumors. Type 0-IIa lesion, 25 mm × 25 mm, mucosal carcinoma, cut-end negative. A: Flat, elevated-type lesion was located in the second portion of the duodenum; B: Performing circumferential incision and submucosal dissection; C: Ulcer findings just after lesion removal. The lesion was resected *en bloc*, and there was no bleeding or perforation in the ulcer just after the procedure; D: After 2 mo of endoscopic submucosal dissection, the wound became a scar, and no residual tumor was found.

SNADETs, including local recurrence and disease-specific mortality, for patients who were under surveillance with an endoscopic observation for 12 mo or longer after ER. The secondary endpoint was short-term outcomes of ER including *en bloc* resection rates and R0 resection rates, and adverse events. Complete (R0) resection was defined as *en bloc* resection with tumor-free margins.

Statistical analysis

Continuous variables were expressed as median (interquartile range (IQR)) and were compared using Student's *t* test or the Mann-Whitney U test. The chi-square test or Fisher's exact test was used to compare data pertaining to categorical variables. A probability value (*P*-value) of < 0.05 was considered significant. Stata software version 14 (Stata Corp., College Station, TX, United States) was used for all statistical analyses.

RESULTS

One hundred and thirty-one patients with 147 SNADETs were analyzed. The patient and tumor characteristics are summarized in Table 1. Ninety-four of the one hundred and thirty-one patients (72%) were men, and the median age was 64 yr. Ninety (61%) and thirty-eight (26%) lesions of 147 SNADETs were located in the second portion and the third or fourth portion, respectively. The median tumor diameter was 10 mm. Thirty (20%), sixty-one (42%), and fifty-six (38%) lesions showed protruded (0-I), slightly elevated (0-IIa), and depressed (0-IIc) macroscopic type, respectively. Final histology showed that 47 (32%) were LGIN, 44 (30%) HGIN, 54 (37%) MC, and 2 (1%) SMC. EMR and ESD were performed for 136 (93%) and 11 (7%) SNADETs, respectively.

Table 2 shows the long-term outcomes of the 121 patients with 135 SNADETs who were under surveillance with an endoscopic observation for 12 mo or longer after ER. The median follow-up period was 43 mo (IQR: 24-60). Local recurrence was found in 4 EMR cases within 12 mo after ER. All recurrence lesions were initially treated by piecemeal EMR ($n = 2$) or *en bloc* EMR with RX ($n = 1$) or R1 ($n = 1$). Eventually, those lesions were completely treated endoscopically.

Table 1 Characteristics of patients and tumors

Patients, *n* = 131		**Value**
Male, *n* (%)		94 (72)
Age, median (IQR), yr		64 (57-70)
Tumors, *n* = 147		**Value**
Location, *n*		
	First/second/third or fourth	19/90/38
	Tumor diameter, median (IQR), mm	10 (7-15)
Macroscopic type[1], *n*		
	0-I / 0-IIa / 0-IIc	30/61/56
Treatment, *n*		
	EMR/ESD	136/11
Histology, *n*		
	LGIN/HGIN/MC/SMC	47/44/54/2

[1]Predominant macroscopic type.
IQR: Interquartile range; EMR: Endoscopic mucosal resection; ESD: Endoscopic submucosal dissection; LGIN: Low-grade intraepithelial tumor; HGIN: High-grade intraepithelial tumor; MC: Mucosal carcinoma; SMC: Submucosal carcinoma.

There was no case of local recurrence in more than 12 mo after ER. Also, no recurrence was noted in 88 cases treated by ER with R0 resection in the follow-up period. No treatment-related death occurred and none of the patients died of SNADET. One patient died of congestive heart failure during the follow-up period. Table 3 shows the details of recurrence cases. All the cases with tumor recurrence occurred after EMR with piecemeal or R1 or RX resection. Table 4 shows the short-term outcomes and adverse events related EMR.

In the EMR cases, 82 (60%) and 54 (40%) tumors were resected with EMR-S and EMR-C, respectively. EMR-S was more frequently used for protruded (0-I) or slightly elevated (0-IIa) tumors than EMR-C for depressed (0-IIc) tumors (82% *vs* 26%, $P < 0.001$). *En bloc* and R0 resection rates of EMR-S and EMR-C were 89%/62%, and 89%/78%, respectively. EMR-C showed a higher rate of R0 resection compared to EMR-S (78% *vs* 62%, $P = 0.06$) (Figure 3). No adverse event occurred in the EMR cases. Table 5 shows the short-term outcomes and adverse events related EMR *vs* ESD.

The median size of lesions treated by ESD was larger than EMR (20 mm *vs* 9 mm, $P < 0.001$). Delayed bleeding, intraoperative perforations, and delayed perforations occurred in 1, 3, and 2 of the ESD cases, respectively. One of the three cases of intraoperative perforation required emergency surgery. In 2 SMC cases, surgical resection was performed after EMR. One case had an SM invasion depth of 500 μm and no vascular invasion and was negative for resection margin, whereas the other had an SM invasion depth of 1000 μm, mild invasion to vessels, and absence of lymphatic invasion, and was negative for VM0 and HMX. Additional surgical partial resection of the duodenum was performed in both patients with SMCs, with no recurrence or metastasis at 3 yr after ER.

DISCUSSION

In this retrospective study, we evaluated therapeutic outcomes of ER for SNADETs in order to clarify the safety, efficacy, and curability of ER in such patients. The long-term prognosis was favorable regardless of the ER technique employed, as no recurrence was noted at more than 12 mo after ER, and no disease-specific death occurred.

This is the third largest case series of patients with SNADETs who were treated *via* ER[7,9,12,19-23]. While this study included few patients treated by ESD, we report the largest number of EMR-C patients; this is particularly relevant for depressed-type SNADET lesions that would be difficult to resect *via* EMR-S. In this series of SNADET patients, all EMR procedures, including EMR-C, were completed without adverse events and no EMR-related complications were noted on follow-up. Although some ESD-treated patients experienced adverse events, previous studies showed a wide variation of local recurrence rates, ranging from 0% to 37.8% after ER of SNADETs[8,9,21,24,25].

Our study demonstrated excellent long-term outcomes of ER for SNADETs because

Table 2 Long-term outcomes of endoscopic resection for 121 patients with 135 superficial non-ampullary duodenal epithelial tumors

		Value
Follow-up period		
	Median (IQR), mo	43 (24-60)
Local recurrence, *n* (%)		
	≤ 12 mo[3]	4 (3)[1]
	> 12 mo[4]	0
Prognosis		
	Death by duodenal tumor, *n*	0
	Death by other causes, *n* (%)	1 (0.9)[2]

IQR, interquartile range.
[1]Detail is provided in Table 3.
[2]Death by cardiac failure.
[3]Within 12 mo after endoscopic resection.
[4]More than 12 mo after endoscopic resection.

the recurrence rate was only 3%, and no one died of SNADET in the median follow-up period of 43 mo, longer than 3 yr. There are two likely explanations for the small recurrence rate noted in this study. First, tumor diameter of SNADET in this study was smaller than those in other published studies[24,27]. Second, we used magnifying endoscopy to observe marginal areas of mucosal defect immediately after ER precisely. If we found a suspected lesion of residual tumor, we performed additional coagulation therapy by using argon plasma or hot biopsy. Tumor recurrence occurred only after piecemeal resection or *en bloc* resection with RX or R1, and all recurrent tumors were identified within 12 mo after EMR. Therefore, strict follow-up in a short interval will be required in such patients.

The incidence of depressed (0-IIc) type of SNADETs was higher in our case series than in previous studies (38% *vs* 5%-26% of SNADETs analyzed)[6,8,9,26,27]. Furthermore, the depressed type tumors were resected using the EMR-C method significantly more often than the EMR-S method in this study. As we found a higher rate of R0 resection for EMR-C than for EMR-S, we believe that EMR-C will be a more suitable method for depressed type SNADETs than EMR-S. Interestingly, we found no EMR-associated adverse events regardless of technique (EMR-C or EMR-S), whereas previous studies reported a higher incidence of adverse events for EMR-C than for EMR-S[23,24,28]. During EMR-C, the step involving sucking the lesion carries the risk of perforation[29]. We must always be careful to avoid perforation during EMR-C for a duodenal tumor, because the muscularis propria layer of the duodenum is very thin.

We recommend the following procedures of EMR-C, namely the "suck and shake" technique: (1) sucking on a target area after submucosal injection and closing of the snare, followed by (2) slightly loosening o the snare and shaking it. Considering no perforation occurred in EMR cases in this study, the "suck and shake" technique may work to release entrapment of the muscularis propria layer and avoid perforation. Neither intraoperative nor delayed perforation could be avoided in ESD-treated patients, likely because we failed to completely close or cover the mucosal defect using clipping or tissue shielding. We expect that the development of simpler endoscopic techniques for closing or shielding large mucosal defects may help reduce the incidence of delayed perforation.

Based on our present findings, relatively small lesions (< 20 mm) represented a good indication for EMR, as *en bloc* resection was achieved for most such tumors, with no local recurrence. ESD was mainly performed for larger lesions (≥ 20 mm). The *en bloc* resection rate was higher for ESD than for EMR (100% *vs* 89%), and no recurrence was noted after ESD. We found no EMR-related adverse events in this series of SNADET patients. Studies on EMR for SNADETs reported an incidence of 0-33% for delayed bleeding[9,21,24,28,30-33] and 0-4% for perforation (intraoperative or delayed)[9,22,30,34,35]. On the other hand, studies on ESD for SNADETs reported an incidence of 0-18.4% for delayed bleeding[8,26,27,36] and 0-50% for perforation[21,25,37-39].

Thus, our present findings confirm previous data suggesting that perforation rates are considerably higher for ESD than for EMR, though the absence of adverse events following EMR may affect the statistical robustness of these conclusions. Although ESD allows *en bloc* resection even for large lesions, the decision to perform ESD should be taken in full consideration of all circumstances, and duodenal ESD should be performed by a skillful endoscopist. Taken together, these observations suggest

Table 3 Characteristics of recurrence cases after endoscopic resection

	Location	Diameter (mm)	Macroscopic type	Treatment	*En bloc*/Piecemeal (*n*)	R0 status	Histology		
1	Second	8	0-IIc	EMR-C	*En bloc*	RX	MC	HMX	VM0
2	Second	18	0-IIc	EMR-C	Piecemeal (3)	RX	MC	HMX	VM0
3	Second	18	0-IIa	EMR-C	Piecemeal (2)	RX	HGIN	HMX	VM0
4	Second	25	0-IIa	EMR-S	*En bloc*	R1	HGIN	HM1	VM0

EMR-C: Cap-assisted endoscopic mucosal resection; EMR-S: Conventional method with a snare; MC: Mucosal carcinoma; HGIN: High-grade intraepithelial neoplasia; RX: Involvement of the horizontal and/or vertical margin could not be assessed histopathologically; R1: Involvement of the horizontal and/or vertical margin histopathologically; HMX: Involvement of the horizontal margin could not be assessed histopathologically; HM1: Involvement of the horizontal margin histopathologically; VM0: No involvement of the vertical margin histopathologically.

that EMR may become the standard endoscopic treatment for SNADETs, particularly if the lesions are relatively small.

We generally avoided taking a biopsy during preoperative endoscopy. The reasons are that the fibrosis after biopsy can increase the risk of perforation due to poor mucosal lifting and the diagnostic accuracy of preoperative biopsy may not be highly reliable. In fact, a multicenter case-series study showed that the overall accuracy of the preoperative diagnosis was significantly higher in endoscopic diagnosis than in histology from biopsy (endoscopy and biopsy, 75% and 68%, respectively)[6]. The other study also showed similar results that the accuracy of endoscopic diagnosis is superior to that of biopsy (endoscopy and biopsy, 78% and 74%, respectively) in preoperative endoscopy[40].

This study has several limitations. First, this was a retrospective, single-center study. Furthermore, we could not follow-up some patients, although the number of such patients was low (7.6%, 10/131). Second, very few ESD procedures were performed in this series. To confirm our present findings and promote the standardization of ER for SNADETs, future studies should have multi-center sampling and a prospective design.

In conclusion, this study suggests that ER would provide good long-term outcomes in patients with SNADETs, albeit a high incidence of adverse events is associated with ESD. EMR should be a first-line treatment for SNADETs, especially small lesions.

Table 4 Short-term outcomes and adverse events (EMR-S *vs* EMR-C)

Outcome	EMR-S, *n* = 82	EMR-C, *n* = 54	*P*-value
Macroscopic type; 0-I or 0-IIa/0-IIc	67 (82)/15 (18)	14 (26)/40 (74)	< 0.001
En bloc resection	73 (89)	48 (89)	NS
R0 resection	51 (62)	42 (78)	NS
Success rate of clip closure	80 (98)	52 (96)	NS
Adverse events	0	0	NA
Perforation			
Intraoperative	0	0	NA
Delayed	0	0	NA
Delayed bleeding	0	0	NA

Data are presented as *n* (%). EMR-S: Conventional endoscopic mucosal resection using a snare; EMR-C: Cap-assisted endoscopic mucosal resection; NS: Not significant; NA: Not available.

Table 5 Short-term outcomes and adverse events (endoscopic mucosal resection *vs* endoscopic submucosal dissection)

Outcome	EMR, *n* = 136	ESD, *n* = 11	*P*-value
Tumor diameter, median (IQR)	9 (7-14.5)	20 (15-33)	< 0.001
Macroscopic type; 0-I or 0-IIa/0-IIc	81 (60)/55 (40)	10 (91)/1 (9)	NS
En bloc resection	121 (89)	11 (100)	NS
R0 resection	93 (68)	8 (73)	NS
Success rate of defect closure	132 (97)	7 (64)	< 0.001
Adverse events	0	5 (45)	< 0.001
Perforation			
Intraoperative	0	3 (27)[1]	< 0.001
Delayed	0	2 (18)[2]	0.004
Delayed bleeding	0	1 (9)[2]	NS

Data are presented as *n* (%).
[1]One required surgery, two recovered with conservative treatment.
[2]Recovered with conservative treatment.
EMR: Endoscopic mucosal resection; ESD: Endoscopic submucosal dissection; NS: Not significant; IQR: Interquartile range.

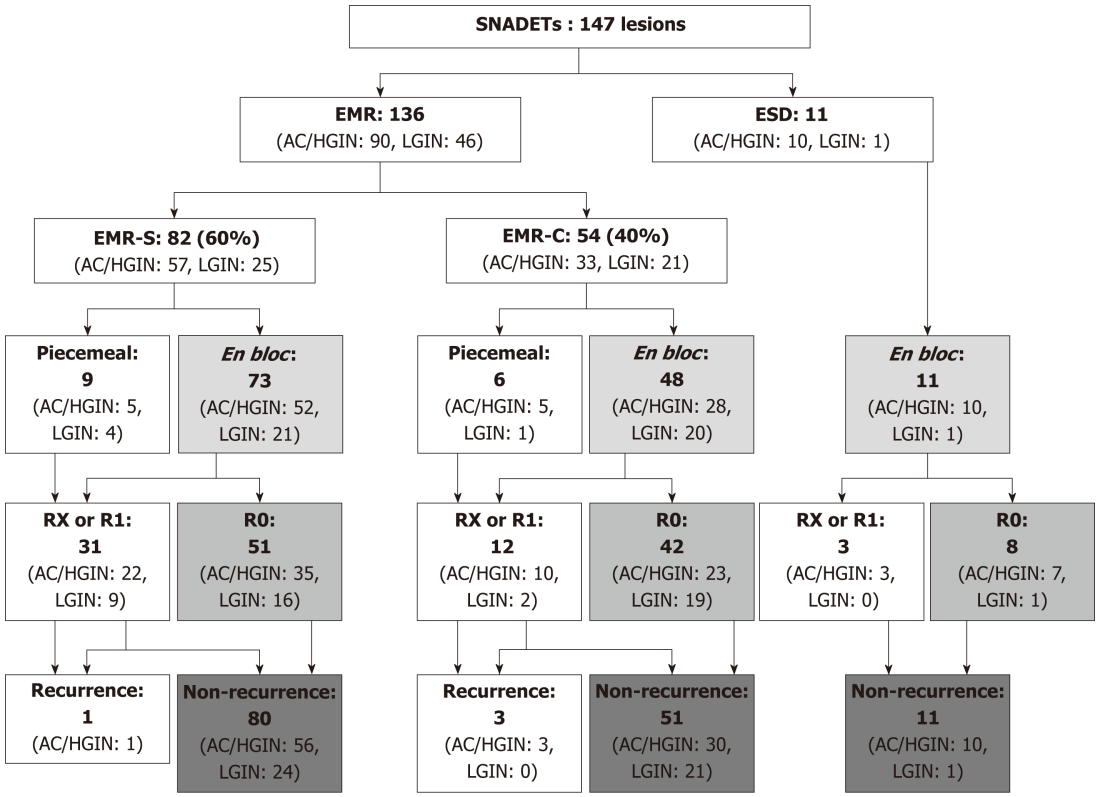

Figure 3 The study flow diagram based on the therapeutic outcomes of endoscopic resections. EMR: Endoscopic mucosal resection; ESD: Endoscopic submucosal dissection; EMR-S: Conventional method with snare; EMR-C: Cap-assisted EMR; R0: *En bloc* resection with tumor-free margins histopathologically; RX: Involvement of the horizontal and/or vertical margin could not be assessed histopathologically; R1: Involvement of the horizontal and/or vertical margin histopathologically; AC: Adenocarcinoma; HGIN: High-grade intraepithelial neoplasia; LGIN: Low-grade intraepithelial neoplasia.

ARTICLE HIGHLIGHTS

Research background

Endoscopic resection (ER) for superficial non-ampullary duodenal epithelial tumor (SNADET) is a challenging technique, due to the anatomical peculiarity of the procedure and the high frequency of the adverse event. Moreover, there are few reports on the treatment outcome of ER in many cases because of its relative rarity.

Research motivation

We aimed to determine the standardized criteria for endoscopic management of SNADNETs.

Research objectives

Based on the research background, we analyzed the results of the short-term and long-term treatment of over 100 cases of SNADET and investigated the effectiveness of ER in these cases.

Research methods

This study analyzed the short- and long-term outcomes of ER. Short-term outcomes of ER included *en bloc* and R0 resection rates, as well as the adverse events. Long-term outcomes included local recurrence detected on endoscopic surveillance and disease-specific mortality in patients followed up for ≥ 12 mo after ER. This retrospective study included a case series of 131 patients (147 SNADETs) who underwent endoscopic mucosal resection (EMR) or endoscopic submucosal dissection (ESD) between March 2004 and July 2017.

Research results

Over a median follow-up of 43 mo, recurrence was found in four lesions and those were treated endoscopically. No adverse events were observed in EMR-treated patients, whereas ESD for SNADETs carries a risk of bleeding and perforation. No patient died due to tumor recurrence.

Research conclusions

Our findings suggest that ER provides good long-term outcomes in patients with SNADETs. EMR was not associated with any adverse events and, therefore, could be considered as a standard treatment for small SNADETs.

Research perspectives

For small SNADETs, EMR is likely to become the standard treatment strategy.

REFERENCES

1 **Shukla SK**, Elias EG. Primary neoplasms of the duodenum. *Surg Gynecol Obstet* 1976; **142**: 858-860 [PMID: 936029]
2 **Murray MA**, Zimmerman MJ, Ee HC. Sporadic duodenal adenoma is associated with colorectal neoplasia. *Gut* 2004; **53**: 261-265 [PMID: 14724161 DOI: 10.1136/gut.2003.025320]
3 **Jepsen JM**, Persson M, Jakobsen NO, Christiansen T, Skoubo-Kristensen E, Funch-Jensen P, Kruse A, Thommesen P. Prospective study of prevalence and endoscopic and histopathologic characteristics of duodenal polyps in patients submitted to upper endoscopy. *Scand J Gastroenterol* 1994; **29**: 483-487 [PMID: 8079103 DOI: 10.3109/00365529409092458]
4 **Howe JR**, Karnell LH, Menck HR, Scott-Conner C. The American College of Surgeons Commission on Cancer and the American Cancer Society. Adenocarcinoma of the small bowel: Review of the National Cancer Data Base, 1985-1995. *Cancer* 1999; **86**: 2693-2706 [PMID: 10594865 DOI: 10.1002/(SICI)1097-0142(19991215)86:123.0.CO;2-U]
5 **Klimstra DS**, Bosman FT, Carneiro F, Hruban RH, Theise ND. Tumours of the ampullary region. Bosman FT, Carneiro F, Hruban RH, Theise ND. *WHO classification of tumours of the digestive system*. Lyon: IARC Publications 2010; 82-86
6 **Goda K**, Kikuchi D, Yamamoto Y, Takimoto K, Kakushima N, Morita Y, Doyama H, Gotoda T, Maehata Y, Abe N. Endoscopic diagnosis of superficial non-ampullary duodenal epithelial tumors in Japan: Multicenter case series. *Dig Endosc* 2014; **26** Suppl 2: 23-29 [PMID: 24750144 DOI: 10.1111/den.12277]
7 **Yahagi N**, Kato M, Ochiai Y, Maehata T, Sasaki M, Kiguchi Y, Akimoto T, Nakayama A, Fujimoto A, Goto O, Uraoka T. Outcomes of endoscopic resection for superficial duodenal epithelial neoplasia. *Gastrointest Endosc* 2018; **88**: 676-682 [PMID: 29753040 DOI: 10.1016/j.gie.2018.05.002]
8 **Yamamoto Y**, Yoshizawa N, Tomida H, Fujisaki J, Igarashi M. Therapeutic outcomes of endoscopic resection for superficial non-ampullary duodenal tumor. *Dig Endosc* 2014; **26** Suppl 2: 50-56 [PMID: 24750149 DOI: 10.1111/den.12273]
9 **Nonaka S**, Oda I, Tada K, Mori G, Sato Y, Abe S, Suzuki H, Yoshinaga S, Nakajima T, Matsuda T, Taniguchi H, Saito Y, Maetani I. Clinical outcome of endoscopic resection for nonampullary duodenal tumors. *Endoscopy* 2015; **47**: 129-135 [PMID: 25314330 DOI: 10.1055/s-0034-1390774]
10 **Japanese Gastric Cancer Association**. Japanese classification of gastric carcinoma: 3rd English edition. *Gastric Cancer* 2011; **14**: 101-112 [PMID: 21573743 DOI: 10.1007/s10120-011-0041-5]
11 **Yoshimura N**, Goda K, Tajiri H, Ikegami M, Nakayoshi T, Kaise M. Endoscopic features of nonampullary duodenal tumors with narrow-band imaging. *Hepatogastroenterology* 2010; **57**: 462-467 [PMID: 20698209 DOI: 10.1002/hed.21133]
12 **Abbass R**, Rigaux J, Al-Kawas FH. Nonampullary duodenal polyps: characteristics and endoscopic management. *Gastrointest Endosc* 2010; **71**: 754-759 [PMID: 20363416 DOI: 10.1016/j.gie.2009.11.043]
13 **Alexander S**, Bourke MJ, Williams SJ, Bailey A, Co J. EMR of large, sessile, sporadic nonampullary duodenal adenomas: technical aspects and long-term outcome (with videos). *Gastrointest Endosc* 2009; **69**: 66-73 [PMID: 18725157 DOI: 10.1016/j.gie.2008.04.061]
14 **Iizuka T**, Kikuchi D, Hoteya S, Yamada A, Yamashita S, Fujimoto A, Nakamura A, Matsui A, Kuroki Y, Mitani T, Kaise M. How to manage duodenal tumors with EMR or ESD. *Gastroenterol Endosc* 2011; **53**: 87-94 [DOI: 10.11280/gee.53.87]
15 **Ono H**, Nonaka S, Uedo N, Kaise M, Oyama T, Doyama H, Kokawa A, Kaneko K, Kodashima S, Tanabe S, Toyonaga T. Clinical issues of duodenal EMR/ESD. *Stomach Intestine* 2011; **46**: 1669-1677
16 **Tajiri H**, Kitano S. Complications associated with endoscopic mucosal resection: Definition of bleeding that can be viewed as accidental. *Dig Endosc* 2004; **16** Suppl 1: S134-S136 [DOI: 10.1111/j.1443-1661.2004.00377.x]
17 **Lauwers GY**, Bosman FT, Carneiro F, Hruban RH, Theise ND. Gastric carcinoma. In: Bosman FT, Carneiro F, Hruban RH, Theise ND, editors. WHO classification of tumours of the digestive system. 4th ed. Lyon: IARC Publications, 2010: 48-58. Bosman FT, Carneiro F, Hruban RH, Theise ND.
18 **Mitsuishi T**, Hamatani S, Hirooka S, Fukasawa N, Aizawa D, Hara Y, Dobashi A, Goda K, Fukuda T, Saruta M, Urashima M, Ikegami M. Clinicopathological characteristics of duodenal epithelial neoplasms: Focus on tumors with a gastric mucin phenotype (pyloric gland-type tumors). *PLoS One* 2017; **12**: e0174985 [PMID: 28376132 DOI: 10.1371/journal.pone.0174985]
19 **Fanning SB**, Bourke MJ, Williams SJ, Chung A, Kariyawasam VC. Giant laterally spreading tumors of the duodenum: endoscopic resection outcomes, limitations, and caveats. *Gastrointest Endosc* 2012; **75**: 805-812 [PMID: 22305507 DOI: 10.1016/j.gie.2011.11.038]
20 **Inoue T**, Uedo N, Yamashina T, Yamamoto S, Hanaoka N, Takeuchi Y, Higashino K, Ishihara R, Iishi H, Tatsuta M, Takahashi H, Eguchi H, Ohigashi H. Delayed perforation: A hazardous complication of endoscopic resection for non-ampullary duodenal neoplasm. *Dig Endosc* 2014; **26**: 220-227 [PMID: 23621427 DOI: 10.1111/den.12104]
21 **Hoteya S**, Furuhata T, Takahito T, Fukuma Y, Suzuki Y, Kikuchi D, Mitani T, Matsui A, Yamashita S, Nomura K, Kuribayashi Y, Iizuka T, Kaise M. Endoscopic Submucosal Dissection and Endoscopic Mucosal Resection for Non-Ampullary Superficial Duodenal Tumor. *Digestion* 2017; **95**: 36-42 [PMID: 28052275 DOI: 10.1159/000452363]
22 **Klein A**, Nayyar D, Bahin FF, Qi Z, Lee E, Williams SJ, Byth K, Bourke MJ. Endoscopic mucosal resection of large and giant lateral spreading lesions of the duodenum: success, adverse events, and long-term outcomes. *Gastrointest Endosc* 2016; **84**: 688-696 [PMID: 26975231 DOI: 10.1016/j.gie.2016.02.049]
23 **Tomizawa Y**, Ginsberg GG. Clinical outcome of EMR of sporadic, nonampullary, duodenal adenomas: A 10-year retrospective. *Gastrointest Endosc* 2018; **87**: 1270-1278 [PMID: 29317270 DOI: 10.1016/j.gie.2017.12.026]
24 **Conio M**, De Ceglie A, Filiberti R, Fisher DA, Siersema PD. Cap-assisted EMR of large, sporadic, nonampullary duodenal polyps. *Gastrointest Endosc* 2012; **76**: 1160-1169 [PMID: 23021169 DOI: 10.1016/j.gie.2012.08.009]
25 **Maruoka D**, Arai M, Kishimoto T, Matsumura T, Inoue M, Nakagawa T, Watanabe Y, Katsuno T, Tsuyuguchi T, Imazeki F, Yokosuka O. Clinical outcomes of endoscopic resection for nonampullary duodenal high-grade dysplasia and intramucosal carcinoma. *Endoscopy* 2013; **45**: 138-141 [PMID: 23322475 DOI: 10.1055/s-0032-1325799]
26 **Hoteya S**, Yahagi N, Iizuka T, Kikuchi D, Mitani T, Matsui A, Ogawa O, Yamashita S, Furuhata T, Yamada A, Kimura R, Nomura K, Kuribayashi Y, Kaise M. Endoscopic submucosal dissection for

nonampullary large superficial adenocarcinoma/adenoma of the duodenum: feasibility and long-term outcomes. *Endosc Int Open* 2013; **1**: 2-7 [PMID: 26135505 DOI: 10.1055/s-0033-1359232]
27 **Matsumoto S**, Yoshida Y. Selection of appropriate endoscopic therapies for duodenal tumors: An open-label study, single-center experience. *World J Gastroenterol* 2014; **20**: 8624-8630 [PMID: 25024618 DOI: 10.3748/wjg.v20.i26.8624]
28 **Jamil LH**, Kashani A, Peter N, Lo SK. Safety and efficacy of cap-assisted EMR for sporadic nonampullary duodenal adenomas. *Gastrointest Endosc* 2017; **86**: 666-672 [PMID: 28257791 DOI: 10.1016/j.gie.2017.02.023]
29 **Inoue H**, Kawano T, Tani M, Takeshita K, Iwai T. Endoscopic mucosal resection using a cap: techniques for use and preventing perforation. *Can J Gastroenterol* 1999; **13**: 477-480 [PMID: 10464347 DOI: 10.1155/1999/198230]
30 **Hirasawa R**, Iishi H, Tatsuta M, Ishiguro S. Clinicopathologic features and endoscopic resection of duodenal adenocarcinomas and adenomas with the submucosal saline injection technique. *Gastrointest Endosc* 1997; **46**: 507-513 [PMID: 9434217 DOI: 10.1016/s0016-5107(97)70005-1]
31 **Ahmad NA**, Kochman ML, Long WB, Furth EE, Ginsberg GG. Efficacy, safety, and clinical outcomes of endoscopic mucosal resection: a study of 101 cases. *Gastrointest Endosc* 2002; **55**: 390-396 [PMID: 11868015 DOI: 10.1067/mge.2002.121881]
32 **Oka S**, Tanaka S, Nagata S, Hiyama T, Ito M, Kitadai Y, Yoshihara M, Haruma K, Chayama K. Clinicopathologic features and endoscopic resection of early primary nonampullary duodenal carcinoma. *J Clin Gastroenterol* 2003; **37**: 381-386 [PMID: 14564184 DOI: 10.1097/00004836-200311000-00006]
33 **Heresbach D**, Kornhauser R, Seyrig JA, Coumaros D, Claviere C, Bury A, Cottereau J, Canard JM, Chaussade S, Baudet A, Casteur A, Duval O, Ponchon T; OMEGA group. A national survey of endoscopic mucosal resection for superficial gastrointestinal neoplasia. *Endoscopy* 2010; **42**: 806-813 [PMID: 20821362 DOI: 10.1055/s-0030-1255715]
34 **Lépilliez V**, Chemaly M, Ponchon T, Napoleon B, Saurin JC. Endoscopic resection of sporadic duodenal adenomas: An efficient technique with a substantial risk of delayed bleeding. *Endoscopy* 2008; **40**: 806-810 [PMID: 18828076 DOI: 10.1055/s-2008-1077619]
35 **Park SM**, Ham JH, Kim BW, Kim JS, Kim CW, Kim JI, Lim CH, Oh JH. Feasibility of endoscopic resection for sessile nonampullary duodenal tumors: a multicenter retrospective study. *Gastroenterol Res Pract* 2015; **2015**: 692492 [PMID: 25810715 DOI: 10.1155/2015/692492]
36 **Endo M**, Abiko Y, Oana S, Kudara N, Chiba T, Suzuki K, Koizuka H, Uesugi N, Sugai T. Usefulness of endoscopic treatment for duodenal adenoma. *Dig Endosc* 2010; **22**: 360-365 [PMID: 21175499 DOI: 10.1111/j.1443-1661.2010.01014.x]
37 **Takahashi T**, Ando T, Kabeshima Y, Kawakubo H, Shito M, Sugiura H, Omori T. Borderline cases between benignancy and malignancy of the duodenum diagnosed successfully by endoscopic submucosal dissection. *Scand J Gastroenterol* 2009; **44**: 1377-1383 [PMID: 19821793 DOI: 10.3109/00365520903287551]
38 **Kakushima N**, Kanemoto H, Tanaka M, Takizawa K, Ono H. Treatment for superficial non-ampullary duodenal epithelial tumors. *World J Gastroenterol* 2014; **20**: 12501-12508 [PMID: 25253950 DOI: 10.3748/wjg.v20.i35.12501]
39 **Miura Y**, Shinozaki S, Hayashi Y, Sakamoto H, Lefor AK, Yamamoto H. Duodenal endoscopic submucosal dissection is feasible using the pocket-creation method. *Endoscopy* 2017; **49**: 8-14 [PMID: 27875854 DOI: 10.1055/s-0042-116315]
40 **Kakushima N**, Kanemoto H, Sasaki K, Kawata N, Tanaka M, Takizawa K, Imai K, Hotta K, Matsubayashi H, Ono H. Endoscopic and biopsy diagnoses of superficial, nonampullary, duodenal adenocarcinomas. *World J Gastroenterol* 2015; **21**: 5560-5567 [PMID: 25987780 DOI: 10.3748/wjg.v21.i18.5560]

P- Reviewer: Barret M, Handra-Luca A, Skok P
S- Editor: Yan JP **L- Editor:** Filipodia **E- Editor:** Yin SY

World Journal of Gastroenterology

Submit a Manuscript: https://www.f6publishing.com

World J Gastroenterol 2019 February 14; 25(6): 719-728

DOI: 10.3748/wjg.v25.i6.719

ISSN 1007-9327 (print) ISSN 2219-2840 (online)

ORIGINAL ARTICLE

Observational Study

Serum hepatitis B virus RNA is a predictor of HBeAg seroconversion and virological response with entecavir treatment in chronic hepatitis B patients

Hao Luo, Xia-Xia Zhang, Li-Hua Cao, Ning Tan, Qian Kang, Hong-Li Xi, Min Yu, Xiao-Yuan Xu

ORCID number: Hao Luo (0000-0002-2067-7217); Xia-Xia Zhang (0000-0002-0512-9001); Li-Hua Cao (0000-0002-4664-9003); Ning Tan (0000-0001-9917-2192); Qian Kang (0000-0001-5825-1660); Hong-Li Xi (0000-0003-0389-7602); Min Yu (0000-0001-7784-7830); Xiao-Yuan Xu (0000-0002-1759-4330).

Author contributions: Luo H and Zhang XX equally designed the research; Luo H performed the research, acquired and analyzed the data, and wrote the article; Cao LH and Xi HL analyzed the data; Tan N, Kang Q, and Yu M acquired the data; Xu XY edited, reviewed, and approved the final article.

Supported by the 13th Five-Year Plan, No. 2018ZX09206005-002.

Institutional review board statement: The study protocol conformed to the ethical guidelines of the Declaration of Helsinki and was approved by the Ethic Committee of Shanghai Jing An Central Hospital (Approval No. 090f51e6809a26e1 v1.0).

Informed consent statement: Patients who were enrolled in the work provided informed consent.

Conflict-of-interest statement: There are no conflicts of interest to report.

Data sharing statement: No additional data are available.

STROBE statement: The guidelines

Hao Luo, Ning Tan, Qian Kang, Hong-Li Xi, Min Yu, Xiao-Yuan Xu, Department of Infectious Diseases, Peking University First Hospital, Beijing 100034, China

Xia-Xia Zhang, Department of Gastroenterology, Capital Medical University Beijing Tiantan Hospital, Beijing 100070, China

Li-Hua Cao, Department of Infectious Diseases, the Third Hospital of Qinhuangdao, Qinhuangdao 066000, Hebei Province, China

Corresponding author: Xiao-Yuan Xu, MD, Professor, Department of Infectious Diseases, Peking University First Hospital, 8 Xishiku Street, Beijing 100034, China.
xiaoyuanxu6@163.com
Telephone: +86-10-83575787
Fax: +86-10-83575787

Abstract

BACKGROUND

Characteristics of alterations of serum hepatitis B virus (HBV) RNA in different chronic hepatitis B (CHB) patients still cannot be fully explained. Whether HBV RNA can predict HBeAg seroconversion is still controversial.

AIM

To investigate whether HBV RNA can predict virological response or HBeAg seroconversion during entecavir (ETV) treatment when HBV DNA is undetectable.

METHODS

The present study evaluated 61 individuals who were diagnosed and treated with long-term ETV monotherapy at the Department of Infectious Diseases of Peking University First Hospital (China) from September 2006 to December 2007. Finally, 30 treatment-naive individuals were included. Serum HBV RNA were extracted from 140 μL serum samples at two time points. Then they were reverse transcribed to cDNA with the HBV-specific primer. The product was quantified by real-time quantitative PCR (RT-PCR) using TAMARA probes. Statistical analyses were performed with IBM SPSS 20.0.

RESULTS

Level of serum HBV RNA at baseline was 4.15 ± 0.90 $\log_{10}$ copies/mL. HBV RNA levels showed no significant difference between the virological response (VR)

Manuscript source: Unsolicited manuscript

Received: November 5, 2018
Peer-review started: November 5, 2018
First decision: December 28, 2018
Revised: January 11, 2019
Accepted: January 18, 2019
Article in press: January 18, 2019
Published online: February 14, 2019

and partial VR (PVR) groups at baseline (P = 0.940). Serum HBV RNA significantly decreased among patients who achieved a VR during ETV therapy (P < 0.001). The levels of HBV RNA in both HBeAg-positive patients with seroconversion group and those with no seroconversion increased after 24 wk of treatment. Overall, HBV RNA significantly but mildly correlated to HBsAg (r = 0.265, P = 0.041), and HBV RNA was not correlated to HBV DNA (r = 0.242, P = 0.062). Furthermore, serum HBV RNA was an independent indicator for predicting HBeAg seroconversion and virological response. HBeAg seroconversion was more likely in CHB patients with HBV RNA levels below 4.12 $\log_{10}$ copies/mL before treatment.

CONLUSION
The level of serum HBV RNA could predict HBeAg seroconversion and PVR during treatment. In the PVR group, the level of serum HBV RNA tends to be increasing.

Key words: Chronic hepatitis B; Hepatitis B virus RNA; Virological response; HBeAg seroconversion; Entecavir

Core tip: HBeAg seroconversion was more likely to be achieved for chronic hepatitis B patients with hepatitis B virus (HBV) RNA levels below 4.12 $\log_{10}$ copies/mL before treatment. In the partial virological response group, serum HBV RNA showed an increasing trend.

Citation: Luo H, Zhang XX, Cao LH, Tan N, Kang Q, Xi HL, Yu M, Xu XY. Serum hepatitis B virus RNA is a predictor of HBeAg seroconversion and virological response with entecavir treatment in chronic hepatitis B patients. *World J Gastroenterol* 2019; 25(6): 719-728
URL: https://www.wjgnet.com/1007-9327/full/v25/i6/719.htm
DOI: https://dx.doi.org/10.3748/wjg.v25.i6.719

INTRODUCTION

Globally, more than 240 million individuals are infected with hepatitis B virus (HBV)[1]. Nucleos(t)ide analogues (NAs) are effective therapies that are widely used to target reverse transcriptases[2]. However, NAs only suppress HBV DNA replication, resulting in decreased serum HBV DNA, but they do not suppress covalently closed circular DNA (cccDNA), which still resides in the nucleus and leads to long-term infection[3]. Pregenome RNA (pgRNA) is the direct product of cccDNA, and HBV DNA polymerase reverse transcribes pgRNA into rcDNA. Therefore, blocking reverse transcription does not influence the generation of HBV pgRNA. In most studies, HBV pgRNA increased after blocking reverse transcription activity[3,4]. Lu's studies showed that serum HBV RNA was pgRNA that appeared in virus-like particles.

In 1996, Kock *et al*[5] first demonstrated that HBV RNA was present in free virus, and a number of studies have shown that the HBV RNA levels in serum were related to virological response (VR) and prognosis[3,4,6-8]. However, characteristics of alterations of serum HBV RNA in different chronic hepatitis B (CHB) patients still cannot be fully explained. Whether HBV RNA can predict HBeAg seroconversion is still controversial.

In this work, we investigated the characteristics of HBV RNA alterations in CHB patients with different treatment effects. The relationships of HBV RNA with other serological markers were also analyzed. Finally, we calculated the predictive value of HBV RNA in anticipating HBeAg seroconversion.

MATERIALS AND METHODS

Patients

We evaluated 61 individuals from September 2006 to December 2007 at the

Department of Infectious Diseases of Peking University First Hospital (China) who had begun long-term entecavir (ETV) monotherapy (Table 1). The criteria for inclusion were: (1) patients who were naive to NA treatment; (2) patients who received monotherapy with ETV, without termination; and (3) patient's written consent was obtained. The criteria for exclusion were: (1) patients who had severe liver-related complications (including decompensated liver cirrhosis, hepatocellular carcinoma, and liver transplantation); (2) patients with co-infection with human immunodeficiency virus (HIV) or hepatitis C virus (HCV); (3) patients receiving combination therapy with other NAs; (4) an absence of samples at the time points; and (5) patients with poor compliance. Finally, we collected 30 treatment-naive individuals.

Patient cohort A included 13 patients who had a VR. Patient cohort B included 17 patients who had a partial VR (PVR). Through 48 weeks of therapy, HBV DNA that was undetected was identified as a VR. After 48 wk of treatment, positive HBV DNA (with a decrease of > 2 $\log_{10}$ copy/mL) was defined as a PVR. At baseline, there were 25 HBeAg positive patients, 10 of whom achieved HBeAg seroconversion during antiviral treatment.

Informed consent was obtained from all enrolled patients and the study protocol conformed to the ethical guidelines of the Declaration of Helsinki and was approved by the Ethic Committee of Shanghai Jing An Central Hospital (Approval No. 090f51e6809a26e1 v1.0).

Standard laboratory assessments

An automatic biochemical analyzer was used to test the biochemical indicators, including alanine aminotransferase (ALT) and aspartate transaminase (AST). Quantitative HBsAg, HBeAg, and anti-HBe were determined with ELISA kits (Abbott Laboratories, Chicago, IL, United States). COBAS TaqMan assay (Roche Diagnostics, Basel, Switzerland) was used to quantify serum HBV DNA levels, with 100 IU/mL as the lower limit of detection. Identification of HBV genotypes was performed by comparison with the generated preS/S gene sequences in GenBank (NCBI) data[9].

Evaluation of serum HBV RNA utilizing real-time PCR

HBV RNA was extracted from 140 μL of serum samples based on the manufacturer's instructions (QIAamp Viral Mini Kit, Qiagen, Germany). Then, we used a RevertAid First Strand cDNA synthesis Kit (Thermo scientific, MA, United States) to reverse transcribe HBV RNA to cDNA with the HBV-specific primer (5'-ACCACGCTATCGCTACTC-3'). The evaluation of HBV RNA was accomplished by quantitative PCR (qPCR) using the ABI Prism 7500 Sequence Detection System (Applied Biosystems, Foster City, CA, United States) by a Taqman probe method, according to the guidelines provided by the manufacturer. The target section was ligated with the constructed PMD19-T vector. The product was evaluated by real-time quantitative PCR (RT-PCR) using TAMARA probes. The primers and probe utilized to ascertain HBV RNA were as follows: Fw: 5'-ACCACGCTATCGCTACTCAC-3', Rw: 5'-CAACTTTTTCACCTCTGCCTA-3' and probe: (TAMARA) CATGTCCTACTGTTCAA GCCTCCAAG (BHQ2). The qPCR reaction mixture (25 μL) contained 2.5 μL 10 × Buffer, 2 μL dNTPs (2.5 mmol/L), 1 μL cDNA, 1 μL primer each, 0.5 μL probe, 0.25 μL Taq DNA polymerase, and 17.75 μL double-distilled water (ddH_2O). The reaction mixture was denatured at 95 °C for 10 min, followed by 40 cycles at 95 °C for 15 s and 60 °C for 1 min.

Statistical analysis

Statistical analyses were performed using IBM SPSS statistics, version 18.0.0.1 (SPSS, Chicago, IL, United States). Data are expressed as the mean ± SD or count number. Differences between groups were examined for statistical significance utilizing Student's *t*-test. We used the chi-square test of independence to evaluate the distribution of HBeAg positivity in various groups. $P < 0.05$ was considered statistically significant. The linear relationships between various viral markers were evaluated by Pearson's correlation coefficient (r) and tested for the significance of the correlation coefficient (P-value reported). Categorical variables were evaluated using Spearman's correlation coefficient (r). We applied a multivariate regularized linear model to identify the factors closely related to HBV RNA. We used a receiver operating characteristic (ROC) curve to calculate the predictive value.

RESULTS

Dynamic changes of HBV RNA after NAs treatment

We studied 30 patients in total, who were divided into two groups depending on

Table 1 Baseline characteristics of enrolled patients

Characteristic	Value
Gender (male/female)	25/5
Age (yr)	35.47 ± 11.05 (17-58)
Body mass index	24.40 ± 3.50 (18.64-32.27)
HBeAg+ (%)	25 (83%)
Alanine aminotransferase (IU/mL)	159.90 ± 226.70 (40-1308)
HBsAg (log_{10} IU/mL)	3.97 ± 0.74 (2.29-4.88)
HBV DNA (log_{10} IU/mL)	7.99 ± 1.32 (4.28-9.52)
HBV RNA (log_{10} copies/mL)	4.15 ± 0.90 (2.24-5.66)
HBV genotype	
B (%)	6 (20.00%)
C (%)	24 (80.00%)

HBV: Hepatitis B virus.

whether HBV DNA was undetectable at week 24 of treatment: a VR group (n = 13) and a PVR group (n = 17). The baseline characteristics of the included patients are listed in Table 2. The ratio of males to females was 5:1. The average age was 35 years. Most patients had a body mass index (BMI) of 24.4, within the normal range. The average value of glutamic-pyruvic transaminase was 159.9, two-fold higher than the normal value. There were 25 HBeAg-positive patients (83%). The average value of serum HBV RNA was 4.15 log_{10} copies/mL. Comparing the baseline characteristics of the VR and PVR groups statistically, the HBV DNA showed a significant difference (P = 0.014), as did HBsAg (P = 0.04). HBV RNA levels showed no significant difference between the VR and PVR groups (P = 0.940).

Before NAs treatment, the HBV RNA level had a medium correlation with respect to whether the patient had a VR (r = -0.515, P = 0.004), and the HBV RNA level had no correlation with other clinical characteristics. After 24 wk of treatment, the HBV RNA level had a high correlation with respect to whether the patient had a VR (r = -0.843, P < 0.001), and HBV RNA also had a high correlation with the HBV DNA level (r = 0.758, P < 0.001). The AST and HBsAg levels had medium correlations with the HBV RNA level (r = 0.379, P = 0.039; r = 0.368, P = 0.045).

After 24 wk of treatment, we found a significant variation in HBV RNA between the VR and PVR groups (P = 0.041). In the VR group, the level of HBV RNA decreased, and the changes were significantly different (P < 0.001). In the PVR group, the level of HBV RNA showed an increasing trend, and the changes were significantly different (P < 0.001) (Figure 1A).

Thirty patients were also divided by whether they achieved HBeAg seroconversion. The baseline characteristics of the individuals are listed in Table 3. Comparing the HBeAg-positive patients with seroconversion (group A) with the HBeAg-positive patients with no seroconversion (group B), there were no significant differences in terms of clinical characteristics before treatment except for age: group A was younger than group B (37 ± 6 *vs* 33 ± 12, P = 0.034). After 24 weeks of treatment, the HBV RNA level showed a difference (3.1 ± 1.4 *vs* 5.5 ± 1.51, P = 0.032). Comparing group A with the HBeAg-negative group, only the HBV DNA level before treatment showed a significant difference (Figure 1B). The HBV RNA levels in groups A and B increased after 24 wk of treatment.

Connection between serum HBV RNA and other common serum biomarkers

Overall, HBV RNA and HBsAg had a poor correlation (r = 0.265, P = 0.041) (Figure 1C), and HBV RNA had no significant correlation with HBV DNA (r = 0.242, P = 0.062) (Figure 1D).

In the VR group, we only found a moderate correlation between HBV RNA and HBV DNA before treatment (r = 0.568, P = 0.043) (Figure 2A). After 24 wk of treatment, HBV RNA had no correlation with other biomarkers (Figure 2B). In the PVR group, we found that HBV RNA had no correlation with HBV DNA before treatment. After 24 wk of treatment, HBV RNA and HBV DNA had a moderate correlation (r = 0.517, P = 0.034) (Figure 2C). HBV RNA and HBsAg had no correlation before treatment (Figure 2D and E). After 24 wk of treatment, HBV RNA had no correlation with HBsAg in the VR group (Figure 2F). After 24 wk of treatment, HBV RNA had a significant high correlation with HBsAg in the PVR group (r = 0.673, P =

Table 2 Baseline characteristics of enrolled patients (virological response group *vs* partial virological response group)

Characteristic	Virological response (*n* = 13)	Partial virological response (*n* = 17)	*P* value
Gender (male/female)	11/2	14/3	
Age (yr)	35.69 ± 10.85	35.29 ± 11.52	0.924
Body mass index	24.11 ± 3.66	24.62 ± 3.46	0.704
HBeAg+ (%)			
Week 0	9 (69.23%)	16 (94.12%)	
Week 24	8 (61.54%)	16 (94.12%)	
Alanine aminotransferase (IU/mL)			
Week 0	213.85 ± 72.11	118.65 ± 74.25	0.262
Week 24	30.23 ± 15.76	56.71 ± 46.12	0.058
HBsAg (log_{10} IU/mL)			
Week 0	3.66 ± 0.66	4.21 ± 0.73	0.040
Week 24	3.49 ± 0.55	3.84 ± 0.61	0.116
HBV DNA (log_{10} IU/mL)			
Week 0	7.26 ± 1.56	8.54 ± 0.75	0.014
Week 24	2.79 ± 0.27	4.20 ± 0.74	0.000
HBV RNA (log_{10} copies/mL)			
Week 0	4.17 ± 0.87	4.14 ± 0.95	0.936
Week 24	2.58 ± 0.90	5.24 ± 0.51	0.000
HBV genotype			
B (%)	3 (23.08%)	3 (17.65%)	
C (%)	10 (76.92%)	14 (82.35%)	

HBV: Hepatitis B virus.

0.003) (Figure 2G).

In group A, HBV RNA had only a moderate correlation with HBV DNA after 24 wk of therapy (r = 0.688, P = 0.028) (Figure 2K). In group B, HBV RNA also had a moderate correlation with HBV DNA after 24 wk of therapy (r = 0.755, P = 0.001) (Figure 2O). HBV RNA had no correlation with HBsAg before or after treatment (Figure 2H, I, L, and M). HBV RNA had no correlation with HBV DNA before treatment (Figure 2J and N).

Multivariate analysis of the factors related with HBV RNA

As HBV patients might have various personal background and their risk factors for prognosis including seroconversion are unknown. It might cause the existence of confounding factors among study subjects which might interfere with the precision of the study. The typical method to adjust confounding factors is multivariate analysis. To evaluate whether HBV RNA was an independent predictor of HBeAg seroconversion and VR, we applied a multivariate regularized linear model. The model was suitable for the following explanatory variables: age, sex, BMI, levels of ALT, HBV DNA, HBsAg, whether there was a VR, and whether there was HBeAg seroconversion.

Before treatment, we identified two models: the first model, whether HBeAg seroconversion was identified as the best indicator associated with HBV RNA level, and the second model, whether HBeAg seroconversion and baseline HBV DNA were the strongest linear factors; however, the P-value for baseline HBV DNA was 0.092, greater than 0.05.

After 24 wk of treatment, we identified one best result model: whether VR was considered the strongest single linear factor related to HBV RNA.

Predictive value of HBV RNA in HBeAg seroconversion

To analyze the predictive value of HBV RNA in HBeAg seroconversion, we generated a ROC curve. We evaluated HBV RNA at baseline and after 24 wk of therapy, measuring the variation in HBV RNA between the time points in terms of three characteristics. The HBV RNA level at baseline had the best predictive value (AUC = 0.847, P = 0.004). The cutoff value was 4.12 (sensitivity = 0.8, specificity = 0.8), suggesting that in CHB patients, an HBV RNA level below 4.12 log_{10} copies/mL before treatment was more likely to achieve HBeAg seroconversion. The variation and

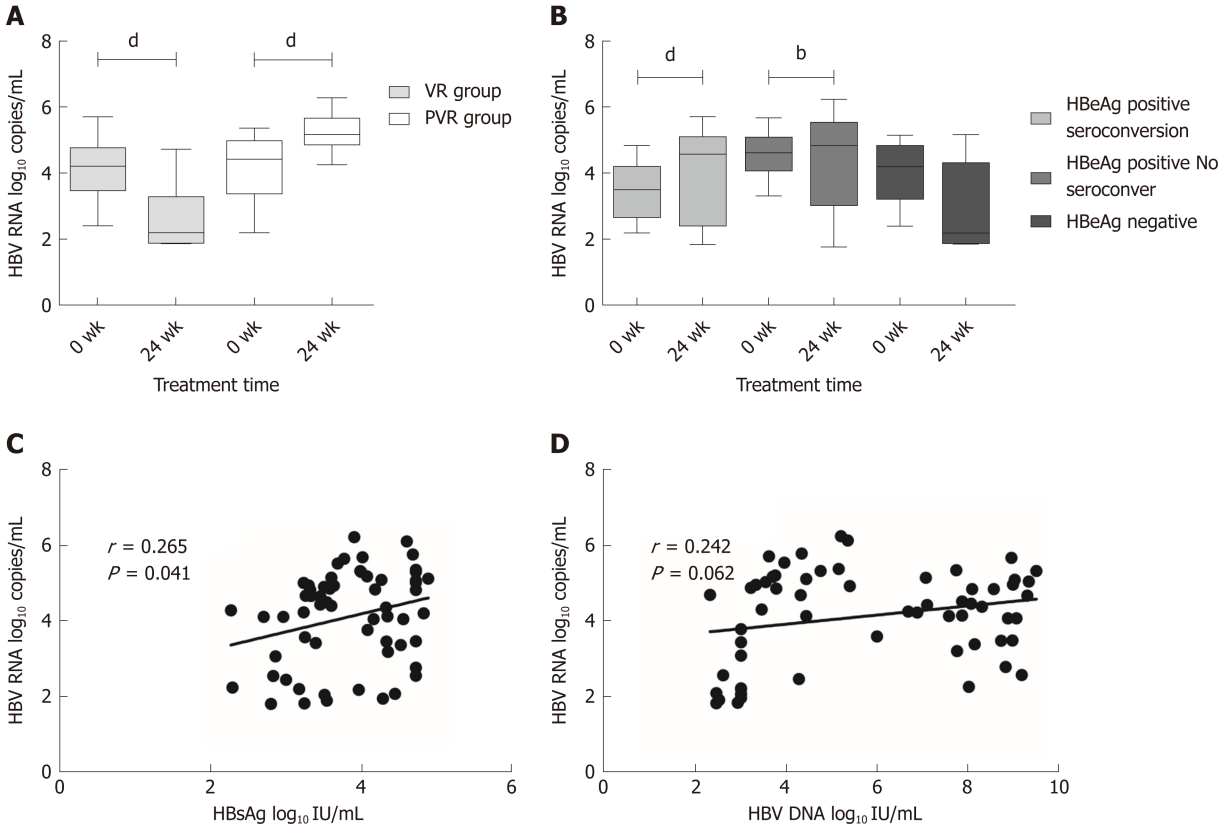

Figure 1 Hepatitis B virus RNA variation and correlation of hepatitis B virus RNA with other biomarkers. A: The level of hepatitis B virus (HBV) RNA in the virological response group and partial virological response group; B: The level of HBV RNA in the HBeAg-positive patients with seroconversion, the HBeAg-positive patients with no seroconversion, and the HBeAg negative patients; C: HBV RNA and HBsAg had a poor correlation; D: HBV RNA had no significant correlation with HBV DNA. HBV: Hepatitis B virus; VR: Virological response; PVR: Partial virological response.

level of HBV RNA at 24 wk did not have predictive value (P = 0.542, P = 0.437) (Figure 3).

DISCUSSION

Studies have shown that NAs treatment can help more than 60% patients achieve undetectable HBV DNA after 1 year of therapy. However, several patients can achieve serological responses (HBeAg and HBsAg loss, with or without detection of corresponding antibodies)[10]. As a result, if HBV DNA is maintained at undetectable levels, it is difficult to predict whether a patient will have a serological response. To address this question, we evaluated whether HBV RNA had a relationship with VR and HBeAg antigen seroconversion, how HBV RNA was related to other indicators, whether HBV RNA was an independent indicator of HBeAg seroconversion, and finally, the diagnostic value of HBV RNA.

By comparing the dynamic characteristics of HBV RNA in the VR and PVR groups, we found that HBV RNA showed a strong decrease in the VR group. By contrast, HBV RNA increased in the PVR group (Figure 1A). Thus, effectively suppressed viral replication not only suppressed HBV DNA but also led to a decrease in HBV RNA, probably because NAs depleted the cccDNA that is the transcription template of HBV RNA. The serum HBV RNA level increased in the HBeAg no-seroconversion group compared with the HBeAg seroconversion group (Figure 1B). Wang's study found that blocking HBV polymerase led to HBV pgRNA accumulation *in vitro* and in transgenic mice, but they also found that in 11 CHB patients, the HBV RNA levels declined after NA treatment[3]. Another study reported that for patients with YMDD mutations, serum HBV RNA was significantly higher than that in others[8]. A study in 2015 reported that during NA therapy, HBV RNA showed remarkable drops in patients undergoing HBeAg seroconversion compared to other patients[7]. The findings of these studies were consistent with our results. They all suggested that HBV RNA reflected the antiviral treatment effect and HBeAg seroconversion.

We also evaluated the relationship of HBV RNA to other biomarkers. Overall,

Table 3 Baseline characteristics of enrolled patients (group A *vs* group B)

Characteristic	(A) HBeAg positive patients with seroconversion (*n* = 10)	(B) HBeAg positive patients with no seroconversion (*n* = 15)	*P* value (A) *vs* (B)	(C) HBeAg negative patients (*n* = 5)	*P* value (A) *vs* (C)
Gender (male/female)	8/2	12/3		5/0	
Age (yR)	37 ± 6	33 ± 12	0.034	40 ± 150	0.505
Body mass index	25.29 ± 3.86	23.82 ± 3.25	0.528	24.38 ± 3.87	0.676
Alanine aminotransferase (IU/mL)					
Week 0	156.10 ± 72.94	174.53 ± 317.58	0.272	123.60 ± 71.81	0.428
Week 24	46.10 ± 32.61	50.00 ± 46.83	0.665	29.20 ± 8.17	0.282
HBsAg (log_{10} IU/mL)					
Week 0	3.81 ± 0.84	4.14 ± 0.57	0.068	3.79 ± 1.02	0.967
Week 24	3.51 ± 0.59	3.94 ± 0.59	0.658	3.29 ± 0.32	0.474
HBV DNA (log_{10} IU/mL)					
Week 0	8.05 ± 0.99	8.57 ± 0.76	0.498	6.11 ± 1.64	0.013
Week 24	3.32 ± 1.11	3.68 ± 1.15	0.635	3.03 ± 0.44	0.279
HBV RNA (log_{10} copies/mL)					
Week 0	3.52 ± 0.84	5.59 ± 0.67	0.061	4.08 ± 0.99	0.27
Week 24	3.06 ± 1.39	5.48 ± 1.51	0.032	2.93 ± 1.39	0.161
HBV genotype					
B (%)	3 (30.00%)	2 (13.33%)		1 (20%)	
C (%)	7 (70.00%)	13 (86.67%)		4 (80%)	

HBV: Hepatitis B virus.

HBsAg had a poor correlation with HBV RNA (r = 0.265, P = 0.041), and HBV DNA and HBV RNA did not show a correlation (r = 0.242, P = 0.062) (Figure 2A and B). Other studies showed that HBV RNA was remarkably related to both HBV DNA and HBsAg before treatment. Nevertheless, those molecules did not show correlations during therapy[7,11]. We hypothesize that HBV RNA may be an independent predictor that is less reflected by the polymerase inhibitors than by HBV DNA. HBsAg can be produced either from intrahepatic cccDNA or from integrated HBV DNA. However, HBV RNA was only produced from cccDNA. As a result, HBV RNA was an independent indicator.

The multivariate regularized linear model was analyzed with the following variables: age, sex, BMI, ALT, HBV DNA, HBsAg, whether there was a VR, and whether there was HBeAg seroconversion. Before treatment, whether there was HBeAg seroconversion was the best single linear indicator associated with HBV RNA level. After 24 wk of treatment, we found one best result model: whether VR was the best single linear indicator related with HBV RNA. The results demonstrated that HBV RNA was an independent molecule predicting HBeAg seroconversion and VR. Despite the fact that VR can be detected by HBV DNA level, we found that when patients had a PVR, the level of HBV RNA increased. Because both serum HBV DNA and HBV RNA can only be generated from cccDNA, the partial effect of blocking reverse transcription activity led to an increase in HBV RNA. A potential explanation may be that the detectable rcDNA translocated into the nucleus. There, it is converted into cccDNA. Because viral mRNA is directly transcribed from cccDNA, an increase in cccDNA will lead to an increase in HBV RNA.

Our results suggested that serum HBV RNA levels predicted HBeAg seroconversion during ETV therapy. The result of ROC curve analysis generated the claim that in patients with subsequent HBeAg seroconversion, serum HBV RNA levels were slightly lower before treatment. A previous study appeared to validate such view[7]. Because most patients (67%-80%) achieved HBeAg seroconversion during therapy[10], patients who had high levels of HBV RNA (over 4.12 log_{10} copies/mL) before treatment should be given more attention during treatment.

However, the present study had a limitation of a relative small number of enrolled

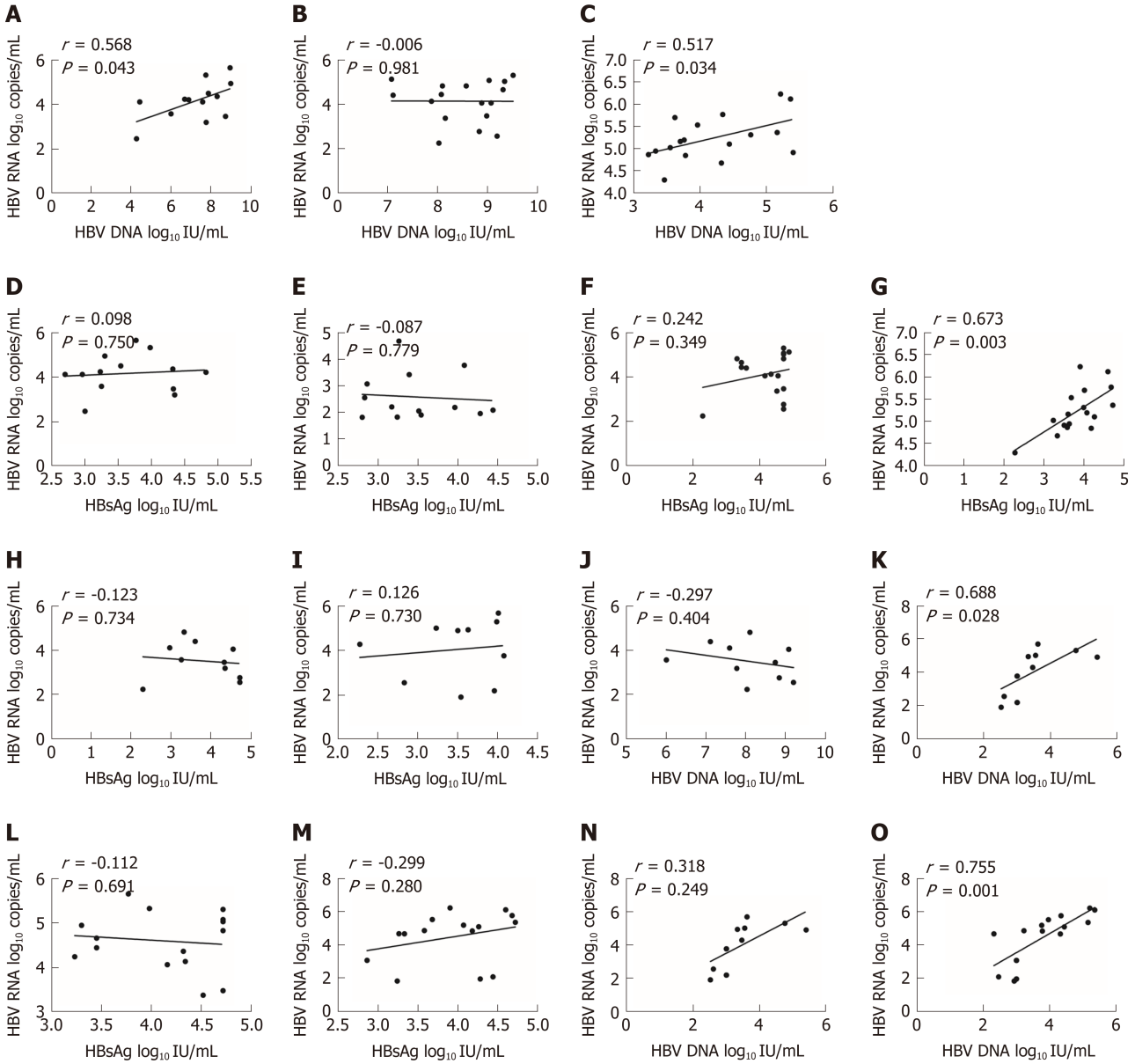

Figure 2 Relationship of hepatitis B virus RNA to other biomarkers. A: In the virological response (VR) group, there was a moderate correlation between hepatitis B virus (HBV) RNA and HBV DNA before treatment; B: In the partial (VR) PVR group, there was no correlation between HBV RNA and HBV DNA before treatment; C: After 24 wk of treatment, HBV RNA and HBV DNA had a moderate correlation in the PVR group; D: In the VR group, HBV RNA and HBsAg had no correlation before treatment; E: In the PVR group, HBV RNA and HBsAg had no correlation before treatment; F: After 24 wk of treatment, HBV RNA had no correlation with HBsAg in the VR group; G: After 24 wk of treatment, HBV RNA had a significant high correlation with HBsAg in the PVR group; H: HBV RNA had no correlation with HBsAg in group A before treatment; I: HBV RNA had no correlation with HBsAg in group A after treatment; J: HBV RNA had no correlation with HBV DNA in group A before treatment; K: HBV RNA had a moderate correlation with HBV DNA in group A after treatment; L: HBV RNA had no correlation with HBsAg in group B before treatment; M: HBV RNA had no correlation with HBsAg in group B after treatment; N: HBV RNA had no correlation with HBV DNA in group B before treatment; O: HBV RNA had a moderate correlation with HBV DNA in group B after treatment. HBV: Hepatitis B virus; VR: Virological response; PVR: Partial virological response.

patients. As a result, the conclusion of present study needs to be confirmed by using much larger sample size.

In conclusion, we found that serum HBV RNA predicted both VR and HBeAg seroconversion. The data appeared to suggest that serum HBV RNA decreased in patients who achieved a VR during ETV therapy, and *vice versa*. Overall, HBsAg and HBV RNA had a poor correlation (r = 0.265, P = 0.041), and HBV DNA had no correlation to HBV RNA (r = 0.242, P = 0.062). Furthermore, serum HBV RNA was an independent predictor of HBeAg seroconversion and VR. HBeAg seroconversion was more likely to be achieved for CHB patients with HBV RNA levels below 4.12 $\log_{10}$ copies/mL before treatment.

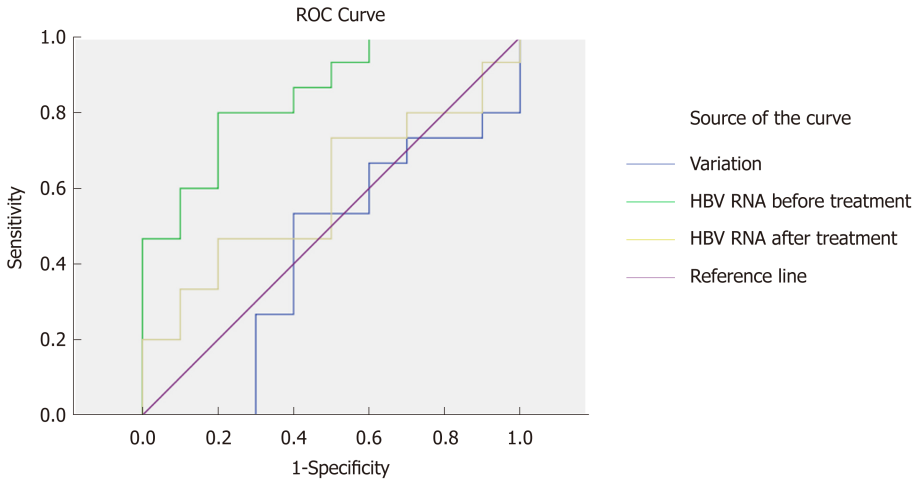

Figure 3 Predictive value of hepatitis B virus RNA for HBeAg seroconversion. ROC: Receiver operating characteristic.

ARTICLE HIGHLIGHTS

Research background

Nucleos(t)ide analogues (NAs) only suppress hepatitis B virus (HBV) DNA replication, resulting in decreased serum HBV DNA, but they do not suppress covalently closed circular DNA (cccDNA). Pregenome RNA (pgRNA) is the direct product of cccDNA. A number of studies have shown that HBV RNA levels in serum were related to virological response (VR) and prognosis. However, characteristics of alterations of serum HBV RNA in different chronic hepatitis B (CHB) patients still cannot be fully explained. Whether HBV RNA can predict HBeAg seroconversion is still controversial.

Research motivation

In this work, we investigated the characteristics of HBV RNA alterations in CHB patients with different treatment effects. The relationships of HBV RNA with other serological markers were also analyzed. Finally, we calculated the predictive value of HBV RNA in anticipating HBeAg seroconversion. Solving these problems helps to investigate the predictive value of HBV RNA.

Research objectives

If HBV DNA is maintained at undetectable levels, it is difficult to predict whether a patient will have a serological response. To address this question, we evaluated whether HBV RNA had a relationship with VR and HBeAg antigen seroconversion, how HBV RNA was related to other indicators, whether HBV RNA was an independent indicator of HBeAg seroconversion, and finally, the diagnostic value of HBV RNA.

Research methods

The present study evaluated 61 CHB patients from September 2006 to December 2007 at the Department of Infectious Diseases of Peking University First Hospital (China) who had begun long-term entecavir (ETV) monotherapy. Finally, we collected 30 treatment-naive individuals. Serum HBV RNA was extracted from 140 μL serum samples at two time points. Then they were reverse transcribed to cDNA with the HBV-specific primer. The product was quantified by real-time quantitative PCR (RT-PCR) using TAMARA probes. Statistical analyses were performed with IBM SPSS 20.0.

Research results

By comparing the dynamic characteristics of HBV RNA in the VR and partial VR groups, we found that HBV RNA showed a strong decrease in the VR group. By contrast, HBV RNA increased in the partial VR group. The serum HBV RNA level increased in the HBeAg no-seroconversion group compared with the HBeAg seroconversion group. Overall, HBsAg had a poor correlation with HBV RNA (r = 0.265, P = 0.041), and HBV DNA and HBV RNA did not show a correlation (r = 0.242, P = 0.062). Furthermore, serum HBV RNA was an independent predictor of HBeAg seroconversion and VR. HBeAg seroconversion was more likely to be achieved for CHB patients with HBV RNA levels below 4.12 $\log_{10}$ copies/mL before treatment.

Research conclusions

In conclusion, we found that serum HBV RNA predicted both VR and HBeAg seroconversion. The data appeared to suggest that serum HBV RNA decreased in patients who achieved a VR during ETV therapy, and *vice versa*. Overall, HBsAg and HBV RNA had a poor correlation (r = 0.265, P = 0.041), and HBV DNA had no correlation to HBV RNA (r = 0.242, P = 0.062). Furthermore, serum HBV RNA was an independent predictor of HBeAg seroconversion and VR. HBeAg seroconversion was more likely to be achieved for CHB patients with HBV RNA levels

below 4.12 $\log_{10}$ copies/mL before treatment.

Research perspectives

The present study suggested that serum HBV RNA decreased in patients who achieved a VR during ETV therapy, and *vice versa*. HBeAg seroconversion was more likely to be achieved for CHB patients with HBV RNA levels below 4.12 $\log_{10}$ copies/mL before treatment. In the future, the study could focus on the application value of HBV RNA in CHB patients with disease progression.

ACKNOWLEDGEMENTS

The authors would like to sincerely thank Professor Ding-Fang Bu (Peking University First Hospital) for his guidance with the statistics.

REFERENCES

1 **Schweitzer A**, Horn J, Mikolajczyk RT, Krause G, Ott JJ. Estimations of worldwide prevalence of chronic hepatitis B virus infection: a systematic review of data published between 1965 and 2013. *Lancet* 2015; **386**: 1546-1555 [PMID: 26231459 DOI: 10.1016/S0140-6736(15)61412-X]
2 **Nassal M**. HBV cccDNA: viral persistence reservoir and key obstacle for a cure of chronic hepatitis B. *Gut* 2015; **64**: 1972-1984 [PMID: 26048673 DOI: 10.1136/gutjnl-2015-309809]
3 **Wang J**, Shen T, Huang X, Kumar GR, Chen X, Zeng Z, Zhang R, Chen R, Li T, Zhang T, Yuan Q, Li PC, Huang Q, Colonno R, Jia J, Hou J, McCrae MA, Gao Z, Ren H, Xia N, Zhuang H, Lu F. Serum hepatitis B virus RNA is encapsidated pregenome RNA that may be associated with persistence of viral infection and rebound. *J Hepatol* 2016; **65**: 700-710 [PMID: 27245431 DOI: 10.1016/j.jhep.2016.05.029]
4 **Jansen L**, Kootstra NA, van Dort KA, Takkenberg RB, Reesink HW, Zaaijer HL. Hepatitis B Virus Pregenomic RNA Is Present in Virions in Plasma and Is Associated With a Response to Pegylated Interferon Alfa-2a and Nucleos(t)ide Analogues. *J Infect Dis* 2016; **213**: 224-232 [PMID: 26216905 DOI: 10.1093/infdis/jiv397]
5 **Köck J**, Theilmann L, Galle P, Schlicht HJ. Hepatitis B virus nucleic acids associated with human peripheral blood mononuclear cells do not originate from replicating virus. *Hepatology* 1996; **23**: 405-413 [PMID: 8617418 DOI: 10.1002/hep.510230303]
6 **Tsuge M**, Murakami E, Imamura M, Abe H, Miki D, Hiraga N, Takahashi S, Ochi H, Nelson Hayes C, Ginba H, Matsuyama K, Kawakami H, Chayama K. Serum HBV RNA and HBeAg are useful markers for the safe discontinuation of nucleotide analogue treatments in chronic hepatitis B patients. *J Gastroenterol* 2013; **48**: 1188-1204 [PMID: 23397114 DOI: 10.1007/s00535-012-0737-2]
7 **van Bömmel F**, Bartens A, Mysickova A, Hofmann J, Krüger DH, Berg T, Edelmann A. Serum hepatitis B virus RNA levels as an early predictor of hepatitis B envelope antigen seroconversion during treatment with polymerase inhibitors. *Hepatology* 2015; **61**: 66-76 [PMID: 25132147 DOI: 10.1002/hep.27381]
8 **Hatakeyama T**, Noguchi C, Hiraga N, Mori N, Tsuge M, Imamura M, Takahashi S, Kawakami Y, Fujimoto Y, Ochi H, Abe H, Maekawa T, Kawakami H, Yatsuji H, Aisaka Y, Kohno H, Aimitsu S, Chayama K. Serum HBV RNA is a predictor of early emergence of the YMDD mutant in patients treated with lamivudine. *Hepatology* 2007; **45**: 1179-1186 [PMID: 17465002 DOI: 10.1002/hep.21581]
9 **Ward H**, Tang L, Poonia B, Kottilil S. Treatment of hepatitis B virus: an update. *Future Microbiol* 2016; **11**: 1581-1597 [PMID: 27855500 DOI: 10.2217/fmb-2016-0128]
10 **Tang LSY**, Covert E, Wilson E, Kottilil S. Chronic Hepatitis B Infection: A Review. *JAMA* 2018; **319**: 1802-1813 [PMID: 29715359 DOI: 10.1001/jama.2018.3795]
11 **Lai CL**, Wong D, Ip P, Kopaniszen M, Seto WK, Fung J, Huang FY, Lee B, Cullaro G, Chong CK, Wu R, Cheng C, Yuen J, Ngai V, Yuen MF. Reduction of covalently closed circular DNA with long-term nucleos(t)ide analogue treatment in chronic hepatitis B. *J Hepatol* 2017; **66**: 275-281 [PMID: 27639844 DOI: 10.1016/j.jhep.2016.08.022]

P- Reviewer: Dogan UB, Tabll AA, Taylor J
S- Editor: Ma RY **L- Editor:** Wang TQ **E- Editor:** Yin SY

World Journal of Gastroenterology

Submit a Manuscript: https://www.f6publishing.com

World J Gastroenterol 2019 February 14; 25(6): 729-743

DOI: 10.3748/wjg.v25.i6.729

ISSN 1007-9327 (print) ISSN 2219-2840 (online)

META-ANALYSIS

Body-mass index correlates with severity and mortality in acute pancreatitis: A meta-analysis

Dalma Dobszai, Péter Mátrai, Zoltán Gyöngyi, Dezső Csupor, Judit Bajor, Bálint Erőss, Alexandra Mikó, Lajos Szakó, Ágnes Meczker, Roland Hágendorn, Katalin Márta, Andrea Szentesi, Péter Hegyi, on behalf of the Hungarian Pancreatic Study Group

ORCID number: Dalma Dobszai (0000-0002-8703-1381); Péter Mátrai (0000-0001-5144-0733); Zoltán Gyöngyi (0000-0001-9330-9119); Dezső Csupor (0000-0002-4088-3333); Judit Bajor (0000-0002-3941-4871); Bálint Erőss (0000-0003-3658-8427); Alexandra Mikó (0000-0002-5322-4425); Lajos Szakó (0000-0001-9783-4076); Ágnes Meczker (0000-0002-2646-2217); Roland Hágendorn (0000-0002-9984-2309); Katalin Márta (0000-0002-2213-4865); Andrea Szentesi (0000-0003-2097-6927); Péter Hegyi (0000-0003-0399-7259).

Author contributions: Dobszai D, Bajor J, Hágendorn R and Szakó L conducted the search in the databases. Mikó A, Meczker Á, Márta K and Csupor D read the articles for eligibility; in the case of conflict, the decision was left to a third participant, Hegyi P. Dobszai D, Meczker Á and Mikó A entered the data from the articles in an Excel file, while Mátrai P analyzed the data. Dobszai D and Gyöngyi Z carried out the bias analysis. Dobszai D, Mikó A and Márta K drafted the manuscript, and Szentesi A, Hágendorn R and Bajor J edited it. Meczker Á and Szentesi A edited the tables and figures. Dobszai D, Bajor J and Szakó L completed the items on the PRISMA-recommended checklist. Hegyi P and Erőss B made a critical revision of the finalized manuscript. All the authors read and approved the final manuscript.

Supported by a Project Grant (No.

Dalma Dobszai, Péter Mátrai, Bálint Erőss, Alexandra Mikó, Lajos Szakó, Ágnes Meczker, Katalin Márta, Andrea Szentesi, Péter Hegyi, Institute for Translational Medicine, Medical School, University of Pécs, Pécs 7624, Hungary

Dalma Dobszai, Andrea Szentesi, Clinical Medicine Doctoral School, University of Szeged, Szeged 6720, Hungary

Péter Mátrai, Institute for Bioanalysis, Medical School, University of Pécs, Pécs 7624, Hungary

Zoltán Gyöngyi, Department of Public Health Medicine, Medical School, University of Pécs, Pécs 7624, Hungary

Dezső Csupor, Department of Pharmacognosy, University of Szeged, Szeged 6720, Hungary

Judit Bajor, Roland Hágendorn, Division of Gastroenterology, First Department of Medicine, University of Pécs, Medical School, Pécs 7624, Hungary

Katalin Márta, János Szentágothai Research Center, University of Pécs, Pécs 7624 Hungary

Péter Hegyi, MTA-SZTE Momentum Translational Gastroenterology Research Group, University of Szeged, Szeged 6720, Hungary

Corresponding author: Péter Hegyi, MD, PhD, DSc, Professor of Medicine, Director, Institute for Translational Medicine, Medical School, University of Pécs, 12 Szigeti Street, Pécs H-7624, Hungary. hegyi2009@gmail.com
Telephone: +36-70-3751031

Abstract

BACKGROUND

Obesity rates have increased sharply in recent decades. As there is a growing number of cases in which acute pancreatitis (AP) is accompanied by obesity, we found it clinically relevant to investigate how body-mass index (BMI) affects the outcome of the disease.

AIM

To quantify the association between subgroups of BMI and the severity and mortality of AP.

METHODS

A meta-analysis was performed using the Preferred Reporting Items for

KH125678 to PH); an Economic Development and Innovation Operative Program Grant (GINOP 2.3.2-15-2016-00048 to PH; and a Human Resources Development Operational Program Grant (No. EFOP-3.6.2-16-2017-00006 to PH) from the National Research, Development and Innovation Office as well as by a Momentum Grant from the Hungarian Academy of Sciences (No. LP2014-10/2014 to PH); EFOP-3.6.3-VEKOP-16-2017-00009 and UNKP-18-3-INew National Excellence Program of the Ministry of Human Capacities (No. PTE/38329-1/2018 to KM).

Conflict-of-interest statement: The authors declare that no conflict of interest exists. There are no financial or other competing interests for principal investigators, patients included or any member of the trial.

PRISMA 2009 Checklist statement: The authors have read the PRISMA 2009 Checklist, and the manuscript was prepared and revised according to the PRISMA 2009 Checklist.

Manuscript source: Unsolicited manuscript

Received: November 7, 2018
Peer-review started: November 12, 2018
First decision: November 22, 2018
Revised: December 4, 2018
Accepted: December 19, 2018
Article in press: December 20, 2018
Published online: February 14, 2019

Systematic Review and Meta-Analysis (PRISMA) Protocols. Three databases (PubMed, EMBASE and the Cochrane Library) were searched for articles containing data on BMI, disease severity and mortality rate for AP. English-language studies from inception to 19 June 2017 were checked against our predetermined eligibility criteria. The included articles reported all AP cases with no restriction on the etiology of the disease. Only studies that classified AP cases according to the Atlanta Criteria were involved in the severity analyses. Odds ratios (OR) and mean differences (MD) were pooled using the random effects model with the DerSimonian-Laird estimation and displayed on forest plots. The meta-analysis was registered in PROSPERO under number CRD42017077890.

RESULTS

A total of 19 articles were included in our meta-analysis containing data on 9997 patients. As regards severity, a subgroup analysis showed a direct association between AP severity and BMI. BMI < 18.5 had no significant effect on severity; however, BMI > 25 had an almost three-fold increased risk for severe AP in comparison to normal BMI (OR = 2.87, 95%CI: 1.90-4.35, $P < 0$ .001). Importantly, the mean BMI of patients with severe AP is higher than that of the non-severe group (MD = 1.79, 95%CI: 0.89-2.70, $P < 0.001$). As regards mortality, death rates among AP patients are the highest in the underweight and obese subgroups. A BMI < 18.5 carries an almost two-fold increase in risk of mortality compared to normal BMI (OR = 1.82, 95%CI: 1.32-2.50, $P < 0.001$). However, the chance of mortality is almost equal in the normal BMI and BMI 25-30 subgroups. A BMI > 30 results in a three times higher risk of mortality in comparison to a BMI < 30 (OR = 2.89, 95%CI: 1.10-7.36, $P = 0.026$).

CONCLUSION

Our findings confirm that a BMI above 25 increases the risk of severe AP, while a BMI > 30 raises the risk of mortality. A BMI < 18.5 carries an almost two times higher risk of mortality in AP.

Key words: Acute pancreatitis; Body-mass index; Obesity; Severity; Mortality; Prognostic; Meta-analysis

Core tip: It is the first detailed analysis on all World Health Organization body-mass index (BMI) categories, by comparing the normal BMI subgroup to all other subgroups of BMI with regard to both severity and mortality in acute pancreatitis (AP). Here we show that a BMI above 25 increases the risk of severe AP, while a BMI > 30 raises the risk of mortality. A BMI lower than eighteen point five carries an almost two times higher risk of mortality in AP.

Citation: Dobszai D, Mátrai P, Gyöngyi Z, Csupor D, Bajor J, Erőss B, Mikó A, Szakó L, Meczker Á, Hágendorn R, Márta K, Szentesi A, Hegyi P, on behalf of the Hungarian Pancreatic Study Group. Body-mass index correlates with severity and mortality in acute pancreatitis: A meta-analysis. *World J Gastroenterol* 2019; 25(6): 729-743
URL: https://www.wjgnet.com/1007-9327/full/v25/i6/729.htm
DOI: https://dx.doi.org/10.3748/wjg.v25.i6.729

INTRODUCTON

Obesity is one of the dominant public health concerns worldwide. It is a major risk factor for various diseases such as diabetes, cardiovascular disease, some cancers, kidney disease, obstructive sleep apnea, gout, osteoarthritis, and hepatobiliary disease[1]. The increasing prevalence of obesity (Figures 1 and 2)[2] also places a huge financial burden on national healthcare systems: according to a review published in 2010, obesity alone accounts for between 0.7% and 2.8% of total healthcare expenditures, while costs associated with a body-mass index (BMI) ≥ 25 reach as high as 9.1% of total spending on medical care[3].

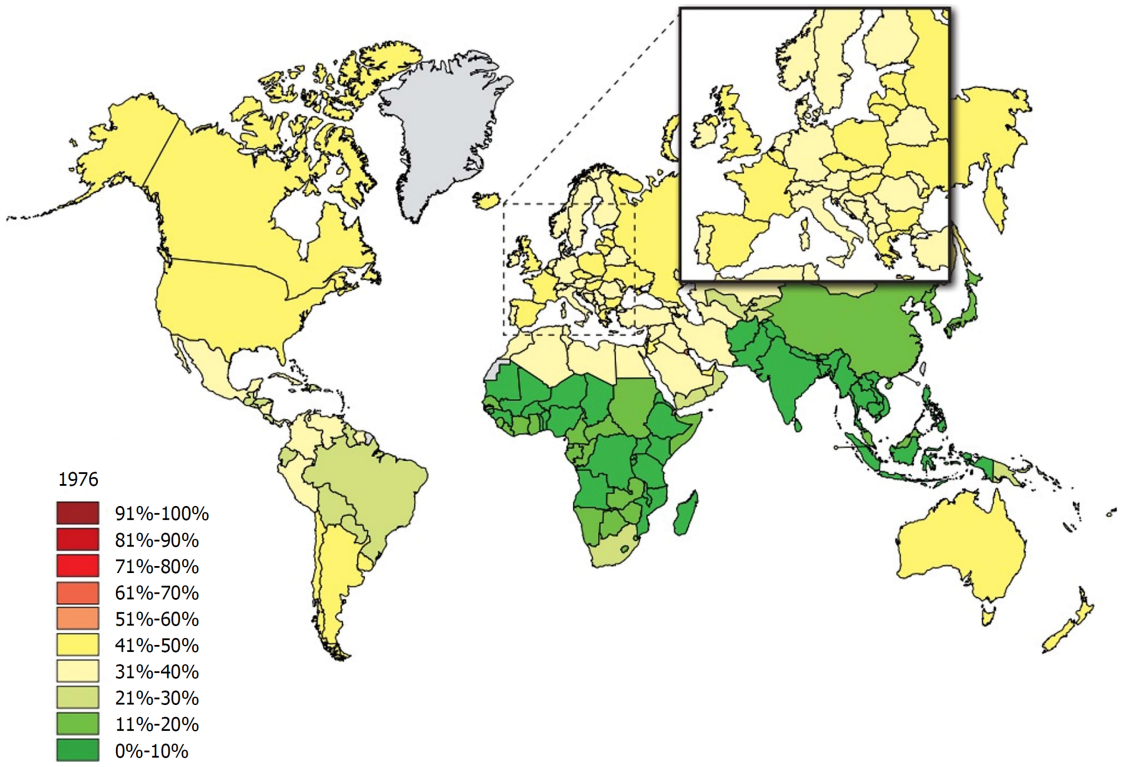

Figure 1 The rate of individuals with a body-mass index ≥ 25 among adults in 1976. Source: Global Health Observatory data repository http://apps.who.int/gho/data/node.main.A897A?lang=en.

The most common method for measuring obesity is BMI, which is calculated from a person's weight in kilograms and height in meters (kg/m^2). BMI is divided into five categories according to the World Health Organization (WHO) classification: underweight (< 18.5 kg/m^2), normal weight (18.5-24.9 kg/m^2), overweight (25-29.9 kg/m^2), obese class I (30-34.9 kg/m^2), obese class II (35-39.9 kg/m^2) and obese class III (≥ 40 kg/m^2)[4].

Among various other diseases, there is an increasing number of clinical cases in which acute pancreatitis (AP) is also accompanied by high BMI. Characterized by high mortality, AP is the most frequent cause of acute hospitalization among all gastrointestinal disorders with a prevalence of 10-100/100000 cases worldwide [5]. The B5 point of the IAP/APA evidence-based guidelines highlights the importance of predicting the primary endpoints of AP, namely severity and mortality, therefore, we found it crucially important to investigate how obesity affects the outcome of the disease[6]. Numerous studies have also linked severe acute pancreatitis (SAP) with obesity. The majority of the clinical trials conducted with the aim of determining the sensitivity and specificity of the predictive score systems of AP with the obesity factor added to it resulted in greater diagnostic accuracy[7-9].

Despite the fact that there is evidence of high BMI exacerbating AP, there has been a lack of structured and completed analyses. Until now, four meta-analyses have been performed to investigate the prognostic role of BMI in AP; however, none of them (1) analyzed all five WHO BMI categories, (2) compared the normal BMI group to every other subgroup, (3) investigated the effect of underweight on AP outcome or (4) suggested cut-off values[10-13]. The last meta-analysis on this topic was conducted in 2011, so our update involves new articles published during the last six years, leading to a remarkably higher patient number than before.

MATERIALS AND METHODS

Literature search

This meta-analysis was conducted following the guidelines proposed by the PRISMA Statement[14]. The protocol was previously registered on PROSPERO under CRD42017077890. A systematic search of the medical literature was performed using PubMed, EMBASE and the Cochrane Library. In all the databases, the following keywords were used for the search: acute pancreatitis AND BMI AND (severity OR

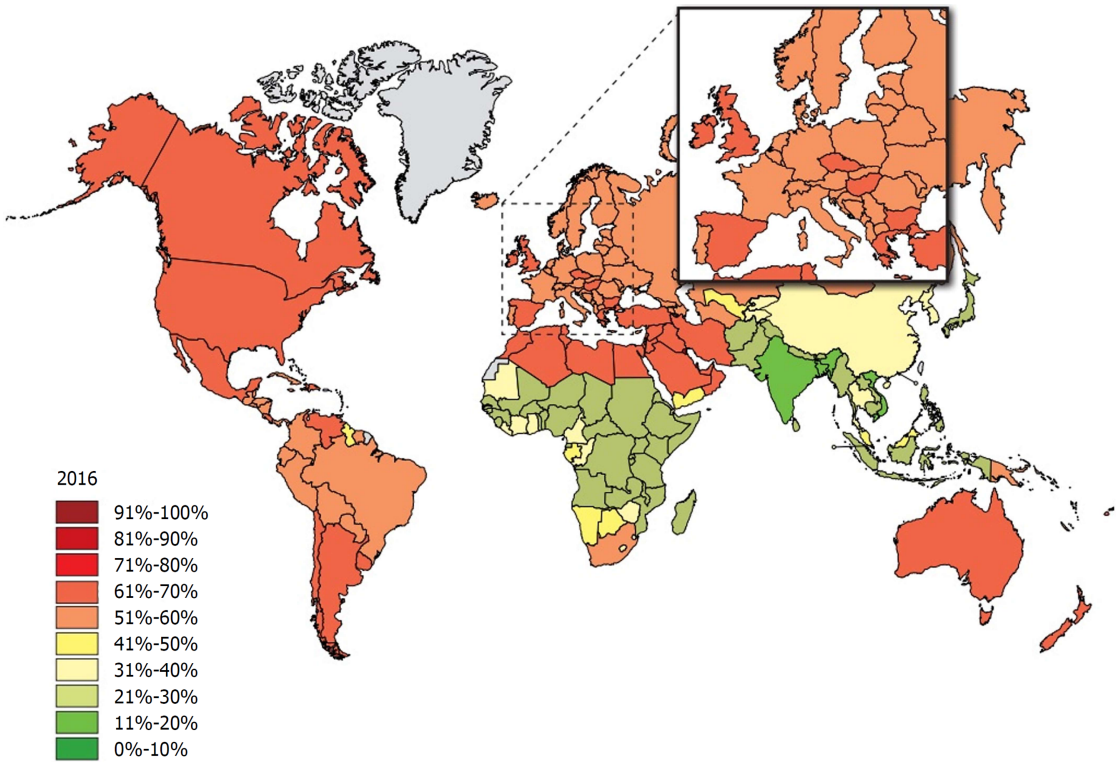

Figure 2 The rate of individuals with a body-mass index ≥ 25 among adults 40 years later in 2016. Source: Global Health Observatory data repository (http://apps.who.int/gho/data/node.main.A897A?lang=en).

mortality). Results were imported into reference manager software (EndNote X7.5). The reference lists in the articles were also checked to capture all relevant articles published within our topic of interest. The last literature search in the same databases was completed on 22nd December 2017. The details of these literature searches are included in the Supporting Material. We adapted the PICO format to set the inclusion criteria. Our PICO items were the following: (P) patients with AP, (I) low/high BMI, (C) normal BMI, and (O) severity and mortality of pancreatitis. Besides these two major endpoints of AP, we also collected data on the length of hospitalization and local or systemic complications for the purpose of analysis.

Study selection

Two of the authors independently checked whole texts with figures and tables against our predetermined eligibility criteria. During the selection process, meta-analyses, reviews, case reports and abstracts with inadequate data were excluded. Articles were declared eligible if the study enrolled all AP patients with no restriction on one specific etiology. In the severity analysis, we only included studies in which the original[15] or the revised[16] version of the Atlanta Criteria were used to determine the severity of AP. However, in the analysis of the effect of BMI on mortality, the use of the Atlanta Classification was not a criterion.

Data extraction

Review authors entered the following main data from the eligible articles (Table 1) on an Excel sheet: (1) First author, year of publication, country; (2) Study type; (3) Group of enrolled patients; (4) BMI subgroups and sample sizes; (5) Method used to define disease severity; (6) Mean BMI; (7) Number of severe cases and mortality; (8) Mean length of hospitalization and mean Intensive Care Unit stay in days; (9) Mean or median severity scores: Acute Physiology and Chronic Health Disease Classification System II (APACHE II) and Ranson's score; and (10) Number of cases with necrosis development. Discrepancies were resolved by consensus.

Risk of bias

Risk of bias assessment was carried out according to a modified version of the Newcastle-Ottawa Scale (NOS) to rate the internal validity of the individual studies, and funnel plots were constructed to assess the risk of publication bias (Supporting Material).

Table 1 Characteristics of the included studies

Ref.	Country	Type of study	Total no. of patients	Groups	BMI groups	Sample size
Bota *et al*[32]	Romania	Retrospective	334	Mild		207
				Severe		127
Duarte-Rojo *et al*[18]	Mexico	Prospective	99	Mild		74
				Severe		25
Funnel *et al*[29]	South Africa	Prospective	99		< 19	15
					19-25	48
					26-29	17
					≥ 30	19
Karpavicius *et al*[23]	Lithuania	Prospective	102	Mild and moderate		82
				Severe		20
Katuchova *et al*[21]	Slovakia	Prospective	384	IEP		293
				SAP		91
Mery *et al*[25]	Mexico	Prospective	88		< 25	34
					25-29.9	32
					≥ 30	22
Papachristou *et al*[8]	United States	Prospective	102		< 30	74
					≥ 30	28
Párniczky *et al*[5]	Hungary	Prospective, multicenter	446		< 18.5	26
					18.5-24.9	136
					25-29.9	154
					30-34.9	86
					35-39.9	24
					> 40	20
Sharma *et al*[30]	United States	Prospective	128		< 30	87
					≥ 30	41
Shin *et al*[20]	South Korea	Retrospective	374		18.5-22.9	170
					23-24.9	96
					25-29.9	97
					≥ 30	11
Suazo-Barahona *et al*[26]	Mexico	Retrospective	150		< 25	65
					≥ 25	85
Taguchi *et al*[31]	Japan	Retrospective	6002		< 18.5	839
					18.5-24.9	3767
					25-29.9	1106
					30-34.9	220
					> 35	70
Thandassery *et al*[27]	India	Prospective	280		18.5-22.9	131
					23-24.9	83
					>25	66
Tsai *et al*[34]	Taiwan	Prospective	320		< 30	294
					≥ 30	26
Türkoglu *et al*[24]	Turkey	Prospective cohort study	92	Mild		62
				Severe		30
Yang *et al*[28]	China	Prospective, multicenter	161		≥ 25	82
					≥ 25	79
Yashima *et al*[22]	Japan	Prospective	124	Mild		76
				Severe		48
Yeung *et al*[19]	China	Prospective	101		< 25	19
					≥ 25	82
Yoon *et al*[17]	South Korea	Retrospective	203	Mild		128
				Moderate		62
				Severe		13

BMI: Body-mass index; IEP: Interstitial edematous pancreatitis; SAP: Severe acute pancreatitis.

Statistical analysis

The statistical analysis was conducted with Stata 11 SE (Stata Corp, College Station, TX, United States). First, we calculated mean differences from BMI in severe and non-severe groups and odds ratios (OR) for severity and mortality outcomes based on patient numbers in different BMI categories. ORs and mean differences were pooled using the random effects model with the DerSimonian-Laird estimator and displayed on forest plots. Summary OR and mean estimation, *P*-value and 95% confidence interval (CI) were calculated. $P < 0.05$ was considered a significant difference from summary OR = 1 or mean = 0. Statistical heterogeneity was analyzed using the I^2 statistic and the chi-square test to obtain probability values; $P < 0.05$ was determined to indicate significant heterogeneity. We investigated the possible signs of a small study effect, displaying the studies on a funnel plot with the trim and fill algorithm.

RESULTS

The systematic search of the literature yielded 262 items. After eliminating duplicates, 217 records were screened by title and abstract. 156 articles were included in the full-text assessment, of which 15 studies met our predetermined eligibility criteria. An additional four articles included in the quantitative synthesis were found by checking the references of the originally identified articles (Figure 3).

The interpretation of cut-off values was not unified in the enrolled studies that investigated the effect of obesity in AP. As articles used different BMI grouping and not all articles contained data on all BMI subgroups, we decided to use several statistical approaches.

Severity

Nine articles[17-24,32] presented data on the mean BMI of the non-severe and severe patient groups (Figure 4). This meta-analysis showed that severe AP patients have a significantly higher BMI compared to those with moderately severe and severe AP (MD = 1.79, 95%CI: 0.89-2.70, $P < 0.001$). AP patients with a BMI > 25 are almost three times more likely to develop a severe disease than normal weight and underweight patients (OR = 2.87, 95%CI: 1.90-4.35, $P < 0.001$) according to the analysis of data from eight additional studies[5,19-20,25-29] (Figure 5). Data from five articles[5,20,25,29-30] also made it possible to set a BMI of 30 kg/m^2 as a cut-off value in our severity analysis. There is a sharp difference between obese and non-obese patients in the chance for developing a severe disease: a patient with a BMI > 30 has an almost four times higher odds of SAP than one with a BMI < 30 (OR = 3.61, 95%CI: 1.56-8.36, $P = 0.003$) (Figure 6).

Comparing the normal BMI group to every other BMI category (< 18.5; 25-30; 30-35; > 35 kg/m^2) in a summary effect analysis (Figure 7) showed that overweight and obese patients are more likely to develop a severe disease than patients in all other BMI categories (OR = 2.53, 95%CI: 1.64-3.90, $P = 0.000$ and OR = 2.99, 95%CI: 1.13-7.92, $P = 0.028$). Underweight compared to normal BMI also seems to increase the risk of severe AP (OR = 1.89, 95%CI: 0.52-6.87, $P = 0.336$); however, the differences are not significant. The reason behind the lack of significance may be the particularly low number of patients in the underweight subgroup ($n = 184$). Forming subgroups from each BMI category (underweight, normal weight, overweight and obese) confirmed the previously identified tendency: the higher the BMI, the higher the chance of developing severe AP (Figure 8).

Mortality

A total of ten[5,8,19-20,25-29,31] of the 19 enrolled studies were included in this part of the meta-analysis. While a BMI > 25 represents a higher chance of developing severe AP, it does not significantly increase the mortality of the disease (OR = 2.46, 95%CI: 0.78-7.79, $P = 0.125$) (Figure 9). However, obese patients are at a three-fold increased risk of mortality compared to those with a BMI < 30 (OR = 2.89, 95%CI: 1.14-7.36, $P = 0.026$) (Figure 10). One with a BMI < 18.5 is also at a significantly higher risk of mortality in AP than a normal weight patient (OR = 1.82, 95%CI: 1.32-2.50, $P = 0.000$) (Figure 11). Death rates among AP patients are the highest in the underweight and obese subgroups (Figures 12 and 13), while the chance of mortality is almost equal in the normal BMI and BMI 25-30 subgroups.

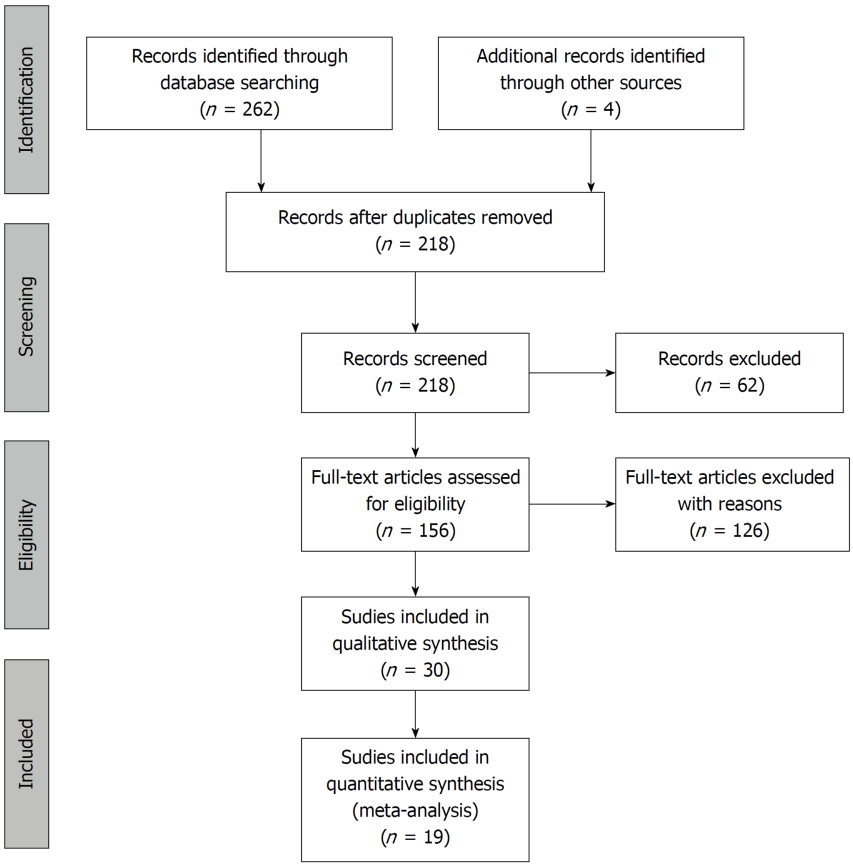

Figure 3 Flowchart of the study selection procedure.

DISCUSSION

The first meta-analysis[10] on the topic of AP and BMI was published by Martínez *et al* in 2004, concluding that obesity significantly increases the risk of local or systemic complications in AP. Since then, three more meta-analyses have also confirmed the prognostic role of BMI in the disease, leading to even more specific results. The first meta-analysis was updated two years later by the same author[11], confirming that obesity not only raises the risk of complications, but also increases the mortality in AP. In 2011, Wang *et al*[12] highlighted that overweigh (BMI > 25) also increases the incidence of SAP, while Hong *et al*[13] drew attention to the prognostic role of body weight in AP development in their meta-analyses.

The main purpose of the present meta-analysis was to precisely evaluate the predictive value of BMI in AP by assessing what is already known and confirmed by evidence and to offer guidance on its use in clinical practice.

Severity

Seven of the included articles in this meta-analysis found a clear correlation between overweight or obesity and the development SAP. Two studies showed no significant relation between BMI and disease severity in AP[5,32]. Three articles[17-18,22] analyzed the effect of BMI in comparison with other tools for measuring obesity. These studies stated that abdominal obesity (waist circumference), peripancreatic visceral adipose tissue and visceral fat-to-muscle ratio have a stronger correlation with SAP than BMI or body weight. We were also prepared to do an analysis of these data, but abdominal obesity is measured differently in each study[18,21-22,25,33], making a meta-analysis inapplicable. One of the enrolled studies compared the accuracy of different scoring systems in predicting the severity of AP[19], in which the addition of the obesity factor did not seem to improve the accuracy of the APACHE II scoring system. An interventional clinical trial[28] was also conducted in this area, resulting in the successful prevention of severe AP in obese patients with the intravenous administration of octreotide.

Although previous studies have already confirmed the relation between BMI and the major endpoints of AP, it is still not incorporated into the scoring systems that aim to predict disease outcome. A prospective study involving 186 consecutive patients

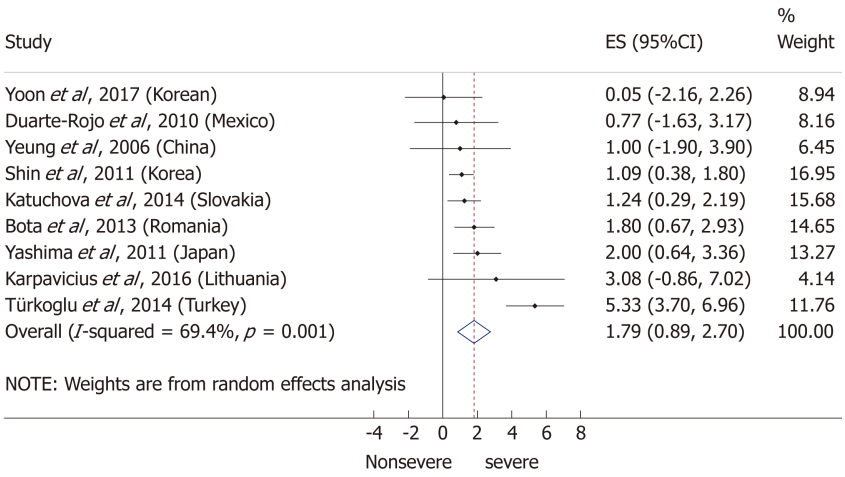

Figure 4 Forest plot of mean body-mass index in the non-severe and severe patient subgroups. Filled circles represent the mean difference derived from the studies analyzed. Horizontal bars represent 95%CI. Empty rhombuses show the overall, combined mean difference (point estimation is the middle of the rhombus and CIs are the edges). BMI: Body-mass index; CI: Confidence interval; OR: Odds ratio.

published by Johnson *et al*[7] in 2004 resulted in the improved prediction of severity in AP by adding the obesity factor to the APACHE II scoring system (Admission APACHE-O > 9: sensitivity 82%, specificity 86%, PPV 74%, NPV 91% and accuracy 85%; admission APACHE II > 9: sensitivity 68%, specificity 84%, PPV 71%, NPV 81% and accuracy 80%). Prevalence of complications increased among patients with a BMI 26-30 (score = 1), while mortality rates were significantly higher among BMI > 30 (score = 2) patients. Two years later, a prospective study of 101 patients[8] also stated that obesity is an independent risk factor for severe AP and that the APACHE-O scoring system is not significantly better, but it has a similar predictive ability compared to APACHE II (Admission APACHE-O > 9: sensitivity 84%, specificity 82%, PPV 52%, NPV 96% and accuracy 83%; admission APACHE II > 9: sensitivity 74%, specificity 85%, PPV 47%, NPV 93% and accuracy 80%). In 2012, a cross-sectional retrospective study by Guzman *et al*[9] added the BMI parameter to the Bedside Index of Severity in Acute Pancreatitis (BISAP) score and achieved higher diagnostic accuracy than the original scoring system (sensitivity 75%, specificity 96.4%, PPV 80%, NPV 95.2% and accuracy 92.3%).

Mortality

All the included articles found a correlation between BMI and mortality in AP. One study[31] identified underweight as another independent risk factor for a fatal disease outcome, and our meta-analysis confirmed this. However, the number of patients was very low in this subgroup.

Limitations

Overweight and obesity are often accompanied by other chronic diseases and metabolic derangements such as hypertension, diabetes and hypertriglyceridemia. As we did not take demographic factors and comorbidities into consideration, we cannot conclude if BMI is an independent or associated risk factor in AP, which is a limitation of this study.

Strengths

Our meta-analysis is much more comprehensive and detailed compared to the earlier ones. This work performs the first detailed analysis on all WHO BMI categories, by comparing the normal BMI subgroup to all other subgroups of BMI with regard to both severity and mortality in AP. Our subgroup analysis also investigated each BMI category, this way, we are now able to determine which BMI groups are most in danger of a severe or even fatal outcome in AP.

In conclusion, the findings of this meta-analysis demonstrated that a BMI above 25 increases the risk of severe AP, but not mortality, while a BMI > 30 raises the risk of both severity and mortality in AP. A BMI < 18.5 carries an almost two times higher risk of mortality in AP.

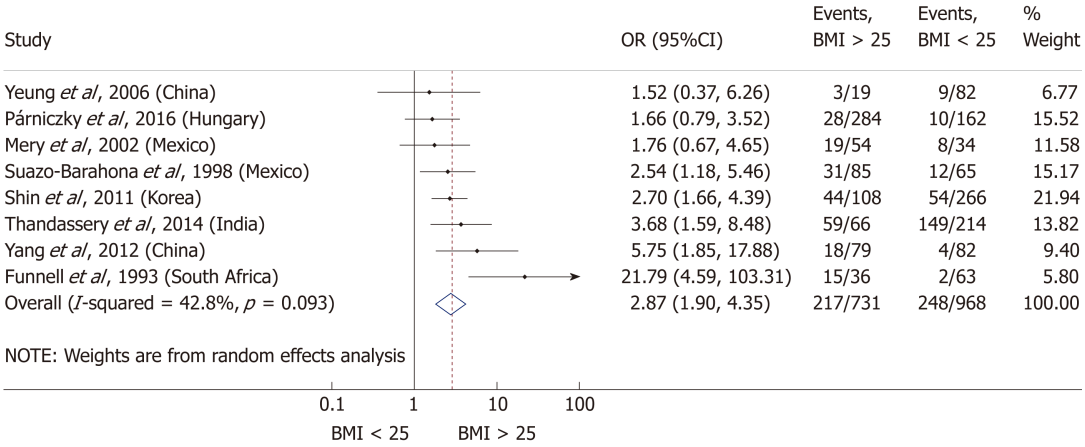

Figure 5 Forest plot of severe acute pancreatitis in the body-mass index < 25 and body-mass index > 25 subgroups. Filled circles represent the odds ratio derived from the studies analyzed. Horizontal bars represent 95%CI. Empty rhombuses show the overall, combined effect (OR is the middle of the rhombus and CIs are the edges). BMI: Body-mass index; CI: Confidence interval; OR: Odds ratio.

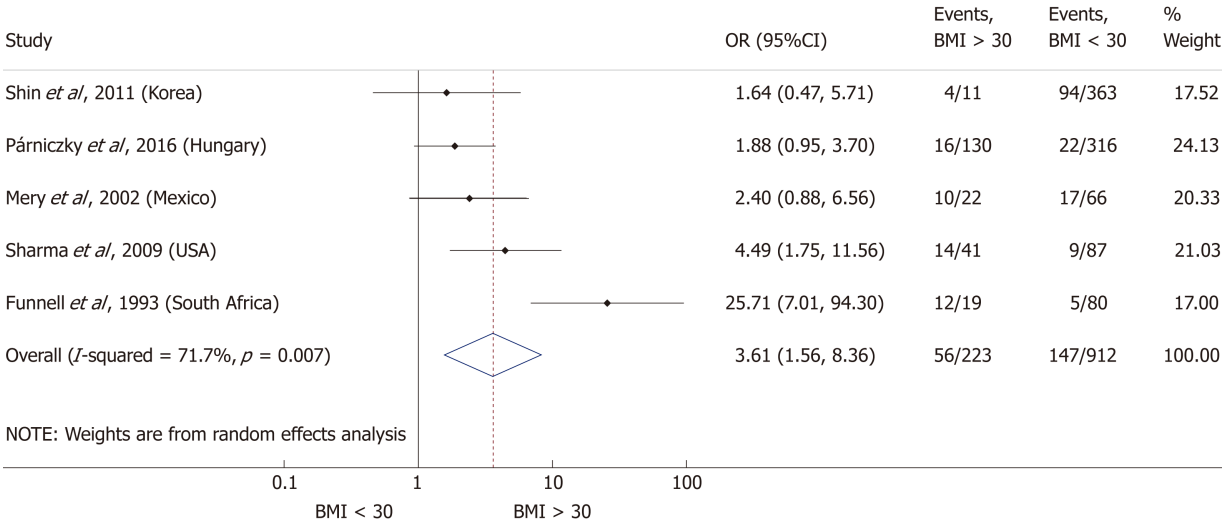

Figure 6 Forest plot of severe acute pancreatitis in the body-mass index < 30 and body-mass index > 30 subgroups. Filled circles represent the odds ratio derived from the studies analyzed. Horizontal bars represent 95%CI. Empty rhombuses show the overall, combined effect (OR is the middle of the rhombus and CIs are the edges). BMI: Body-mass index; CI: Confidence interval; OR: Odds ratio.

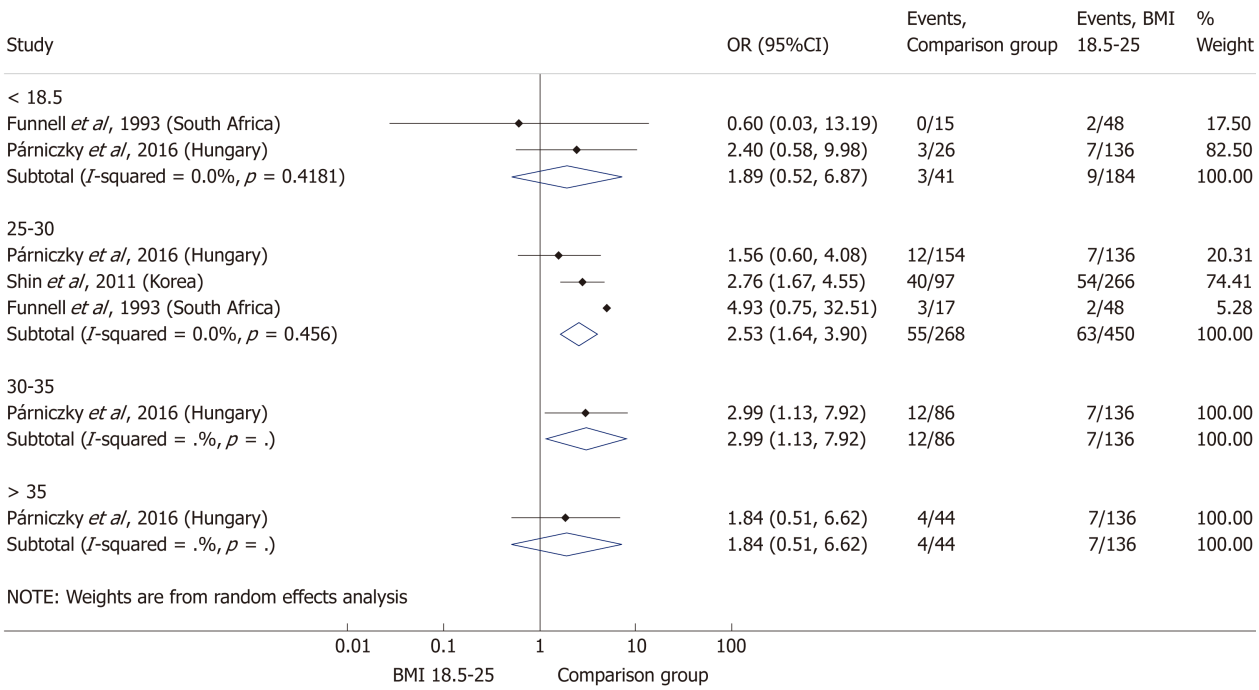

Figure 7 Forest plot of acute pancreatitis severity comparing the normal body-mass index group (body-mass index 18.5-25) to other body-mass index categories. Filled circles represent the odds ratio derived from the studies analyzed. Horizontal bars represent 95% CI. Empty rhombuses show the overall, combined effect (OR is the middle of the rhombus and CIs are the edges). BMI: Body-mass index; CI: Confidence interval; OR: Odds ratio.

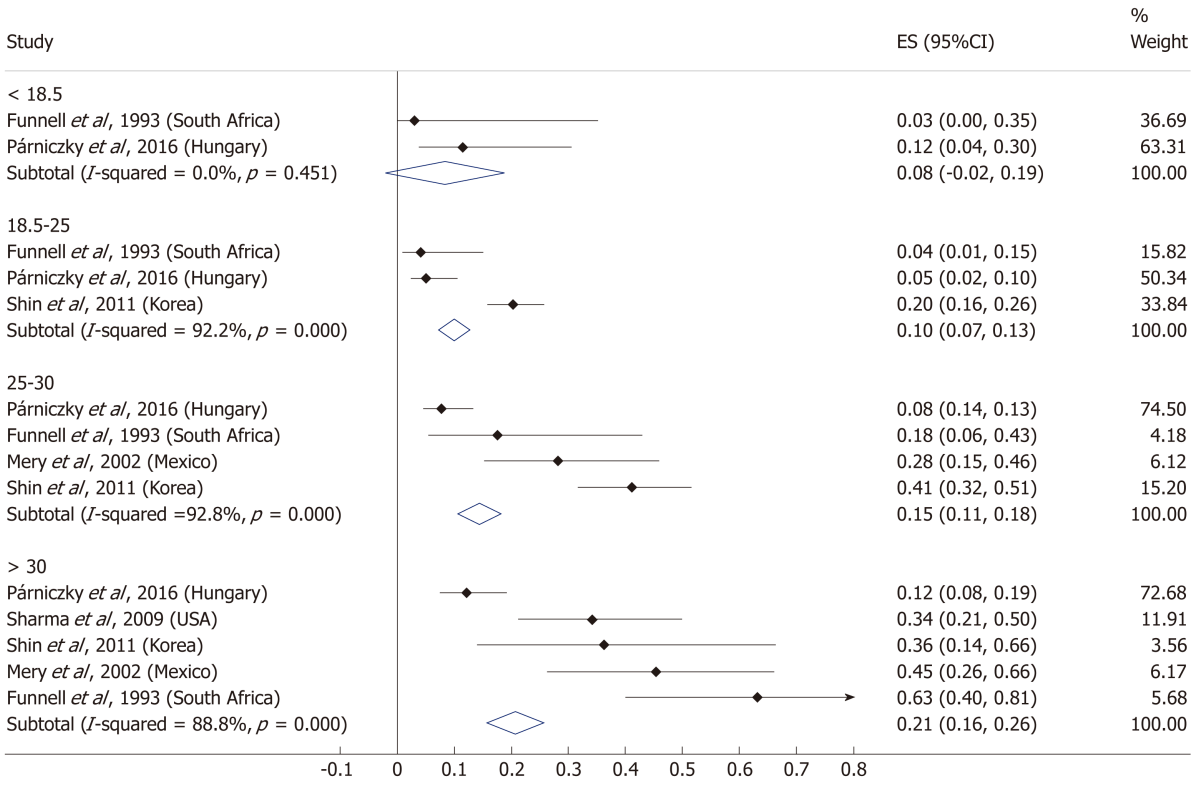

Figure 8 Subgroup analysis of body-mass index and acute pancreatitis severity displayed on forest plot. Filled circles represent the odds ratio derived from the studies analyzed. Horizontal bars represent 95%CI. Empty rhombuses show the overall, combined effect (OR is the middle of the rhombus and CIs are the edges). BMI: Body-mass index; CI: Confidence interval; OR: Odds ratio.

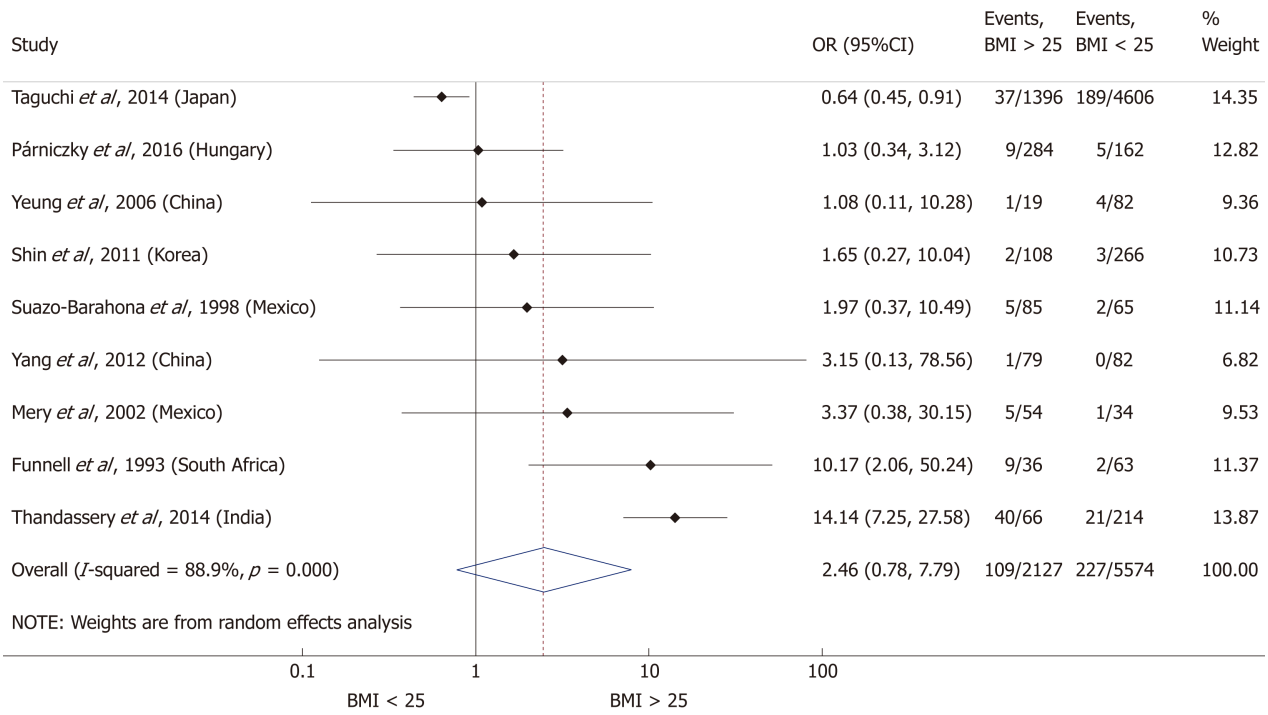

Figure 9 Forest plot of mortality comparing the body-mass index < 25 and body-mass index > 25 subgroups. Filled circles represent the odds ratio derived from the studies analyzed. Horizontal bars represent 95% CI. Empty rhombuses show the overall, combined effect (OR is the middle of the rhombus and CIs are the edges). BMI: Body-mass index; CI: Confidence interval; OR: Odds ratio.

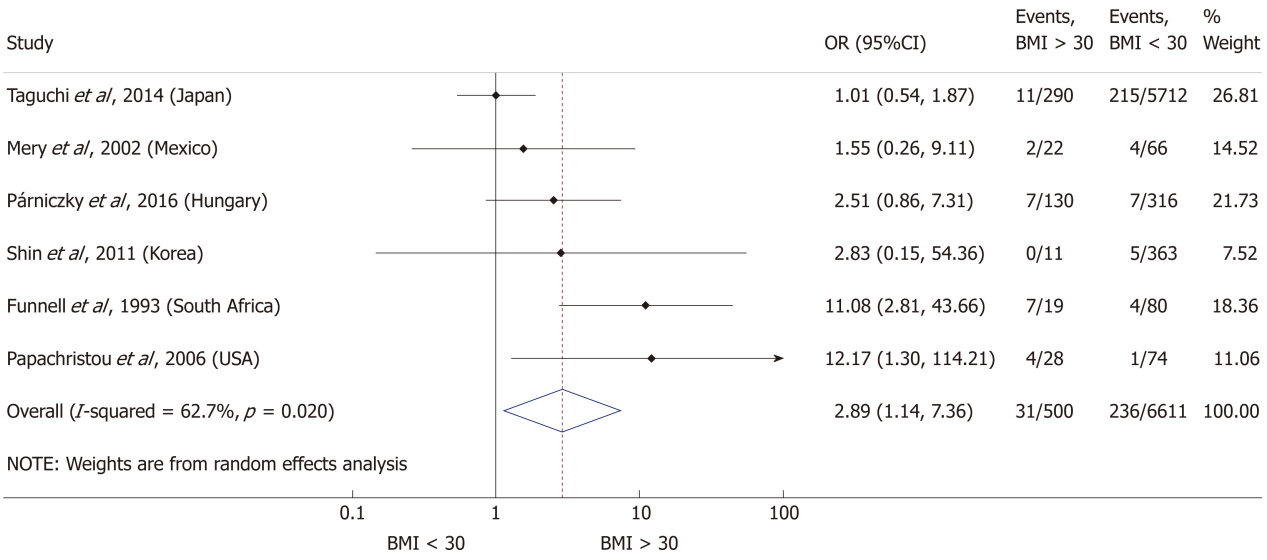

Figure 10 Forest plot of mortality comparing the body-mass index < 30 and body-mass index > 30 subgroups. Filled circles represent the odds ratio derived from the studies analyzed. Horizontal bars represent 95%CI. Empty rhombuses show the overall, combined effect (OR is the middle of the rhombus and CIs are the edges). BMI: Body-mass index; CI: Confidence interval; OR: Odds ratio.

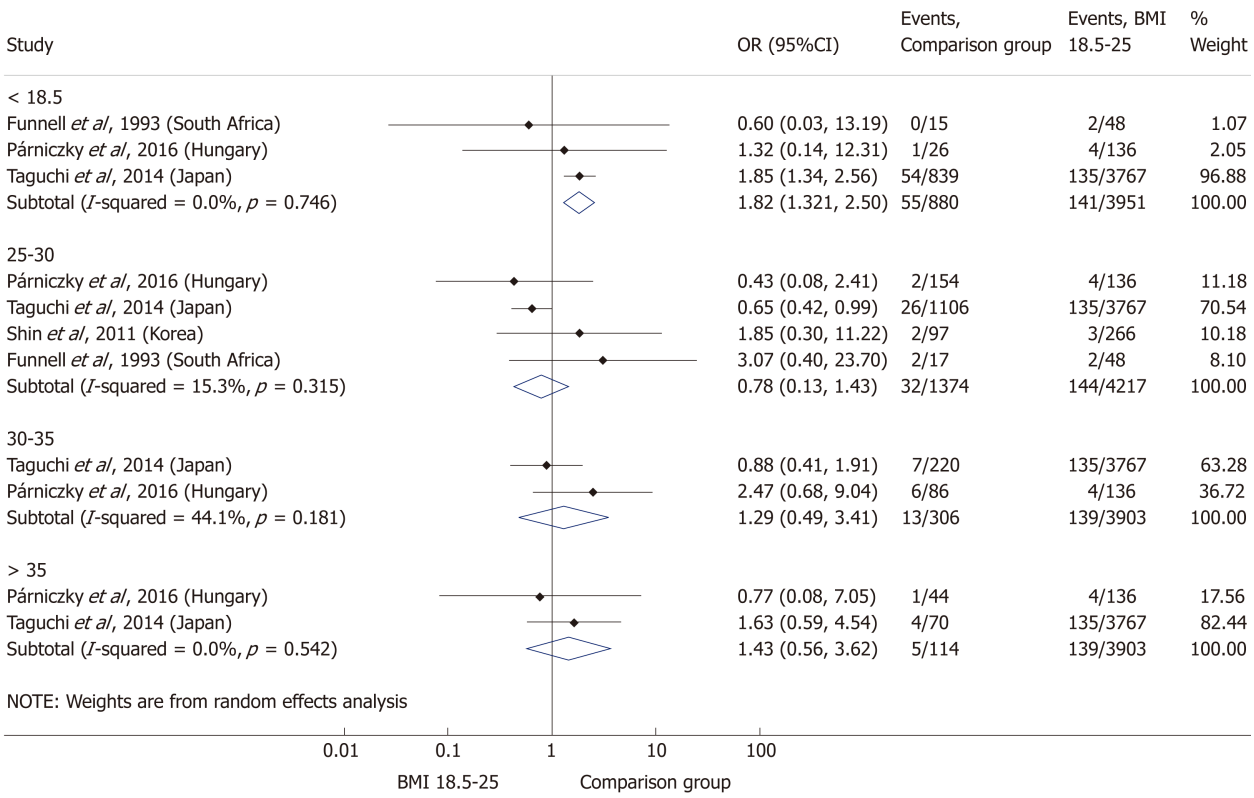

Figure 11 Forest plot of mortality comparing the normal body-mass index group (body-mass index 18.5-25) to other body-mass index categories. Filled circles represent the odds ratio derived from the studies analyzed. Horizontal bars represent 95% CI. Empty rhombuses show the overall, combined effect (OR is the middle of the rhombus and CIs are the edges). BMI: Body-mass index; CI: Confidence interval; OR: Odds ratio.

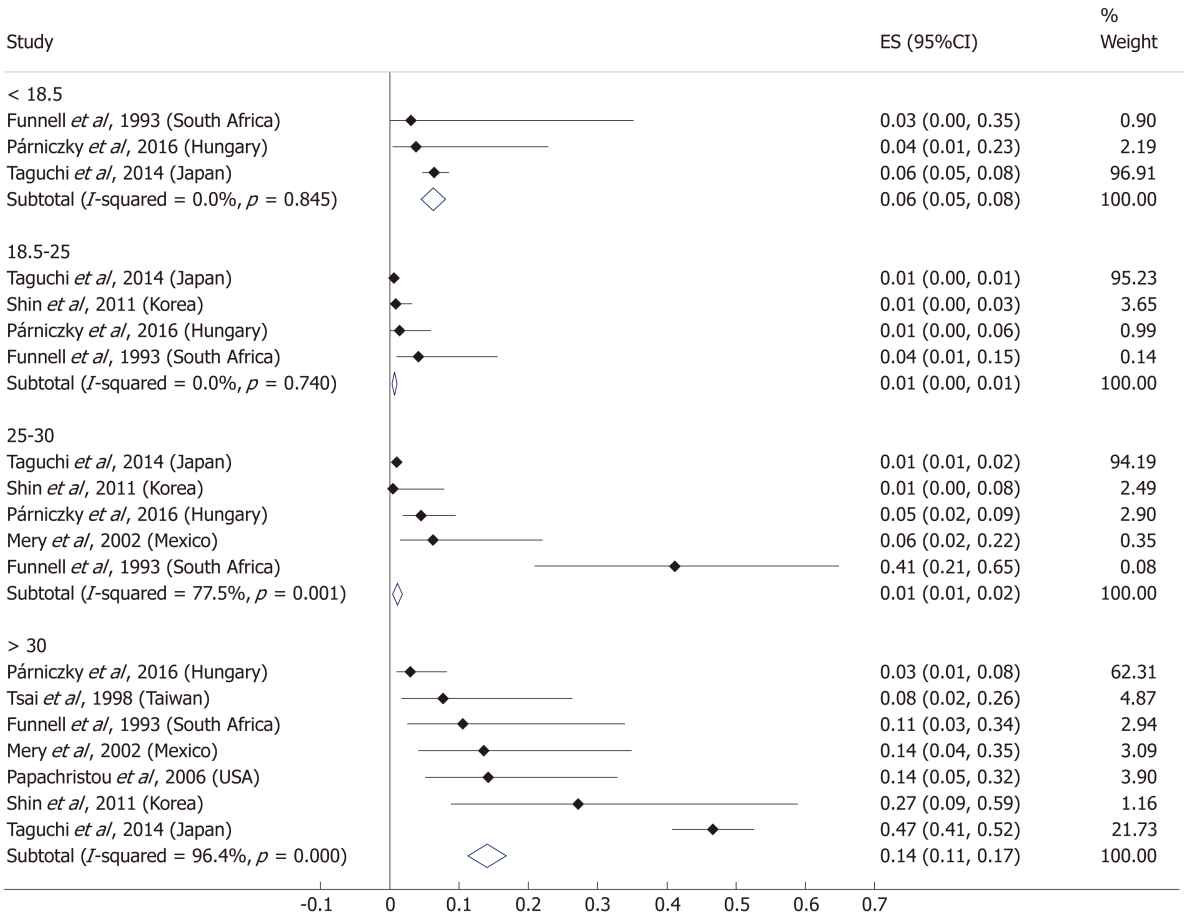

Figure 12 Subgroup analysis of body-mass index and acute pancreatitis mortality displayed on forest plot. Filled circles represent the odds ratio derived from the studies analyzed. Horizontal bars represent 95%CI. Empty rhombuses show the overall, combined effect (OR is the middle of the rhombus and CIs are the edges). BMI: Body-mass index; CI: Confidence interval; OR: Odds ratio.

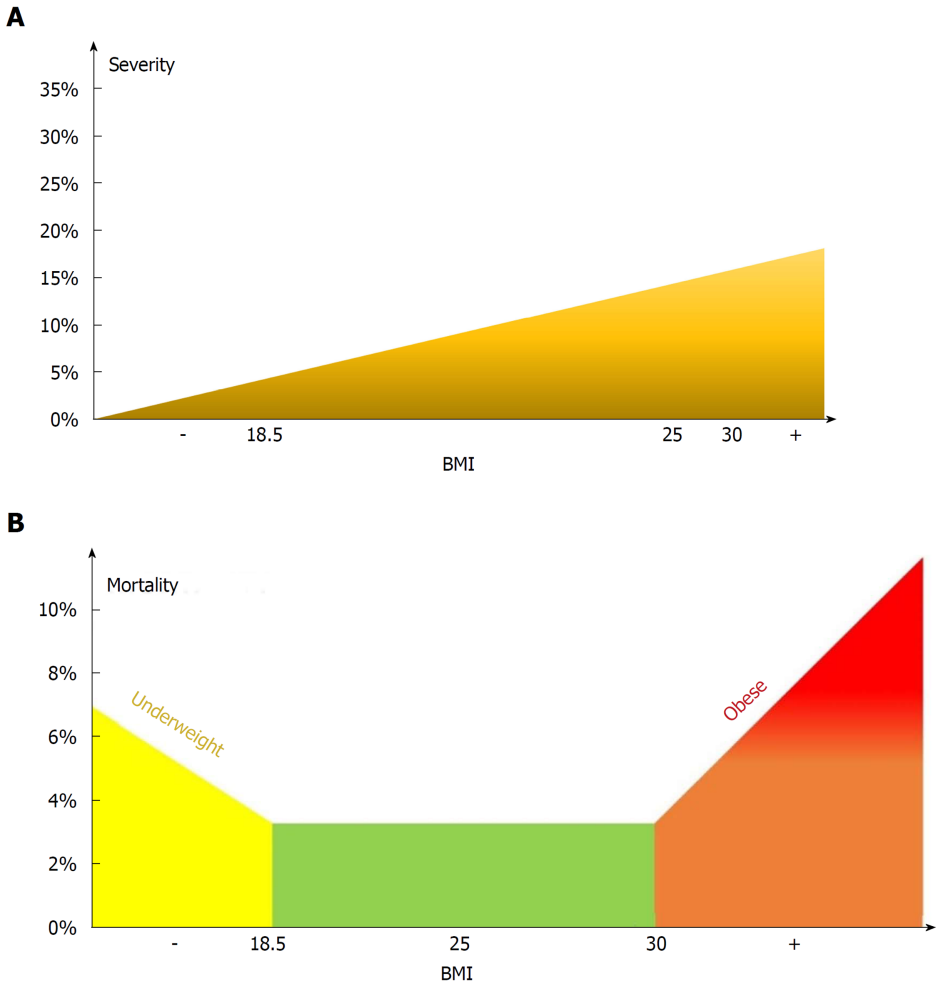

Figure 13 Model for the effect of body-mass index on severity (A) and mortality (B).

ARTICLE HIGHLIGHTS

Research background

The worldwide incidence of obesity is increasing and previous studies stated that it worsens the outcome of AP.

Research motivation

We wanted to provide detailed guidance on the clinical use of BMI in prognostic scoring.

Research objectives

To exactly identify which BMI subgroups are most in danger of a severe or even fatal disease outcome in AP.

Research methods

A systematic search was carried out in PubMed, Embase and Cochrane Library databases for studies investigating the effect of BMI on the outcome of AP. We used the PRISMA protocol, registered our project in PROSPERO and assessed the quality of the included articles by using a modified version of the Newcastle-Ottawa Scale. The statistical calculations were performed with Stata 11 SE, using the random effects model (DerSimonian-Laird method).

Research results

9997 patients with acute pancreatitis were included (19 articles) in this analysis. We found that AP patients with a BMI > 25 have a significantly increased risk of SAP with an OR of 2.87. A BMI > 30 means a significantly increased risk of mortality (OR = 2.89) while one with a BMI < 18.5 is

also at a significantly higher risk of mortality compared to normal weight patients with an OR of 1.82.

Research conclusions

The new findings of this study identified that a BMI above 25 increases the risk of severe AP, but not mortality, while a BMI > 30 raises the risk of mortality. A BMI < 18.5 carries an almost two times higher risk of mortality in AP. It is the first meta-analysis that performs a detailed analysis on all WHO BMI categories with regard to both primary endpoints of AP. This helps to determine which BMI groups are at the highest risk of severe or even fatal outcome in AP.

Research perspectives

Our results give the opportunity for researchers to prepare the guidelines and scoring systems more precisely.

REFERENCES

1 **Bray GA**, Heisel WE, Afshin A, Jensen MD, Dietz WH, Long M, Kushner RF, Daniels SR, Wadden TA, Tsai AG, Hu FB, Jakicic JM, Ryan DH, Wolfe BM, Inge TH. The Science of Obesity Management: An Endocrine Society Scientific Statement. *Endocr Rev* 2018; **39**: 79-132 [PMID: 29518206 DOI: 10.1210/er.2017-00253]

2 Available from: http://apps.who.int/gho/data/node.main.A897A?lang=en

3 **Withrow D**, Alter DA. The economic burden of obesity worldwide: a systematic review of the direct costs of obesity. *Obes Rev* 2011; **12**: 131-141 [PMID: 20122135 DOI: 10.1111/j.1467-789X.2009.00712.x]

4 **Seidell JC**, Flegal KM. Assessing obesity: classification and epidemiology. *Br Med Bull* 1997; **53**: 238-252 [PMID: 9246834]

5 **Párniczky A**, Kui B, Szentesi A, Balázs A, Szűcs Á, Mosztbacher D, Czimmer J, Sarlós P, Bajor J, Gódi S, Vincze Á, Illés A, Szabó I, Pár G, Takács T, Czakó L, Szepes Z, Rakonczay Z, Izbéki F, Gervain J, Halász A, Novák J, Crai S, Hritz I, Góg C, Sümegi J, Golovics P, Varga M, Bod B, Hamvas J, Varga-Müller M, Papp Z, Sahin-Tóth M, Hegyi P; Hungarian Pancreatic Study Group. Prospective, Multicentre, Nationwide Clinical Data from 600 Cases of Acute Pancreatitis. *PLoS One* 2016; **11**: e0165309 [PMID: 27798670 DOI: 10.1371/journal.pone.0165309]

6 **Working Group IAP/APA Acute Pancreatitis Guidelines**. IAP/APA evidence-based guidelines for the management of acute pancreatitis. *Pancreatology* 2013; **13**: e1-15 [PMID: 24054878 DOI: 10.1016/j.pan.2013.07.063]

7 **Johnson CD**, Toh SK, Campbell MJ. Combination of APACHE-II score and an obesity score (APACHE-O) for the prediction of severe acute pancreatitis. *Pancreatology* 2004; **4**: 1-6 [PMID: 14988652 DOI: 10.1159/000077021]

8 **Papachristou GI**, Papachristou DJ, Avula H, Slivka A, Whitcomb DC. Obesity increases the severity of acute pancreatitis: performance of APACHE-O score and correlation with the inflammatory response. *Pancreatology* 2006; **6**: 279-285 [PMID: 16636600 DOI: 10.1159/000092689]

9 **Guzmán Calderon E**, Montes Teves P, Monge Salgado E. [Bisap-O: obesity included in score BISAP to improve prediction of severity in acute pancreatitis]. *Rev Gastroenterol Peru* 2012; **32**: 251-256 [PMID: 23128944]

10 **Martínez J**, Sánchez-Payá J, Palazón JM, Suazo-Barahona J, Robles-Díaz G, Pérez-Mateo M. Is obesity a risk factor in acute pancreatitis? A meta-analysis. *Pancreatology* 2004; **4**: 42-48 [PMID: 14988657 DOI: 10.1159/000077025]

11 **Martínez J**, Johnson CD, Sánchez-Payá J, de Madaria E, Robles-Díaz G, Pérez-Mateo M. Obesity is a definitive risk factor of severity and mortality in acute pancreatitis: an updated meta-analysis. *Pancreatology* 2006; **6**: 206-209 [PMID: 16549939 DOI: 10.1159/000092104]

12 **Wang SQ**, Li SJ, Feng QX, Feng XY, Xu L, Zhao QC. Overweight is an additional prognostic factor in acute pancreatitis: a meta-analysis. *Pancreatology* 2011; **11**: 92-98 [PMID: 21577040 DOI: 10.1159/000327688]

13 **Hong S**, Qiwen B, Ying J, Wei A, Chaoyang T. Body mass index and the risk and prognosis of acute pancreatitis: a meta-analysis. *Eur J Gastroenterol Hepatol* 2011; **23**: 1136-1143 [PMID: 21904207 DOI: 10.1097/MEG.0b013e32834b0e0e]

14 **Moher D**, Liberati A, Tetzlaff J, Altman DG; PRISMA Group. Preferred reporting items for systematic reviews and meta-analyses: the PRISMA statement. *BMJ* 2009; **339**: b2535 [PMID: 19622551 DOI: 10.1136/bmj.b2535]

15 **Bradley EL**. A clinically based classification system for acute pancreatitis. Summary of the International Symposium on Acute Pancreatitis, Atlanta, Ga, September 11 through 13, 1992. *Arch Surg* 1993; **128**: 586-590 [PMID: 8489394]

16 **Sarr MG**, Banks PA, Bollen TL, Dervenis C, Gooszen HG, Johnson CD, Tsiotos GG, Vege SS. The new revised classification of acute pancreatitis 2012. *Surg Clin North Am* 2013; **93**: 549-562 [PMID: 23632143 DOI: 10.1016/j.suc.2013.02.012]

17 **Yoon SB**, Choi MH, Lee IS, Lim CH, Kim JS, Cho YK, Park JM, Lee BI, Cho YS, Choi MG. Impact of body fat and muscle distribution on severity of acute pancreatitis. *Pancreatology* 2017; **17**: 188-193 [PMID: 28190685 DOI: 10.1016/j.pan.2017.02.002]

18 **Duarte-Rojo A**, Sosa-Lozano LA, Saúl A, Herrera-Cáceres JO, Hernández-Cárdenas C, Vázquez-Lamadrid J, Robles-Díaz G. Methods for measuring abdominal obesity in the prediction of severe acute pancreatitis, and their correlation with abdominal fat areas assessed by computed tomography. *Aliment Pharmacol Ther* 2010; **32**: 244-253 [PMID: 20374222 DOI: 10.1111/j.1365-2036.2010.04321.x]

19 **Yeung YP**, Lam BY, Yip AW. APACHE system is better than Ranson system in the prediction of severity of acute pancreatitis. *Hepatobiliary Pancreat Dis Int* 2006; **5**: 294-299 [PMID: 16698595]

20 **Shin KY**, Lee WS, Chung DW, Heo J, Jung MK, Tak WY, Kweon YO, Cho CM. Influence of obesity on the severity and clinical outcome of acute pancreatitis. *Gut Liver* 2011; **5**: 335-339 [PMID: 21927663 DOI: 10.5009/gnl.2011.5.3.335]

21 **Katuchova J**, Bober J, Harbulak P, Hudak A, Gajdzik T, Kalanin R, Radonak J. Obesity as a risk factor for severe acute pancreatitis patients. *Wien Klin Wochenschr* 2014; **126**: 223-227 [PMID: 24522641 DOI:

10.1007/s00508-014-0507-7]
22 **Yashima Y**, Isayama H, Tsujino T, Nagano R, Yamamoto K, Mizuno S, Yagioka H, Kawakubo K, Sasaki T, Kogure H, Nakai Y, Hirano K, Sasahira N, Tada M, Kawabe T, Koike K, Omata M. A large volume of visceral adipose tissue leads to severe acute pancreatitis. *J Gastroenterol* 2011; **46**: 1213-1218 [PMID: 21805069 DOI: 10.1007/s00535-011-0430-x]
23 **Karpavicius A**, Dambrauskas Z, Gradauskas A, Samuilis A, Zviniene K, Kupcinskas J, Brimas G, Meckovski A, Sileikis A, Strupas K. The clinical value of adipokines in predicting the severity and outcome of acute pancreatitis. *BMC Gastroenterol* 2016; **16**: 99 [PMID: 27549125 DOI: 10.1186/s12876-016-0514-4]
24 **Türkoğlu A**, Böyük A, Tanrıverdi MH, Gündüz E, Dusak A, Kaplan İ, Gümüş M. The potential role of BMI, plasma leptin, nesfatin-1 and ghrelin levels in the early detection of pancreatic necrosis and severe acute pancreatitis: a prospective cohort study. *Int J Surg* 2014; **12**: 1310-1313 [PMID: 25448651 DOI: 10.1016/j.ijsu.2014.10.040]
25 **Mery CM**, Rubio V, Duarte-Rojo A, Suazo-Barahona J, Peláez-Luna M, Milke P, Robles-Díaz G. Android fat distribution as predictor of severity in acute pancreatitis. *Pancreatology* 2002; **2**: 543-549 [PMID: 12435867 DOI: 10.1159/000066099]
26 **Suazo-Baráhona J**, Carmona-Sánchez R, Robles-Díaz G, Milke-García P, Vargas-Voracková F, Uscanga-Domínguez L, Peláez-Luna M. Obesity: a risk factor for severe acute biliary and alcoholic pancreatitis. *Am J Gastroenterol* 1998; **93**: 1324-1328 [PMID: 9707059 DOI: 10.1111/j.1572-0241.1998.442_l.x]
27 **Thandassery RB**, Appasani S, Yadav TD, Dutta U, Indrajit A, Singh K, Kochhar R. Implementation of the Asia-Pacific guidelines of obesity classification on the APACHE-O scoring system and its role in the prediction of outcomes of acute pancreatitis: a study from India. *Dig Dis Sci* 2014; **59**: 1316-1321 [PMID: 24374646 DOI: 10.1007/s10620-013-3000-7]
28 **Yang F**, Wu H, Li Y, Li Z, Wang C, Yang J, Hu B, Huang Z, Ji R, Zhan X, Xie H, Wang L, Zhang M, Tang C. Prevention of severe acute pancreatitis with octreotide in obese patients: a prospective multi-center randomized controlled trial. *Pancreas* 2012; **41**: 1206-1212 [PMID: 23086244 DOI: 10.1097/MPA.0b013e3182523bdf]
29 **Funnell IC**, Bornman PC, Weakley SP, Terblanche J, Marks IN. Obesity: an important prognostic factor in acute pancreatitis. *Br J Surg* 1993; **80**: 484-486 [PMID: 8495317]
30 **Sharma A**, Muddana V, Lamb J, Greer J, Papachristou GI, Whitcomb DC. Low serum adiponectin levels are associated with systemic organ failure in acute pancreatitis. *Pancreas* 2009; **38**: 907-912 [PMID: 19696691 DOI: 10.1097/MPA.0b013e3181b65bbe]
31 **Taguchi M**, Kubo T, Yamamoto M, Muramatsu K, Yasunaga H, Horiguchi H, Fujimori K, Matsuda S, Fushimi K, Harada M. Body mass index influences the outcome of acute pancreatitis: an analysis based on the Japanese administrative database. *Pancreas* 2014; **43**: 863-866 [PMID: 24786667 DOI: 10.1097/MPA.0000000000000137]
32 **Bota S**, Sporea I, Sirli R, Popescu A, Strain M, Focsa M, Danila M, Chisevescu D. Predictive factors for severe evolution in acute pancreatitis and a new score for predicting a severe outcome. *Ann Gastroenterol* 2013; **26**: 156-162 [PMID: 24714801]
33 **Sadr-Azodi O**, Orsini N, Andrén-Sandberg Å, Wolk A. Abdominal and total adiposity and the risk of acute pancreatitis: a population-based prospective cohort study. *Am J Gastroenterol* 2013; **108**: 133-139 [PMID: 23147519 DOI: 10.1038/ajg.2012.381]
34 **Tsai CJ**. Is obesity a significant prognostic factor in acute pancreatitis? *Dig Dis Sci* 1998; **43**: 2251-2254 [PMID: 9790461]

P- Reviewer: Gonoi W, Löhr JM
S- Editor: Gong ZM **L- Editor:** A **E- Editor:** Yin SY

Published By Baishideng Publishing Group Inc
7901 Stoneridge Drive, Suite 501, Pleasanton, CA 94588, USA
Telephone: +1-925-2238242
Fax: +1-925-2238243
E-mail: bpgoffice@wjgnet.com
Help Desk:http://www.f6publishing.com/helpdesk
http://www.wjgnet.com